

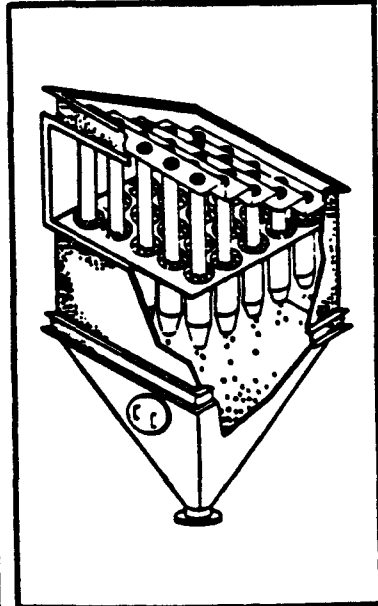
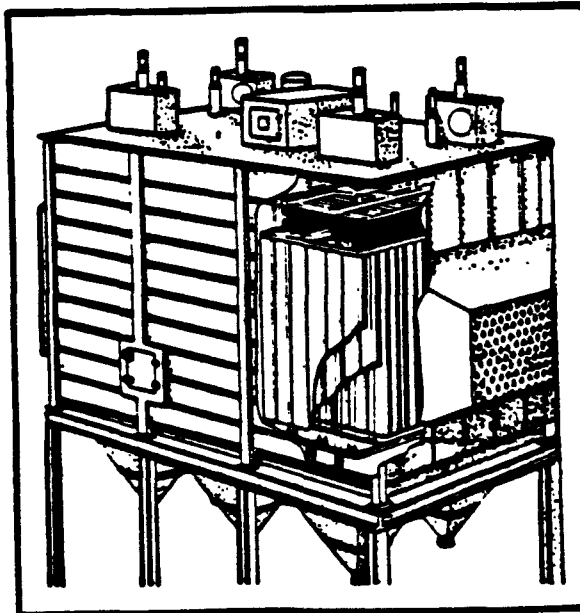
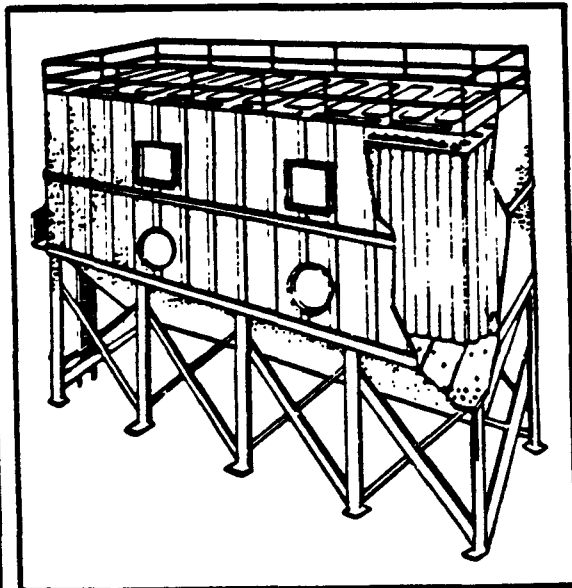
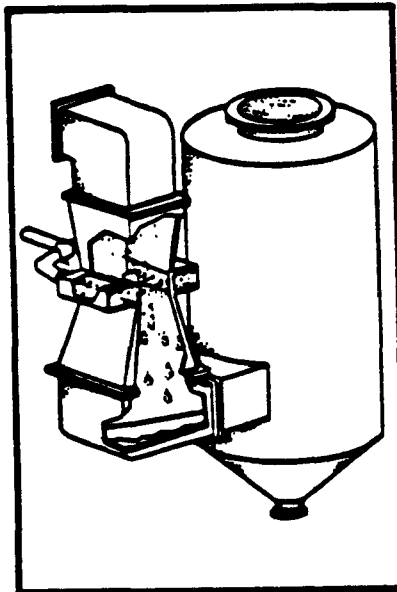


Air

APTI Course 413 Control of Particulate Emissions

Do not remove. This document
should be retained in the EPA
Region 5 Library Collection.

Student Manual



Air

APTI

Course 413

Control of Particulate Emissions

Student Manual

Written by:
David S. Beachler
James A. Jahnke, Ph.D.

Northrop Services, Inc.
P.O. Box 12313
Research Triangle Park, NC 27709

Under Contract No.
68-02-2374
EPA Project Officer
R. E. Townsend

United States Environmental Protection Agency
Office of Air, Noise, and Radiation
Office of Air Quality Planning and Standards
Research Triangle Park, NC 27711



U.S. Environmental Protection Agency
Region 5, Library (5PL-16)
270 S. Dearborn Street, Room 1670
Chicago, IL 60604

Notice

This is not an official policy and standards document. The opinions and selections are those of the authors and not necessarily those of the Environmental Protection Agency. Every attempt has been made to represent the present state of the art as well as subject areas still under evaluation. Any mention of products or organizations does not constitute endorsement by the United States Environmental Protection Agency.

Availability

This document is issued by the Manpower and Technical Information Branch, Control Programs Development Division, Office of Air Quality Planning and Standards, USEPA. It was developed for use in training courses presented by the EPA Air Pollution Training Institute and others receiving contractual or grant support from the Institute. Other organizations are welcome to use the document.

This publication is available, free of charge, to schools or governmental air pollution control agencies intending to conduct a training course on the subject covered. Submit a written request to the Air Pollution Training Institute, USEPA, MD 20, Research Triangle Park, NC 27711.

Others may obtain copies, for a fee, from the National Technical Information Service (NTIS), 5825 Port Royal Road, Springfield, VA 22161.

Sets of slides and films designed for use in the training course of which this publication is a part may be borrowed from the Air Pollution Training Institute upon written request. The slides may be freely copied. Some films may be copied; others must be purchased from the commercial distributor.

Table of Contents

	Page
Chapter 1. Air Pollution Control Overview	1-1
Introduction	1-1
Collection Forces	1-3
Factors Affecting Control Equipment Selection	1-5
Chapter 2. Basic Concepts of Gases	2-1
Expression of Gas Temperature	2-1
Expression of Gas Pressure	2-2
Molecular Weight	2-4
Mole	2-5
The Laws of Ideal Gases	2-5
Density	2-6
Viscosity	2-7
Specific Heat	2-9
Reynolds Number	2-9
Chapter 3. Particle Dynamics	3-1
Forces Acting on a Particle	3-1
Balance of Forces on a Particle	3-8
Determination of the Flow Regime	3-10
References	3-12
Chapter 4. Particle Sizing	4-1
Introduction	4-1
Size	4-1
Various Sizing Devices	4-2
Comparison of Particle Sizing Devices	4-10
Mathematical Treatment of Data	4-12
Example of a Typical Particle Size Data Reduction	4-19
References	4-23
Chapter 5. Gravity Settling Chambers	5-1
Introduction	5-1
Equipment Description	5-1
Baffle Chambers	5-3
Design Parameters	5-4
Process Variables	5-7
References	5-8
Chapter 6. Cyclones	6-1
Introduction	6-1
Cyclone Types	6-2
Characterizing Cyclone Performance	6-15
Summary of Performance Characteristics	6-23
References	6-27

Chapter 7. Electrostatic Precipitators	7-1
Introduction	7-1
Types of ESPs	7-2
Theory of Precipitation	7-5
Collection Efficiency	7-9
Design Parameters	7-11
Precipitator Equipment	7-19
Electrostatic Precipitator Applications	7-27
References	7-29
Chapter 8. Fabric Filtration	8-1
Filtration for Particle Collection	8-1
Baghouses	8-4
Fabric Filter Material	8-16
Bag Cleaning	8-21
Baghouse Design Variables	8-29
Baghouse Design Review	8-33
References	8-37
Chapter 9. Wet Collectors	9-1
General Characteristics—Particulate Matter Removal	9-1
Theory of Operation	9-3
General Theories	9-4
Collection Mechanisms	9-5
The Johnstone Equation	9-10
The Cut Power Method	9-12
The Contact Power Theory	9-15
Pilot Methods	9-21
Wet Collector Systems	9-22
Gas Phase Contacting Scrubbers	9-22
Liquid Phase Contacting Scrubbers	9-36
Liquid Phase/Gas Phase Contacting Scrubbers	9-41
Mechanically Aided Scrubbers	9-49
Miscellaneous Devices	9-52
References	9-58
Appendix A. Common SI Units	A-1
Appendix B. Conversion Factors	B-1
Appendix C. Constants and Useful Information	C-1
Appendix D. Capital and Operating Cost Estimations	D-1
Appendix E. Characteristics of Air Pollution Control Equipment	E-1
Appendix F. Industry Pollutant Sources and Typical Control Devices	F-1
Appendix G. Characteristics of Particles	G-1
Appendix References	H-1

Figures

Figure		Page
1-1	Gravity	1-3
1-2	Centrifugal force	1-3
1-3	Impaction	1-4
1-4	Direct interception	1-4
1-5	Diffusion	1-5
1-6	Electrostatic attraction	1-5
2-1	Comparison of degree-units between Fahrenheit and Celsius	2-1
2-2	Two examples of absolute pressure determination	2-4
2-3	Shearing stress in a moving fluid	2-7
3-1	Identical objects in two different fluids	3-2
3-2	Buoyant and gravitational forces acting on a particle	3-3
3-3	Drag force	3-4
3-4	Drag coefficient versus Reynolds Number for spheres	3-5
3-5	Collisions of air molecules on particles greater than $3\ \mu\text{m}$ in diameter	3-6
3-6	Collisions of air molecules on particles less than $3\ \mu\text{m}$ in diameter	3-7
3-7	Vector sum of forces acting on a particle	3-9
4-1	Diameters of nonspherical particles	4-1
4-2	Aerodynamic diameter	4-2
4-3	Microscope	4-3
4-4	Operating principle for an optical particle counter	4-5
4-5	Coaxial cylinder mobility analyzer	4-6
4-6	Bahco sampler	4-7
4-7	Schematic diagram, operation of an inertial impactor	4-8
4-8	Schematics of two commercial cascade impactors	4-9
4-9	Particle size distribution with one preferential size	4-12
4-10	Skewed particle size distribution plotted on a linear scale	4-13
4-11	Typical particle size distribution plotted on a log scale	4-13
4-12	Typical particle size distribution with two preferential sizes	4-14
4-13	Cumulative particle size distribution plotted on a linear scale	4-15
4-14	Cumulative distribution plotted on log probability paper	4-17
4-15	Geometric mean and standard deviation from a log-normal distribution plot	4-18
4-16	Mass concentration versus particle diameter on a linear scale	4-20
4-17	Mass concentration versus particle size on a log scale	4-21
4-18	Log-probability distribution for data in Table 4-6	4-22

Figure		Page
5-1	Horizontal flow settling chamber.....	5-2
5-2	Howard settling chamber (multiple tray).....	5-3
5-3	Baffle chamber.....	5-3
5-4	Settling chamber dimensions.....	5-4
5-5	Fractional efficiency curve for dusts from a sinter plant.....	5-6
6-1	Particle collection mechanisms.....	6-1
6-2	Types of cyclones.....	6-3
6-3	Common cyclone.....	6-4
6-4	Inlet interference.....	6-5
6-5	Types of cyclone inlets.....	6-6
6-6	Nomenclature for a tangential entry cyclone.....	6-7
6-7	Standard cyclone designs.....	6-8
6-8	Cyclone vortices.....	6-9
6-9	Fines eductor.....	6-11
6-10	Discharge systems.....	6-12
6-11	Cyclone outlet devices.....	6-14
6-12	Typical size efficiency curve.....	6-16
6-13a	Cut size in micrometers for cyclones of conventional type.....	6-17
6-13b	Viscosity and velocity correction factors for cut size particle of conventional cyclones.....	6-18
6-13c	Inlet width/cyclone diameter and effective number of turns correction factors for cut size particle of conventional cyclones.....	6-18
6-14	Cyclone efficiency versus particle diameter. Experimental results and theoretical predictions.....	6-21
6-15	Cyclone efficiency versus particle size ratio.....	6-22
6-16	Cyclones in series.....	6-24
6-17	Battery of four involute cyclones in parallel.....	6-25
6-18	Battery of vane axial cyclones.....	6-26
7-1	Typical plate and wire single-stage electrostatic precipitator.....	7-1
7-2	Typical two-stage precipitator.....	7-3
7-3	Gas flow through wire and tubular pipe precipitators.....	7-4
7-4	Gas flow through a wire and plate precipitator.....	7-4
7-5	Electric field generation (top view).....	7-5
7-6	Generation of corona.....	7-6
7-7	Avalanche multiplication.....	7-6
7-8	Gas ionization in the inter-electrode region.....	7-7
7-9	Field lines modified by the particle.....	7-8
7-10	Effect of temperature and moisture content on apparent resistivity of precipitated cement dust.....	7-13
7-11	Fly ash resistivity versus coal sulfur content for several flue gas temperature bands.....	7-14
7-12	Gas inlet with diffuser-perforated plates.....	7-16
7-13	Stage or field sectionalization.....	7-18

Figure		Page
7-14	Parallel sectionalization.....	7-18
7-15	Guide frames and shrouds for discharge wires.....	7-19
7-16	Typical discharge wire shapes.....	7-20
7-17	Rigid frame discharge electrode design.....	7-21
7-18	Typical collection plates.....	7-21
7-19	Typical hammer/anvil collection plate rapper.....	7-23
7-20	Typical impulse collection plate rappers.....	7-24
7-21	Typical vibrator rappers used for discharge electrodes.....	7-25
7-22	High voltage system.....	7-26
8-1	Impaction.....	8-1
8-2	Direct interception.....	8-2
8-3	Diffusion.....	8-2
8-4	Bags and support.....	8-4
8-5	Envelope baghouse.....	8-5
8-6	Bags and hopper.....	8-6
8-7	Positive and negative pressure baghouses.....	8-7
8-8	Interior filtration (particles collected on the inside of the bag).....	8-8
8-9	Exterior filtration (particles collected on the outside of the bag).....	8-9
8-10	Dust inlet to the baghouse.....	8-10
8-11	Bag attachment.....	8-11
8-12	Hopper.....	8-13
8-13	Trickle valve discharge device.....	8-13
8-14	Rotary airlock discharge device.....	8-14
8-15	Screw conveyor.....	8-15
8-16	Pneumatic conveyor.....	8-16
8-17	Woven fabric filter; twill weave and sateen weave.....	8-17
8-18	Sieving.....	8-18
8-19	Felted fabric filter.....	8-18
8-20	Shaking.....	8-22
8-21	Reverse air cleaning.....	8-23
8-22	Pulse jet cleaning.....	8-25
8-23	Pulse jet air supply.....	8-26
8-24	Reverse jet cleaning using blow rings.....	8-28
8-25	Performance curve for a single bag of a fabric filter.....	8-31
8-26	Overall pressure drop of a multicompartment baghouse.....	8-31
9-1	Zones of a wet scrubber.....	9-3
9-2	Collection efficiency for a mobile bed scrubber as a function of particle size.....	9-4
9-3	Inertial impaction collection efficiency: target efficiency.....	9-6
9-4	Target efficiency: the area ratios.....	9-7
9-5	Collection by interception.....	9-8
9-6	Penetration and the cut diameter.....	9-14
9-7	Correlation of scrubber outlet dust loading with theoretical power consumption.....	9-19

Figure		Page
9-8	Cut diameter $[d_p]_{cut}$ as a function of gas pressure drop and power consumption.....	9-20
9-9	Sieve plate scrubber.....	9-23
9-10	Impingement plate scrubber.....	9-24
9-11	Detail of an impingement plate.....	9-25
9-12	Detail of bubble caps.....	9-25
9-13	Detail of orifice action.....	9-27
9-14	Swirl orifice scrubber.....	9-28
9-15	Typical venturi scrubber.....	9-29
9-16	Swirl venturi scrubber.....	9-31
9-17	Spray venturi scrubber.....	9-32
9-18	Variable throat venturi scrubber.....	9-33
9-19	Variable throat venturi scrubber.....	9-34
9-20	Venturi-rod scrubber.....	9-35
9-21	Types of spray nozzles.....	9-37
9-22	Simple spray chamber.....	9-38
9-23	Mist eliminators.....	9-39
9-24	Ejector venturi scrubber.....	9-40
9-25	Irrigated cyclone scrubber.....	9-42
9-26	Cyclonic spray scrubber.....	9-43
9-27	Centrifugal scrubber.....	9-44
9-28	Moving bed scrubber.....	9-45
9-29	Baffle spray scrubber.....	9-47
9-30	Combination device A.....	9-48
9-31	Combination device B.....	9-49
9-32	Centrifugal fan scrubber.....	9-50
9-33	Vertical spray rotor scrubber.....	9-51
9-34	Common packing materials.....	9-53
9-35	Countercurrent packed tower.....	9-54
9-36	Cocurrent packed tower.....	9-55
9-37	Crossflow scrubber.....	9-56
9-38	Fiber bed scrubber.....	9-57
D-1	Dry type electrostatic precipitator purchase prices versus plate area. Data valid for December 1977.....	D-2
D-2	1/8" thick carbon steel fabricated scrubber price versus volume. Data valid for December 1977.....	D-4
D-3	Metal thickness required versus volume and design pressure.....	D-4
D-4	Price adjustment factors versus plate thickness and volume. Data valid for December 1977.....	D-5
D-5	Scrubber internal surface area and separator diameter and height versus waste inlet gas volume.....	D-5
D-6	Internal gas cooler bubble tray cost versus separator diameter. Data valid for December 1977.....	D-6
D-7	Intermittent, pressure, mechanical shaker baghouse prices versus net cloth area. Data valid for December 1977.....	D-7

Figure		Page
D-8	Continuous, suction or pressure, pulse jet baghouse prices versus net cloth area. Data valid for December 1977.....	D-8
D-9	Continuous, pressure, mechanical shaker baghouse prices versus net cloth area. Data valid for December 1977.....	D-8
D-10	Continuous, pressure, reverse air baghouse prices versus net cloth area. Data valid for December 1977.....	D-9
D-11	Custom pressure or suction baghouse prices versus net cloth area. Data valid for December 1977.....	D-9
D-12	Capacity estimates for cyclones.....	D-11
D-13	Critical particle size estimates for cyclones.....	D-12
D-14	Cyclone prices for carbon steel construction versus inlet area. Data valid for December 1977.....	D-12
D-15	Cyclone prices for stainless steel construction versus inlet area. Data valid for December 1977.....	D-13
D-16	Cyclone support prices versus collector inlet area. Data valid for December 1977.....	D-13
D-17	Cyclone dust hopper prices for carbon and stainless steel construction versus collector inlet area. Data valid for December 1977.....	D-14
D-18	Cyclone scroll outlet prices for carbon and stainless steel construction versus collector inlet area. Data valid for December 1977.....	D-14

Tables

Table		Page
3-1	Values of C_f (for air at atmospheric pressure).....	3-7
3-2	K values for flow regime determination.....	3-10
4-1	Size range capabilities of measuring devices.....	4-11
4-2	Comparison of particle sizing devices.....	4-11
4-3	Size ranges in arithmetic increments.....	4-14
4-4	Size ranges with the same ratio.....	4-15
4-5	Typical particle size data.....	4-19
4-6	Cumulative particle size data.....	4-21
5-1	Pickup velocities of various materials.....	5-8
6-1	Dimensionless design ratios for tangential entry cyclones.....	6-8
6-2	Changes in performance characteristics.....	6-23

Table		Page
7-1	Typical precipitation rate parameters for various applications.....	7-10
7-2	Typical design parameter ranges for fly ash precipitators.....	7-28
8-1	Triboelectric series for some production fabrics.....	8-3
8-2	Typical fabrics used for bags.....	8-19
8-3	Typical air-to-cloth ranges.....	8-35
8-4	Typical A/C ratios [(ft ³ /min)/ft ²] for selected industries.....	8-36
8-5	Typical A/C ratios for fabric filters used for control of particulate emissions from industrial boilers.....	8-37
9-1	Parameters α and β for the contact power theory.....	9-17
9-2	Methods for predicting venturi scrubber pressure requirements.....	9-21
9-3	Categories of wet collectors and energy input.....	9-22
9-4	Operating characteristics of plate scrubbers.....	9-26
9-5	Operating characteristics of orifice scrubbers.....	9-29
9-6	Operating characteristics of venturi scrubbers.....	9-36
9-7	Operating characteristics of spray towers.....	9-39
9-8	Operating characteristics of ejector venturis.....	9-41
9-9	Operating characteristics of cyclonic scrubbers.....	9-45
9-10	Operating characteristics of moving bed scrubbers.....	9-46
9-11	Baffle spray chamber.....	9-47
9-12	Operating characteristics of mechanically aided scrubbers.....	9-52
9-13	Operating characteristics of packed towers.....	9-57
D-1	Approximate guide to estimate gross cloth area.....	D-7
D-2	Bag prices (\$/ft ²). Data valid for December 1977.....	D-10

Nomenclature

a_p	acceleration of the particle
A	effective collecting plate area of an ESP
A_b	area of a bag
A_c	area of cloth filter
A_{cut}	parameter characterizing particle size distribution for cut power method
$A_{cleared}$	area cleared of particles
A/C	air-to-cloth ratio
A_{drop}	frontal area of a water droplet
$A.R.$	aspect ratio
B	width of a settling chamber
B_c	cyclone inlet width
B_{cut}	empirical constant for cut power method
c	cyclone dimension factor
c_i	dust concentration loading
C_D	drag coefficient
C_f	Cunningham correction factor
d'	diameter of the area cleared of particles
d_{gm}	geometric mean diameter
d_o	droplet diameter
d_p	particle diameter
d_p^*	minimum particle size (diameter) collected in a settling chamber
$[d_p]_{cut}$	particle cut diameter
$[d_p]_{crit}$	particle critical diameter
d_{pmax}	maximum particle diameter
dv/dt	change in velocity with respect to time
dv/dy	velocity gradient
D_c	cyclone body diameter
D_e	cyclone exit tube diameter
e	base of the natural logarithm = 2.718
E_o	strength of electric field in which particles are charged
E_p	strength of electric field in which particles are collected
F	force
F_B	buoyant force
F_D	drag force
F_G	gravitational force
F_R	resultant force
g	acceleration due to gravity
g_c	dimensional constant
h_p	height particle must fall to be collected in a settling chamber
H	settling chamber height
H_c	cyclone inlet height

k	dimensionless parameter
k_1	fabric resistance
k_2	filter cake resistance
k_B	Boltzmann's constant
k_c	dimensionless factor descriptive of cyclone vanes
K	factor to determine flow regimes
K_c'	proportionality factor (cyclones)
L	settling chamber length
L_c	cyclone body length
m	mass
m_a	mass of air
m_w	true weight of water (specific gravity calculation)
m_p	mass of a particle
M	molecular weight of a gas
n	vortex exponent (cyclones)
n_t	effective number of turns (vortex in a cyclone)
N_c	number of parallel chambers (Howard settling chamber)
N_t	number of transfer units
p	partial pressure of each individual gas component
p_g	gage pressure
p_L	liquid inlet pressure (scrubber)
Δp	pressure drop
Δp_c	pressure drop across a filter cake
Δp_f	pressure drop across a fabric filter
Δp_T	total pressure drop (across a baghouse)
P	absolute pressure
P_b	barometric pressure
P_T	total pressure of a gas mixture
Pe	Peclet number
P_t	penetration
\mathcal{P}_G	power input from gas stream
\mathcal{P}_L	power input from liquid stream
\mathcal{P}_T	total contacting power
q	particle charge
Q	volumetric flow rate
Q_G	gas flow rate
Q_L	liquid flow rate
r	radius of a circular path
R	universal gas constant
Re	Reynolds Number
Re_p	Reynolds Number of a particle

S	filter drag
S_c	length of exit tube in a cyclone
S_o	total number of exposures
SCA	specific collection area
t	time (filtration time)
T	absolute temperature
v	velocity
v_f	filtration velocity
v_i	inlet gas velocity
v_p	particle velocity
v_R	relative velocity of a gas to liquid
v_t	settling velocity
v_x	horizontal velocity
v_y	vertical velocity
V	volume
V_p	volume of a particle
w	migration velocity
w_i	weight fraction
Z_c	cone length
α	empirical constant for contact power theory
β	empirical constant for contact power theory
η	collection efficiency
η_c	collection efficiency of a droplet
η_i	fractional efficiency
η_{TOT}	overall collection efficiency
μ	gas viscosity
μ_l	liquid viscosity
μ^o	gas viscosity at 0°C and prevailing pressure
ν	kinematic viscosity
ρ	density
ρ_a	fluid density (air)
ρ_g	gas density
ρ_l	density of a liquid
ρ_m	density of manometer fluid used to determine v_t for cyclones
ρ_p	particle density
σ	standard deviation
σ_{gm}	geometric standard deviation
σ_l	liquid surface tension
τ	shearing stress
ψ	impaction parameter

Chapter 1

Air Pollution Control Overview

Introduction

Air pollution control is important for protecting the quality of air in our atmosphere. One pollutant affecting ambient air quality, particulate matter, is defined as any finely divided solid or liquid material other than uncombined water as measured by the Federal reference methods (Code of Federal Regulations, 1980). Control of particulate matter is necessary to maintain or improve air quality in our atmosphere.

Air cleaning devices have reduced particulate emissions from various industrial sources for the past fifty years. However, legislation such as the 1970 Clean Air Act and the 1977 Clean Air Act amendments have mandated stricter control of particulate emissions from industrial sources in order to meet National Ambient Air Quality Standards. In addition, State and local air pollution agencies have adopted regulations that are in some cases more stringent than Federal emission standards. These air pollution regulations have necessitated the application of improved control technology to industrial processes.

The Clean Air Act as amended in 1977 contains basically three classes of control technology which are to reduce emissions from existing sources, and from new and modified sources. These are: Reasonably Available Control Technology (RACT), Best Available Control Technology (BACT), and controls that reflect the Lowest Achievable Emission Rate (LAER).

In order to understand the distinctions between these various types of control technologies it is necessary to become familiar with their regulatory definitions.

- First consider the following definitions from the Code of Federal Regulations:

A *new source* is one which is contracted and installed at a facility after the date emission standards are proposed for that industry.

Modification means any physical change or change in the operation of an existing facility which increases the amount of an air pollutant emitted, or results in the emission of an air pollutant not previously emitted into the atmosphere to which a standard applies.

The term *existing source* refers to an air pollution source which was constructed before the proposal date of the emission standard.

- On this basis, then:

Reasonably Available Control Technology is control technology applied to existing sources to meet ambient air quality standards. This technology is generally designated in the State Implementation Plan (SIP) so as to reduce emissions to achieve ambient standards. RACT considers both the cost and technology available for emission control. This control is usually less stringent than both BACT or LAER.

Best Available Control Technology is control technology applied to new and modified sources. Prevention of Significant Deterioration (PSD) is the review process for sources in attainment areas and is required for each pollutant subject to regulation under the Act. An attainment area is an air quality control region that meets the National Ambient Air Quality Standards.

New Source Performance Standards (NSPS) are set for a number of source categories. Best Available Control Technology must reduce emissions at least as much as the NSPS limit. New Source Performance Standards that have been promulgated are published first in the Federal Register and then in the U.S. Code of Federal Regulations. BACT applied to a source must be technologically feasible and must also reflect considerations of cost and energy usage. The BACT requirement is to be applied on a case-by-case basis review by EPA regional engineers.

Lowest Achievable Emission Rate refers to control technology applied to new and modified sources in a nonattainment area. A nonattainment area is an area or region where the National Ambient Air Quality Standards are being violated. LAER is the most stringent emission limitation which is contained in the SIP of any State or the most stringent emission limitation achieved in practice by that source category. LAER may be in some cases considered to be technology forcing, involving the transfer of technology from one source category to another. LAER is usually more stringent than BACT or RACT but must be at least as stringent as control specified by the NSPS.

The type of control equipment which can satisfy the requirements of RACT, BACT or LAER is generally specific to a given source category. For example, a particulate emission source may satisfy RACT requirements by applying a wet scrubber. BACT may require the application of an electrostatic precipitator. In another industry however, due to the explosive nature of the materials, wet scrubbers might be the only feasible type of collection equipment that can be used. BACT, in this case, might specify the use of a wet scrubber at a given pressure drop.

These control limitations clearly show that particulate air pollutants must be controlled from industrial sources. The stringency of control might also include other methods in addition to the traditional add-on control devices. This calls for the consideration and application of alternative production procedures, modifications of processes and control techniques that result in minimum emissions from a source.

This training manual is intended to be used in APTI Course 413, Control of Particulate Emissions. This document presents the fundamental concepts of the operation of particulate emission control equipment for stationary sources. The authors of this manual suggest that the reader turn to the many EPA publications from the Office of Air Quality Planning and Standards and the Industrial Environmental Research Laboratory for additional information concerning this subject. Many recent publications include NSPS and LAER control strategies that describe the latest technological advances in the field of particulate emission control.

Collection Forces

All particulate emission control devices collect particles by mechanisms involving an applied force, the simplest being *gravity*. Large particles moving slow enough in a gas stream can be overcome by gravity and be collected (Figure 1-1). Gravity is responsible for particle collection in the simplest devices such as settling chambers.

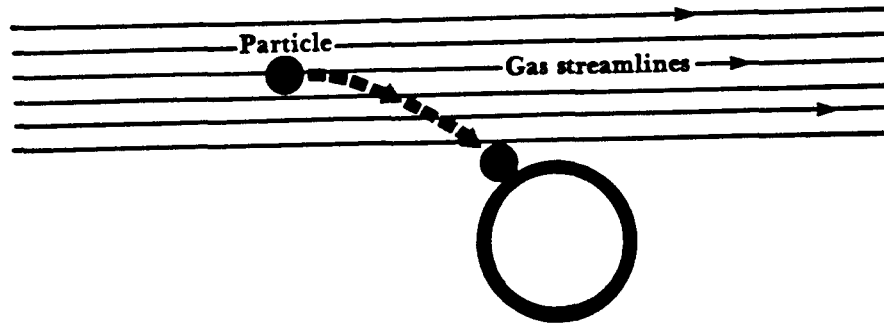


Figure 1-1. Gravity.

Centrifugal force is another collection mechanism used for particle capture. The shape or curvature of the collector causes the gas stream to rotate in a spiral motion. Larger particles move toward the outside of the wall by virtue of their momentum (Figure 1-2). The particles lose kinetic energy there and are separated from the gas stream. Particles then are overcome by gravitational force and are collected. Centrifugal and gravitational forces are both responsible for particle collection in a cyclone.

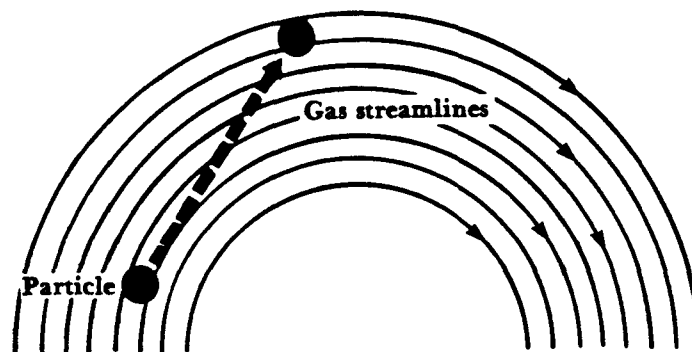


Figure 1-2. Centrifugal force.

In both fabric filters and wet collectors three separate forces are responsible for particle collection: impaction, direct interception, and diffusion. In a fabric filter, the target object for particle capture is a stationary fiber. In a wet collector, the target object is a water droplet that is introduced into the gas stream generally through a nozzle.

Consider the case of an individual fiber in a fabric filter. *Impaction* occurs when the particle is so large that it cannot follow the gas streamlines around the stationary fiber and impacts on the fiber (Figure 1-3). *Direct interception* is a special case of the impaction mechanism. The center of a particle may follow the streamlines formed around the fibers. A collision will occur if the distance between the particle center and the collection surface is less than the particle radius (Figure 1-4). Particles below $0.1\ \mu\text{m}$ in aerodynamic diameter undergo Brownian motion, randomly moving or diffusing throughout the gas volume. The mechanism of *diffusion* is responsible for the collection of particles which are so small that they become affected by collisions of molecules in the gas stream. The randomly moving particles then move or diffuse through the gas to impact on the fiber and are collected (Figure 1-5).

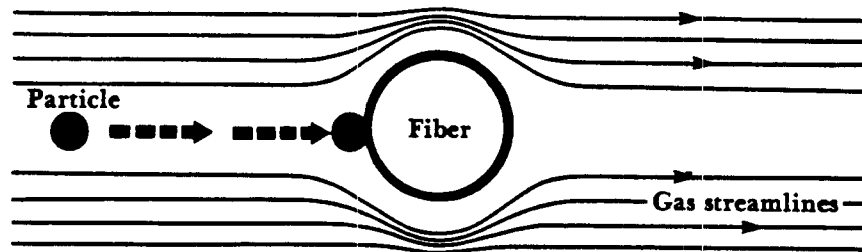


Figure 1-3. Impaction.

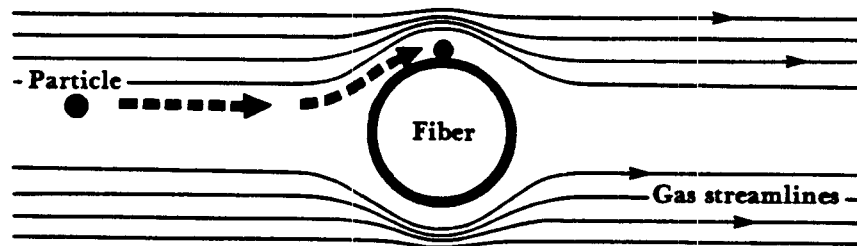


Figure 1-4. Direct interception.

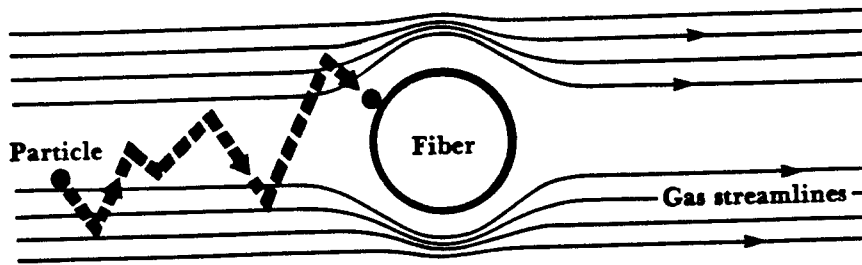


Figure 1-5. Diffusion.

The other primary particle collection mechanism involves electrostatic forces. The particles can be naturally charged, or, as in most cases involving *electrostatic attraction*, be charged by subjecting the particle to a strong electric field. The charged particles migrate to an oppositely charged collection surface (Figure 1-6). This is the collection mechanism responsible for particle capture in both electrostatic precipitators and charged droplet scrubbers. In an electrostatic precipitator, particle collection occurs due to electrostatic forces only. In a charged droplet scrubber, particle removal occurs by the combined effects of impaction, direct interception, diffusion and electrostatic attraction. Particles are charged in these scrubbers in order to enhance both diffusion and direct interception.

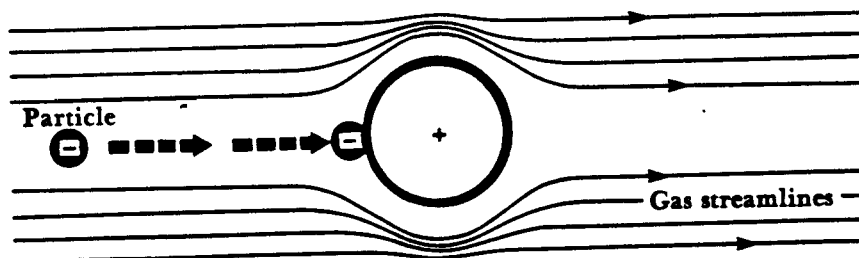


Figure 1-6. Electrostatic attraction.

Particle collection can occur from the combined effect of the mechanisms discussed. In addition, particles can agglomerate or grow in size by cooling, increasing humidity or from electrostatic effects. Agglomerated particles thus have a larger aerodynamic diameter and can be collected by impaction, interception or gravitational forces.

Factors Affecting Control Equipment Selection

Many factors influence the choice of a control device used to reduce industrial particulate emissions. The composition of the particles in terms of concentration, size, chemical and physical characteristics must be considered. If emitted material can be used in the process, dry collection should be used. If the pollutant has little

economic value, collection should be accomplished and the pollutant disposed of safely and economically. The industrial process and potential control devices must both be carefully reviewed. The conversion of an air pollution problem into a water pollution problem can create a more difficult disposal problem.

One selection factor to be considered is the **concentration** or grain loading of particulate pollutants in the process exhaust stream. Pollutant concentration is typically expressed in terms of pounds per cubic foot (lb/ft^3), grains per cubic foot (gr/ft^3), and grams per cubic meter (g/m^3). Both the level and fluctuation of grain loading are very important. Some control devices are not affected by high levels or great fluctuations in particle concentration such as in fabric filters. Others, such as electrostatic precipitators, do not function effectively with large fluctuating concentration levels. Another related problem can occur when the exhaust gas velocity changes rapidly. Some control devices are designated to operate at specific exhaust gas velocities; large changes can drastically affect the collection efficiency of the unit.

Particle characteristics such as **size, shape, and density** must also be considered. Particle size is usually expressed in terms of the aerodynamic diameter. The aerodynamic diameter describes how the particle moves in a gas stream. The larger particles ($> 60 \mu\text{m}$ aerodynamic diameter) can be collected in simple devices such as settling or baffle chambers. Particles greater than $10 \mu\text{m}$ can be collected in cyclones or multicyclones. Smaller particles ($< 5 \mu\text{m}$) must be collected in more sophisticated devices such as scrubbers, baghouses or electrostatic precipitators. Particle size thus plays a large role in the collection efficiency of a specific control device. Methods used to size particles and the effect of size on particle collection will be discussed in later chapters.

Chemical and physical properties of particulate emissions greatly affect the selection of control devices. Electrical properties of the particle can be both a hinderance and aid to collection. Static electricity can create solid buildup in both inertial and baghouse collectors. Cakes can form on the bag filters as a result of the static electric forces and can be difficult to dislodge. In an electrostatic precipitator, on the other hand, the collection of particulate matter depends on the ability of the precipitator to charge the particle. Particles passing through an electric field are charged and consequently migrate to an oppositely charged collection plate. Although there are many factors that govern the ease of charging the particles, the primary factor governing adequate particle collection is particle dust resistivity (a term that describes the resistance of the collected dust layer to the flow of electric current).

If the particles in the gas stream are explosive, electrostatic precipitators cannot be used. Fabric filters might be used, but only if no static electric effects exist in the baghouse. The logical choice of control would be a scrubber in which water is used as the scrubbing liquid. The water has a dampening effect on the explosive dust.

Hygroscopicity is the tendency of a material to absorb water. It is a physical characteristic of some particles which causes changes in the crystal structure as water is added. Some particles such as sodium sulfate can absorb up to 12 moles of

water per mole of anhydrous salt in high humidity conditions. Other particles from processes such as alfalfa dehydration and pelleting, and cotton ginning are hygroscopic to varying degrees. The hygroscopic nature of the particle affects the performance of mechanical collectors by causing dust deposits to build up on their internal surfaces. This may cause internal plugging or unpredictable dust cake discharges into collection hoppers at various times. Hygroscopic particles also affect the choice of cleaning in a baghouse by forming cakes on the bags that are difficult to remove.

Particle toxicity will influence the location of the control device and the air moving system (fan). Highly toxic materials require the use of a negative pressure system so that leaks will be contained within the collector. A positive pressure system could cause fugitive emissions creating an occupational health and safety problem. In a negative pressure system the fan is located downstream of the air pollution control device. The volume of gas to be handled may increase slightly by air leakage into the collector, but little or no contaminant leakage from the collector should occur.

The behavior of the carrier gas stream is also important in the design phases of air pollution control systems. Gas stream temperature affects a number of variables in the design stages of the control device. The size and thus the cost of the unit depends on the temperature of the exhaust gas stream being treated. The volume of gas to be cleaned would be larger at high temperatures than that at corresponding lower gas temperatures. Reducing the temperature reduces the volume of exhaust gas to be handled, however this could create some additional problems. The gas stream temperature must be maintained above the dew point of the gas to prevent water and acid from condensing in the collector. Water and acid mists could cause corrosion and complete deterioration of the structural material of the collector. High gas stream temperatures can also cause equipment failure to components of a fabric filtration system. At exhaust gas temperatures greater than 300°C most fabric materials deteriorate. Gas temperature can also affect conditions such as particle resistivity. By changing the temperatures of the exhaust stream in an electrostatic precipitator, one can also change the resistivity of the particles, and thus the collection efficiency of the unit.

Efficiency/Cost Trade-Offs

In air pollution work, the control equipment should be designed to meet emission limitations at minimum cost with maximum reliability. The basic trade-offs involve decisions between collection efficiency, pressure drop, installation cost, and operating costs. Of these, the principle one is the trade off between collection efficiency and pressure drop (which can be translated into power requirements) across the control device.

Collection efficiency (by weight) can be defined by the following formula:

$$\text{collection efficiency} = \frac{\text{inlet loading} - \text{outlet loading}}{\text{inlet loading}} \times 100\%$$

Emission limits are usually set by existing air pollution regulations. The control to be achieved is dependent on the allowed outlet concentration and the quantity of emissions generated from the process.

Equipment should be operated at the pressure drop specified by the design. *Pressure drop* describes the pressure loss between the inlet and outlet sections of the control device. Collectors with large pressure drops would require larger fans (and greater power requirements) to either push or pull the exhaust gas through the system. An increase in pressure drop means that there is a larger pressure loss in the system. Some control devices such as venturi scrubbers are designed to operate at high pressure drops (as great as 60 in. H_2O ; 14.9 kPa). On the other hand, electrostatic precipitators are designed to operate at much lower pressure drops (usually less than 10 in. H_2O ; 2.49 kPa) for similar collection efficiencies as venturi scrubbers. It may be advantageous however, to choose the scrubber as the control device in this case, especially if the dust to be collected is explosive.

Other conditions such as space limitations for installation may affect the ultimate decision for control equipment. Scrubbers generally require less installation space than either baghouses or electrostatic precipitators. There are, of course, water disposal problems with wet collectors that could sway the choice toward some other type of control. Installed cost and operating costs vary for each type of collector. For a given process, electrostatic precipitators may be more expensive to install than baghouses. However, baghouses may be more expensive to operate and maintain on an annual basis. The cost trade-offs must be examined carefully in making the final choice in control equipment..

This training manual discusses the operating principles, design specifications, parameters affecting efficiency, and examples of equipment used in selected applications. It is intended to assist in evaluating plans for particulate emission control systems and in conducting plan reviews.

Chapter 2

Basic Concepts of Gases

Expression of Gas Temperature

The Fahrenheit and Celsius Scales

The range on the Fahrenheit scale between freezing and boiling is 180 degree-units; on the Celsius or Centigrade scale, the range is 100 degree-units. Therefore, 1.0 Celsius degree-unit is equivalent to 1.8 Fahrenheit degree-units on a temperature scale (Figure 2-1). The following relationships convert one scale to the other:

(Eq. 2-1)

$$^{\circ}\text{F} = 1.8^{\circ}\text{C} + 32$$

(Eq. 2-2)

$$^{\circ}\text{C} = (^{\circ}\text{F} - 32)/1.8$$

Where: $^{\circ}\text{F}$ = degrees Fahrenheit
 $^{\circ}\text{C}$ = degrees Celsius or degrees Centigrade

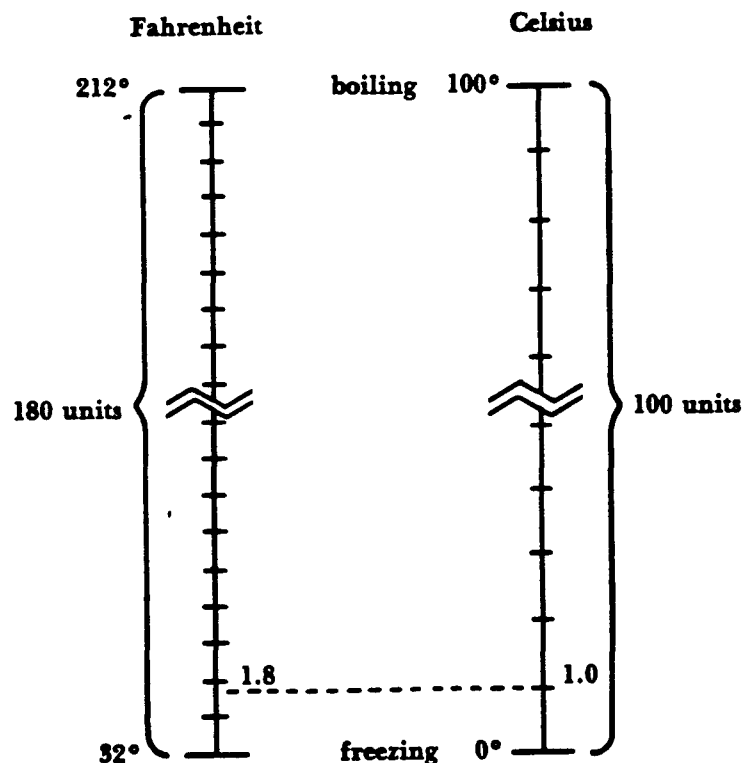


Figure 2-1. Comparison of degree-units between Fahrenheit and Celsius.

NOTE: SI units are listed in Appendix A.

Absolute Temperature

Experiments with perfect gases have shown that, under constant pressure, for each change in Fahrenheit degree below 32°F the volume of gas changes 1/491.67. Similarly, for each Celsius degree, the volume changes 1/273.16. Therefore, if this change in volume per temperature degree is constant, the volume of gas would, theoretically, become zero at 491.67 Fahrenheit degrees below 32°F or at -459.67°F. On the Celsius or Centigrade scale, this condition occurs at 273.16 Celsius degrees below 0°C, or at a temperature of -273.16°C.

Absolute temperatures determined by using Fahrenheit units are expressed as degrees Rankine (°R); those determined by using Celsius units are expressed as degrees Kelvin (K).^{*} The following relationships convert one scale to the other:

$$\text{(Eq. 2-3)} \quad {}^{\circ}\text{R} = {}^{\circ}\text{F} + 459.67$$

$$\text{(Eq. 2-4)} \quad \text{K} = {}^{\circ}\text{C} + 273.16$$

The symbol T will be used to denote absolute temperature.

Expression of Gas Pressure

Definition of Pressure

A body may be subjected to three kinds of stress: shear, compression, and tension. Fluids are unable to withstand tensile stress; hence, they are subject to shear and compression only. Unit compressive stress in a fluid is termed pressure and is expressed as force per unit area (e.g., lb/in.² or psi, Newtons/m² or Pa). Pressure is equal in all directions at a point within a volume of fluid, and acts perpendicular to a surface.

Barometric Pressure

Barometric pressure and atmospheric pressure are synonymous. These pressures are measured with a barometer and are usually expressed as inches, or millimeters, of mercury (Hg). Standard barometric pressure is the average atmospheric pressure at sea level, 45° north latitude at 35°F. It is equivalent to a pressure of 14.696 pounds force per square inch exerted at the base of a column of mercury 29.92 inches high. Weather and altitude are responsible for barometric pressure variations.

^{*}NOTE: Using the metric system the degree mark (°) is not used with the unit in the Kelvin system. Throughout this manual degrees Celsius will be °C, degrees Kelvin will be K.

Gage Pressure

Measurements of pressure by ordinary gages are indications of difference in pressure above, or below, that of the atmosphere surrounding the gage. Gage pressure, then, is ordinarily the pressure of the system. If greater than the pressure prevailing in the atmosphere, the gage pressure is expressed as a positive value; if smaller, the gage pressure is expressed as negative. The term *vacuum* designates a negative gage pressure.

The symbol p_g is used to specify a gage pressure. Also, psig means pounds force per square inch gage pressure.

Absolute Pressure

Most pressure measurements are taken with atmospheric (barometric) pressure as a reference. The gage pressure (either positive or negative) is the pressure relative to atmospheric pressure. The absolute pressure is the algebraic sum of the atmospheric pressure and the gage pressure and is given as:

$$(Eq. 2-5) \quad P = P_b + p_g$$

Where: P = absolute pressure
 P_b = barometric pressure
 p_g = gage pressure

The symbol P is used to indicate that the pressure is absolute. Also, psia means pounds per square inch absolute pressure.

The absolute pressure allows conversion of one pressure system to the other. Relationship of the pressure systems are shown graphically in Figure 2-2 using two typical gage pressures, (1) and (2). Gage pressure (1) is above the zero from which gage pressures are measured, and, hence, is expressed as a positive value; gage pressure (2) is below the gage pressure zero, and, therefore, is expressed as a negative value.

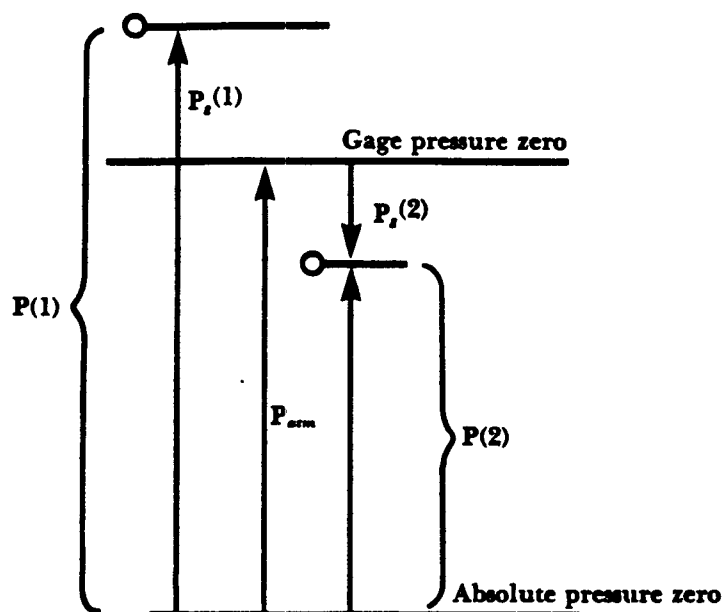


Figure 2-2. Two examples of absolute pressure determination.

Dalton's Law of Partial Pressure

Dalton's Law is used to determine the partial pressure of a gas compound in a gas mixture. The pressure exerted by a mixture of gases is equal to the sum of the partial pressures which each gas would exert if it alone occupied the whole volume. The pressure exerted by one component of a gas mixture is called partial pressure. The total pressure of the gas mixture is the sum of the partial pressures. Dalton's Law is given as:

(Eq. 2-6)
$$P_T = p_1 + p_2 + p_3$$

Where: P_T = total pressure of the gas mixture
 p = partial pressure of each individual gas component

Molecular Weight

The molecular weight of a compound or an element is simply the sum of all the atomic weights of all the atoms in the molecule. The atomic weight of an element is the average isotopic mass and can be generally assumed to be constant. The chemical identity of an atom is determined by the number of protons contained in the nucleus. The number of protons contained in the nucleus is also called the atomic number.

Examining the element sulfur from the Periodic Table of Elements, one can see the following:

16 Atomic number

S

32 Atomic weight

The atomic number specifies that the number of protons in the nucleus of the sulfur atom is 16. Sulfur has an atomic weight of 32 (amu) atomic mass units.

However, a molecule of oxygen, O_2 , is comprised of two atoms of oxygen. Since the atomic weight of oxygen is 16, one molecule of oxygen gas would have a molecular weight of 32 amu.

$O = O$

16 16

Molecular weight = 32 amu

Mole

The mole concept in chemistry is described as the amount of substance that numerically equals the molecular weight of that compound (usually expressed in grams). Thus, one mole or gram-mole of oxygen gas, O_2 , weighs 32 grams and one mole of water, H_2O , weighs 18 grams. The mole concept is used extensively in chemistry since it greatly simplifies calculations.

The Laws of Ideal Gases

The Laws of Boyle and Charles

Boyle's Law states that, when the temperature (T) is held constant, the volume (V) of a given mass of a perfect gas of a given composition varies inversely as the absolute pressure, i.e.,

$$V \propto \frac{1}{P} \text{ at constant } T$$

Where: \propto = proportional to

Charles' Law states that, when the volume is held constant, the absolute pressure of a given mass of a perfect gas of a given composition varies directly as the absolute temperature, i.e., $P \propto T$ at constant volume.

The Ideal Gas Law

Both Boyle's and Charles' Law are satisfied in the following equation:

$$(Eq. 2-7) \quad PV = \frac{mRT}{M}$$

Where: P = absolute pressure
 V = volume of a gas
 m = mass of gas
 M = molecular weight of a gas
 T = absolute temperature
 R = universal gas constant

The unit of R depends upon the units of measurement used in the equation. Some useful values are:

$$1544 \frac{(\text{lb})(\text{ft})}{(\text{lb mole})(^\circ\text{R})}$$

$$21.83 \frac{(\text{in. Hg})(\text{ft}^3)}{(\text{lb mole})(^\circ\text{R})}$$

$$554.6 \frac{(\text{mm Hg})(\text{ft}^3)}{(\text{lb mole})(^\circ\text{R})}$$

$$82.06 \frac{(\text{cm}^3)(\text{atm})}{(\text{g mole})(\text{K})}$$

Any value of R can be obtained by using the fact, with appropriate conversion factors, that there are 22.414 liters per g mole or 359 ft³ per lb mole at 32°F and 29.92 in. Hg.

Density

Density is defined as mass per unit volume, or:

$$(Eq. 2-8) \quad \rho = \frac{m}{V}$$

In the case of liquids and solids, the temperature at which density is measured is given in tables of physical data such as those in Perry's Chemical Engineer Handbook. Gas densities refer to the density of that particular gas at a given temperature and pressure.

A concept related to density is specific gravity, which is defined as the ratio:

(Eq. 2-9)
$$\frac{m/V}{m_w/V}$$

Where m is the true weight of the substance being measured, and m_w is the true weight of water, both in the same volume and at a specified temperature.

Density is related to specific gravity by the following relationship:

$$\text{Density} = \text{specific gravity} \times \text{density of water.}$$

As an example, the specific gravity of a calcium sulfate particle is 2.61. The density of the particle is:

$$\begin{aligned} \text{Density} &= 2.61 \times 62.4 \text{ lb/ft}^3 \\ &= 162.86 \text{ lb/ft}^3 \end{aligned}$$

Viscosity

Origin and Definition of Viscosity

Viscosity is the proportionality constant associated with a fluid resistance to flow. Viscosity is the result of two phenomena: (a) intermolecular cohesive forces, and (b) momentum transfer between flowing strata caused by molecular agitation perpendicular to the direction of motion. Between adjacent strata of a moving fluid, a shearing stress (τ) that is directly proportional to the velocity gradient occurs (Figure 2-3).

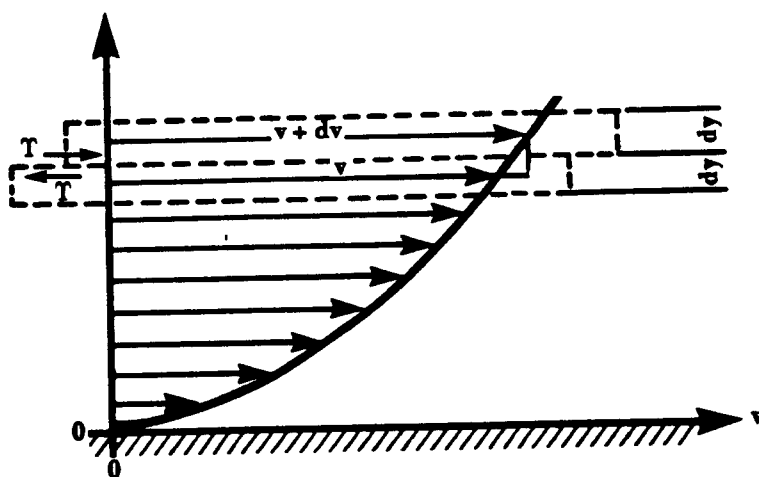


Figure 2-3. Shearing stress in a moving fluid.

This is expressed in the equation:

$$(Eq. 2-10) \quad \tau = \mu \frac{dv}{dy}$$

Where: τ = unit shearing stress between adjacent layers of fluid
 dv/dy = velocity gradient
 μ = proportionality constant (viscosity)

The proportionality constant, μ , is called the coefficient of viscosity, or merely, viscosity. It should be noted that the pressure does not appear in Equation 2-10 which indicates that the shear (τ) and the viscosity (μ) are independent of pressure. (Viscosity actually increases very slightly with pressure but this variation is negligible in most engineering problems.)

Kinematic Viscosity

The ratio of the absolute viscosity to the density of a fluid often appears in dimensionless numbers such as the Reynolds Number. The expression for kinematic viscosity is used to simplify calculations. Kinematic viscosity is defined according to the following relationship:

$$(Eq. 2-11) \quad \nu = \frac{\mu}{\rho}$$

Where: ν = kinematic viscosity, m^2/sec
 μ = viscosity of the gas, $Pa \cdot sec$
 ρ = density of the gas, kg/m^3

Liquid Viscosity

In a liquid, transfer of momentum between strata having a relative velocity is small compared to the cohesive forces between molecules. Hence, shear stress is predominantly the result of intermolecular cohesion. Because forces of cohesion decrease rapidly with an increase in temperature, the shear stress decreases with an increase in temperature. Equation 2-10 shows that shear stress is directly proportional to viscosity. Therefore, liquid viscosity decreases when the temperature increases.

Gas Viscosity

In a gas, the molecules are too far apart for intermolecular cohesion to be effective. Thus, shear stress is predominantly the result of an exchange of momentum between flowing strata caused by molecular activity. Because molecular activity increases as temperature increases, the shear stress increases with a rise in the temperature. Therefore, gas viscosity increases as the temperature rises.

Determination of Viscosity of Gases

The viscosity of a gas for prevailing conditions may be found accurately from the following formula:

$$\text{(Eq. 2-12)} \quad \frac{\mu}{\mu^{\circ}} = \left(\frac{T}{273.2} \right)^n$$

Where: μ = viscosity prevailing
 μ° = viscosity at 0°C and prevailing pressure
 T = absolute prevailing temperature (K)
 n = an empirical exponent ($n = 0.768$ for air)

The viscosity of air and other gases at various temperatures and at a pressure of 1 atmosphere may be found in engineering tables.

Units of Viscosity

The metric unit used to describe absolute viscosity is the Pascal second (Pa•sec). English units are obtained by multiplying the value of Pascal second by 0.672. English units for viscosity are lb_m/ft•sec.

Specific Heat

The specific heat of a gas is the amount of heat required to change the temperature of a unit-mass of gas one temperature-degree. Units of specific heat are, therefore, (Btu/lb•°F) or (joule/kg•K) depending upon the dimensional system used.

Heat may be added while the volume or pressure of the gas remains constant. Hence, there may be two values of specific heat: the specific heat at constant volume (C_v), and the specific heat at constant pressure (C_p). Because the heat energy added at constant pressure is used in raising the temperature and doing work against the pressure as expansion takes place, C_p is greater than C_v .

Reynolds Number

Definition

A typical inertial force per unit volume of fluid is qv^2/L ; a typical viscous force per unit volume of fluid is $\mu v/L^2$. The first expression divided by the second provides the dimensionless ratio known as **Reynolds Number**:

$$\text{(Eq. 2-13)} \quad Re = \frac{Lv\rho}{\mu}$$

Where: ρ = density of the fluid (mass/volume)
 v = velocity of the fluid
 L = linear dimension
 μ = viscosity of the fluid
 Re = Reynolds Number

The larger the Reynolds Number, the smaller is the effect of viscous forces; the smaller the Reynolds Number, the greater the effect of the viscous forces.

The linear dimension, L , is a length characteristic of the flow system. It is equal to four times the mean hydraulic radius, which is the cross-sectional area divided by the wetted perimeter. Thus for a circular pipe, L = diameter of the pipe; for a particle settling in a fluid medium, L = diameter of the particle; for a rectangular duct, L = twice the length times the width divided by the sum; and for an annulus such as a rotameter system, L = outer diameter minus the inner diameter.

Laminar and Turbulent Flow

In **laminar** flow, the fluid is constrained to motion in layers (or laminae) by the action of viscosity. The layers of fluid move in parallel paths that remain distinct from one another; any agitation is of a molecular nature only. Laminar flow occurs when the Reynolds Number for circular pipes is less than 2000 and less than 0.1 for particles settling in a fluid medium.

In **turbulent** flow, the fluid is not restricted to parallel paths but moves forward in a haphazard manner. Fully turbulent flow occurs when Reynolds Number is greater than 2500 for circular pipes and greater than 1000 for settling particles.

Chapter 3

Particle Dynamics

Collection of solid or liquid particles in an air pollution control device is based upon the movement of a particle in the gas (fluid) stream. In order to understand the mechanisms of particle capture, it is necessary to examine the basic concepts of particle behavior in a fluid. To be captured, the particle must be subjected to external forces large enough to separate the particle from the gas stream. In this chapter, we will examine the various forces acting on a particle and how they affect particle collection.

Forces Acting on a Particle

A force acting on a particle can be described by the general equation:

(Eq. 3-1)
$$F = m_p a_p$$

Where: F = the force on the particle ($\text{kg} \cdot \text{m}/\text{sec}^2$) or (N)
 m_p = mass of the particle (g)
 a_p = acceleration of the particle (m/sec^2)

A number of forces act on a particle moving in a fluid. Three major ones are the gravitational force, F_G , the buoyant force, F_B , and the drag force, F_D . Others are magnetic, inertial, electrostatic and thermal forces. All forces must be considered when evaluating the capture of a particle in an air pollution control device. This discussion of particle movement in a fluid will examine the gravitational, buoyant and drag forces. Electrostatic, inertial, and other forces will be discussed in more detail in later chapters.

Gravitational Force, F_G

All particles are subjected to gravity. The gravitational force, F_G , which causes particles and masses to fall to the earth can be expressed in the form of the general Equation 3-1. Assuming that there are no other forces acting on the particle F_G is given as:

(Eq. 3-2)
$$F_G = m_p g$$

Where: m_p = mass of the particle (kg)
 g = acceleration of the particle due to gravity ($980 \text{ cm}/\text{sec}^2$)

The mass of the particle is equal to the particle density (ρ_p) multiplied by the particle volume (V_p).

$$m_p = \rho_p V_p$$

The volume of a spherical particle is equal to:

$$V_p = \frac{4}{3} \pi r^3 = \frac{\pi d_p^3}{6}$$

Where: d_p = particle diameter (μm)

Equation 3-2, gravitational force, can then be written as:

$$\text{(Eq. 3-3)} \quad F_G = \frac{\rho_p \pi d_p^3 g}{6}$$

Where: ρ_p = density of the particle (g/cm^3)
 d_p = particle diameter (μm)
 g = acceleration of the particle due to gravity ($980 \text{ cm}/\text{sec}^2$)

Buoyant Force, F_b

Another force acting on a particle suspended in an air stream is the buoyant force, F_b . The buoyant force acting on a particle is equal to the weight of the displaced fluid. The concept of buoyant forces can be seen from the following example. Let's say we have two identical buckets, one containing water, the other containing air (Figure 3-1). A block of wood with identical size, shape, and density is placed in each bucket. The density of air is much less than the density of water. The buoyant force of the fluid (air) acting on the piece of wood in the bucket filled with air is not great enough to displace the weight of the object. However, the buoyant force of the fluid (water) in the second bucket is large enough to displace the object. The object thus rises and floats on the fluid.

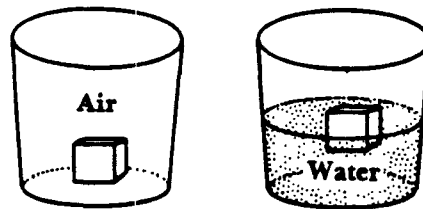


Figure 3-1. Identical objects in two different fluids.

Particles in a fluid have both a gravitational and buoyant force acting on them as shown in Figure 3-2.



Figure 3-2. Buoyant and gravitational forces acting on a particle.

The buoyant force can also be written from the general equation (Equation 3-1) of a force.

$$(Eq. 3-4) \quad F_B = m_a g$$

Where: m_a = mass of air or fluid displaced (g)
 g = acceleration of the particle due to gravity (980 cm/sec²)

F_B can also be written as:

$$(Eq. 3-5) \quad F_B = \rho_a V_a g = \rho_a \frac{\pi d_p^3}{6} g$$

Where: ρ_a = density of the (air) fluid (g/cm³)

Comparing Equations 3-3 and 3-5, one can see that these equations are very similar except that ρ_p and ρ_a represent the density of the particle and the density of the fluid, respectively. For air pollution applications, ρ_p is always much greater than ρ_a when air is the fluid in which the particle is suspended. Therefore, the term F_B can frequently be ignored.

Drag Force, F_D

Whenever there is particle motion in a gas stream, there will be a resisting force caused by the fluid (gas) molecules resisting the motion of the particle (Figure 3-3).

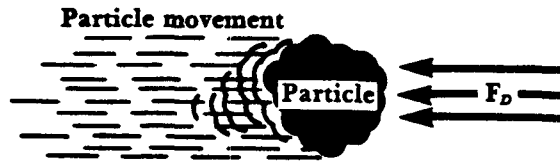


Figure 3-3. Drag force.

The resistive force caused by the fluid on the particle is called the drag force, F_D . The drag force is given by the expression:

$$\text{(Eq. 3-6)} \quad F_D = \frac{\pi d_p^2 \rho_a v_p^2 C_D}{8}$$

Where: C_D = drag coefficient (unitless)
 v_p = particle velocity (m/sec)
 d_p = particle diameter (μm)
 ρ_a = density of the (air) fluid (g/cm^3)

The drag force arises when a particle moves through a fluid. The particle cleaves or displaces the fluid immediately in front of it, imparting momentum to the fluid. The drag force produced is equal to the momentum (mv) per unit time imparted to the fluid by the particle. Since the moving particle has a velocity, v_p , a portion of the particle's velocity is transferred by momentum to the fluid as fluid velocity, v_a . The amount of energy imparted from v_p to v_a is related to a friction factor which is called the drag coefficient, C_D .

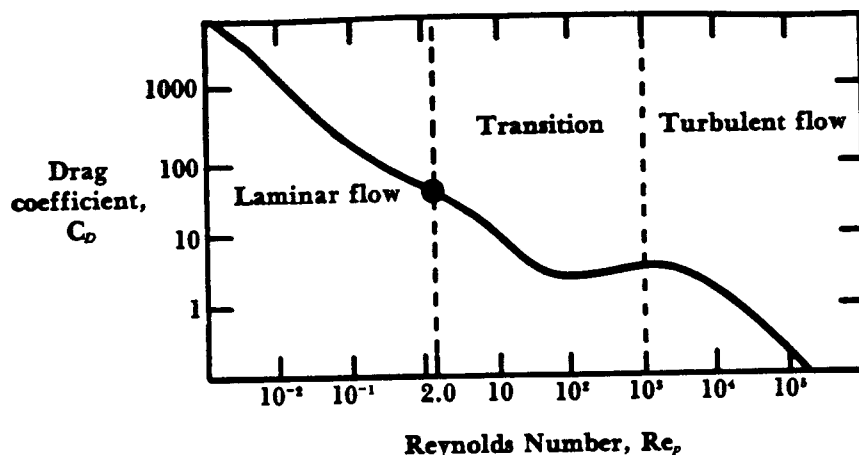
Drag Coefficient, C_D

The value of C_D is related to the velocity of the particle and the flow pattern of the fluid around the particle. The Reynolds Number, Re_p , of the particle is used as an indication of this flow pattern. The Reynolds Number of the particle is a function of the fluid density, particle diameter, particle velocity and fluid viscosity (and is dimensionless). The Reynolds Number (developed by Osborne Reynolds in 1883) is given as:

$$\text{(Eq. 3-7)} \quad Re_p = \frac{\rho_a v_p d_p}{\mu} \text{ (dimensionless)}$$

Where: ρ_a = density of the (air) fluid (g/cm^3)
 v_p = particle velocity (m/sec)
 d_p = particle diameter (μm)
 μ = air (fluid) viscosity ($\text{g}/\text{cm}\cdot\text{sec}$)

A mathematical expression describing C_D is very complex, if one could be written at all. Values of C_D can be estimated by using plots of C_D versus Reynolds Number constructed from experimental data. It is essential to determine C_D so that one can solve for F_D , the drag force, as in Equation 3-6. From experiment it has been observed that three particle flow regimes exist. The three regimes are laminar (or Stokes), transition and turbulent (sometimes called the Newtonian regime). These regimes are related to the Reynolds Number of the particle (Re_p). The relationship of C_D versus Re_p is shown in Figure 3-4.



Source: Chemical Engineer's Handbook, 1951.

Figure 3-4. Drag coefficient versus Reynolds Number for spheres.

For low values of the Reynolds Number ($Re_p < 2$) the flow is said to be laminar. Laminar flow is defined as flow in which the fluid moves in layers, one layer gliding smoothly over an adjacent layer with only a molecular interchange of momentum between layers. For much higher values of the Reynolds Number ($Re_p > 1,000$) the flow is turbulent. Turbulent flow has erratic motion of fluid, with a violent interchange of momentum throughout the fluid. For Reynolds Number values between 2 and 1,000, the flow pattern is said to be in the transition regime where the flow can be either laminar or turbulent.

Mathematical expressions relating the values of C_D and Re_p can be derived from Figure 3-4. Equations for determining C_D in each flow regime are:

$$(Eq. 3-8) \quad C_D = \frac{24}{Re_p} \text{ (dimensionless)} \quad \text{Laminar } (Re_p < 2.0)$$

$$(Eq. 3-9) \quad C_D = \frac{18.5}{Re_p^{0.6}} \text{ (dimensionless)} \quad \text{Transition } (2 < Re_p < 500)$$

(Eq. 3-10)

$$C_D = 0.44$$

Turbulent ($500 < Re_p < 2 \times 10^5$)

Cunningham Correction Factor, C_f

If the size of the particle is greater than $3 \mu\text{m}$ in diameter, the fluid appears *continuous* around the particle. What we mean by the description *continuous* is that the particle is not affected by collisions with individual air molecules. Collisions occur frequently on all sides of the particle (Figure 3-5).

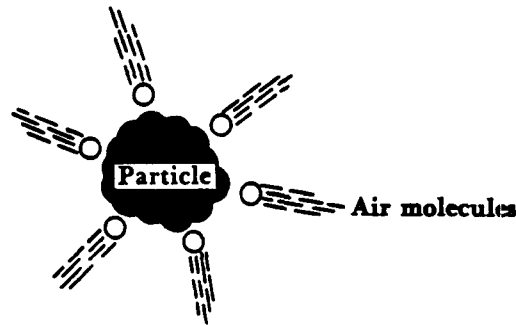


Figure 3-5. Collisions of air molecules on particles greater than $3 \mu\text{m}$ in diameter.

However, if the particles are smaller than $3.0 \mu\text{m}$ in diameter, the fluid appears *discontinuous*. This occurs for particles in the laminar flow regime. In this case, the particles are affected by collisions of air molecules. These collisions will cause the particle to move in a direction related to the combined forces acting on the particle. The particle is said to be *slipping* between the fluid molecules (Figure 3-6). To correct for this, Cunningham deduced that the drag coefficient should be reduced. Thus the drag coefficient equation includes a term called the Cunningham slip correction factor, C_f . In the laminar flow regime Equation 3-8 is corrected to include C_f . The drag coefficient for the laminar regime thus becomes:

(Eq. 3-11)

$$C_D = \frac{24}{Re_p C_f}$$

Where: C_f = Cunningham correction factor (dimensionless)

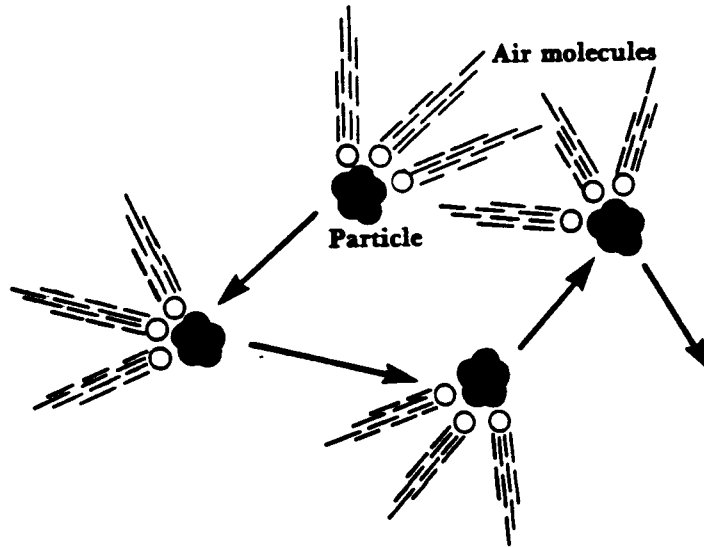


Figure 3-6. Collisions of air molecules on particles less than 3 μm in diameter.

The Cunningham correction factor can be estimated by:

(Eq. 3-12)
$$C_r = 1 + \frac{(6.21 \times 10^{-4})(T)}{d_p}$$

Where: T = absolute temperature (degrees Kelvin)
 d_p = particle diameter (μm)

A compilation of values of C_r at various temperatures is provided in Table 3-1.

Table 3-1. Values of C_r (for air at atmospheric pressure).

Particle diameter (micrometers)	Value of C_r at temperature of:		
	70°F	212°F	500°F
0.1	2.88	3.61	5.14
0.25	1.682	1.952	2.528
0.5	1.325	1.446	1.711
1.0	1.160	1.217	1.338
2.5	1.064	1.087	1.133
5.0	1.032	1.043	1.067
10.0	1.016	1.022	1.033

Source: Lapple, 1951.

Calculation of F_D

The drag force can be calculated by substituting the proper C_D expression into Equation 3-6. The equations for calculating F_D in all three flow regimes are:

(Eq. 3-13)	$F_D = \frac{3\pi\mu v_p d_p}{C_f}$	Laminar (Stokes)
------------	-------------------------------------	------------------

(Eq. 3-14)	$F_D = 2.31\pi(d_p v_p)^{1.4} \mu^{0.6} \rho^{0.4}$	Transition
------------	---	------------

(Eq. 3-15)	$F_D = 0.055\pi(d_p v_p)^2 \rho$	Turbulent
------------	----------------------------------	-----------

The streamline (laminar) flow of a fluid around a sphere (particle) was investigated by G. Stokes in 1845 for small values of the Reynolds Number. Stokes found that the drag force of the fluid around a particle is a function of the gas viscosity, particle velocity, and particle diameter and is given by Equation 3-13. This is known as **Stokes law** and is valid for Reynolds Numbers less than 2.0. Stokes law is important in determining the settling velocity of a particle and is used in the design of settling chambers for particulate emission control.

Balance of Forces on a Particle

Newton's second law of motion states that the acceleration produced in a given mass by the action of a given force is proportional to the force and in the direction of that force. The second law is simply a statement of the equation $F = ma$. The sum of the forces can be written as:

$$\sum F = ma = m \frac{dv}{dt}$$

Where: dv/dt = acceleration or change in velocity with respect to time

A particle in motion in a fluid will be affected by a number of forces (Figure 3-7).

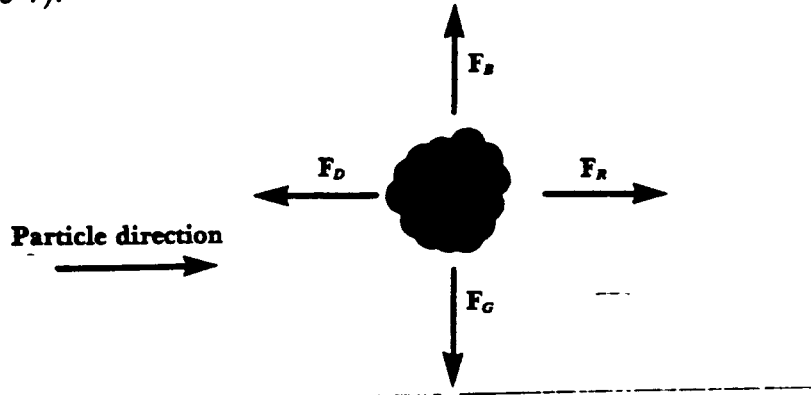


Figure 3-7. Vector sum of forces acting on a particle.

The vector sum of the forces is equal to a resultant force, F_R .

$$F_R = F_G - F_B - F_D = m \frac{dv}{dt}$$

As previously stated, the density of the particle is much greater than the density of air and the term F_B can be ignored. As the particle accelerates the velocity will increase. The drag force on the particle also increases with increasing velocity. At some point there will be a value of velocity where F_D will be as large as the other forces. At this point the resultant force will be zero, and the particle will no longer accelerate. If the particle is not accelerating, then it must be at a constant velocity. This constant velocity, where all the forces balance out, is called the terminal settling velocity.

$$F_R = F_G - F_B - F_D = 0 \quad \text{at terminal settling velocity}$$

then:

$$F_G = F_D$$

Derivation of Particle Settling Velocity Equations

The particle settling velocity equation is derived by setting F_G equal to F_D . Substitute the values for F_G and F_D from Equations 3-3 and 3-13 respectively.

$$\text{(Eq. 3-3)} \quad F_G = \frac{\rho_p \pi d_p^3 g}{6}$$

$$\text{(Eq. 3-13)} \quad F_D = \frac{3 \pi d_p v_p \mu}{C_f}$$

$$\frac{\rho_p \pi d_p^3 g}{6} = \frac{3 \pi d_p v_p \mu}{C_f}$$

Solving for v_p (which is now v_t):

$$(Eq. 3-16) \quad v_t = \frac{g Q_p d_p^2}{18 \mu} C_f \text{ (m/sec)} \quad \text{Laminar Regime}$$

Similar derivations for the settling velocity for the other regimes are:

$$(Eq. 3-17) \quad v_t = \frac{0.153 g^{0.71} d_p^{1.14} Q_p^{0.71}}{\mu^{0.43} Q_a^{0.29}} \text{ (m/sec)} \quad \text{Transition Regime}$$

$$(Eq. 3-18) \quad v_t = 1.74 \left(\frac{g d_p Q_p}{Q_a} \right)^{0.5} \text{ (m/sec)} \quad \text{Turbulent Regime}$$

Determination of the Flow Regime

To solve for an unknown particle settling velocity, the flow regime of particle motion must be determined. This is done to select the correct settling velocity equation. In other words, the Re_p and consequent flow regime cannot be determined because the velocity is unknown. The flow regime can be determined by the following equation:

$$(Eq. 3-19) \quad K = d_p \left(\frac{g Q_p Q_a}{\mu^2} \right)^{0.33} \text{ (dimensionless)}$$

Values of K correspond to the different flow regime as can be seen from Table 3-2.

Table 3-2. K values for flow regime determination.

Laminar regime	$K < 3.3$
Transition regime	$3.3 < K < 43.6$
Turbulent regime	$K > 43.6$

Once the flow regime has been determined, the correct formula can be used to calculate the settling velocity of the particle.

Example Problem

Calculate the settling velocity of a particle moving in a gas stream. Assume the following information:

$$\begin{aligned} \rho_p &= 0.899 \text{ g/cm}^3 \\ \rho_s &= 0.012 \text{ g/cm}^3 \\ \mu_{(AIR)} &= 1.82 \times 10^{-4} \text{ g/cm} \cdot \text{sec} \\ g &= 980 \text{ cm/sec}^2 \\ d_p &= 45 \text{ } \mu\text{m} \\ C_f &= 1.0 \text{ (if applicable)} \end{aligned}$$

Solution:

1. Calculate the K parameter to determine the proper flow regime. Use Equation 3-19.

$$\begin{aligned} K &= d_p [g \rho_p \rho_s / \mu^2]^{1/3} \\ &= 45 \times 10^{-4} \text{ cm} \left[\frac{\left(980 \frac{\text{cm}}{\text{sec}^2}\right) \left(0.899 \frac{\text{g}}{\text{cm}^3}\right) \left(0.012 \frac{\text{g}}{\text{cm}^3}\right)}{\left(1.82 \times 10^{-4} \frac{\text{g}}{\text{cm} \cdot \text{sec}}\right)^2} \right]^{1/3} \\ &= 3.07 \end{aligned}$$

Therefore, the flow regime is laminar.

2. The settling velocity is calculated using Equation 3-16.

$$\begin{aligned} v_t &= \frac{g \rho_p d_p^2}{18 \mu} C_f \\ &= \frac{\left(980 \frac{\text{cm}}{\text{sec}^2}\right) \left(0.899 \frac{\text{g}}{\text{cm}^3}\right) (45 \times 10^{-4} \text{ cm})^2}{18 \left(1.82 \times 10^{-4} \frac{\text{g}}{\text{cm} \cdot \text{sec}}\right)} (1.0) \\ &= 5.38 \text{ cm/sec} \end{aligned}$$

References

1. *Notes and Personal Communication* with Donald A. Deieso, Rutgers University,, 1980.
2. *Notes and Personal Communication* with Cliff I. Davidson, Carnegie Mellon University, 1979.
3. Lapple, C. E. 1951. *Fluid and Particle Mechanics*. Newark, Delaware: University of Delaware.
4. Theodore, L. and Buonicore, A. J. 1976. *Industrial Air Pollution Control Equipment*. Cleveland: CRC Press, Inc.
5. Cheremisinoff, P. N. and Young, R. A., eds. 1977. *Air Pollution Control and Design Handbook, Part 1*. New York: Marcel Dekker, Inc.
6. Streeter, V. and Wylie, E. B. 1975. *Fluid Mechanics*. 6th ed. New York: McGraw-Hill Book Company.
7. Perry, J. H., ed. 1950. *Chemical Engineer's Handbook*. 3rd ed. New York: McGraw-Hill Book Company.

Chapter 4

Particle Sizing

Introduction

With the high cost of particulate control equipment and more stringent regulations, particle sizing data has become an increasingly important consideration in the design of particulate control equipment. Appropriate design is directly dependent on good particle size data.

Several methods are used to obtain particle size data from industrial sources. This section will briefly describe a number of these methods and their operating principles. The mathematical treatment of collected data will also be presented.

Size

Particle size is usually expressed by some diameter that is measured. A particle diameter, however, is dependent on the measurement method by which it is determined. Diameters can be based on projected area, surface area, volume, mass, etc.

Particle size is uniquely defined by particle diameter only for the case of spherical particles. Unfortunately, except for liquid droplets, certain metallurgical fumes, and combustion emissions, particles are usually not spherical. To deal with nonspherical particles it becomes necessary to define an *equivalent diameter* term that depends upon the various geometrical or physical properties of the particles. Some of the methods used to express the size of a nonspherical particle measured by microscopy are illustrated in Figure 4-1.

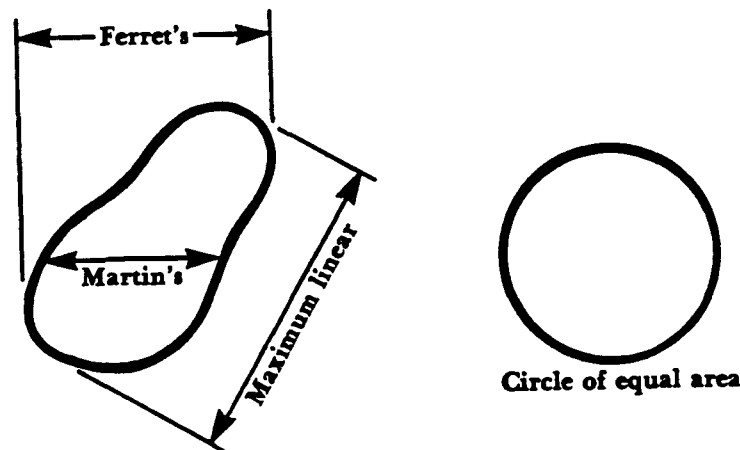


Figure 4-1. Diameters of nonspherical particles.

Ferret's diameter is the mean length between two tangents on opposite sides of the particle perpendicular to the fixed direction of the microscope scan. Martin's diameter measures the diameter of the particle parallel to the microscope scan that divides the particle into two equal areas. The diameter of a circle of equal area is obtained by estimating the projected area of the particle and comparing it with a sphere that approximates its size.

In terms of particulate control equipment, interest is centered primarily on the aerodynamic behavior of the particle. The aerodynamic diameter is defined as the diameter of a sphere of unit density having the same falling speed in air as the particle (Figure 4-2). The aerodynamic diameter is a function of the physical size, shape, and density of the particle. The aerodynamic diameter is useful when designing certain control devices and is usually measured by a device called an impactor.

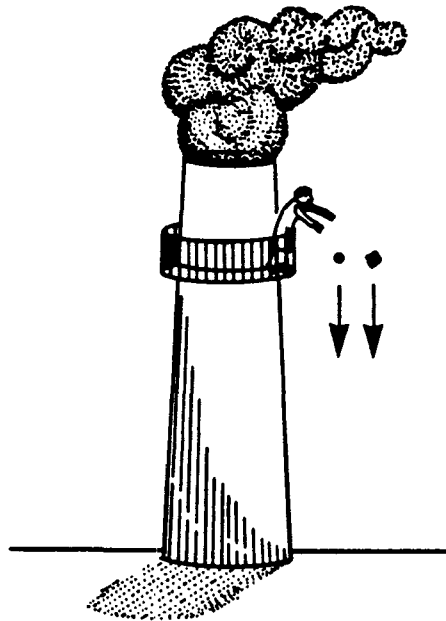


Figure 4-2. Aerodynamic diameter.

Various Sizing Devices

If one were able to design an ideal particle measuring device, the device would have the following features.

It would be able to:

1. measure the exact size of each particle.
2. report data instantaneously without averaging data over some specified time interval.
3. determine the complete composition of each particle including shape, density, chemical nature, etc.

It would be an extremely difficult task to produce such an instrument. At this time there are devices which incorporate only one or two of these ideal functions. Various sizing techniques will be examined and will be compared to such an ideal device, listing advantages and disadvantages of each. While this discussion is not intended to be exhaustive, the more commonly employed methods will be reviewed.

Microscopy

The microscope is one common instrument used in particle size analysis (Figure 4-3). The microscope measures the geometric diameter of each individual particle. The determination of particle size analysis is carried out by measuring the size of a number of particles. Particles are sized as they are traversed past the eyepiece micrometer. Each particle, presented in a fixed area of the eyepiece, is sized and tallied into a number of size classes. The number of particles sized may range from 100 to several thousand depending on the accuracy desired. This method can be time consuming and extremely tedious.

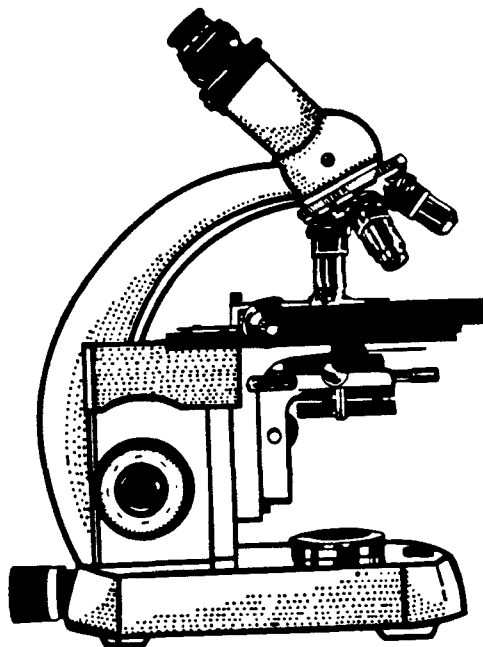


Figure 4-3. Microscope.

The particles can be collected by deposition on a glass slide or on a filter by using an EPA Method 5 sampling train. The glass slide or filter would subsequently be analyzed by a microscope in the lab. The analysis of size distribution of particles collected in the field and transported to the lab must be viewed with great caution. It is difficult to collect a representative sample in the first place, and it is almost impossible to maintain the original size distribution under laboratory conditions. For example, laboratory measurements cannot determine whether some of the par-

ticles existed in the process stream as agglomerates of smaller particles. In spite of the limitations of the microscopic method, this method is useful in the determination of some properties of interest.

Generally speaking, the chemical composition of the particle cannot be obtained by using an optical microscope. However, a subsequent chemical analysis can be performed on the sample. The electron microscope, on the other hand, can give a detailed chemical analysis of the particle. The electron microscope is used in conjunction with an x-ray diffraction attachment to determine the molecular weight of the particle. Particles with molecular weights greater than carbon can be determined by the amount of radiation diffracted by each particle analyzed.

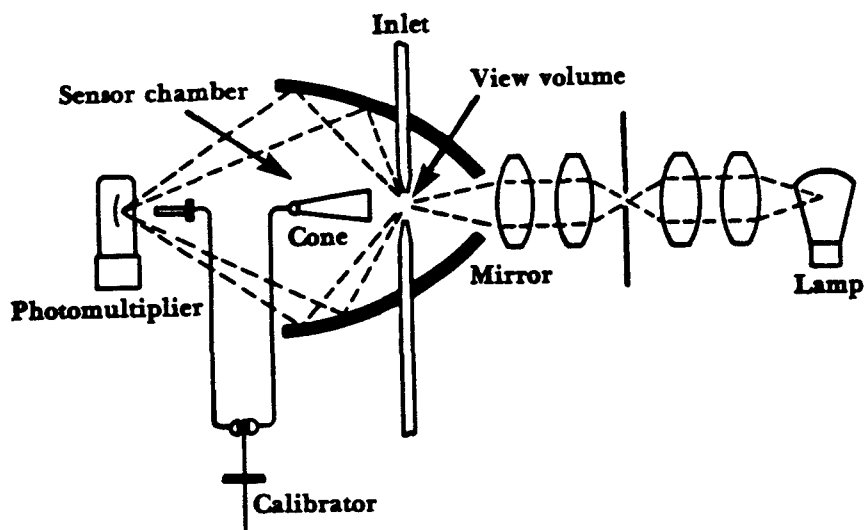
The optical microscope can measure particles from about $0.5\text{ }\mu\text{m}$ to about $100\text{ }\mu\text{m}$ in diameter. Electron microscopes can measure particles with diameters as small as $0.001\text{ }\mu\text{m}$. This could be useful for examining extremely minute particles (see Table 4-1).

Optical Counters

Optical particle counters have not been widely used for particle sizing because they cannot be directly applied to the stack exhaust gas stream. The sample must be extracted, cooled, and diluted before entering the counter. This procedure must be done with extreme care to avoid introducing serious errors in the sample. The major advantage of the counter is its capability of observing emission (particle) fluctuations on an instantaneous level. One can size particles as small as $0.3\text{ }\mu\text{m}$ with the optical counter (Table 4-1).

Optical particle counters work on the principle of light scattering. Each particle in a continuously flowing sample stream is passed through a small illuminated viewing chamber. Light scattered by the particle is sensed by the photodetector during the time the particle is in the viewing chamber (Figure 4-4). The intensity of the scattered light is a function of particle size, shape and index of refraction. Optical counters will give reliable particle size information if only one particle is in the viewing chamber at a single time. The simultaneous presence of more than one particle can be interpreted by the photodetector as a larger sized particle. This error can be avoided by maintaining sample dilution less than 300 particles per cubic centimeter.

A disadvantage of the optical counter is the dependence of calibration instrument upon the index of refraction and shape of the particle. Errors in counting can also occur from the presence of high concentrations of very small particles which are sensitive to the light wavelength used.



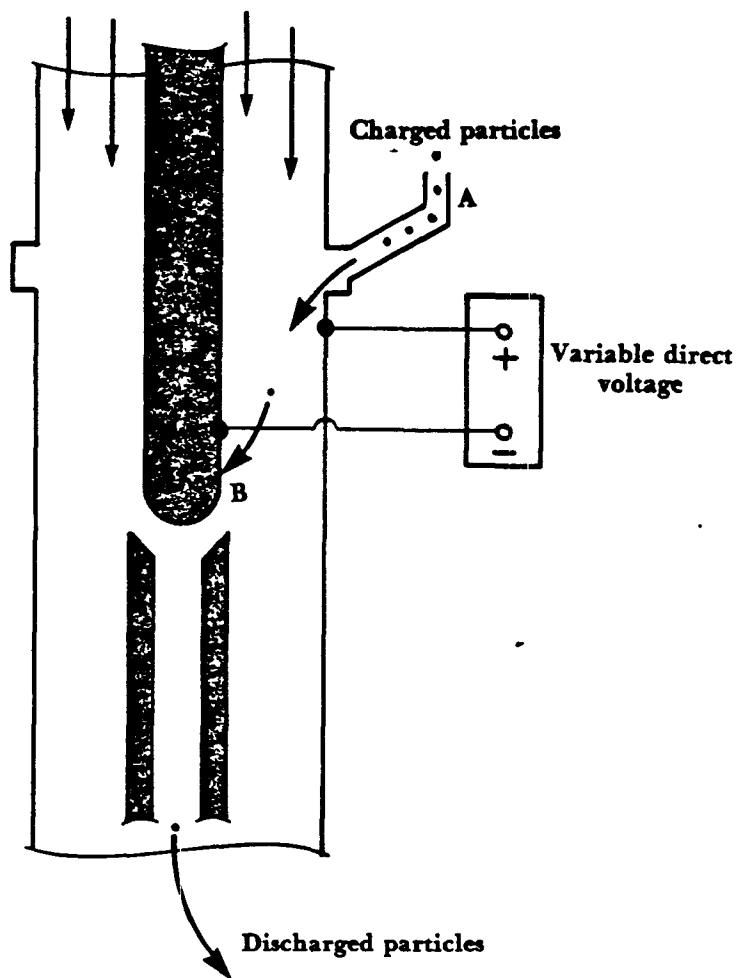
Source: EPA, 1979. EPA/4-79-028.

Figure 4-4. Operating principle for an optical particle counter.

Electrical Aerosol Analyzer

The electrical aerosol analyzer (EAA) is an aerosol size distribution measuring device that was commercially developed at the University of Minnesota. The EAA uses an electric field (which is set at an intensity dependent upon the size and mass of the particle) to measure the mobility of a charged aerosol. The analyzer operates by first placing a unipolar charge on the aerosol being measured, and measuring the resulting mobility distribution of the charged particles by means of a mobility analyzer.

Charged particles enter through a narrow passage (A) and experience a radial force toward the central cylinder due to the applied field. By moving the sampling groove (B), axially, or by varying the applied field, the mobility of the charged particles can be measured. One type of EAA is shown in Figure 4-5 (Hewitt, 1957).



Source: EPA, June 1977. EPA 600/7-77-059.

Figure 4-5. Coaxial cylinder mobility analyzer.

The EAA has been used for source analysis by pulling a sample from the stack into the chamber and introducing the gas stream into the analyzer. The instrument requires that enough particles pass through the chamber so that a charge can be detected. The concentration range for most efficient operation of the EAA is from 1 to 1000 $\mu\text{g}/\text{m}^3$. Since stack gas concentrations usually exceed 1000 $\mu\text{g}/\text{m}^3$, sample dilution with clean air is required (EPA, 1979, EPA 600/7-79-028). No information on the chemical composition of the particles is possible since the particles are not collected. The major advantage of the EAA is that the instrument can measure particles from 0.003 to 1.0 μm in diameter.

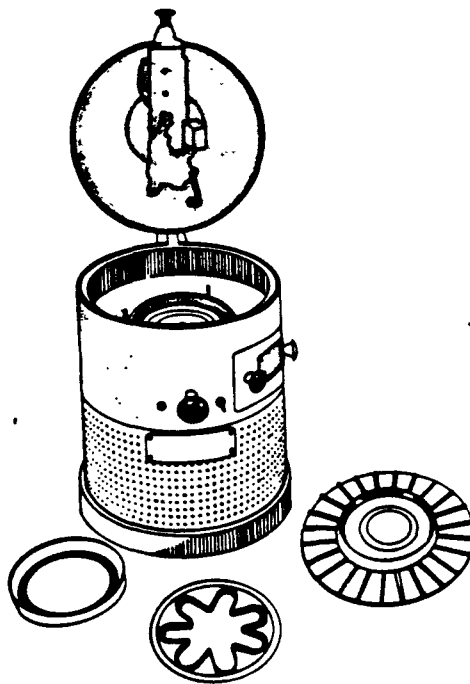
Bahco Microparticle Classifier

The Bahco (Figure 4-6) is a versatile particle classifier used for measuring powders, dust, and other finely divided solid materials. The Bahco's working range is approximately 1 to 60 μm (Table 4-1). Developed in the 1950s, the Bahco has lost some of its initial appeal to more recently developed techniques.

The Bahco uses a combination of elutriation and centrifugation to separate particles in an air stream. Particles can be collected onto a filter by using an EPA Method 5 sampling train. The collected particles are subsequently analyzed in the lab (Figure 4-6).

A weighed sample, usually 5 grams, is introduced into a spiral-shaped air current to separate the particle fractions. The larger particles overcome the viscous forces of the fluid and migrate to the wall of the chamber, while the smaller particles remain suspended. After the two size fractions are separated, one of them is reintroduced into the device and is fractionated further. A different spin speed is used to give a slightly different centrifugal force. This is repeated as many times as desired to give an adequate size distribution. The measurements are grouped into discrete size ranges (i.e., 40-60 μm , 20-40 μm , etc.).

The Bahco provides information on the aerodynamic size of particles. This data can be translated into settling velocity information useful in the design of emission control devices. Several hours are required to complete the fractionation analysis. Once the particles have been fractionated into the discrete ranges, a chemical analysis can be done on the collected particles.



Source: Stockman and Fochtman, 1977.

Figure 4-6. Bahco sampler.

Some of the major drawbacks of the Bahco are that:

- the working range is limited between 1 and 60 μm ;
- care must be exercised when measuring certain types of particles especially those which are friable, or hygroscopic;
- the sample may not be representative due to particle agglomeration either in the stack or during the transfer of the collected sample to the lab;
- the length of time required for analysis is several hours or more; and
- the size grading regimes are not as sharp as with newer devices.

Impactors

Inertial impactors are commonly used to determine the particle size distribution of exhaust streams from industrial sources. Inertial impactors measure the aerodynamic diameter of the particles. The inertial impactor can be directly attached to an EPA Method 5 sampling train and easily inserted into the stack of an industrial source.

The mechanism by which an impactor operates is illustrated in Figure 4-7. The impactor is constructed using a succession of stages each containing orifice openings with an impaction slide or collection plate behind the openings. In each stage, the gas stream passes through the orifice opening and forms a jet which is directed towards the impaction plate. The larger particles will impact on the plate if their momentum is large enough to overcome the drag of the air stream as it moves around the plate. Since each successive orifice opening is smaller than those on the preceeding stage, the velocity of the air stream, and therefore that of the dispersed particles, is increased as the gas stream advances through the impactor. Consequently, smaller particles eventually acquire enough momentum to break away from the gas streamlines to impact on a plate. A complete particle size classification of the gas stream is therefore achieved.

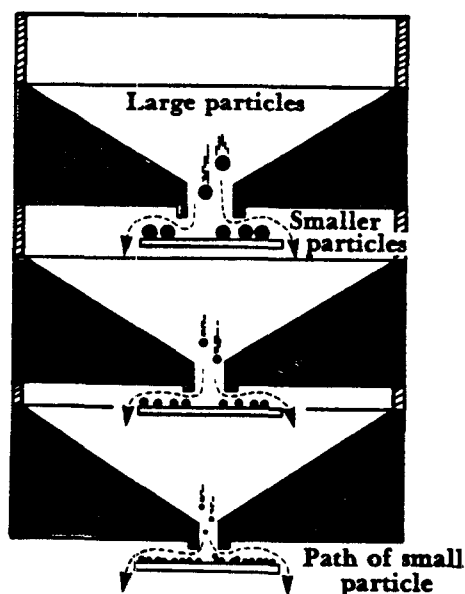


Figure 4-7. Schematic diagram, operation of an inertial impactor.

Typical impactors consist of a series of stacked stages and collection surfaces. Depending on the calibration requirements, each stage contains from one to as many as 400 precisely drilled jet orifices, identical in diameter in each stage but decreasing in diameter in each succeeding stage (Figure 4-8). Adhesive, electrostatic, and van der Waals forces hold the particles to each other and to the collection surfaces. Moreover, the particles are not blown off the collecting plate by the jets of air because these jets follow laminar flow paths so that no turbulent areas exist. This results in complete dead air spaces over and around the samples.

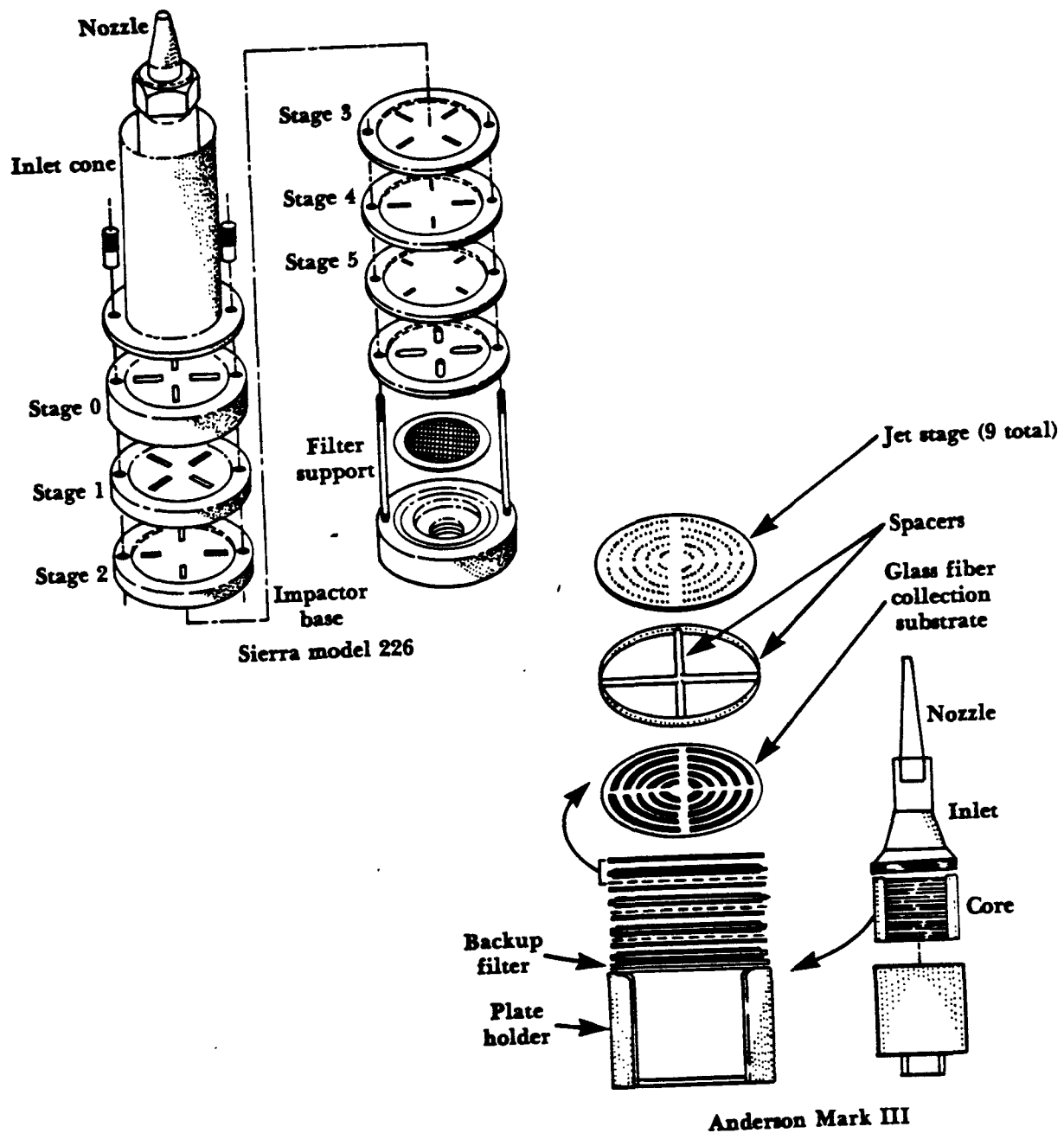


Figure 4-8. Schematics of two commercial cascade impactors.

Particles are collected on preweighed individual stages, usually filters made of glass fiber or thin metal foil. Once the sample is complete, the collection filters are weighed again, yielding particle size distribution data for the various collection stages. Occasionally there are some dusts that are very difficult to collect, and require grease on the collection filter for adequate particle capture. Once the particles have been fractionated into discrete ranges, a chemical analysis can be performed on the collected particles.

The effective range for measuring the aerodynamic diameter is generally between 0.3 and 20 μm (Table 4-1). Some vendors have claimed size fractionation as small as 0.02 μm with the use of 20 or more stages. Impactors are one of the most useful devices for determining particle size. This is because of the impactor's compact arrangement, mechanical stability, and its ability to draw a sample directly from a stack. In addition, the impactor measures the aerodynamic diameter of particles, which describes the movement of the particles in a gas stream. Particle movement information is extremely useful in designing air pollution control equipment, especially mechanical collectors which depend on aerodynamic drag forces for particle collection.

Comparison of Particle Sizing Devices

Five particle sizing instruments have been briefly described in the previous sections. These are by no means the only ones available; there are others such as the condensation nuclei counter and the diffusion battery, cyclones placed in series, laser backscattering instruments, and multiwavelength transmissometers (EPA, 1979, EPA-600/7-79-028).

Comparisons have been made among the various devices mentioned by listing several advantages/disadvantages of each.* As previously stated, the ideal instrument would measure the exact size of each particle, yield instantaneous response, and determine the complete composition of the particle. Table 4-1 shows the effectiveness of each device over different particle size ranges. Table 4-2 shows the major features of each device.

From Table 4-2 one can compare the major features of the various measuring devices. One can see that the single particle level symbol (\triangleleft) describes how the device measures each individual particle from the sample. The discrete ranges symbol (\trianglelefteq) is used to describe the devices that classify the particles into discrete ranges such as 5-10 μm , 10-15 μm , 15-20 μm , etc. The integrated averaging process symbol (\int) is used to describe the time period (averaged) in which the device measures size and chemical composition of the particle.

*EPA Guidelines for Particulate Sampling in Gaseous Effluents from Industrial Processes. EPA-600/7-79-028, IERL, RTP, NC 27711, January 1979.

Table 4-1. Size range capabilities of measuring devices.

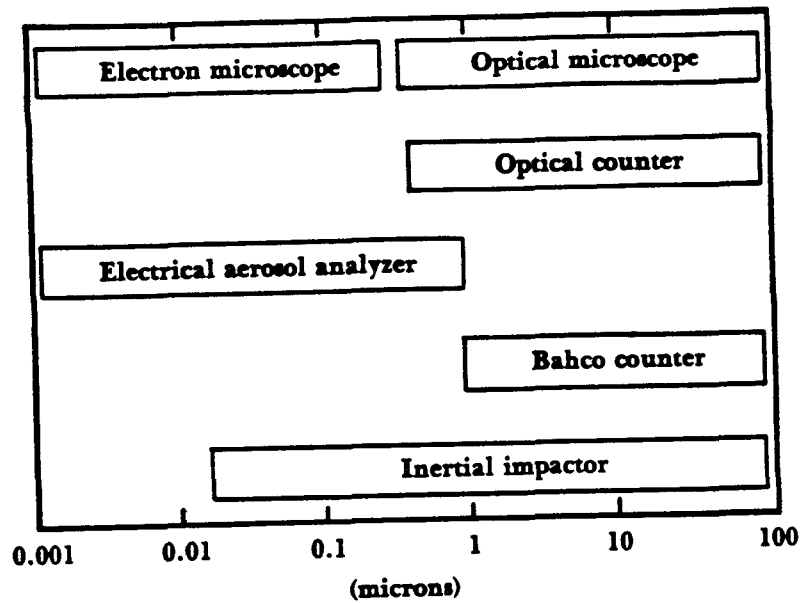


Table 4-2. Comparison of particle sizing devices.

Device	Size	Time	Composition
Ideal			
Microscope			
Optical counter			
EEA			
Bahco counter			
Impactor			

- Single particle level
 Discrete ranges
 Integrated averaging process

Mathematical Treatment of Data

There are various ways to analyze or reduce the data generated from a particle sizing device. The most common methods of expressing particle size data are through the use of frequency distribution curves (histograms) or cumulative distribution curves. The cumulative plot is a cumulative distribution curve. All forms of graphical presentation employ one axis to represent particle size and the other axis to represent particle amount. The particle amount can be expressed by either the mass of particles or the number of particles.

Frequency Distribution Curve

Frequency distribution curves are usually plotted on regular coordinate (linear) paper. The curve describes the amount of material (particles) falling within each size range. When gas borne particles produced in industrial operations are measured, the data has a tendency to show a preferential particle size. A plot of percent mass versus particle size (d_p) on a linear scale gives a curve with a peak at the preferential size. Such a curve is shown in Figure 4-9.

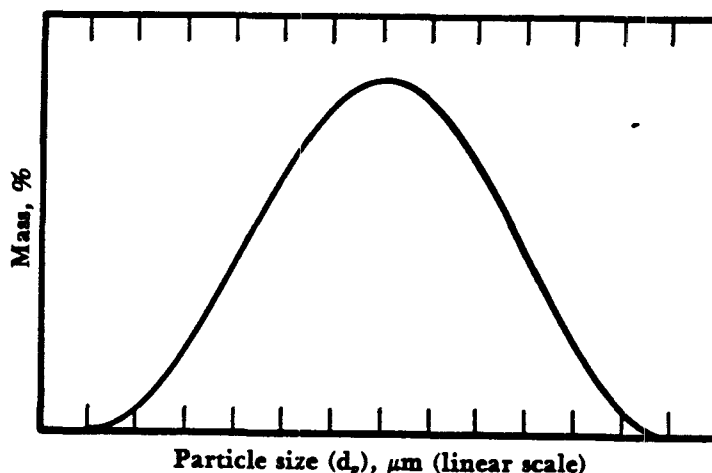


Figure 4-9. Particle size distribution with one preferential size.

Figure 4-9 shows a *normal* probability distribution which is symmetrical about the preferential size. This curve is rarely encountered for dusts consisting of very fine particles. This curve may be found for particles such as fumes formed by vapor phase reaction and condensation or for tar and acid mists.

Another representation of the normal probability of the distribution can be seen in Figure 4-10. This curve is skewed or off-center about the preferential size. This type of curve usually occurs when very fine industrial dust data are plotted.

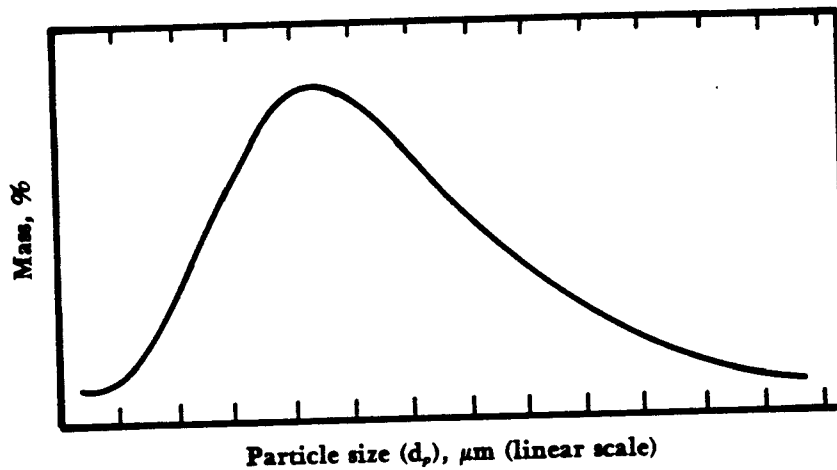


Figure 4-10. Skewed particle size distribution plotted on a linear scale.

The normal probability of the distribution can also be plotted on log scale. The representation of the distribution can be seen in Figure 4-11. The percent mass (concentration) is plotted on a linear scale as the y-axis. The particle size, d_p , is plotted on a log scale as the x-axis. If the curve takes on the bell-shape, the distribution appears normal.

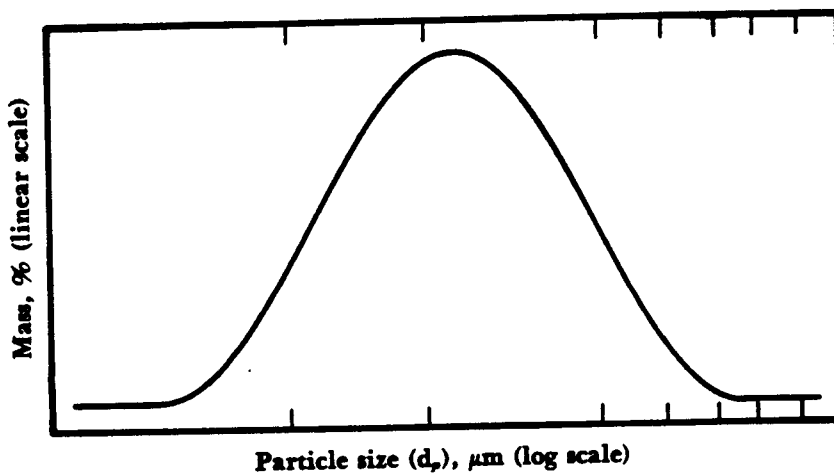


Figure 4-11. Typical particle size distribution plotted on a log scale.

Figure 4-12 shows a particle size distribution with two peaks. The curve simply shows that the data has two preferential sizes instead of one, as shown in Figure 4-9.

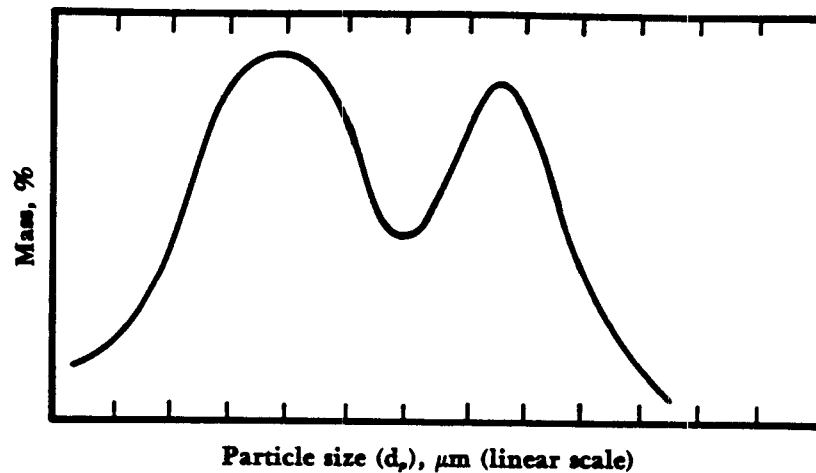


Figure 4-12. Typical particle size distribution with two preferential sizes.

Construction of the Frequency Distribution Curve

Frequency distribution curves are usually plotted on linear coordinate paper. The percentage by weight (or the frequency) is plotted as the ordinate. The average particle size of each size range (size fraction) is plotted on the abscissa.

Since the curve is plotted using average particle diameters within each range, there may be several positions of the curve for a given dust. Each position is dependent on the series of size ranges used.

There are a number of methods for selecting size ranges for the construction of the frequency distribution curve. Two of the more common are:

- select equal arithmetic increments of size as shown in Table 4-3.

Table 4-3. Size ranges in arithmetic increments.

Size range (μm)	Percent in size range
0- 2	10
2- 4	15
4- 6	30
6- 8	30
8-10	10
> 10	5

- choose size ranges bounded by sizes having the same ratio to each other as shown in Table 4-4.

Table 4-4. Size ranges with the same ratio.

Size range (μm)	Percent in size range
0- 5	15
5-10	10
10-20	30
20-40	20
40-80	20
> 80	10

It is evident from this discussion that a large number of points are necessary to fix the position of the frequency curve. If this were the only method of representing the particle size data of a particulate sample, particle size analysis would be an extremely laborious and time consuming procedure.

Cumulative Distribution Curves

Particle size data can also be plotted as a cumulative plot. Particle size of each size range is plotted on the ordinate. The cumulative percent by weight (frequency) is plotted on the abscissa. The cumulative percent by weight can be given as cumulative percent less than stated particle size or cumulative percent larger than stated particle size. The cumulative percent by weight can be plotted on either a linear percentage or a probability percentage scale. The particle size range (ordinate) is usually a logarithmic scale.

If the particle size, d_p , of each size range is plotted versus the cumulative percent larger than d_p (linear scale) one could get a distribution curve as shown in Figure 4-13.

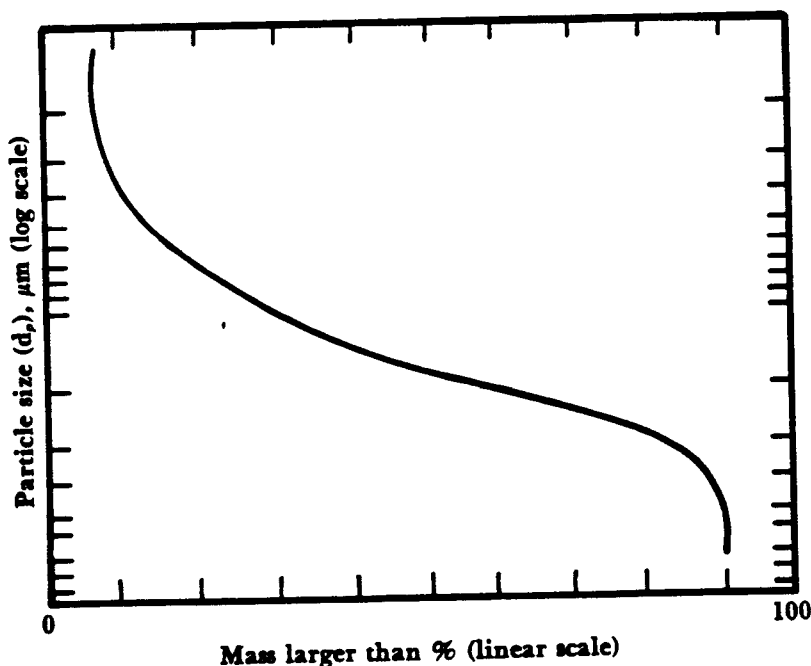


Figure 4-13. Cumulative particle size distribution plotted on a linear scale.

In Figure 4-13, the distribution approaches the 0% and 100% values asymptotically. It is evident that the cumulative distribution in this figure is not a straight line for the entire range of particle size in the sample. The majority of the size ranges occur toward the 0% size and the 100% size.

More frequently the cumulative distribution is plotted on special coordinate paper called log probability paper. The particle size of each size range is plotted on the logarithmic ordinate. The percent by weight larger than d_p is plotted on the probability scale as the abscissa (Figure 4-14). This allows one to expand the cumulative distribution axis near 0% and near 100%. By expanding the axis, the distribution plots out as a straight line if the frequency distribution plot is *skewed* as in Figure 4-10. The cumulative distribution plot in Figure 4-14 is identical to that in Figure 4-13, except that the percentage scale is expanded near 0% and 100%. It should be noted that one can just as easily plot percent mass less than d_p on the abscissa.

The Log-Normal Distribution

When measuring dusts from industrial sources, the graph of the particle size distribution often displays the logarithmic variation of the normal distribution. As can be seen in Figure 4-10 the normal distribution has a fundamental defect related to its use in particle sizing analysis. Implicit in the statement that a random variable is normally distributed is the concept that the values of particle size are at equal distances from the central tendency or preferential size. Suppose the mean particle size or central tendency of the distribution were 20 μm . It would be equally probable to find either a 15 μm or 25 μm particle. One might also find a particle the size of 50 μm in the distribution. Were the distribution normal, it would be equally likely to find a particle the size of minus 10 μm .

However, if it can be assumed that the logarithm of the particle size is randomly distributed, then this problem is avoided. The ratios of particle size about a central tendency are equally probable, and the ratios are bounded on the lower end by zero.

The usefulness of the log-normal distribution is most evident when the frequency distribution curve is characteristically *skewed*, as in Figure 4-10. The data is plotted as a cumulative plot on log probability paper. If the distribution follows the log-normal relationship, then the plot will result in a straight line. The linearity of the relationship allows one to describe the distribution statistically with a minimum of individual observations. The distribution is completely specified by two parameters, the geometric mean, d_{gm} , and the geometric standard deviation, σ_{gm} .

The geometric mean value of a log-normal distribution can be read directly from a plot similar to that represented in Figure 4-15. The geometric mean size is the 50% size on the plot.

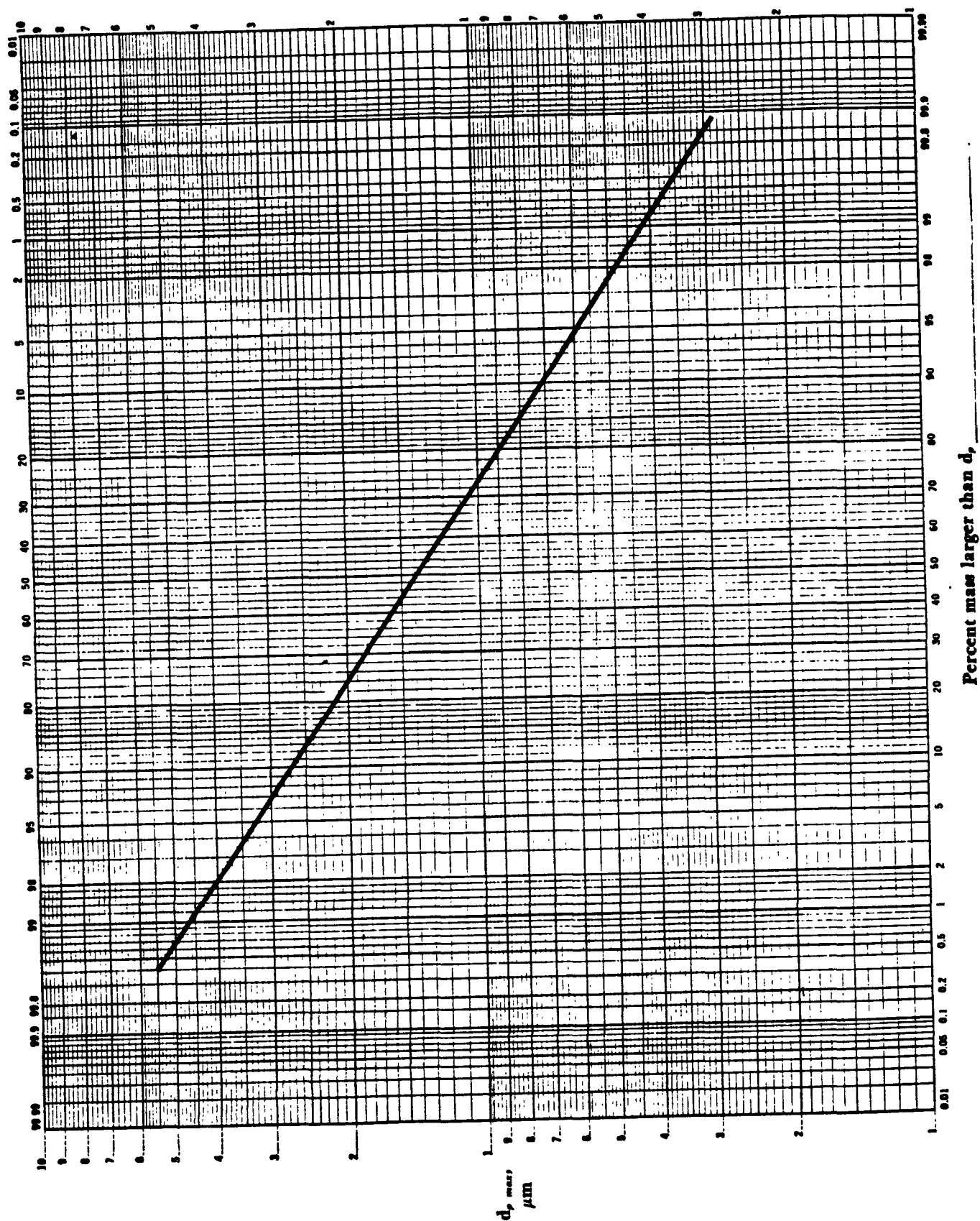


Figure 4-14. Cumulative distribution plotted on log probability paper.

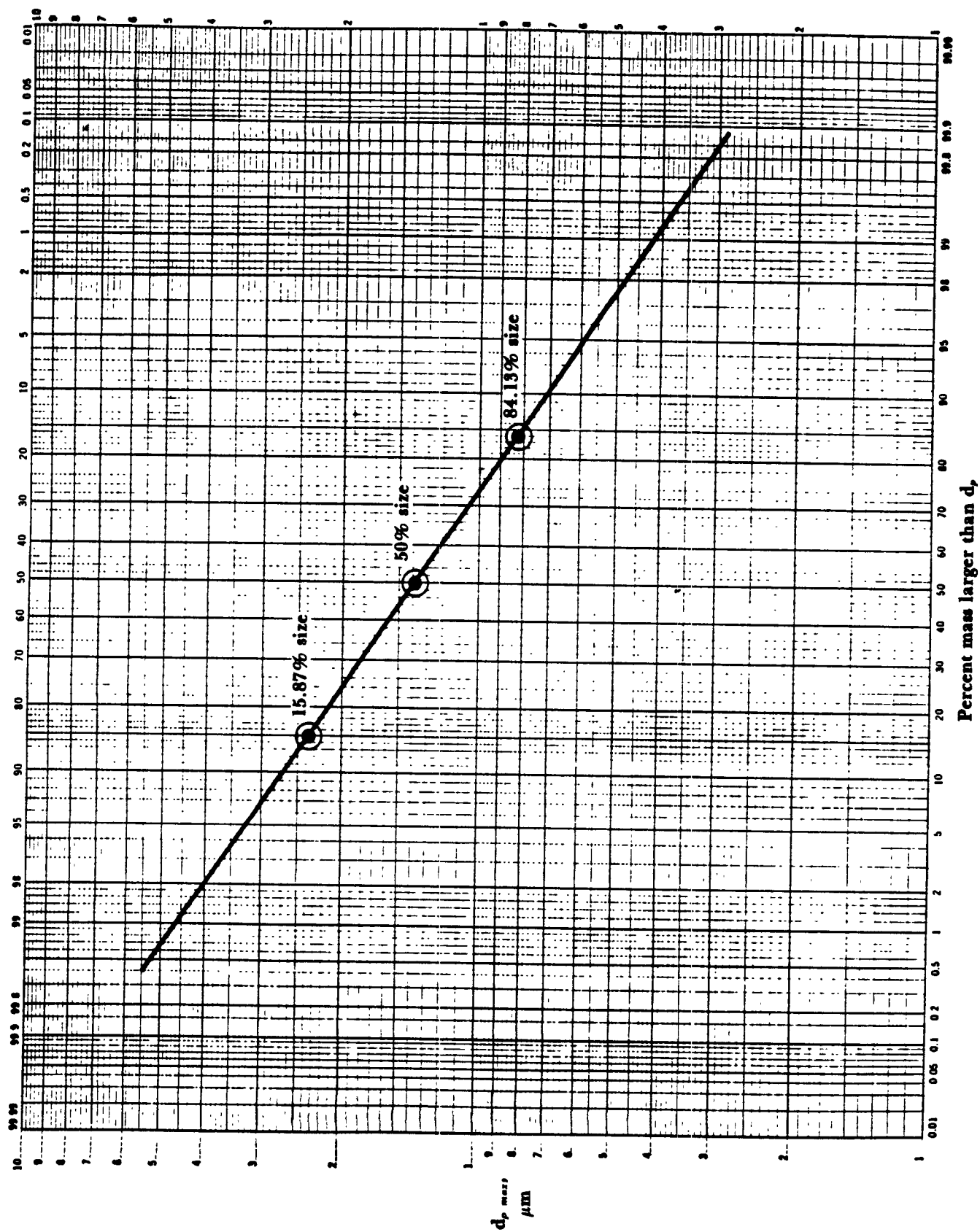


Figure 4-15. Geometric mean and standard deviation from a log-normal distribution plot.

The geometric standard deviation is a good measure of the dispersion or spread of a distribution. The geometric standard deviation is the root-mean square deviation about the mean value. Its derivation and application in significance testing and setting of confidence levels can be found in most statistics textbooks. The geometric standard deviation is identical for specifying the size distribution of a log-normal distribution, whether by particle number, surface, mass, or any other quantity of the form kd_p^n , where k is a parameter common to all particles and d_p is the diameter. Plots of cumulative distribution on log-probability paper are then parallel straight lines for number, mass, or surface which leads to a great simplification and easy graphical technique.

The geometric standard deviation can be read directly from a plot such as shown in Figure 4-15. For a log-normal distribution (that plots d_p maximum versus percent mass larger than d_p), the geometric standard deviation is given by:

$$\sigma_{gm} = \frac{50\% \text{ size}}{84.13\% \text{ size}}$$

or

$$\sigma_{gm} = \frac{15.87\% \text{ size}}{50\% \text{ size}}$$

! All one must do is determine the 50% size and the 84.13% size from the plot and divide to determine the geometric standard deviation.

Example of a Typical Particle Size Data Reduction

Consider the data listed in Table 4-5:

Table 4-5. Typical particle size data.

Size range (m)	Concentration ($\mu\text{g}/\text{m}^3$)	<u>Concentration</u> Δd_p	<u>Concentration</u> $\Delta \log d_p$
1- 2	0.8	$0.8/(2.0 - 1.0) = 0.8$	$0.8/[\log 2 - \log 1] = 2.66$
2- 4	12.2	6.1	40.53
4- 6	25.0	12.5	142.0
6-10	56.0	14.0	252.3
10-20	76.0	7.6	253.2
20-40	27.0	1.35	89.7
> 40	3.0	0.075	10.0

Suppose we were asked to determine if the distribution was log-normal, and if so, determine the geometric mean diameter (d_{gm}) and the geometric standard deviation (σ_{gm}). How would one approach this problem?

First we could plot the mass concentration ($\text{concentration}/\Delta d_p$) versus particle diameter (d_p) on a linear scale (Figure 4-16.)

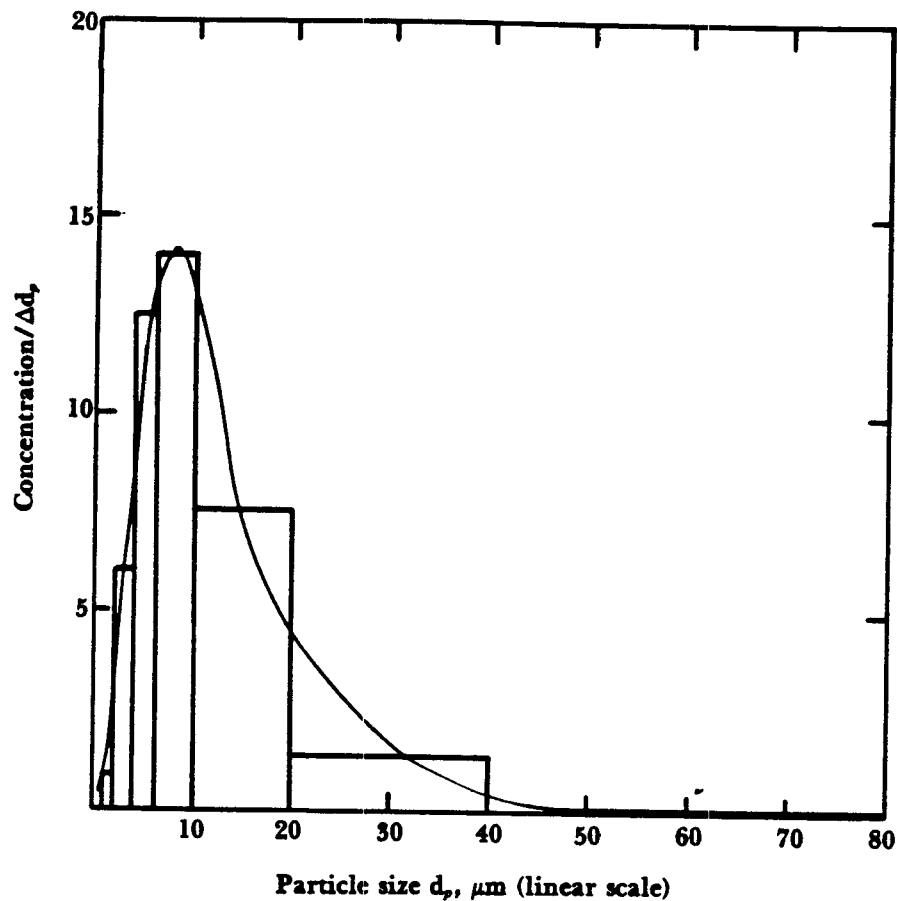


Figure 4-16. Mass concentration versus particle diameter on a linear scale.

The data appears to be skewed and would therefore lead one to believe that the distribution could be log-normal.

We can now plot mass concentration ($\text{concentration}/\Delta \log d_p$) on a log scale (Figure 4-17). The particle size d_p (x-axis) is plotted on a log scale. The area under the smooth curve between two different values of d_p represents the total particle mass concentration between the two values of d_p . If the y-axis is not "concentration divided by $\Delta \log d_p$ " then the distribution shape will be partly determined by the size ranges of the sampling device (i.e. impactor stages) rather than the true particle distribution shape.

We can now plot mass concentration versus particle diameter (d_p) on a log scale (Figure 4-17).

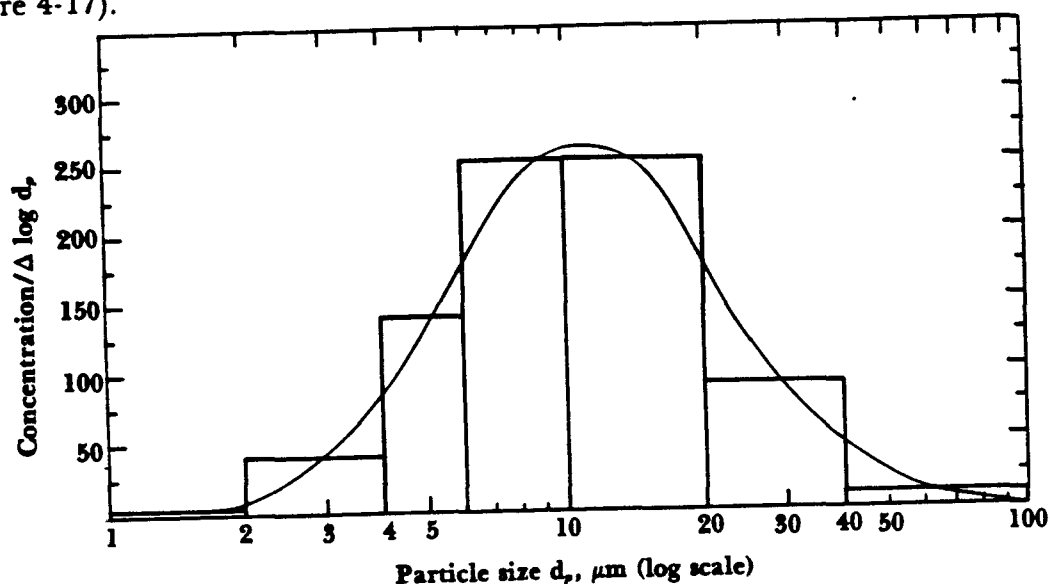


Figure 4-17. Mass concentration versus particle size on a log scale.

This plot yields an appropriately shaped bell curve that appears to indicate that this is a log-normal distribution. However, it is extremely important to plot the data on log-probability paper to see if a straight line results. If the distribution plots a straight line on log probability paper, then the distribution is log-normal.

First we must calculate the percent in each size range and then the cumulative percent larger than d_p maximum (Table 4-6).

Table 4-6. Cumulative particle size data.

Size range (μm)	Concentration ($\mu\text{g}/\text{m}^3$)	Percent weight in size range	Cumulative percent larger than $d_{p\text{max}}$
0- 2	0.8	0.4	99.6
2- 4	12.2	6.1	93.5
4- 6	25.0	12.5	81.
6-10	56	28	53.
10-20	76	38	15.
20-40	27	13.5	1.5
> 40	3	1.5	—
	200		

Now plot the calculated values of cumulative percent larger than $d_{p,max}$ (Figure 4-18).

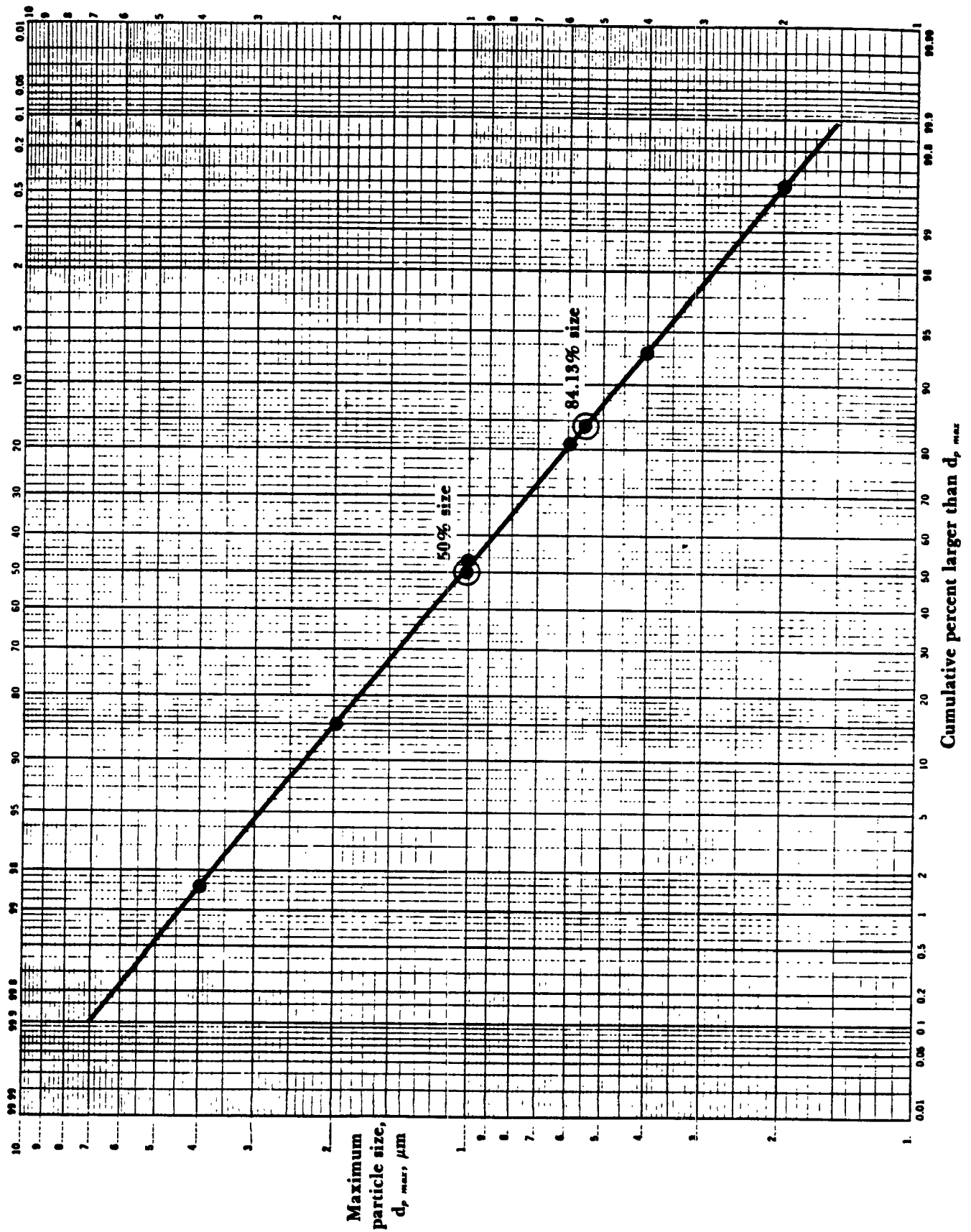


Figure 4-18. Log-probability distribution for data in Table 4-6.

The plot (in Figure 4-18) on log probability paper yields a straight line. Therefore the distribution is log-normal. To determine the geometric mean diameter one can read the 50% size from Figure 4-18.

$$d_{gm} = 10.5 \text{ micrometers}$$

The geometric standard deviation is:

$$\begin{aligned}\sigma_{gm} &= \frac{50\% \text{ size}}{84.13\% \text{ size}} \\ &= \frac{10.5}{5.5} \\ &= 1.9\end{aligned}$$

References

1. Stockman, J. D. and Fochtman, E. G. eds. 1977. *Particle Size Analysis*. Ann Arbor, Mich: Ann Arbor Science Publishers Inc.
2. McFarland, A. R., 1978. *Aerodynamic Particle Sizing*. College Station, Texas: Air Quality Laboratory Publication.
3. Environmental Protection Agency (EPA). 1979. *Guidelines for Particulate Sampling in Gaseous Effluents from Industrial Processes*. EPA 600/7-79-028.
4. Environmental Protection Agency (EPA). 1977. *Inertial Cascade Impactor Substrate Media for Flue Gas Sampling*. EPA 600/7-77-060.
5. Environmental Protection Agency (EPA). 1976. *Particulate Sizing Techniques for Control Device Evaluation: Cascade Impactor Calibrations*. EPA 600/2-76-280.
6. Environmental Protection Agency (EPA). 1979. Proceedings: *Advances in Particle Sampling and Measurement (Asheville, NC, May 1978)*. EPA 600/7-79-065.
7. Environmental Protection Agency (EPA). 1977. *Procedures Manual for Electrostatic Precipitator Evaluation*. EPA 600/7-77-059.
8. Hewitt, G. W. 1957. The Charging of Small Particles for Electrostatic Precipitation. *AIEE Winter General Meeting*. Paper no. 73-283. New York.
9. *Notes and Personal Communication* with Cliff I. Davidson, Carnegie Mellon University, 1979, 1981, 1982.

Chapter 5

Gravity Settling Chambers

Introduction

Long used by industry for removing solids or liquid particulate matter from gaseous streams, gravity settlers or gravity settling chambers have the advantages of simple construction, low initial cost and maintenance, low pressure losses, and simple disposal of collected materials.

The gravity settler was one of the first devices used to control particulate emissions. It is an expansion chamber in which particle velocity is reduced, thus allowing the particle to settle out under the action of gravity. One primary feature of this device is that the external force causing separation of particles from the gas stream is provided free by nature. This chamber's use in industry, however, is generally limited to the removal of larger sized particles, 40-60 μm in diameter.

Today's demands for cleaner air and stricter emission standards have relegated the settling chamber to use in research for testing or as a precleaner for other particulate control devices (cyclones, fabric filters, electrostatic precipitators, and scrubbers).

Settling chambers have been used in a number of research projects to study the flow of particles in a gas stream. The data generated from these studies is useful in the design of other particulate emission control devices.

Equipment Description

There are basically two types of gravity settlers: the simple expansion chamber and the multiple-tray settling chamber. A typical horizontal flow (simple expansion) gravity settling chamber is presented in Figure 5-1. The unit is constructed in the form of a long horizontal box with inlet, outlet and dust collection hoppers. These units depend on gravity for collection of the particles. The particle-laden gas stream enters the unit at the gas inlet. The gas stream then enters the expansion section of the duct. Expansion of the gas stream causes the gas velocity to be reduced. All particles in the gas stream are subject to the force of gravity. However, at reduced gas velocities (in the range of 0.305 to 3.05 m/sec) the larger particles can be overcome by gravity and fall into the dust hoppers. Theoretically, a settling chamber of infinite length could collect even the very small particles ($< 10 \mu\text{m}$).

The collection hoppers located at the bottom of the settler are usually designed with positive seal valves and must be emptied as dust buildup occurs. Dust buildup will vary depending on the concentration levels of particulate matter in the gas streams, especially for heavy concentrations of particles greater than $60\text{ }\mu\text{m}$ in diameter.

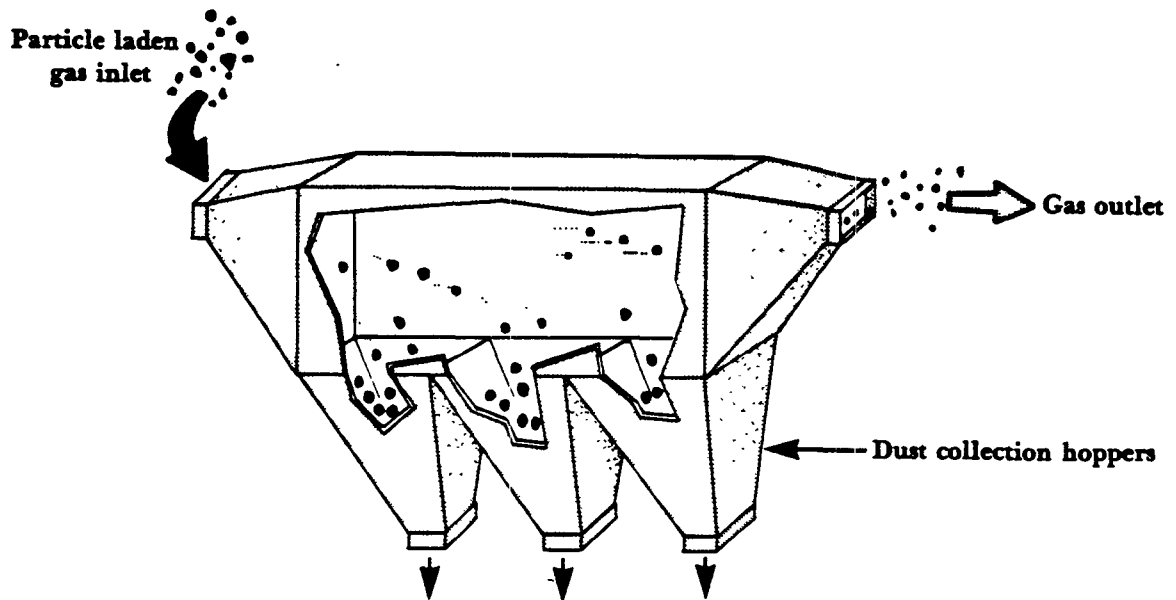


Figure 5-1. Horizontal flow settling chamber.

The multiple-tray settling chamber, also called the Howard settling chamber, is shown in Figure 5-2. Several horizontal collection plates are introduced to shorten the settling path of the particle and to improve the collection efficiency of small particles (as small as $15\text{ }\mu\text{m}$ in diameter). Each shelf or tray in the unit can collect dust that settles out by gravitational force. Since the vertical distance that a particle must fall to be captured is less than the distance in a horizontal settling unit, the overall collection efficiency of the Howard settling chamber can be greater than the horizontal chamber. The gas must be uniformly distributed as it passes through each tray throughout the chamber. Uniform distribution is usually achieved by the use of gradual transitions, guide vanes, distributor screens, and perforated plates. The particles will settle on the individual trays which must be cleaned periodically. The vertical distance between trays may be as little as 1 inch, making cleaning much more difficult than with the horizontal settling chamber. Other disadvantages include the tendency of trays to warp during high temperature operation and the inability of the unit to handle dust concentrations exceeding approximately 1 grain/ft^3 (2.29 g/m^3). For these reasons, the Howard settling chamber is not used very frequently for particulate emission control.

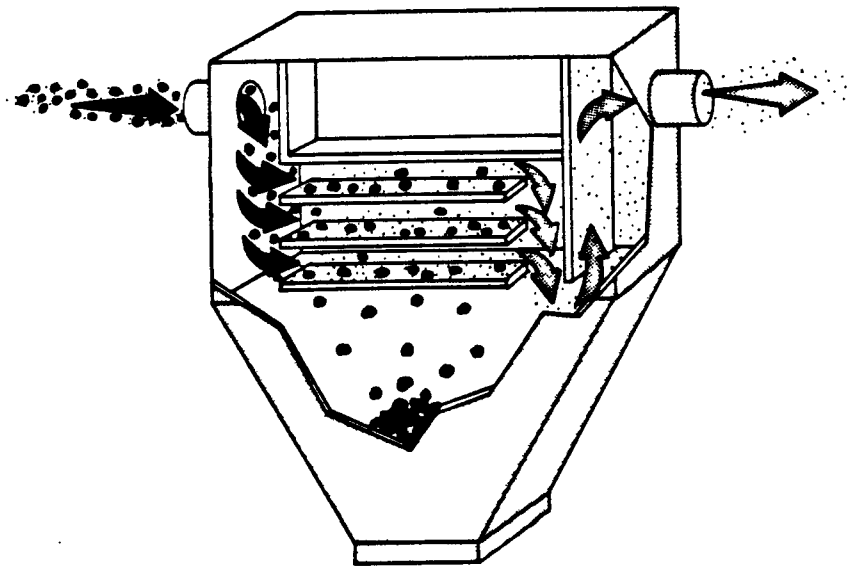


Figure 5-2. Howard settling chamber (multiple tray).

Baffle Chambers

A variation of the gravity settling chamber is a baffle chamber, sometimes referred to as an inertial separator. These units have baffles within the chamber to enhance particle separation and collection. This arises by changing the direction of the gas velocity and imparting a downward motion to the particle. This induced motion is superimposed on the motion due to gravity. Thus, particle collection is accomplished by gravity and an inertial or momentum effect. Particles as small as 20 to 40 μm can be collected. An example of this device is shown in Figure 5-3. These units are more compact and require less space than gravity settling chambers. The pressure drops are slightly higher, ranging from 0.1 to 1.0 in. of H_2O (0.25 to 2.5 cm H_2O).

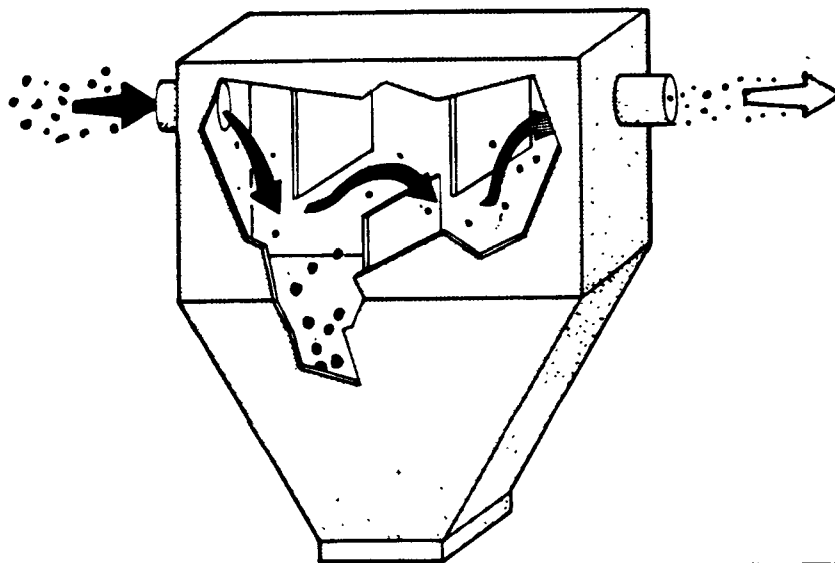


Figure 5-3. Baffle chamber.

Design Parameters

Understanding the principles governing particle collection in a gravity settler begins by examining the behavior of a single spherical particle in the chamber (Figure 5-4). The bulk flow air velocity profile in this case is assumed to be uniform throughout the chamber. The particle flows with the same velocity as the gas stream, and the horizontal velocity is given as v_x . The particle also has a vertical velocity, v_y . The term v_y is also called the terminal settling velocity (v_t) and was discussed in Chapter 3 of this manual. The length, width, and height of the chamber are L , B , and H respectively.

Suppose the particle enters the chamber at a height h_p . The particle must fall this distance (h_p) before it travels the length of the chamber if the particle is to be collected. In other words, the particle will settle if the time required for the particle to settle is less than the time that the particle resides in the chamber.

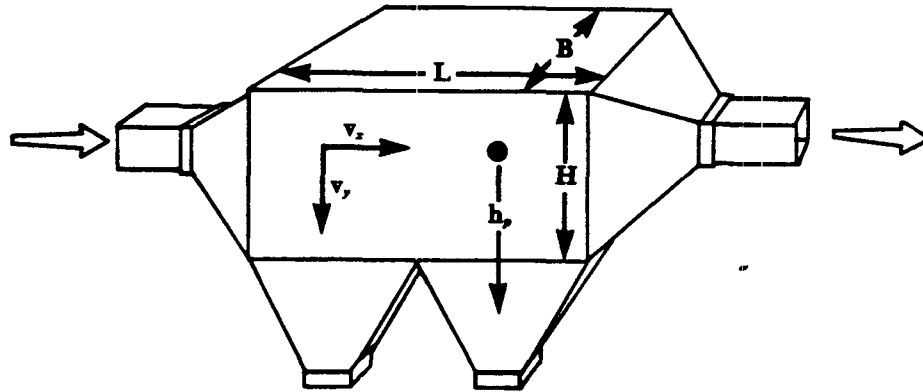


Figure 5-4. Settling chamber dimensions.

The theoretical collection efficiency of the settling chamber is given by the expression.

(Eq. 5-1)
$$\eta = \frac{v_y L}{v_x H}$$

Where: η = fractional efficiency of particle size d_p (one size)

v_y = vertical settling velocity

v_x = horizontal gas velocity

L = chamber length

H = chamber height (greatest distance a particle must fall to be collected)

The settling velocity can be calculated from Stokes law as previously discussed in Chapter 3. As a rule of thumb, Stokes law applies when the particle size d_p is less than $100 \mu\text{m}$ in size. The settling velocity is:

$$(Eq. 5-2) \quad v_s = \frac{gd_p^2(\rho_p - \rho_a)}{18\mu}$$

Where: v_s = settling velocity in Stokes law range, m/sec (ft/sec)
 g = acceleration due to gravity, 9.8 m/sec^2 (32.1 ft/sec^2)
 d_p = diameter of the particle, μm
 ρ_p = particle density kg/m^3 , (lb/ft^3)
 ρ_a = gas density (usually air), kg/m^3 (lb/ft^3)
 μ = gas viscosity, $\text{Pa}\cdot\text{sec}$ (lb/ft sec)

Note: $\text{Pa} = \text{N/m}^2$

$\text{N} = \text{Kg}\cdot\text{m/sec}^2$

Thus, we can rearrange Equation 5-2 to determine the minimum particle size that can be collected in the unit with 100% efficiency. The minimum particle size d_p^* is given as:

$$(Eq. 5-3 \text{ given in } \mu\text{m}) \quad d_p^* = \left(\frac{v_s 18\mu}{g(\rho_p - \rho_a)} \right)^{1/2}$$

The density of the particle ρ_p is usually much greater than the density of the gas ρ_a . Therefore, the quantity $(\rho_p - \rho_a)$ reduces to ρ_p . The velocity can be written as $v = Q/BL$ where Q is the volumetric flow rate and B and L are the width and length respectively. Equation 5-3 is reduced to:

$$(Eq. 5-4) \quad d_p^* = \left(\frac{18\mu Q}{g\rho_p BL} \right)^{1/2}$$

From Equation 5-1 and 5-2, one can rewrite the efficiency equation to be:

$$(Eq. 5-5) \quad \eta = \left[\frac{g\rho_p BLN_c}{18\mu Q} \right] d_p^2$$

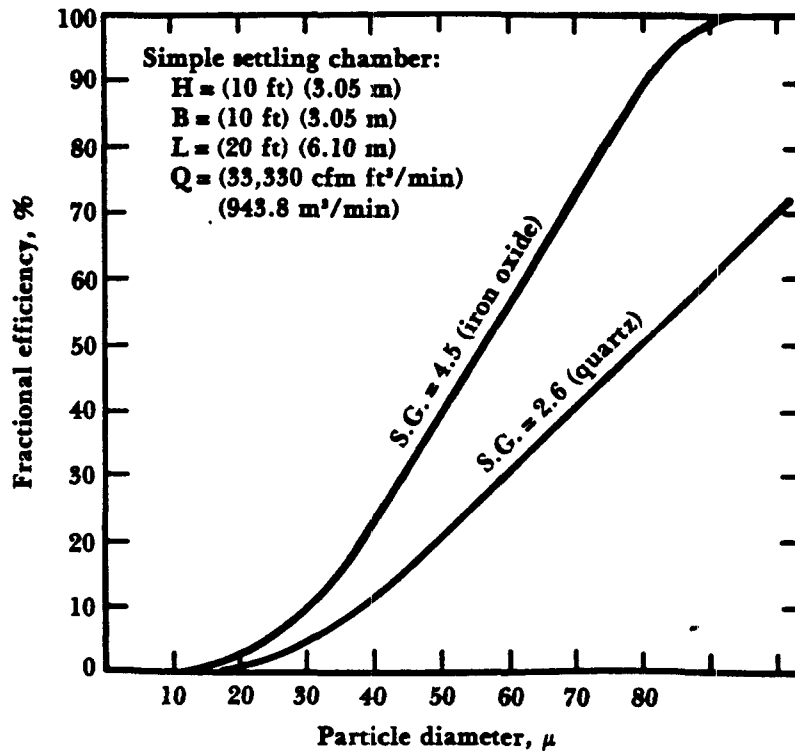
Where: N_c = number of parallel chambers: 1 for simple settling chamber
 and N trays + 1 for a Howard settling chamber

In Equation 5-5, ρ_p (particle density) was assumed to be much greater than ρ_a (gas density), hence $\rho_p - \rho_a = \rho_p$. The term in the brackets in Equation 5-5 is often multiplied by a dimensionless empirical factor to correlate theoretical efficiencies with experimental data. If no information is available, it is suggested that 0.5 be used*. Thus Equation 5-5 can be written:

$$(Eq. 5-6) \quad \eta = 0.5 \left[\frac{g\rho_p BLN_c}{18\mu Q} \right] d_p^2$$

*Theodore and Buonicore, 1976.

Equations 5-1 and 5-5 give the theoretical collection efficiencies of a settling chamber for a single sized particle. Since the gas stream entering a unit consists of a distribution of particles of various sizes, a fractional efficiency curve must be used to determine the overall collection efficiency. This is simply a curve describing the collection efficiency for particles of various sizes (Figure 5-5).



Source: Jennings, R. F., J. Iron Steel Inst. London, 164, 305, 1950.

Figure 5-5. Fractional efficiency curve for dusts from a sinter plant.

One can see from Figure 5-5 that the fractional efficiency for a 40 micrometer iron oxide particle is 22%. The fractional efficiency of an 80 micrometer iron oxide particle is 88%. Figure 5-5 shows that the larger particles have a higher fractional efficiency than the smaller particles. The overall efficiency can be calculated using:

(Eq. 5-7)
$$\eta_{TOT} = \sum \eta_i w_i$$

Where: η_{TOT} = overall collection efficiency
 η_i = fractional efficiency of specific size particle
 w_i = weight fraction of specific size particle

Equations 5-1 and 5-2 were developed with the assumption that the gas flow through the settling chamber is laminar. This assumption is usually incorrect. The gas flow is usually turbulent. The equation for determining efficiency when the flow is turbulent is:

$$(Eq. 5-8) \quad \eta = 1 - e^{-\left[\frac{Lv_y}{Hv_x}\right]}$$

One must be careful when using Equations 5-1 through 5-6. For example, Equation 5-4 is used to find the minimum particle size collected with 100% efficiency. This equation assumes that Stokes law describes particle settling. However, Stokes law does not work for particles greater than 100 micrometers, the particle size more suitable for collection in a settling chamber. Equation 5-4 can, in some cases, give results that are gravely in error.

Process Variables

The process design variables for a settling chamber consist of length (L), width (B), and height (H). These parameters are usually chosen by the chamber manufacturer to remove all particles above a specified size. The chamber design must provide conditions for sufficient particle residence time to capture the desired particle size range. This can be accomplished by keeping the velocity of the exhaust gas through the chamber as low as possible. If the velocity is too high dust reentrainment will occur. However, the design velocity must not be so low as to cause the design of the chamber volume to be exorbitant. Consequently, the units are designed for gas velocities in the range from 1 to 10 ft/sec (0.305 to 3.05 m/sec). Errors in estimating settling velocities from equations such as Equation 5-2 can occur due to agglomeration and electrostatic effects. Therefore, in actual practice, the terminal settling velocities used for design purposes are based upon experience and tests under normal process conditions.

In settling chamber designs, the velocity at which the gas moves through the chamber is usually called the throughput velocity. The velocity at which settled materials (particles) become reentrained is called the pickup velocity. In order to avoid reentrainment of collected dust, the throughput velocity must not exceed the pickup velocity. Experimental data or equipment supplier data such as that presented in Table 5-1 should be used to estimate the pickup velocity. As can be seen from this table, the pickup velocity can exceed 10 ft/sec. If no data for determining the pickup velocity is available, the pickup velocity should be assumed to be 10 ft/sec. In this case, the velocity of gas through the settling chamber (throughput velocity) must be less than 10 ft/sec.

Table 5-1. Pickup velocities of various materials.

Material	Density (g/cm ³)	Median size (μ m)	Pickup velocity (ft/sec)
Aluminum chips	2.72	335	14.2
Asbestos	2.20	261	17.0
Nonferrous foundry dust	3.02	117	18.8
Lead oxide	8.26	14.7	25.0
Limestone	2.78	71	21.0
Starch	1.27	64	5.8
Steel shot	6.85	96	15.2
Wood chips	1.18	1370	15.0
Wood sawdust	—	1400	22.3

Source: Theodore and Buonicore, 1976.

In terms of overall design considerations for gravity settlers, advantages include:

- low cost of construction and operation,
- few maintenance problems,
- relatively low operating pressure drops in the range of approximately 0.2-0.5 in. (0.51-1.27 cm) of water,
- temperature and pressure limitations imposed only by the materials of construction used, and
- dry disposal of solid particulates.

The disadvantages include:

- large space requirements, and
- relatively low overall collection efficiencies (typically ranging from 20 to 60%).

In general, most gravity settlers in use today are precleaners removing the relatively large particles (greater than 60 μ m) before the gas stream enters a more efficient particulate control device such as a cyclone, baghouse, electrostatic precipitator, or scrubber.

References

1. Bethea, R. M. 1978. *Air Pollution Control Technology: An Engineering Analysis Point of View*. New York: Van Nostrand Reinhold Company.
2. Theodore, L. and Buonicore, A. J. 1976. *Industrial Air Pollution Control Equipment for Particulates*. Cleveland: CRC Press.
3. Cheremisinoff, P. N. and Young, R. A., eds. 1977. *Air Pollution Control and Design Handbook Part 1*. New York: Marcel Dekker, Inc.

Chapter 6

Cyclones

Introduction

Cyclones provide a relatively low-cost method of removing particulate matter from exhaust gas streams. Cyclones are somewhat more complicated in design than simple gravity settling systems and their removal efficiency is accordingly much better than that of settling chambers. However, cyclones are not as efficient as baghouses and electrostatic precipitators, but are often installed as precleaners before these more effective devices.

Cyclones come in many sizes and shapes and have no moving parts. From the small one- and two-centimeter diameter source sampling cyclones used for particle size analysis to the large five-meter diameter cyclone separators used after wet scrubbers, the basic separation principle remains the same. Particles enter the device with the flowing gas (Figure 6-1); the gas stream is forced to turn, but the larger particles have too much momentum and can't turn with the gas. These larger particles impact and fall down the cyclone wall, then are collected in a hopper. The gas stream actually turns a number of times in a helical pattern, much like the funnel of a tornado. The repeated turnings provide many opportunities for particles to break through the streamlines, thus hitting the cyclone wall.

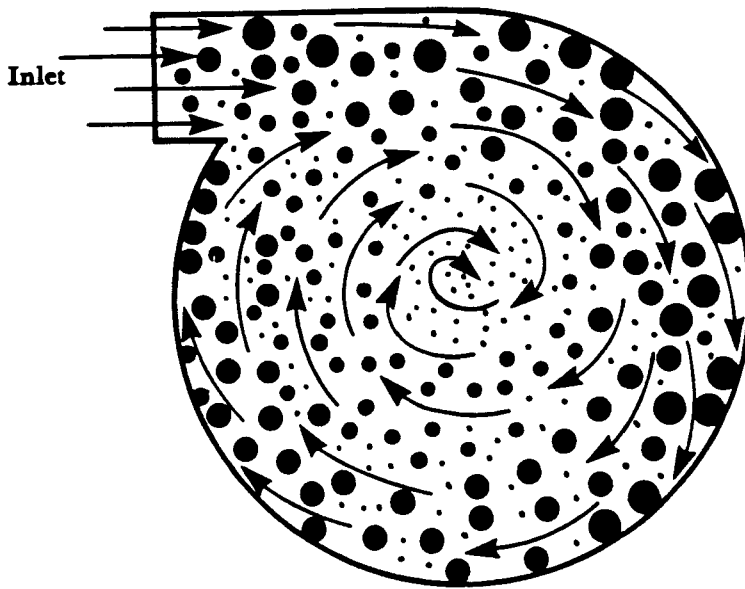


Figure 6-1. Particle collection mechanisms.

The range of particle sizes collected in a cyclone is dependent upon the overall diameter and relative dimensions of the device. Various refinements such as the use of skimmers, turning vanes, and water sprays can in some cases improve efficiency. Stacking cyclones in series or in parallel can provide further alternatives for improving overall collection efficiency.

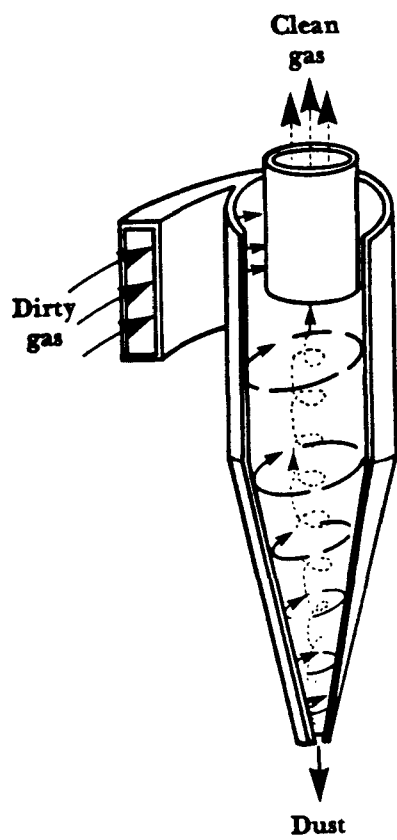
Cyclone Types

Three types of cyclones are shown in Figure 6-2. The first diagram, Figure 6-2a, shows a typical tangential entry cyclone arrangement. These cyclones have a distinctive and easily recognized form and can be found in almost any industrial area of a town or a city—at lumber companies, feed mills, cement plants, power plants, smelters, and at many other process industrial sites. Since top inlet type cyclones are so widely used, most of this chapter will be devoted to their operational characteristics.

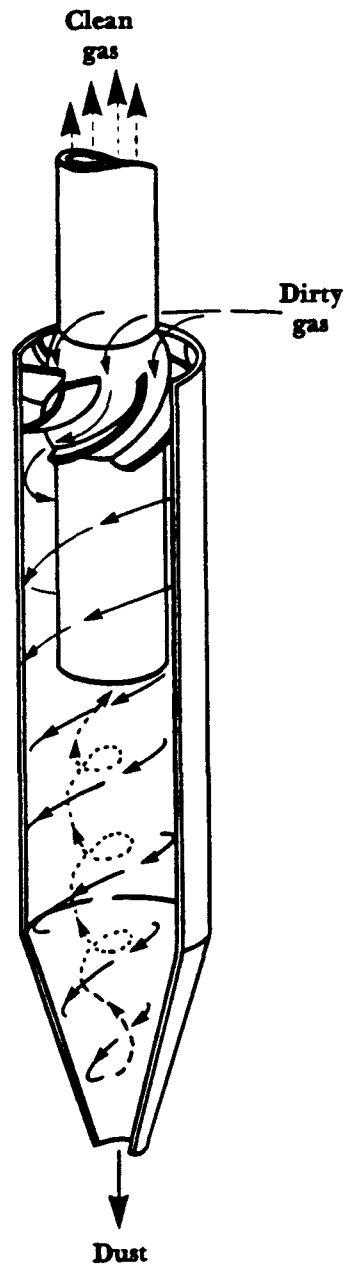
In axial entry cyclones, Figure 6-2b, the gas inlet is parallel to the axis of the cyclone body. Here, the exhaust process gases enter from the top and are directed into a vortex pattern by the vanes attached to the central tube. Axial entry cyclones are commonly used in multicyclone configurations.

The large cyclonic type separator shown in Figure 6-2c is often used after wet scrubbers to collect particulate matter entrained in water droplets. The gas enters tangentially at the bottom of the drum, forming a vortex. The large water droplets are forced against the walls and are removed from the gas stream.

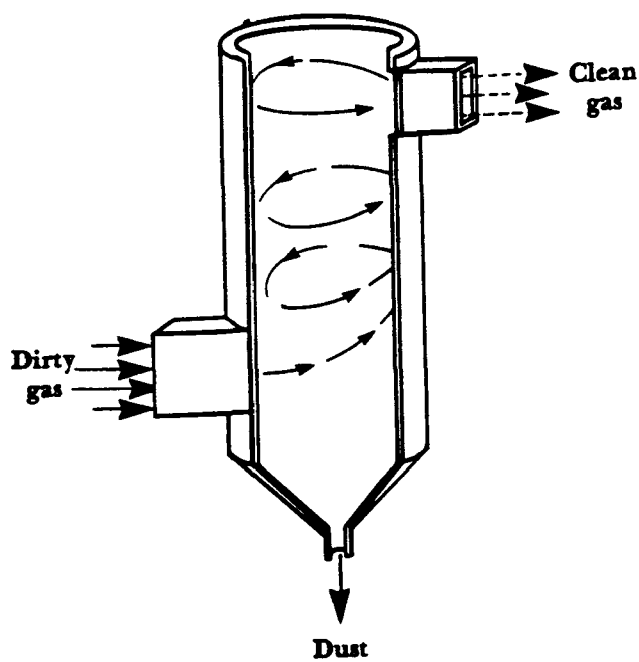
There are other variations in the design of cyclones. One classification scheme, Caplan (1977), characterizes the various types in terms of where the gas enters and exits the cyclone body (tangentially, axially, or peripherally).



a. Top inlet



b. Axial inlet



c. Bottom inlet

Figure 6-2. Types of cyclones.

The common cyclone shown in Figure 6-3 has four major design areas: *inlet*, *cyclone body*, *dust discharge system*, and *outlet*. Each part of the cyclone is important to its overall effectiveness.

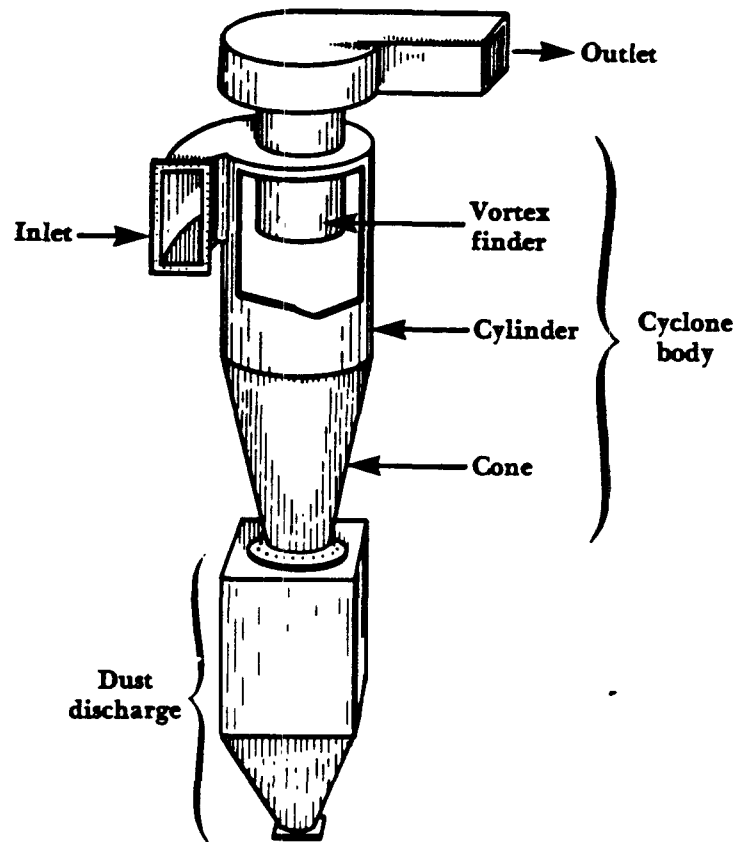


Figure 6-3. Common cyclone.

The inlet directs the gas into the cyclone body and is important in forming the vortex. In the cylindrical section the particulate matter is forced to the wall. The gas spirals down to the cone section where the body is tapered to give the gas enough rotational velocity to keep the dust against the wall. The particulate matter is collected in the hopper or vortex arrestor, and is continuously or periodically removed. The gas vortex changes from the downward to the upward direction at the bottom of the cone.

A tube extends from the top of the cyclone into the cylinder of the body. This tube extension is sometimes called a *vortex finder*. The ascending vortex enters the tube extension and then exits. A helical exhaust duct or a drum may be placed on the exit tube to straighten the gas flow before it flows through further ductwork.

Inlet

Gas coming from a duct into a cyclone is transformed from linear flow into a circular vortex pattern. The shape of the inlet assists in this transformation; however, several problems can arise. First, gas is already present in the cyclone and the incoming gas from the duct has to be squeezed between the cyclone body and the exit tube. Consequently, the gas is accelerated and added to the already rotating gas in the cyclone. In other words, the pressure drop increases and it takes more power to move the gas through the system with increasing pressure drop. If the inlet is poorly designed, turbulence can occur and the energy of the gas stream leading into the inlet is not immediately incorporated into the vortex (Figure 6-4).

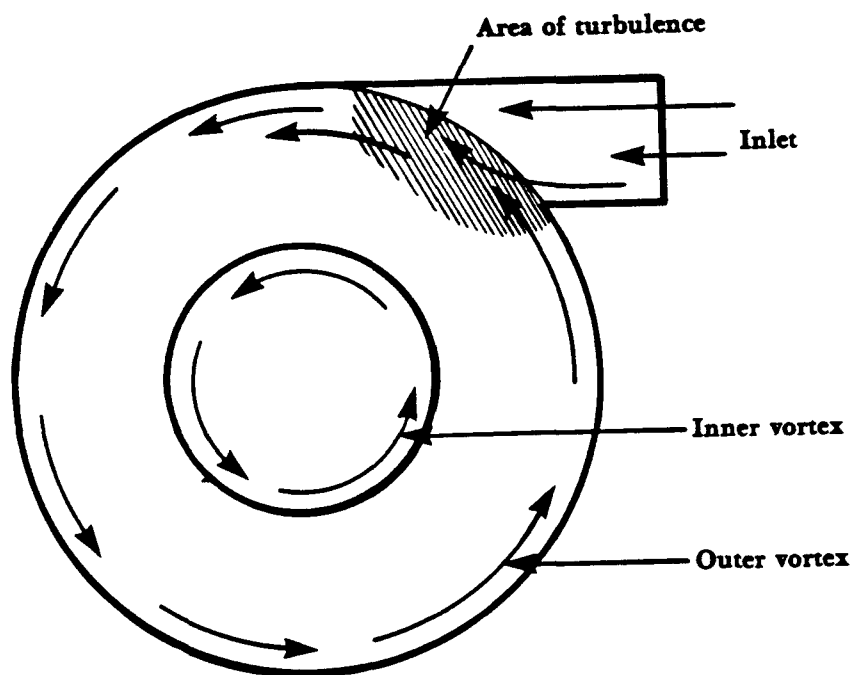


Figure 6-4. Inlet interference.

Several methods have been developed in order to *merge* the incoming gas into that already in the cyclone. These are shown in Figure 6-5.

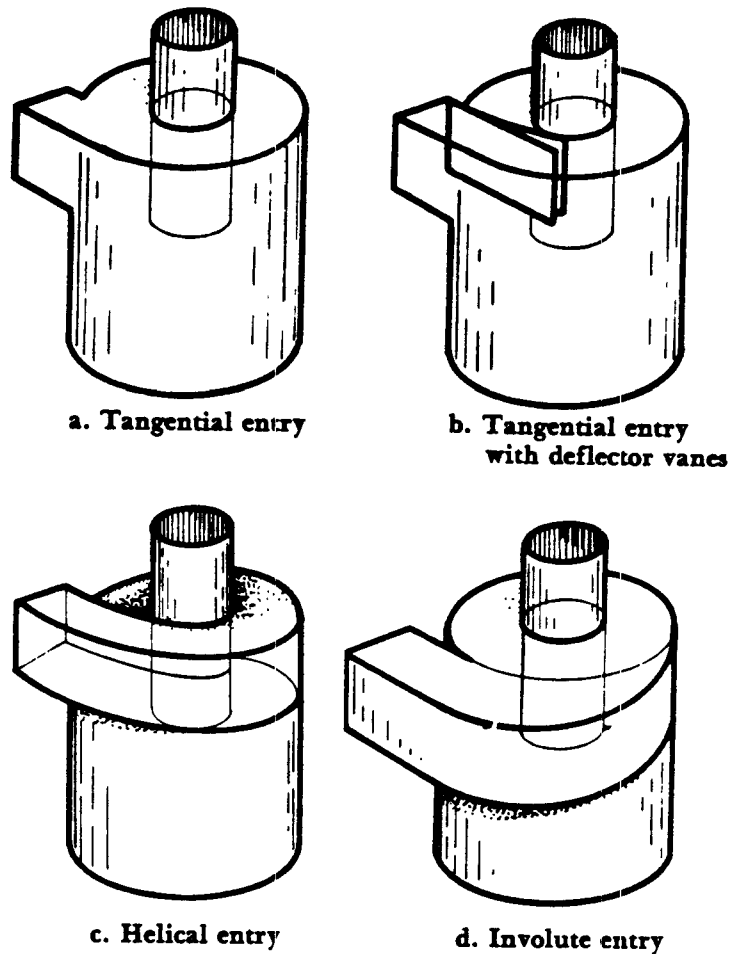


Figure 6-5. Types of cyclone inlets.

The straight *tangential* inlet shown in Figure 6-5a can cause some turbulence and loss of particles directly through the outlet tube. *Inlet deflector vanes* added to a tangential entry as shown in Figure 6-5b can narrow and guide the gas stream to move tangentially against the wall. Inlet vanes will also reduce the pressure drop. It has been found, however, that vanes can suppress the development of the vortex and reduce efficiency.

Helical inlets have been designed to deflect the incoming gas both tangentially and downward in order to provide a smooth transition to the vortex (Figure 6-5c). Present experimental data is inadequate to determine whether this general technique can gain anything in terms of increased efficiency or even in reducing the pressure drop (Stern, 1955).

The *involute* or wraparound design shown in Figure 6-5d allows the incoming gas to enter the top section of the cyclone with a minimum amount of turbulence. It has been found that the pressure drop for the involute design is less than for the tangential entry and that the efficiency is much higher (Bethea, 1979). The particles are thrown to the wall more effectively and fewer fine particles are lost through the exit tube due to turbulence.

Cyclone Body and Cone

The removal efficiency of a cyclone for a given size particle is very dependent upon the cyclone dimensions. The pressure drop at a given volumetric flow rate is most affected by the diameter. The overall length determines the number of turns of the vortex. The greater the number of turns, the greater the efficiency.

The length and width of the inlet are also important, since the smaller the inlet, the greater the inlet velocity becomes. A greater inlet velocity gives greater efficiency but also increases the pressure drop. Consider the dimensions shown in Figure 6-6.

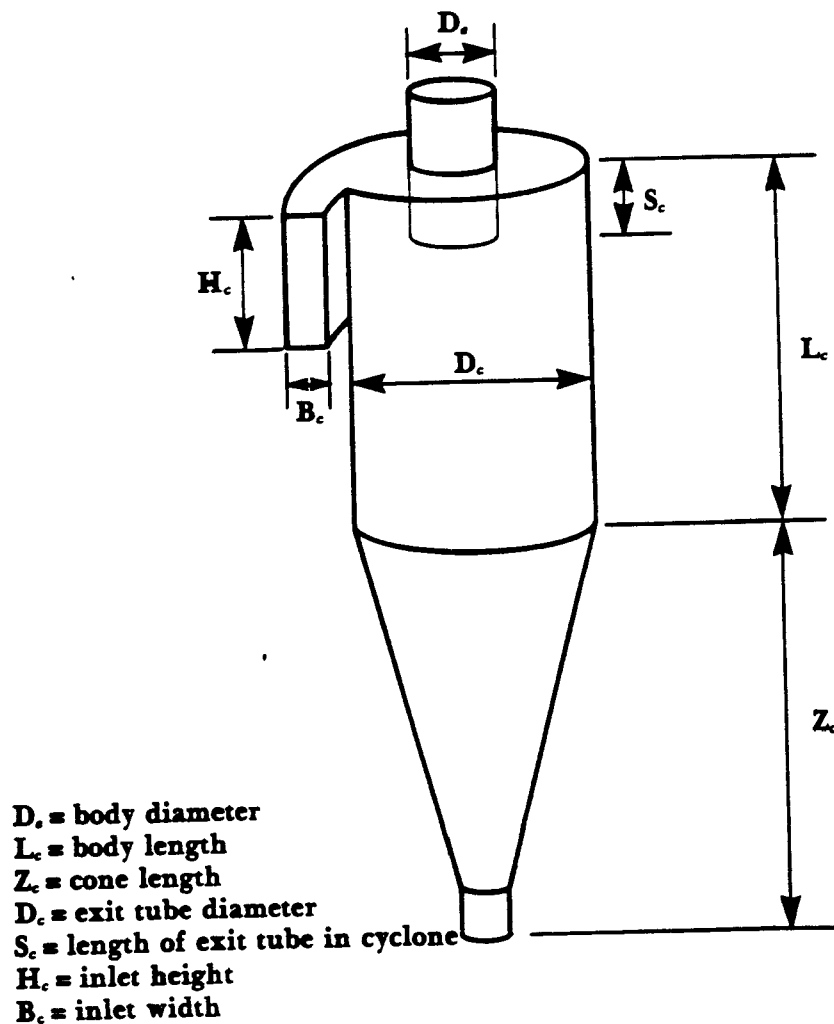


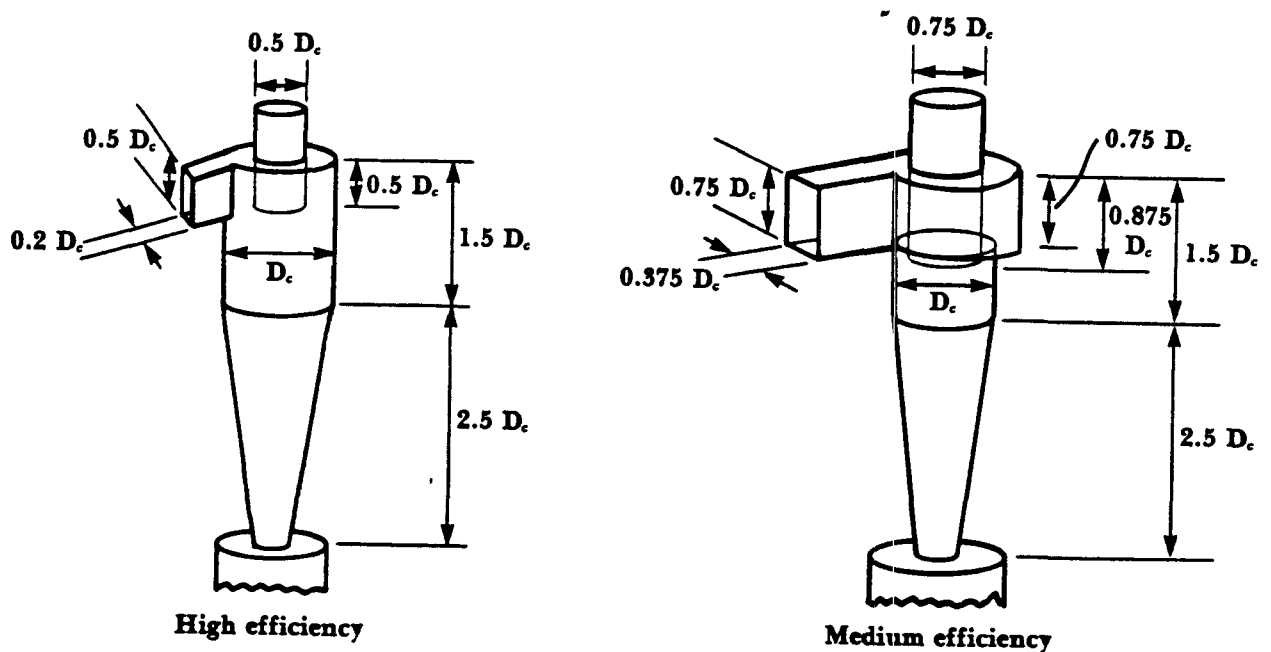
Figure 6-6. Nomenclature for a tangential entry cyclone.

Many different types of cyclones have been designed by merely varying the dimensions highlighted in Figure 6-6. Table 6-1 gives dimensional characteristics of a number of designs reported in the literature. Dimensions are given relative to the body diameter D_c .

Table 6-1. Dimensionless design ratios for tangential entry cyclones.

Symbol	Nomenclature	High efficiency	Medium efficiency	Conventional
		Stairmand		Lapple
D_c	Body diameter	1.0	1.0	1.0
H_c	Inlet height	0.5	0.75	0.5
B_c	Inlet width	0.2	0.375	0.25
S_c	Outlet length	0.5	0.875	0.625
D_o	Outlet diameter	0.5	0.75	0.5
L_c	Cylinder length	1.5	1.5	2.0
Z_c	Cone length	2.5	2.5	2.0

High efficiency cyclones generally have smaller inlet and exit areas with a smaller body diameter and possibly longer overall length. A conventional cyclone will be from 4 to 12 feet (1.2 to 3.6 m) in diameter, with a pressure drop of from 2 to 5 inches (5 to 13 cm) of water. A high efficiency cyclone will be less than 3 feet (0.9 m) in diameter with a pressure drop of from 2 to 6 inches (5 to 15 cm) of water. Two of these designs are shown in Figure 6-7.



Source: Strauss, 1975.

Figure 6-7. Standard cyclone designs.

The motion of the gas in the cyclone is not as simple as it first might appear. There are two vortices, one descending, the other ascending. The descending vortex is often called the main vortex. Figure 6-8 shows a *descending* vortex which has a right-handed orientation.

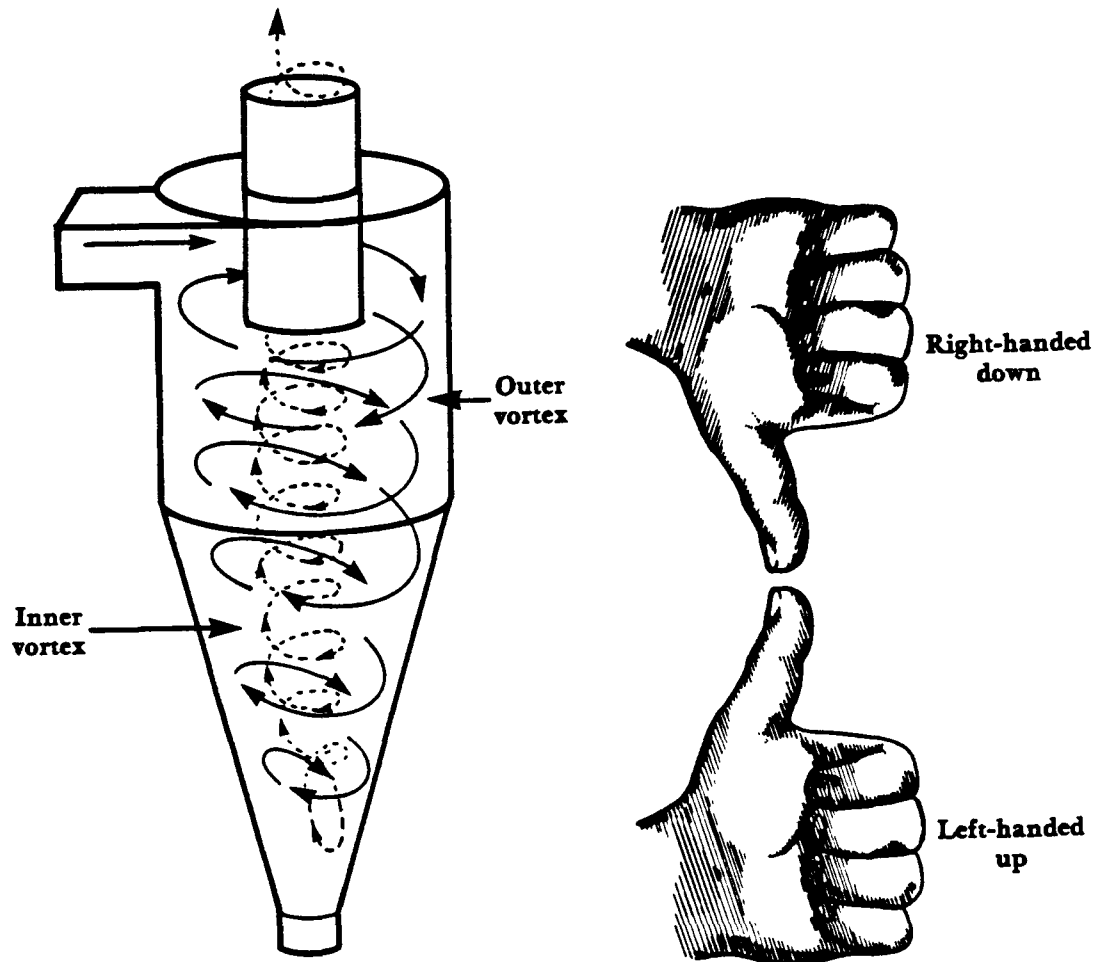


Figure 6-8. Cyclone vortices.

If the thumb of the right hand is pointed downward, the curl of the fingers will show the radial direction of the gas stream as if it were viewed from the top. For a properly designed cyclone, the vortex will change direction and ascend at the bottom of the cone.

The *ascending* vortex is smaller in radius, with faster tangential velocities than the descending vortex. It has a left-handed orientation. If the thumb of the left hand is pointed upwards, the curl of the fingers will again show the radial direction of the vortex. Note that the radial directions are the same in both cases.

The cone primarily serves as a mechanism to remove particulate matter down the walls to the hopper, and to provide greater tangential velocities near the bottom for removal of smaller particles. The vortex formed in a cyclone is, however, eccentric. Just as a tornado moves at an angle to the ground, the cyclone's main vortex can deviate from the vertical axis. For this reason, it has been found that the bottom of the cone should have a diameter of at least $\frac{1}{4}$ of D_c , the cylinder diameter. The outer vortex otherwise could touch the cone wall and entrain already separated particulate matter into the ascending vortex.

Even if optimum dimensions are selected, problems can occur within the cyclone which can reduce the efficiency. Rough walls will slow down the gas, decreasing the velocity of the vortex, thus causing smaller particles to be lost. Particles can bounce off the walls into the inner vortex and also be lost. Secondary flow patterns or eddies can form in the annular region at the inlet. The recirculation and turbulence here can prevent small particles from entering the vortex and instead be drawn into the outlet tube. The lower pressure in the inner vortex caused by its faster velocity can cause particles to drift in from the main vortex (a Bernoulli effect). These problems limit the efficiency of a cyclone.

These problems can, however, be minimized in some cases. First, care should be taken to have the cyclone constructed with smooth interior walls. A *finer eductor* or skimmer can also be added which will bleed off a portion of the gas (and fine particles) from the upper part of the cyclone (Figure 6-9). Since a pressure drop exists from the upper part of the cyclone cylinder to the bottom part, the fines can be reinjected into the main vortex at the cone junction merely by taking advantage of the small vacuum which exists. The fines are bombarded by other particles and forced to the wall, thus increasing the efficiency. If particle bounce is a great problem, water sprays can be added to wet the walls and entrain the particles.

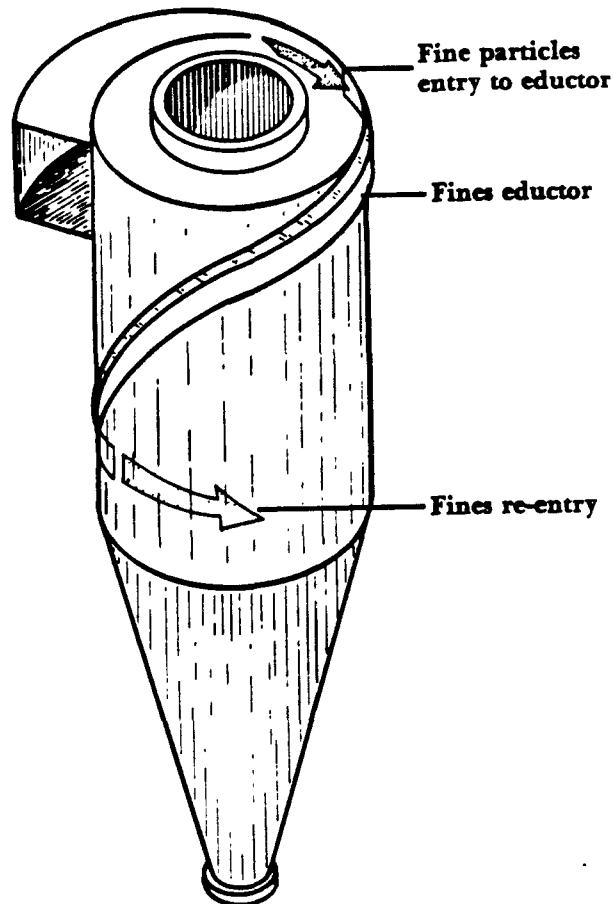
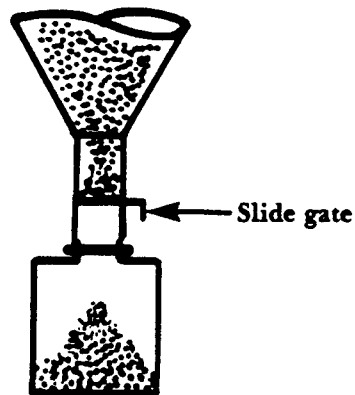


Figure 6-9. Fines eductor.

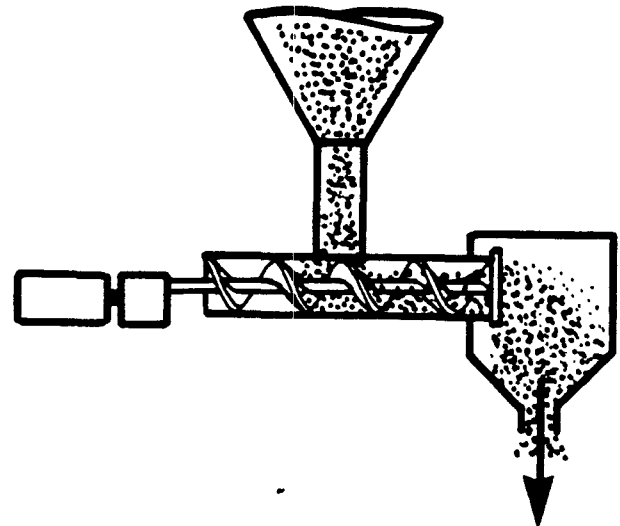
Dust Discharge System (Hopper)

The vortex will extend into the discharge bin if the bin is immediately below the cone and nothing is added at the bottom of the cone to arrest the vortex. Since the static pressure in the vortex core is slightly negative, dust can be reentrained from the hopper into the inner vortex. Also, if leaks exist in the bin, dust can be sucked back up into the cyclone.

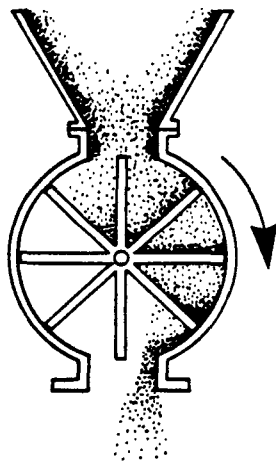
Several methods are used to avoid reentrainment. Straightening vanes added to the inside of the pipe leading from the cone to the hopper can arrest the vortex, as can axial discs added above the discharge tube (Stern, 1955). Reentrainment can be minimized by making the hopper large in volume and deep enough so that the collected dust level will lie below the point where the vortex ends. The addition of a mechanical valve which can periodically or continually remove the dust from the cyclone, can effectively reduce inflow from the hopper. A number of designs are shown in Figure 6-10.



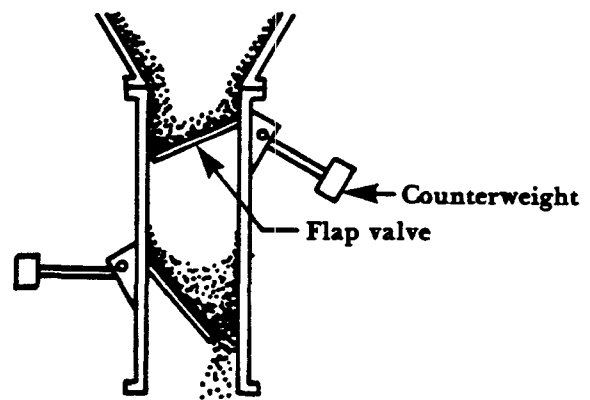
a. Simple manual slide gate



c. Discharge screw feeder



b. Rotary valve



d. Automatic flap valve

Figure 6-10. Discharge systems.

A valve between the cyclone and bin can be a simple manual device as shown in Figure 6-10a, or can provide a continuous discharge as with the rotary valve and screw feeder shown in Figures 6-10b and c. Automatic flap valves shown in Figure 6-10d can periodically swing to discharge accumulated dust in a double-valved arrangement.

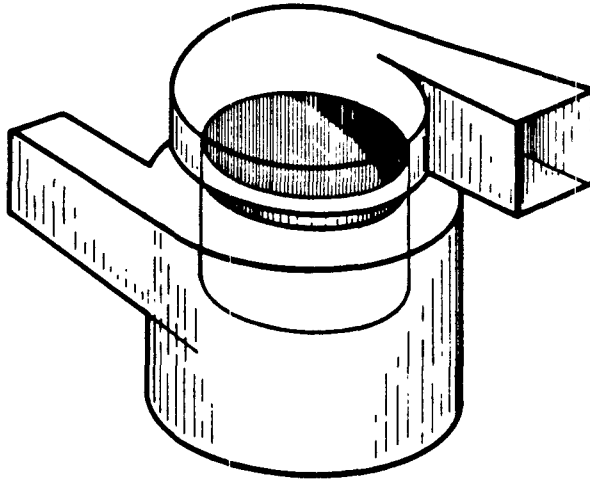
Cyclone efficiency can also be improved if a portion of the flue gas is drawn through the hopper. An additional vane or lower pressure duct can provide this flow. However, it may then become necessary to recirculate or otherwise treat this purge exhaust to remove uncollected particulate matter.

Cyclone Gas Outlet

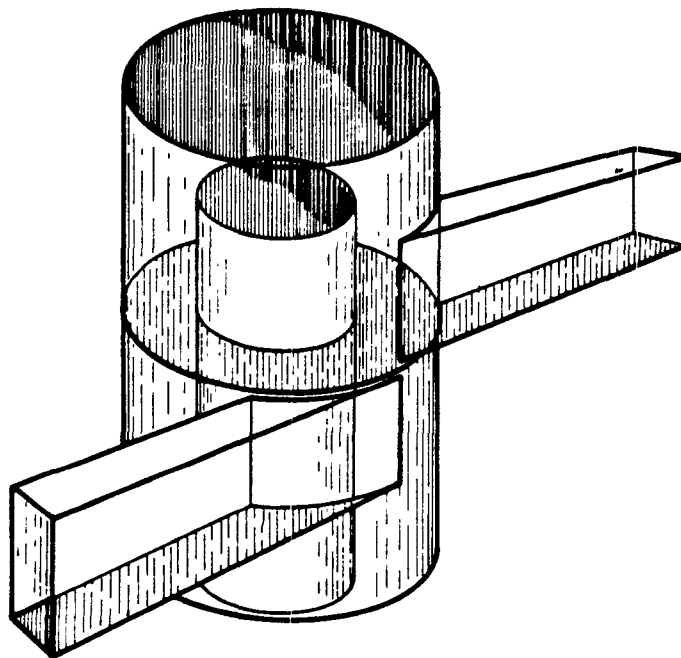
The exit tube is an important consideration in the design of any cyclone. Its length must extend beyond the inlet so that the eddies created in the annulus between the tube and the walls do not mix particles up and into the exit tube.

Some of the energy due to the radial motion of the ascending gases can be recovered by the application of *scroll devices* or by placing *outlet drums* on top of the exit tube (Figure 6-11). These are essentially flow straighteners and can effectively reduce the pressure drop across the cyclone without reducing collection efficiency. This is a unique situation since most other modifications which reduce the pressure drop in a cyclone also reduce the efficiency. For example, straightening vanes added to the inside or bottom of the outlet tube can suppress the vortex and therefore reduce efficiency (Stern, 1955).

It should be apparent from the above discussion, that many things will affect the efficiency and pressure drop of a cyclone. Although the manufacturers of these control devices will start with an optimized set of dimensions such as those given in Table 6-1 "...there is no single cyclone design which will perform best for all dust collection problems" (Leith, 1973). Basic process characteristics such as dust caking properties, particle size distributions, and gas volumetric flow rates and temperatures must be considered. Most of the theoretical cyclone design equations have been developed for simple cyclones not having modifications such as skimmers and outlet drums. The basic design equations can, however, in some cases be used to compare the performance of similar cyclones.



a. Involute scroll outlet



b. Outlet drum

Figure 6-11. Cyclone outlet devices.

Characterizing Cyclone Performance

Objects moving in circular paths tend to move away from the center of their motion. The object moves outward as if a force were pushing it out. This force is known as centrifugal force. The whirling motion of the gas in a cyclone causes particulate matter in the gas to feel this force and move out to the walls. An expression for this phenomenon is as follows:

$$(Eq. 6-1) \quad F = \frac{\rho_p d_p^3 v_p^2}{r}$$

Where: ρ_p = particle density, lb/ft³ (kg/m³)
 d_p = particle diameter, in. (μ m)
 v_p = particle tangential velocity, ft/sec (m/sec)
 r = radius of the circular path, ft (m)

F is the force that the particulate matter views as acting on it. This expression explains several of the cyclone characteristics discussed in the previous section. For example, $\rho_p d_p^3$ is merely proportional to the mass of the particle. The larger the mass, the greater the force. The tendency to move toward the walls is consequently increased and larger particles are more easily collected. The reason all of the particles don't move to the wall is because of the drag resistance of the air. The buffeting molecules in the gas resist the outward motion and act like an opposing force. Particles move to the wall when the centrifugal force is greater than the opposing drag force.

Note also from Equation 6-1, that as r (the radius of the circular path) decreases, the force again increases. This is why smaller cyclones are more efficient for the collection of smaller sized particles than are large cyclones.

These types of considerations in conjunction with considerations of cyclone geometry, and vortex formation have led to the development of numerous performance equations. These equations attempt to characterize the behavior of cyclones. Some work well and some do not (Leith, 1973). None adequately describe performance under all operating conditions, such as at high pressure and high temperatures (Parker, 1981).

There are three important parameters which can be used to characterize cyclone performance. These are:

$[d_p]_{cut}$ = cut diameter
 Δp = pressure drop
 η = overall collection efficiency

Equations for each of these parameters will be given in this section. The equations should be used with caution, however, since there are strict limitations on their applicability.

Cut Diameter

The cut diameter is defined as the size (diameter) of particles collected with 50% efficiency. It is a convenient way of defining efficiency for a control device since it gives an idea of the effectiveness for a particle size range.

A frequently used expression for cut diameter is that given by Lapple (1965):

$$(Eq. 6-2) \quad [d_p]_{cut} = \sqrt{\frac{9\mu B_c}{2\pi n_t v_i (\rho_p - \rho_s)}}$$

Where: μ = viscosity, lbs/sec ft (Pa·s)
 n_t = effective number of turns (5 to 10 for common cyclone)
 v_i = inlet gas velocity, ft/sec (m/sec)
 ρ_p = particle density, lbs/ft³ (kg/m³)
 ρ_s = gas density, lbs/ft³ (kg/m³)
 B_c = inlet width, ft (m)

The cut diameter, $[d_p]_{cut}$, is a characteristic of the control device and should not be confused with the geometric mean particle diameter, d_{gm} , of the size distribution.

Figure 6-12 shows a size efficiency curve and points out the cut diameter and the critical diameter, $[d_p]_{crit}$, the particle size collected at 100% efficiency. Values of $[d_p]_{crit}$ are difficult to obtain from such curves so the cut size is often determined instead.

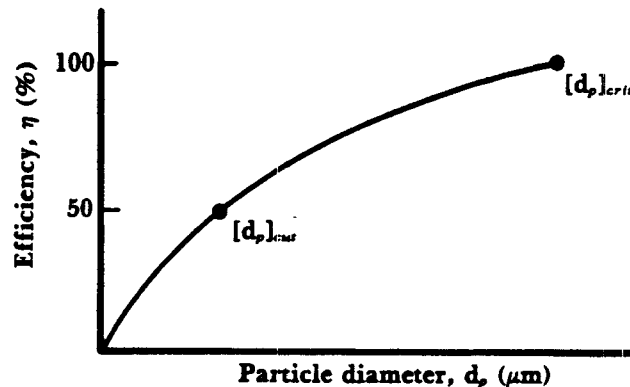
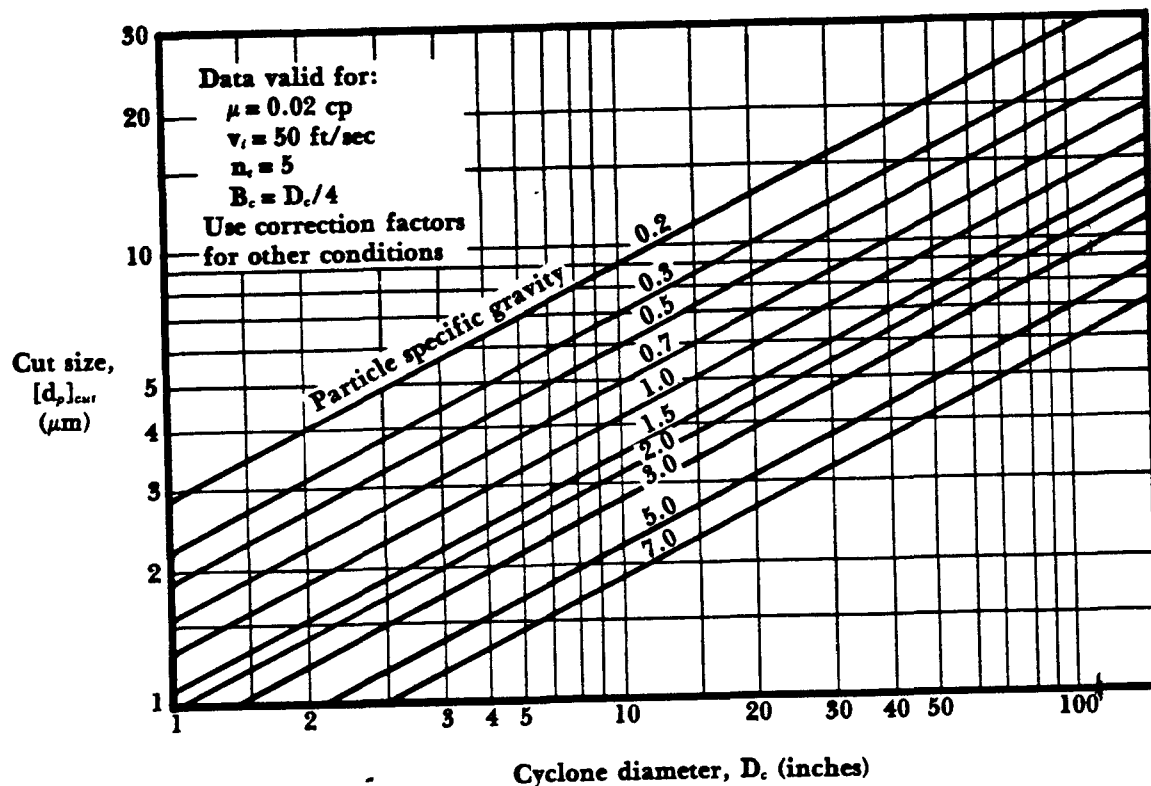


Figure 6-12. Typical size efficiency curve.

A number of formulas exist for the calculation of the cut diameter and critical diameter. Stern (1955) and Strauss (1975) review a number of the expressions. A value of n_t , the number of turns, must be known in order to solve Equation 6-2 for $[d_p]_{cut}$. Given the volumetric flow rate inlet velocity, and dimensions of the cyclone, n_t can be easily calculated (Strauss, 1975).

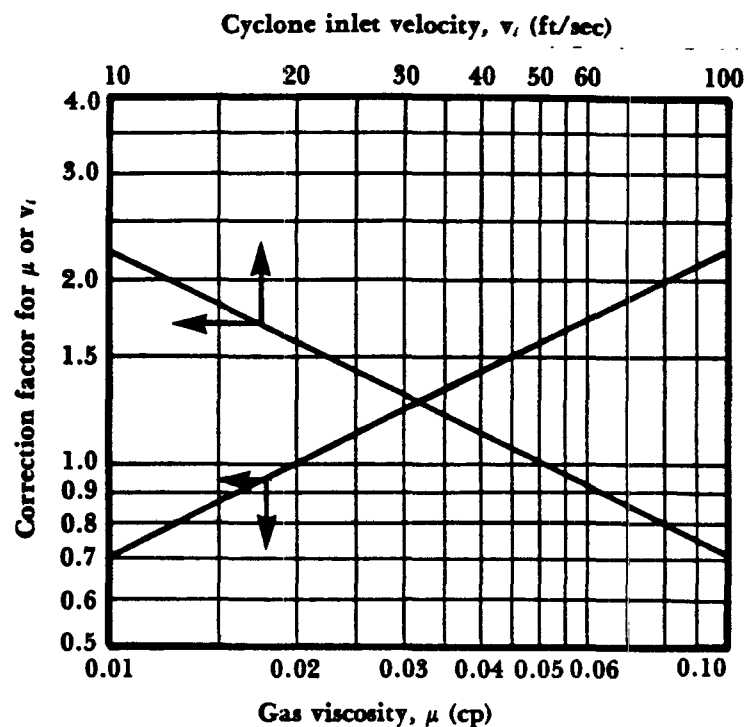
Using Figure 6-13a, Equation 6-2 can be solved graphically for a conventional cyclone having the relative dimensions given in Table 6-1 and if n_t is assumed to equal 5. (Lapple, 1951. See also USEPA AP 40, Air Pollution Engineering Manual).



Source: EPA, 1973.

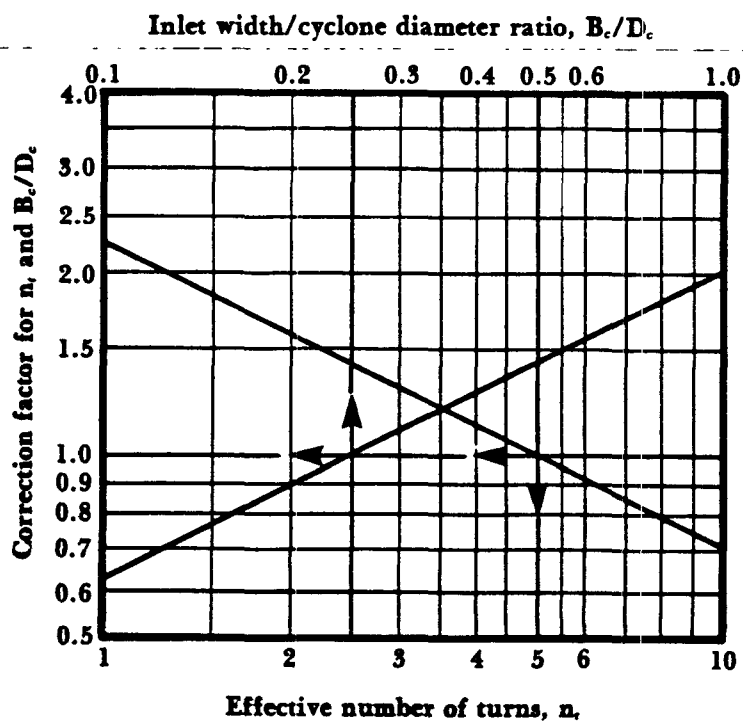
Figure 6-13a. Cut size in micrometers for cyclones of conventional type.

Figure 6-13a assumes certain values for inlet velocity, viscosity, number of turns and relative dimensions. Figures 6-13b and c could be used to correct the $[d_p]_{cut}$ of Figure 6-13a if these values are different from those assumed.



Source: EPA, 1973.

Figure 6-13b. Viscosity and velocity correction factors for cut size particle of conventional cyclones.



Source: EPA, 1973.

Figure 6-13c. Inlet width/cyclone diameter and effective number of turns correction factors for cut size particle of conventional cyclones.

The expression for the cut diameter (Equation 6-2) has been found to agree within $\frac{1}{2}$ micrometer for some experimental data (Lucas, 1974). However, other experimental work (Parker, 1981) has shown limitations to its application. A high efficiency cyclone will have a cut diameter of typically 5 to 10 micrometers. Equation 6-2 is typical of most of those devised for determining the cut or critical diameter. Note that an increase in the number of turns, inlet velocity, or the particle density will decrease the cut size as one would expect. A decrease in viscosity will decrease the drag force opposing the centrifugal force and therefore also reduce the cut size (i.e. smaller size particles will be collected).

Pressure Drop

The pressure drop across a cyclone is an important parameter to the purchaser of such equipment. Increased pressure drop means greater costs for power to move exhaust gas through the control device. With cyclones, an increase in pressure drop usually means that there will be an improvement in collection efficiency (one exception to this is the use of pressure recovery devices attached to the exit tube; these reduce the pressure drop but do not adversely affect collection efficiency). For these reasons, there have been many attempts to predict pressure drops from design variables. The idea is that having such an equation, one could work back and optimize the design of new cyclones.

One of the simplest pressure drop equations which correlates reasonably well with the experiment (Leith, 1973) is that developed by Shepherd and Lapple (1939).

(Eq. 6-3) *use this equation*
$$\Delta p = \frac{v_i^2 \rho_g}{2g\rho_m} K_c \frac{H_c B_c}{D_c^2} \quad (\text{Consistent units})$$

Where: ρ_g = gas density
 ρ_m = density of measuring manometer fluid used to determine v_i
 g = gravitational constant

K_c is an empirical constant. It is equal to 16 for a cyclone with a standard tangential inlet and is equal to 7.5 for a cyclone with an inlet vane. A correlation coefficient of 0.77 between experimental data and calculations based on Equation 6-3 was found by Leith (1977). Perfect correlation equals 1.0. None of the pressure drop equations were found to have better than a 0.80 correlation coefficient.

Another expression frequently used is that given by First (1950).

(Eq. 6-4)
$$\Delta p = \frac{0.0027 Q^2}{k_c D_c^2 B_c H_c \left(\frac{L_c}{D_c}\right)^{1/3} \left(\frac{Z_c}{D_c}\right)^{1/3}} \quad (\text{Consistent units})$$

Where: Q = volumetric flow rate

(In this case k_c is a dimensionless factor descriptive of cyclone inlet vanes. It is equal to 0.5 for cyclones without vanes, 1.0 for vanes that do not expand the entering gas or touch the outlet wall, and 2.0 for vanes that expand and touch the outlet wall.) This equation, when compared to experimental data was found to have a correlation coefficient of only 0.53 (Leith, 1977).

It should be noticed from both of these equations that the pressure drop is a function of the square of the inlet velocity. Most of the empirical pressure drop equations have the form:

$$\text{(Eq. 6-5)} \quad \Delta p = K_c' Q_i v_i^2 \quad \text{(Consistent units)}$$

Where: K_c' = a proportionality factor

If Δp is measured in inches of water, K_c' can vary from 0.013 to 0.024. Velocities for cyclones range from 20 to 70 ft/sec (6 to 21 m/sec), although common velocities range from 50 to 60 ft/sec (15 to 18 m/sec). At velocities greater than 80 ft/sec (24 m/sec), turbulence increases in the cyclone and efficiency will actually decrease. Also, at high loads of particulate matter and high velocities, scouring of the cyclones by the particles will rapidly increase. To minimize erosion in such cases, a cyclone would be designed for lower inlet velocities.

Pressure drops for single cyclones vary depending upon both size and design. Common ranges are:

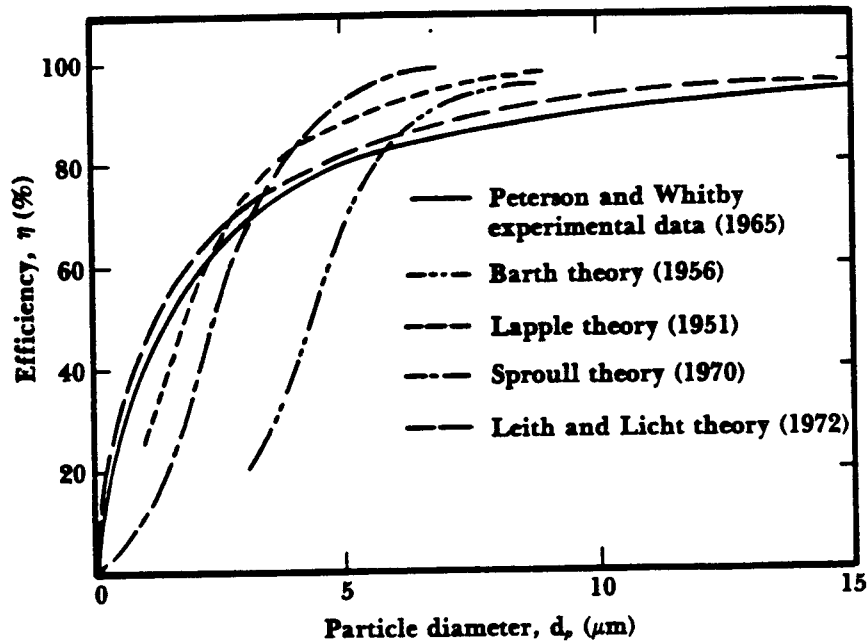
low efficiency cyclones	2-4" H ₂ O (5-10 cm H ₂ O)
medium efficiency cyclones	4-6" H ₂ O (10-15 cm H ₂ O)
high efficiency cyclones	8-10" H ₂ O (20-25 cm H ₂ O)

Collection Efficiency

A number of formulations have been developed for determining the fractional cyclone efficiency, η_i , for a given size particle. Fractional efficiency is defined as the fraction of particles of a given size collected in the cyclone, compared to those of that size going into the cyclone. An excellent discussion and comparison of these theories is given by Leith (1973). Figure 6-14 reproduced from Leith (1973) gives an estimate of the applicability of several theories for the calculated efficiency of a simple cyclone.

No efficiency theory or calculation method provides a description for all cyclones. The modification of inlets and outlets, addition of fines eductors, etc. introduce variables which are difficult to treat theoretically. Although theoretical efficiencies can give estimations of cyclone performance, it should be kept in mind that designers of equipment commonly rely on comparative evaluations between similar designs and on experience.

This section will describe two methods of calculating cyclone efficiency. The Leith and Licht theory for calculating fractional efficiency will be discussed first. A convenient graphical method for estimating efficiency, developed by Lapple (1951), will also be discussed.



Source: Leith and Mehta, 1973.

Figure 6-14. Cyclone efficiency versus particle diameter.
Experimental results and theoretical predictions.

Leith and Licht Theory

The fractional efficiency equation of Leith and Licht has a form similar to many of those developed for particulate control devices. Fractional efficiency is expressed as:

$$\text{(Eq. 6-6)} \quad \eta_i = 1 - e^{[-2(c\psi)^{1/(2n+2)}]}$$

Where: η_i = fraction efficiency
 c = cyclone dimension factor
 ψ = impaction parameter
 n = vortex exponent

This exponential form is quite common since it can give the general form of efficiency plots such as shown in Figure 6-14. In this expression, c is a factor which is a function only of the cyclone's dimensions. The symbol ψ , expresses characteristics of the particles and gas as:

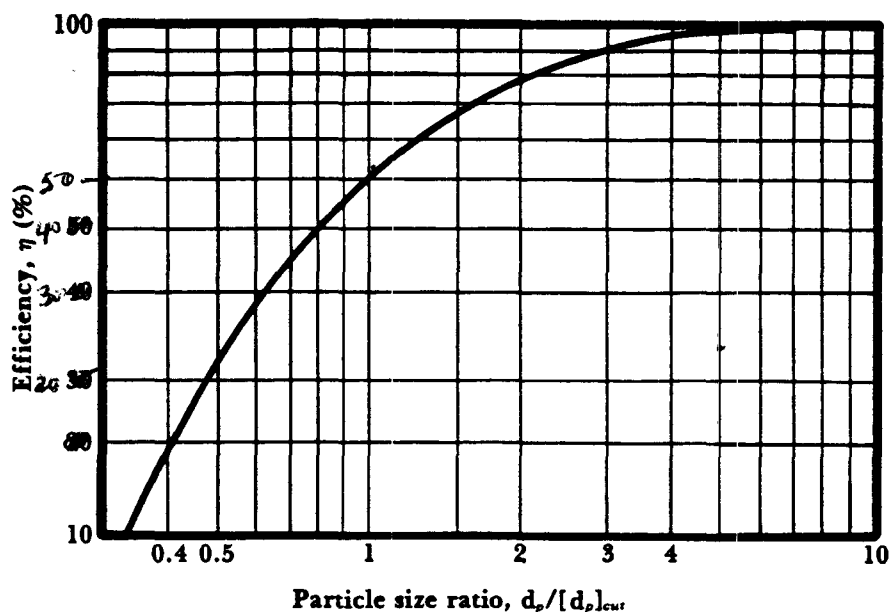
$$\text{(Eq. 6-7)} \quad \psi = \frac{\rho_p d_p^2 v_i}{18\mu D_c} (n+1)$$

and is known as *inertia* or *impaction* parameter. Note that ρ_p times v_i essentially expresses the particle's initial momentum. The value of n is dependent upon the cyclone diameter and temperature of the gas stream.

The calculations involved in this method are straightforward, although tedious. The original reference (Leith, 1973) should be consulted if it is to be applied. The method has also been extended to provide a graphical method of optimizing certain parameters of cyclone design (Koch, 1977).

Lapple Method

An older method of calculating cyclone fractional efficiency and overall efficiency was developed by Lapple (1951). (See also USEPA AP 40, Air Pollution Engineering Manual, pp. 94-99). Lapple first computed the ratios $d_p/[d_p]_{cut}$, the particle diameter versus the cut diameter as determined from Equation 6-2 or Figure 6-12. He found that cyclone efficiency correlates in a general way with this ratio. For a common cyclone, efficiency will increase as the ratio increases as shown in Figure 6-15.



Source: Lapple, 1951.

Figure 6-15. Cyclone efficiency versus particle size ratio.

As a universal curve for common cyclones, this correlation has been found to agree within 5% at a $d_p/[d_p]_{cut}$ near 1.0 (AP 40). To calculate fractional efficiencies, the following procedure is followed:

1. Calculate $[d_p]_{cut}'$ for the cyclone being investigated using Equation 6-2 or Figure 6-12.
2. Multiply $[d_p]_{cut}'$ times several values of the ratio $d_p/[d_p]_{cut}$ given in Figure 6-15.
3. Replot the efficiency given at each $d_p/[d_p]_{cut}$ versus the values obtained in step 2, $(d_p/[d_p]_{cut}) \times [d_p]_{cut}'$.

The replot will give the fractional efficiency curve for the cyclone being evaluated. Since this procedure only gives an estimate (see Figure 6-14 for relative deviations), in practice, a range of $[d_p]_{cut}$ values are used instead of a single value. Maximum and minimum curves determined from these values will then give a range of efficiency for estimation purposes.

The overall efficiency can also be determined if the inlet particle size distribution is known. This can be easily done by constructing a table with the following headings:

d_p range	wt % in range	$d_p/[d_p]_{cut}$	η_i for each d_p from experiment or Lapple's method (%)	wt % $\times \eta_i$ %
----------------	------------------	-------------------	---	------------------------

The fractional efficiency (η_i) for each $(d_p/[d_p]_{cut}) \times [d_p]_{cut}$ is found using the previous method. Each fractional efficiency is multiplied times the weight percent in each range. The sum of these products in the last column will give the overall efficiency.

Summary of Performance Characteristics

Efficiency, pressure drop, and costs are intimately related in cyclones as they are with most other particulate control equipment. Many factors affect efficiency and pressure drop. A number of factors can be taken into account in the theoretical formulations, others cannot. A thorough evaluation of cyclone design will depend on previous experience or empirical information derived from experiments on similar cyclones.

A summary of changes in performance characteristics produced by changes in cyclone design and exhaust gas properties is given in Table 6-2.

Table 6-2. Changes in performance characteristics.

Cyclone and process design changes	Pressure drop	Efficiency	Cost
Increase cyclone size (D_c)	Decreases	Decreases	Increases
Lengthen cylinder (L_c)	Decreases slightly	Decreases	Increases
Lengthen cone (Z_c)	Decreases slightly	Increases	Increases
Increase exit tube diameter (D_e)	Decreases	Decreases	Increases
Increase inlet area — maintaining velocity	Increases	Decreases	Decreases
Increase velocity	Increases	Increases	Operating costs higher
Increase temperature (maintaining velocity)	Decreases	Decreases	No change
Increased dust concentration	Decrease for large increases	Increases	No change
Increasing particle size and/or density	No change	Increases	No change

Source: Bhatia and Cheremisinoff, 1977.

It should be remembered that the addition of fines eductors (skimmers) can also increase efficiency with little effect on pressure drop. Adding water sprays to wet the walls can also improve performance.

Cyclone Arrangements

It should be apparent from the above discussion that small cyclones are more efficient than large cyclones. Small cyclones, however, have a higher pressure drop and are limited with respect to volumetric flow rates. Smaller cyclones can be arranged either in series or in parallel to substantially increase efficiency at lower pressure drops. These gains are somewhat offset however, by increased maintenance problems. Multicyclone arrangements tend to plug more easily. When common hoppers are used in such arrangements, different flows through cyclones can lead to reentrainment problems.

Series Arrangements

A typical series arrangement is shown in Figure 6-16.

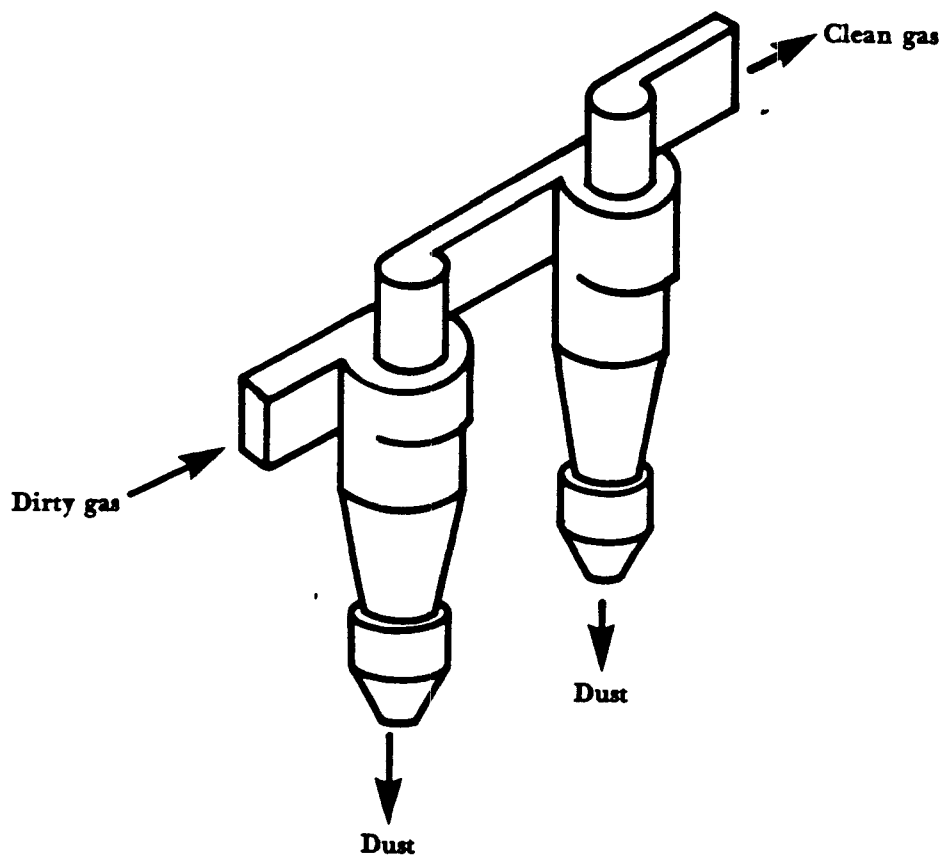


Figure 6-16. Cyclones in series.

Larger particles can be collected in the first cyclone and a smaller, more efficient cyclone can collect smaller particles. Such an arrangement can reduce dust loading in the second cyclone and avoid problems of abrasion and plugging. Also, if the first cyclone should plug there still will be some collection occurring in the second cyclone. The additional pressure drop produced by the second cyclone adds to the overall pressure drop of the system. The higher pressure drop can be a disadvantage in such a series system design.

Parallel Arrangements

Many types of parallel arrangements have been designed for cyclones. An example of a parallel arrangement using tangential entry cyclones is shown in Figure 6-17.

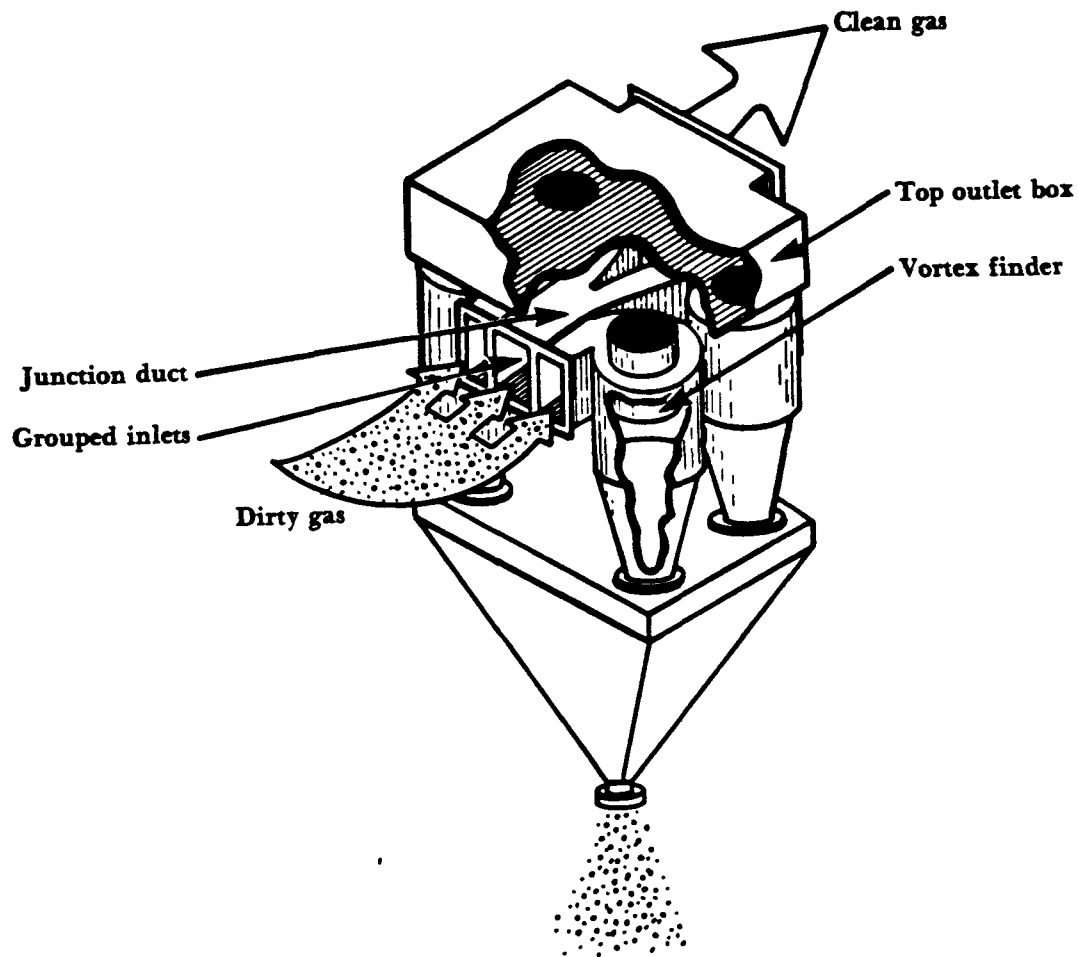


Figure 6-17. Battery of four involute cyclones in parallel.

With batteries of cyclones using a common inlet plenum, higher volumes of gas can be treated at reasonable pressure drops. In configurations where a common hopper is used, each cyclone should have the same pressure drop or the gas will preferentially channel through one cyclone or several cyclones.

Another type of parallel arrangement uses the axial entry cyclone shown in Figure 6-16. Arrangements of high efficiency, small diameter axial cyclones can provide increases in collection efficiency with reductions in pressure drop, space, and cost. Such a multiclone arrangement is shown in Figure 6-18. Pressure drops commonly range from 4 to 6 inches (10 to 15 cm) of water.

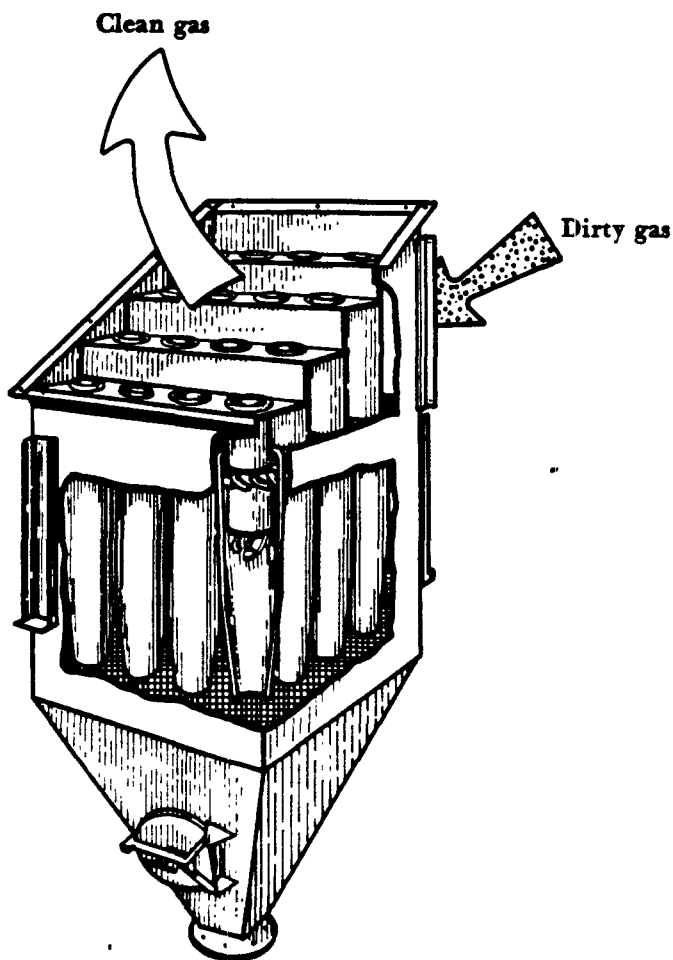


Figure 6-18. Battery of vane axial cyclones.

The axial entry minimizes the eddy formation that is common in tangential entry cyclones. Here, the inlet guide vanes create the vortex.

Care must be taken in designing the inlet plenum for the multiclone since the inlet exhaust gas should have an even distribution to each individual cyclone. Sticky materials should not be collected using multiclones since the vanes and smaller outlet tubes are quite prone to plugging. A good discussion of operation and maintenance problems occurring with multiclones is given by Schneider (1975).

References

1. Bethea, R. M. 1978. *Air Pollution Control Technology*. New York: Van Nostrand Reinhold, pp. 117-144.
2. Bhatia, M. V. and Cheremisinoff, P. N. 1977. Cyclones. In *Air Pollution Control and Design Handbook*. P. N. Cheremisinoff and R. A. Young, eds. pp. 281-316, New York: Marcel Dekker, Inc.
3. Caplan, K. 1964. All About Cyclone Collectors. *Air Eng.* Sept.: 28-38.
4. Caplan, K. 1977. Source Control by Centrifugal Force and Gravity. In *Air Pollution Vol. IV Engineering Control of Air Pollution*, A. C. Stern, ed. pp. 97-148, New York: Academic Press.
5. Danielson, J. A., ed., 1973. *Air Pollution Engineering Manual*, Research Triangle Park, NC: US Environmental Protection Agency, pp. 91-99.
6. Doerschlag, C. and Miczek, G. 1977. How to Choose a Cyclone Dust Collector. *Chem. Eng.* Feb.: 64-72.
7. Hesketh, H. E. 1979. *Air Pollution Control*. Ann Arbor: Ann Arbor Science Publishers, pp. 184-193.
8. Koch, W. H. and Licht, W. 1977. New Design Approach Boosts Cyclone Efficiency, *Chem. Eng.* Nov.: 79-88.
9. Leith, D. and Mehta, D. 1973. Cyclone Performance and Design. *Atmos. Environ.* 7:527-549.
10. McCarty, R. E. 1962. How to Evaluate and Specify Mechanical Dust Collectors. *Air Eng.* Feb.: 22-49.
11. Parker, R.; Jain, R.; Calvert, S.; Drehmel, D.; and Abbott, J. 1981. Particle Collection in Cyclones at High Temperature and High Pressure. *Environ. Sci. Technol.* 15:451-458.
12. Schneider, A. G. 1975. Mechanical Collectors. In *Handbook for the Operation and Maintenance of Air Pollution Control Equipment*, F. L. Cross, Jr. and H. E. Hesketh, eds. pp. 41-68, Westport: Technomic Publishing.
13. Stern, A. C., Caplan, K. J., and Bush, P. D. 1955. *Cyclone Dust Collectors*. Amer. Petrol. Inst., New York.
14. Strauss, W. 1975. *Industrial Gas Cleaning. International Series in Chemical Engineering*, Vol. 8. Oxford: Pergamon Press, pp. 216-276.
15. Theodore, L. and Buonicore, A. J. 1976. *Industrial Air Pollution Control for Particulates*. Cleveland: CRC Press, pp. 91-137.
16. Lapple, C. E., 1951. Processes Use Many Collection Types. *Chem. Eng.* 58:145-51 (May).
17. Shepherd, C. B. and Lapple, C. E. 1939. Flow Pattern and Pressure Drop in Cyclone Dust Collectors. *Ind. Eng. Chem.* 31:972-984.

Chapter 7

Electrostatic Precipitators

Introduction

The fundamental principles underlying the application of electrostatic forces to precipitate particles suspended in a gas were known in the 18th century, however, the successful development of a device that employed electrical gas cleaning methods did not take place until professor Fredrick Cottrell designed and built the first industrial ESP at the Detroit-Edison Trenton Channel Steam generator in 1923. Today there are thousands of ESPs in operation for the control of fly ash emissions from steam generators. The ESP is also an effective device for controlling emissions from cement kilns, pulp and paper plants, acid plants, sintering operations, and other industrial sources. The method is extensively used where dust emissions are less than 10-20 μm in size with a predominant portion in the submicron range.

The electrostatic precipitator is comprised of four essential components, each of which will be discussed in detail in this chapter (see Figure 7-1). The major components are:

- discharge electrodes
- collection electrodes
- rappers
- hoppers

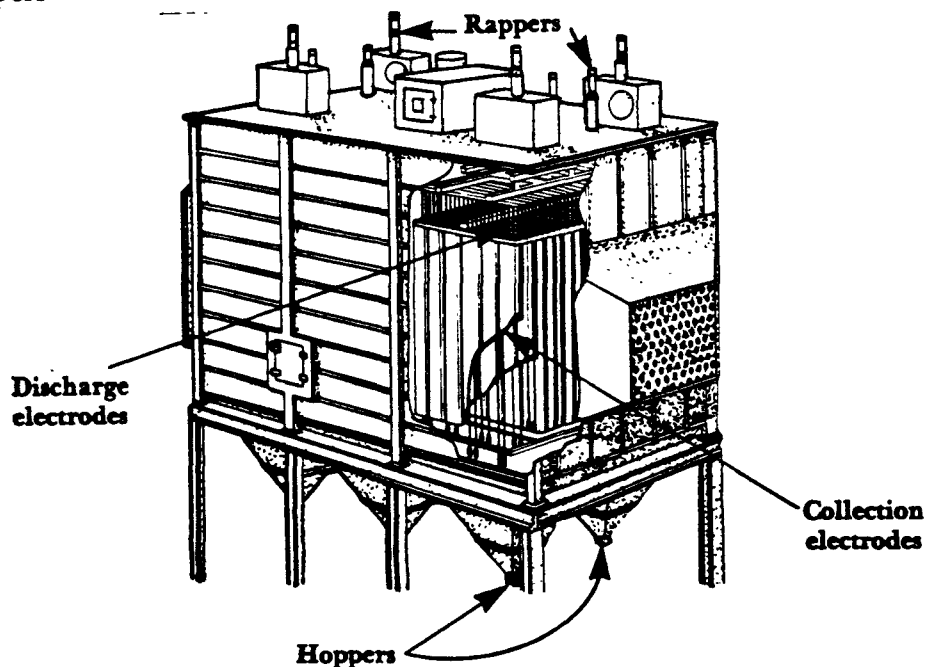


Figure 7-1. Typical plate and wire single-stage electrostatic precipitator.

The discharge electrode is normally a wire where a corona discharge occurs. This electrode is used to ionize the gas (which charges the particles) and create an electric field. The collection electrode consists of either a tube or flat plate which is oppositely charged (relative to the discharge electrode) and is the surface where the charged particles are collected. The rapper is a device used to impart a vibration or shock to dislodge the deposited dust on the electrodes. Rappers are used to remove dust accumulated on both the collection electrodes and discharge electrodes. Hoppers are located at the bottom of the precipitator and are used to collect and store the dust removed by the rapping process.

Types of ESPs

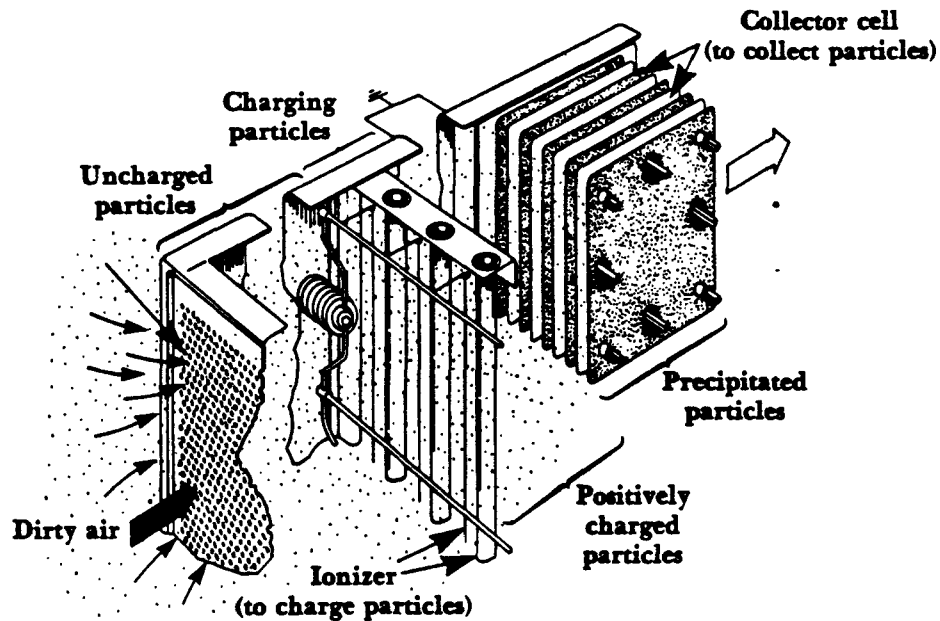
There are basically two types of electrostatic precipitators: high voltage single-stage and low voltage two-stage. The high voltage single-stage precipitator is the more popular type and has been used successfully to collect both solid and liquid particulate matter in industrial facilities such as smelters, steel furnaces, cement kilns, municipal incinerators, and utility boilers. Low voltage two-stage precipitators are limited almost exclusively to the collection of liquid aerosols discharged from sources such as meat smokehouses, pipe coating machines, asphalt paper saturators, and high speed grinding machines.

Low Voltage, Two-Stage ESP

Low voltage two-stage precipitators were originally designed for air purification in conjunction with air conditioning systems (they are also referred to as electronic air filters). Two-stage ESPs have been used primarily for the control of finely divided liquid particles. Controlling solid or sticky materials is usually difficult, and the collector becomes ineffective for dust loadings greater than 0.4 grains per standard cubic foot (7.35×10^{-4} g/m³). Therefore, two-stage precipitators have limited use for particulate emission control.

The low voltage two-stage precipitator differs from the high voltage single-stage precipitator in terms of both design and amount of applied voltage. The two-stage ESP has separate particle charging and collection stages (Figure 7-2). The ionizing stage consists of a series of small (0.007 inch diameter) positively charged wires equally spaced 1 to 2 inches from parallel grounded tubes or rods. A corona discharge between each wire and a corresponding tube charges the particles suspended in the air flow through the ionizer. The direct-current potential applied to the wires is approximately 12 to 13 kV.

The second stage consists of parallel metal plates less than 1 in. (2.5 cm) apart. The liquid particles receive a positive charge in the ionizer stage and are collected at the negative plates in the second stage. Collected liquids drain by gravity to a pan located below the plates.



Source: EPA, 1973.

Figure 7-2. Typical two-stage precipitator.

High Voltage, Single-Stage

The two major types of high voltage single-stage ESP configurations are tubular and plate. Particles are both charged and collected in a single stage.

Tubular precipitators consist of cylindrical collection electrodes with discharge electrodes located in the center of the cylinders. Dirty gas flows into the cylinder where precipitation occurs. The negatively charged particles migrate to and are collected on grounded collecting tubes. The collected dust or liquid is removed by washing the tubes with water sprays located directly above the tubes (Figure 7-3). These precipitators are generally referred to as water-walled ESPs. Tubular precipitators are generally used for collecting mists or fogs. Tube diameters typically vary from 0.5 to 1 ft (0.15 to 0.31 m), with length usually ranging from 6 to 15 ft (1.85 to 4.6 m).

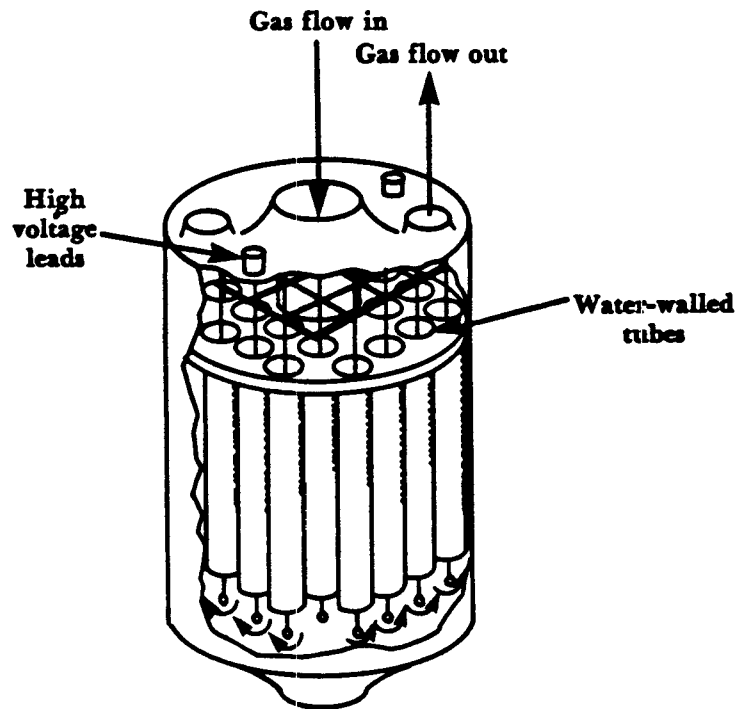


Figure 7-3. Gas flow through wire and tubular pipe precipitators.

Plate electrostatic precipitators are used more often than tubular ESPs in industrial applications. High voltage is used to subject the particles in the gas stream to an intense electric field. Dirty gas flows into a chamber consisting of a series of discharge electrodes (wires) spaced along the center line of adjacent plates (Figure 7-4).

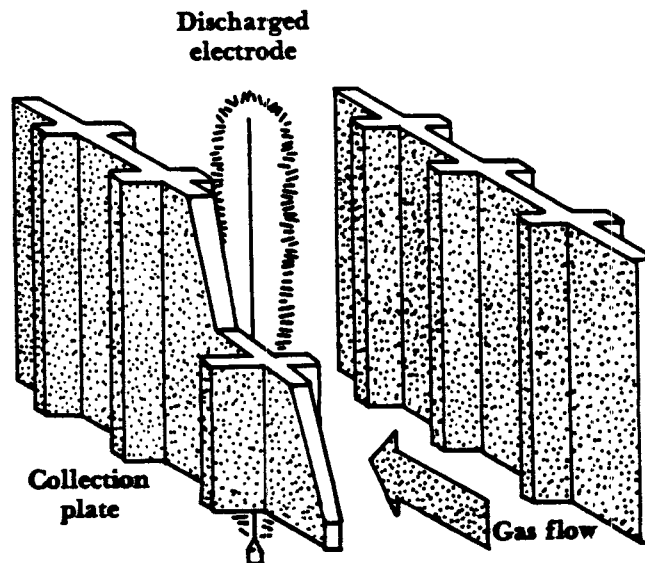


Figure 7-4. Gas flow through a wire and plate precipitator.

Charged particles migrate to and are collected at oppositely charged collection plates. Collected particles are usually removed by rapping (dry precipitator) or by a liquid film (wet precipitator). Particles fall by force of gravity into hoppers where they are stored prior to removal and final disposal. The remainder of the chapter will be devoted to the high voltage single-stage plate ESP.

Theory of Precipitation

Charging the Particles

Electrostatic precipitation occurs in the space between the discharge electrode and the collection surface. A high voltage, pulsating direct current is applied to an electrode system consisting of a small diameter discharge electrode, which is usually negatively charged, and a collecting plate electrode, which is grounded. This produces a unidirectional, nonuniform electric field whose magnitude is highest near the discharge electrode (Figure 7-5).

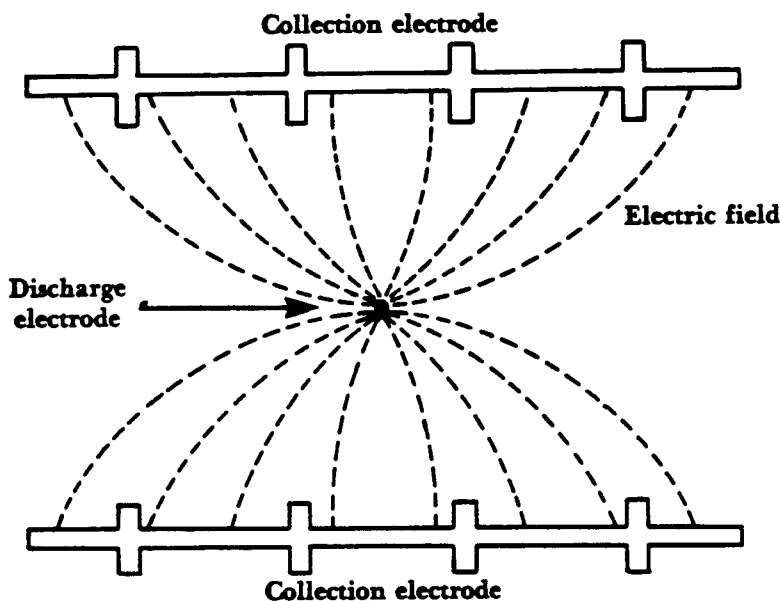


Figure 7-5. Electric field generation (top view).

Corona Generation

The applied voltage is increased until it produces a corona discharge (corona), which can be seen as a luminous blue glow around the discharge electrode. The corona is a discharge phenomenon in which gaseous molecules are ionized by electron collisions in the region of a high electric field. The intense electric field close to the discharge electrode accelerates the free electrons that are present in the gas. These electrons acquire sufficient velocity to ionize gas molecules upon collision; producing a positive ion and an additional free electron (Figure 7-6).

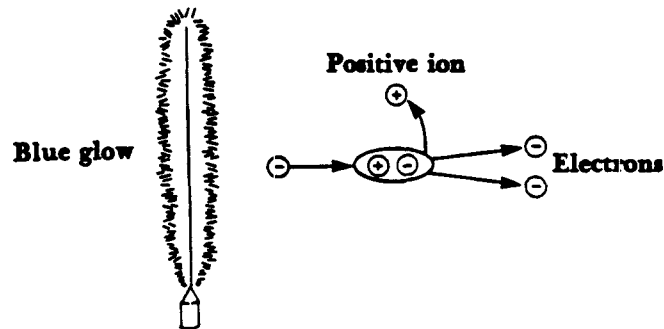


Figure 7-6. Generation of corona.

The additional free electrons create more positive ions and free electrons as they collide with additional gas molecules. This process is called *avalanche multiplication*, and occurs in the corona glow region (Figure 7-7). Avalanche multiplication will continue until the local electric field strength decreases to the point where there is insufficient energy to perpetuate ionization.

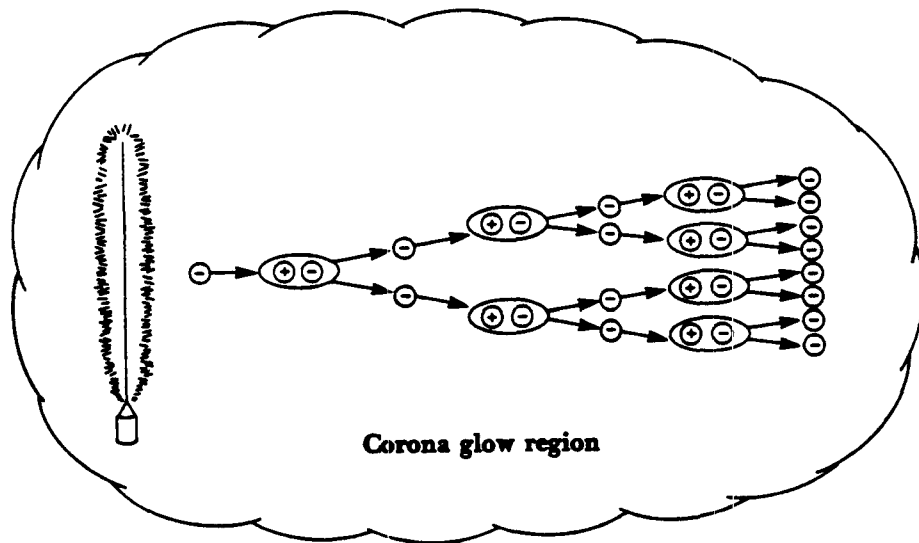


Figure 7-7. Avalanche multiplication.

The sluggish positive ions migrate back to the negative discharge electrode and form new free electrons upon impaction with the discharge wire or gas space around the wire. The electrons produced during the avalanche multiplication process follow the electric field toward the grounded collection electrode.

The electrons leave the corona region and enter the inter-electrode region. The magnitude of the electric field is diminished and the free electrons' velocity decreases. When electrons impact on gas molecules in the inter-electrode region, they are captured, and negative gas ions are created (Figure 7-8). These negative ions serve as the principal mechanism for charging of the dust.

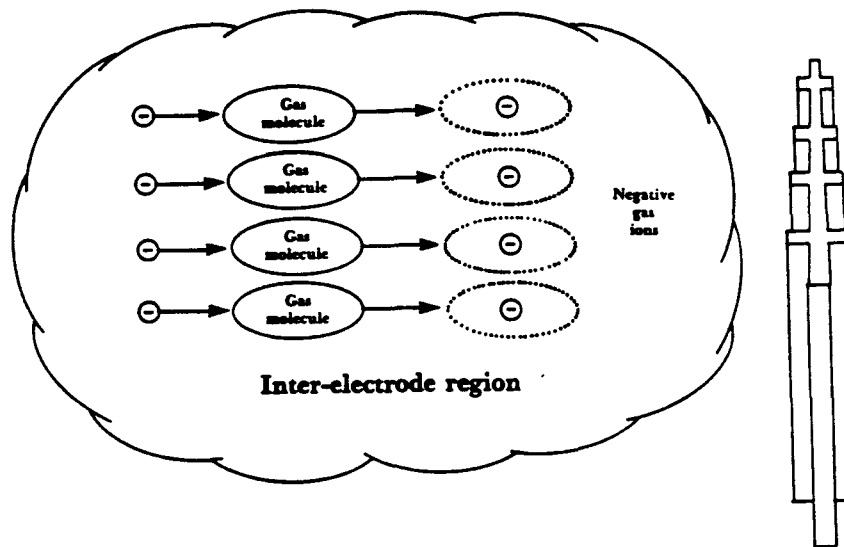


Figure 7-8. Gas ionization in the inter-electrode region.

Negative gas ions migrate toward the grounded collection electrode. A space charge which is a stable concentration of negative gas ions forms in the inter-electrode region. Increases in the applied voltage will increase the field strength and ion formation until sparkover occurs. Sparkover refers to internal sparking between the discharge and collection electrodes. It is a sudden rush of localized electric current through the gas layer between the two electrodes. Sparking causes an immediate short-term collapse of the electric field. In general, it is very desirable to operate at voltages high enough to cause some sparking but not at a frequency such that the electric field constantly collapses. The average sparkover rate for optimum precipitator operation is between 50 and 100 sparks per minute. At this spark rate the gains in efficiency associated with increased voltage compensates for decreased gas ionization due to collapse of the electric field. For optimum efficiency the electric field strength should be as high as possible. This is accomplished by applying a high voltage to the discharge electrode and the consequent high corona current flow from the discharge electrode to the collection electrode.

Field and Diffusion Charging

The negative gas ion movement has two main charging effects on dust particles in the inter-electrode region. These effects are called field charging and diffusion charging. Each type of charging is used to some extent in particle charging, but one dominates depending on the particle size. Field charging dominates for particles with a diameter $> 1.0 \mu\text{m}$, while diffusion charging dominates for particles with a diameter between 0.1 and $0.3 \mu\text{m}$. A combination of the two mechanisms occurs for particles in the range between 0.3 and $1.0 \mu\text{m}$ in diameter. It is also possible to charge particles by electron charging. In this case free electrons that do not combine with gas ions are moving at an extremely fast rate. These electrons hit the particle and impart a charge. However, this effect is responsible for very little particle charging.

In field charging, as particles enter the electric field they cause a local dislocation of the field (Figure 7-9). Negative gas ions traveling along the electric field lines collide with the suspended particles and impart a charge to them. The ions continue to bombard the particle until the charge on the particle is sufficient to divert the electric lines away from the charged particle. This prevents new ions from colliding with the dust particle. When a particle no longer receives an ion charge it is said to be saturated. Saturated charged particles then migrate to the collection electrode and are collected.

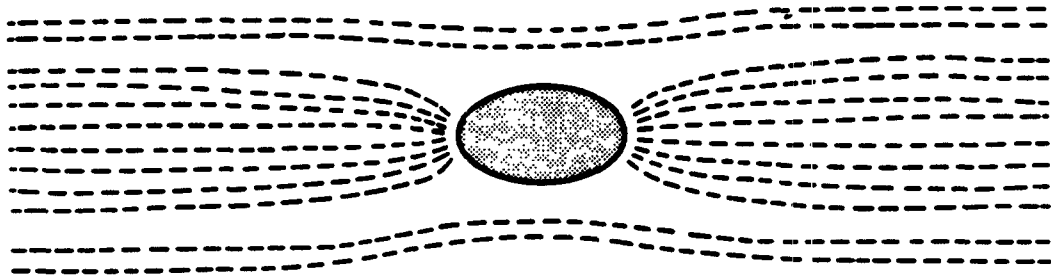


Figure 7-9. Field lines modified by the particle.

Diffusion charging is associated with the random Brownian motion of the negative gas ions. The random motion is related to the thermal velocity of the gas ions: the higher the temperature, the more movement. Negative ions collide with the particles because of the random thermal motion of the ions and impart a charge on the particle. The charged particles migrate to the collection electrode. This mechanism is important for charging particles in the submicron range. In the intermediate size range from 0.3 to $1.0 \mu\text{m}$ in diameter, both field and diffusion charging are important.

Discharging the Particle at the Collection Electrode

Resistivity is related to the ability of a particle to take on a charge. In most industrial applications, the resistivity of the particle is such that the charge on the particle is only partially discharged upon contact with the grounded collection electrode. A portion of the charge is returned and contributes to the intermolecular cohesive and adhesive forces which hold the particles to the collection surfaces. The dust layer builds up on the collection plate to a thickness between 0.03 and 0.5 in. (0.08-1.27 cm). If the dust layer becomes too thick, it is possible for the accumulated layer to act as an insulator, reducing the flow of the electric field lines.

Rapping Particles into the Hopper

To maintain the continuous process of precipitation, it is necessary to periodically remove collected dust particles from the discharge and collecting electrodes. In wet-walled precipitators, the electrodes are cleaned by washing with water sprays. In most other precipitators deposited dry particles are dislodged by mechanical impulses or vibrations to the electrodes, called *rapping*. The electrodes are rapped with sufficient intensity to cause particles collected on them to fall into a hopper.

Rapping is done when the accumulated dust layer is approximately 0.03 to 0.5 inches thick. This allows the dust layer to fall off the collecting plates as large aggregate sheets to help eliminate particle reentrainment. Most precipitators will use adjustable rappers that can change the rapping intensity and frequency according to dust grain-loading conditions. Rapping is done while the ESP is on-line.

Dislodged dust falls from the collecting plates into the hopper. The hopper is a simple collection bin. Hoppers should be cleaned frequently to prevent dust buildup. Most hoppers are emptied by some type of screw or pneumatic conveyor.

Collection Efficiency

Migration Velocity

Once the particle is charged, it migrates toward the grounded collection electrode. An indicator of particle movement toward the collection electrode is denoted by the symbol w and is called the particle migration velocity or drift velocity. The migration velocity parameter represents the collectability of the particle within the confines of a specific collector. The migration velocity can be expressed in terms of:

(Eq. 7-1)
$$w = \frac{d_p E_o E_p}{4\pi\mu}$$

Where:

- d_p = diameter of the particle, micrometers
- E_o = strength of field in which particles are charged, volts per meter
(represented by peak voltage)
- E_p = strength of field in which particles are collected, volts per meter
(normally the field close to the collecting plates)
- μ = viscosity of gas, Pascal•second

Migration velocity is quite sensitive to the voltage since the electric field appears twice in Equation 7-1. Therefore, the precipitator must be designed using the maximum electric field for maximum collection efficiency. The migration velocity is also dependent on particle size; larger particles are collected more easily than smaller ones.

Particle migration velocity can be determined by the following equation:

(Eq. 7-2)
$$w = \frac{qE_p}{6\pi\mu r}$$

Where: q = particle charge (charges)
 E_p = strength of field in which particles are collected (V/m)
 μ = gas viscosity (Pa·sec)
 r = radius of the particle (μm)

The particle migration velocity can be calculated using either Equation 7-1 or 7-2. However, most ESPs are designed using a particle migration velocity based on field experience rather than theory. Typical particle migration velocity rates such as those listed in Table 7-1 have been published by various ESP vendors. These values can be used to estimate the collection efficiency of the ESP.

Table 7-1. Typical precipitation rate parameters for various applications.

Application	Precipitation rate	
	(ft/sec)	(cm/sec)
Utility fly ash	0.13-0.67	4.0-20.4
Pulverized coal fly ash	0.33-0.44	10.1-13.4
Pulp and paper mills	0.21-0.31	6.4- 9.5
Sulfuric acid mist	0.19-0.25	5.8- 7.62
Cement (wet process)	0.33-0.37	10.1-11.3
Cement (dry process)	0.19-0.23	6.4- 7.0
Gypsum	0.52-0.64	15.8-19.5
Smelter	0.06	1.8
Open-hearth furnace	0.16-0.19	4.9- 5.8
Blast furnace	0.20-0.46	6.1-14.0
Hot phosphorous	0.09	2.7
Flash roaster	0.25	7.6
Multiple hearth roaster	0.26	7.9
Catalyst dust	0.25	7.6
Cupola	0.10-0.12	3.0- 3.7

Sources: Theodore and Buonicore, 1976; EPA, 1979.

Deutsch-Anderson Equation

Probably the best way to gain insight into the process of electrostatic precipitation is to study the relationship known as the Deutsch-Anderson Equation. This equation is used to determine the collection efficiency of the precipitator under ideal conditions. The simplest form of the equation is:

(Eq. 7-3)
$$\eta = 1 - e^{-\left(\frac{wA}{Q}\right)}$$

Where: η = collection efficiency of the precipitator
A = the effective collecting plate area of the precipitator, ft² (m²)
Q = gas flow rate through the precipitator, acfs (acms)
e = base of natural logarithm = 2.718
w = migration velocity, ft/sec (cm/sec)

Sources: Deutsch, 1922; Anderson, 1924.

This equation has been used extensively for many years for theoretical collection efficiency calculations. Unfortunately, while the equation is scientifically valid, there are a number of operating parameters that can cause the results to be in error by a factor of two or more. The Deutsch-Anderson Equation neglects three significant process variables. First, it completely ignores the fact that dust reentrainment may occur during the rapping process. Second, it assumes that the particle size and, consequently, the migration velocity is uniform for all particles in the gas stream. Third, it assumes that the gas flow rate is uniform everywhere across the precipitator and that particle sneakeage through the hopper section does not occur. Therefore, this equation should be used only for making preliminary estimates of precipitation collection efficiency.

Design Parameters

Many parameters must be taken into consideration in the design and specification of electrostatic precipitators. The focus of the remainder of this chapter will be on typical design parameters such as those associated with resistivity, specific collection area, aspect ratio, gas flow distribution, electrical sectionalization, and precipitator equipment.

Resistivity

Particle resistivity is a condition of the particle in the gas stream that can alter the actual collection efficiency of an ESP design. Resistivity is a term that describes the resistance of the collected dust layer to the flow of electrical current. By definition, the resistivity is the electrical resistance of a dust sample 1.0 cm² in cross-sectional area, 1.0 cm thick, and recorded in units ohm•cm. It can also be described as the resistance to charge transfer by the dust. Dust resistivity values can be classified roughly into three groups:

- between 10⁴ and 10⁷ ohm•cm — low resistivity
- between 10⁷ and 10¹⁰ ohm•cm — normal resistivity
- above 10¹⁰ ohm•cm — high resistivity

Low Resistivity

Particles that have low resistivity are difficult to collect since they are easily charged and lose their charge upon arrival at the collection electrode. This happens very fast and the particles can take on the charge of the collection electrode. Particles thus bounce off the plates and become reentrained in the gas stream. Examples of low resistivity dusts are unburned carbon in fly ash and carbon black.

If the conductive particles are coarse, they can be removed upstream of the precipitator with another device such as a cyclone. Baffles are often installed on the collection plates to help eliminate this precipitation-repulsion phenomenon.

The use of liquid ammonia (NH_3) as a conditioning agent has found wide use in recent years. It is theorized that ammonia reacts with H_2SO_4 to form an ammonium sulfate substance that increases the resistivity of the dust. Ammonia vapor at rates of 15 to 40 ppm by volume is injected into the duct leading to the precipitator. The injection of NH_3 has improved the resistivity of fly ash from coal fired boilers with low flue gas temperatures (Katz, 1979).

Normal Resistivity

Particles that have normal resistivity do not rapidly lose their charge upon arrival at the collection electrode. These particles slowly leak their charge to ground and are retained on the collection plates by intermolecular adhesive and cohesive forces. This allows a particulate layer to be built up, which is then dislodged into the hoppers. At this range of dust resistivity (between 10^7 and 10^{10} ohm-cm) flyash can be collected most efficiently.

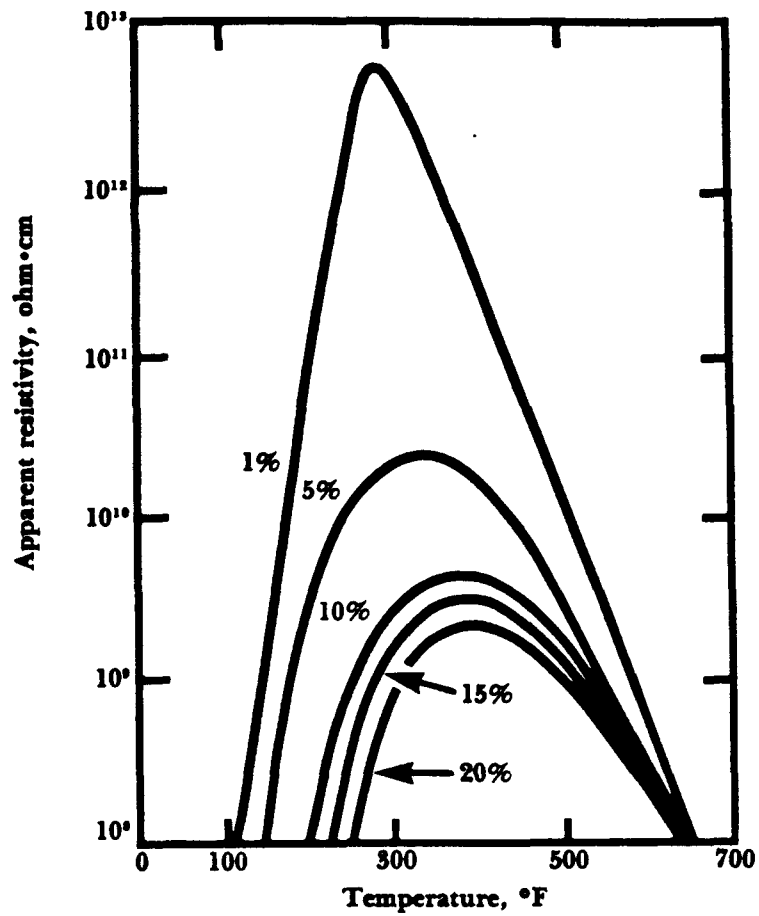
High Resistivity

Particles that exhibit high resistivity are difficult to charge. Once they are finally charged they do not readily give up the acquired negative charge upon arrival at the collection electrode. As the dust layer builds up on the collection electrode, the layer and the electrode form a high potential electric field. The surface of the dust layer is negatively charged, the interior is neutral, and the collection electrode is grounded. This causes a condition known as back corona. Under the influence of the corona discharge, the dust layer breaks down electrically, producing small holes or craters (in the layer) from which back corona discharges occur. Positive ions are generated within the dust layer and are accelerated toward the negative (discharge) electrode. The result of this event would be to counteract the ion generation of the charging electrode with a corresponding reduction in collection efficiency. Disruptions of the normal corona process greatly reduce precipitator collection efficiency, which, in severe cases, may fall below 50%. (White, 1974).

Reducing High Resistivity

High resistivity can generally be reduced by adjusting the temperature and moisture content of the gas stream. Particle resistivity decreases for both high and low temperatures (see Figure 7-10).

The moisture content of the gas stream also affects particle resistivity. Increasing the moisture content of the gas stream lowers the resistivity. This can be accomplished by spraying water or injecting steam into the duct work preceding the ESP. In both temperature adjustment and moisture conditioning one must maintain gas conditions above the dew point to prevent corrosion problems.



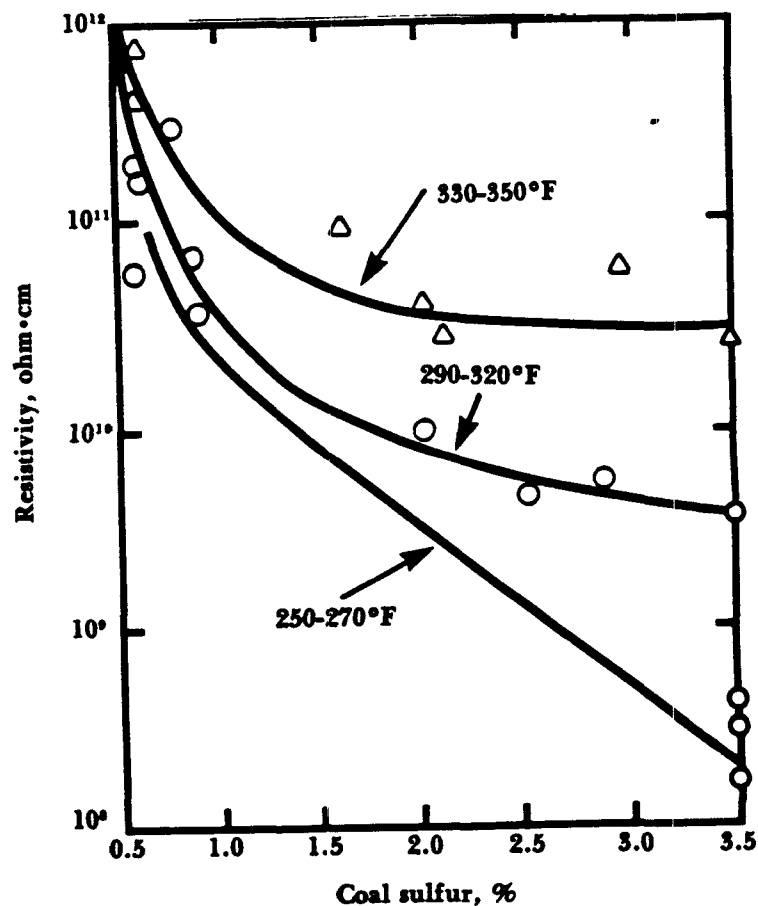
Source: Schmidt, 1949.

Figure 7-10. Effect of temperature and moisture content on apparent resistivity of precipitated cement dust.

The presence of SO_3 in the gas stream has been shown to favor the electrostatic precipitation process when problems with high resistivity occur. Most of the sulfur content in the coal burned for combustion sources converts to SO_2 . However, approximately 1 percent of the sulfur converts to SO_3 . The amount of SO_3 in the flue gas normally increases with increasing sulfur content of the coal. The resistivity of the particles decreases as the sulfur content of the coal increases (Figure 7-11).

The use of low sulfur western coal for boiler operations has caused fly ash resistivity problems for ESP operations. For coal fly ash dusts, the resistivity can be lowered below the critical level by the injection of as little as 10-20 ppm SO_3 into the gas stream. The SO_3 is injected into the duct work preceeding the precipitator. Other conditioning agents such as sulfuric acid, ammonia, sodium chloride, and soda ash have also been used to reduce particle resistivity (White, 1974).

Two other methods to reduce particle resistivity include: increasing the collection surface area and by inletting exhaust gas at higher temperatures. Increasing the collection area of the precipitator will increase the overall cost of the ESP. This may not be the most desirable method to reduce resistivity problems. Hot precipitators, which are usually located before the combustion air preheater section of the boiler, are also used to combat resistivity problems. The use of hot precipitators is discussed in more detail later in this chapter.



Source: White, 1977.

Figure 7-11. Fly ash resistivity versus coal sulfur content for several flue gas temperature bands.

Specific Collection Area

The specific collection area (SCA) is defined as the ratio of collection surface area to the gas flow rate into the collector. The importance of this term is that it represents the A/Q relationship in the Deutsch-Anderson equation.

$$SCA = \frac{\text{Total collecting surface (ft}^2\text{)}}{\text{gas flow rate (1000 acfm)}}$$

or in metric units:

$$SCA = \frac{\text{m}^2}{1000 \text{ m}^3/\text{hr}}$$

Increases in the SCA of a precipitator design will in most cases increase the collection efficiency of the precipitator. Most conservative designs call for an SCA of 350 to 400 ft² per 1000 acfm (20-25 m² per 1000 m³/hr) to achieve 99.5+ percent particle removal. The general range of SCA is between 200-800 ft² per 1000 acfm (11-45 m² per 1000 m³/hr) depending on precipitator design conditions and desired collection efficiency.

Aspect Ratio

The aspect ratio is the ratio of the total length to height of collector surface. The aspect ratio can be calculated by:

$$A.R. = \frac{\text{Effective length}}{\text{Effective height}}$$

Having a precipitator chamber many times larger in length than in height would be ideal. However, space limitations and cost could be prohibitive. The aspect ratio for ESPs can range from 0.5 to 2.0. For 99.5+ percent collection efficiency, the precipitator design should have an aspect ratio of greater than 1.0.

Gas Flow Distribution

Gas flow through the ESP chamber should be slow and evenly distributed throughout the unit. The gas velocities in the duct ahead of the ESP are generally between 20 and 80 ft/sec (6 and 24 m/sec). The gas velocity into the ESP must be reduced for adequate particle collection. This is achieved by using an expansion inlet plenum (see Figure 7-12).

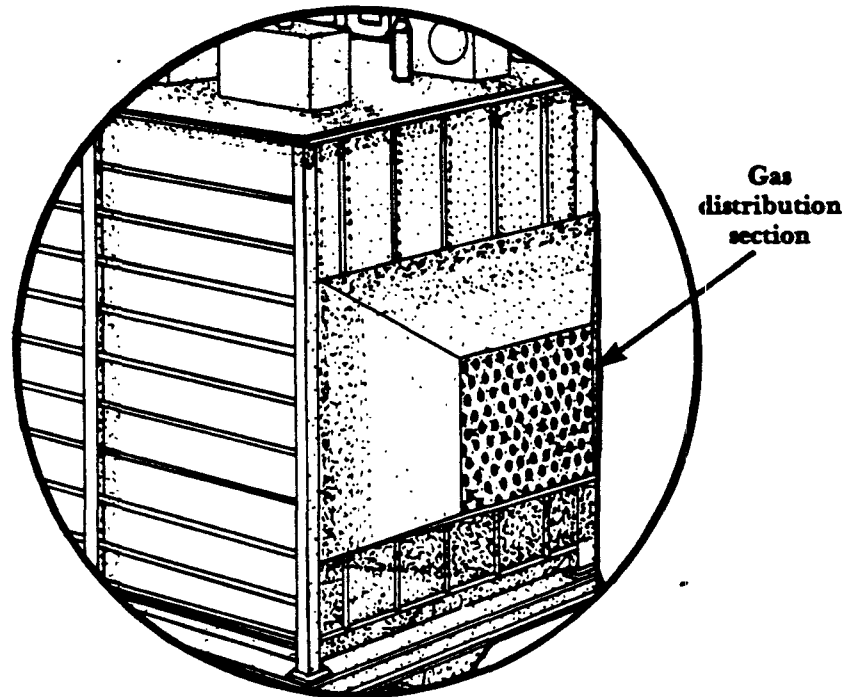


Figure 7-12. Gas inlet with diffuser-perforated plates.

The inlet plenum contains diffuser-perforated plate openings to evenly distribute the gas flow throughout the precipitator. Typical gas velocities in the ESP chamber range from 2 to 8 ft/sec (0.6 to 2.4 m/sec). With aspect ratios of 1.5, the optimum gas velocity is generally between 5 and 6 ft/sec (1.5 and 1.8 m/sec).

Electrical Sectionalization

Stage or Field Sectionalization

Precipitator performance is dependent on the number of individual sections or *fields* installed. The maximum voltage at which a given field can be maintained depends on the properties of the gas and dust being collected. These parameters may vary from one point to another in the unit. To keep each section of the precipitator working at high efficiency, a high degree of sectionalization is recommended. Multiple fields or stages are used to provide electrical sectionalization. Each field has separate power supplies and controls to adjust for varying gas conditions in the unit.

Modern precipitators have voltage control devices that automatically limit precipitator power input. A well designed automatic control system keeps the voltage level at approximately the value needed for optimum particle charging by the discharge electrodes.

The voltage control devices operate in the following manner: increases in voltage will cause a greater spark rate between the discharge and collection electrodes. Occurrence of a spark counteracts high ESP performance since it causes an immediate, short term collapse of the precipitator field. Consequently, less useful power is applied to capture particles. There is, however, an optimal sparking rate where the gains in particle charging are just offset by corona current losses from sparkover.

Measurements on commercial precipitators have determined that the optimal sparking rate is between 50 and 150 sparks per minute per electrical section. The objective in power control is to maintain corona power input at this optimal sparking rate. This can be accomplished by momentarily reducing precipitator power whenever excessive sparking occurs.

The need for separate fields arises mainly because power input requirements differ at various locations in a precipitator. The particulate matter concentration is generally high at the inlet sections of the precipitator. High dust concentrations tend to suppress corona current. Therefore, a great deal of power is needed to generate corona discharge for optimal particle charging.

In the downstream fields of a precipitator, the dust loading is usually lighter. Consequently, corona current flows freer in downstream fields. Particle charging will more likely be limited by excessive sparking in downstream fields than in the inlet fields. The power to the outlet sections must still be high in order to collect small particles, particularly if they exhibit high resistivity.

If the precipitator had only one power set, the excessive sparking would limit the power input to the entire precipitator. This would result in a reduction of overall collection efficiency.

The precipitator is divided into a series of independently energized *bus* sections or fields (see Figure 7-13). Each bus section has individual transformer-rectifier sets, voltage stabilization controls, and high-voltage conductors that energize the discharge electrodes within the section. This allows greater flexibility for individual field energizing for varying conditions in the precipitator. Most ESP vendors recommend that there be at least four or more fields in the precipitator. It might be necessary to design the unit with seven or more fields for 99.9+ percent collection efficiency.

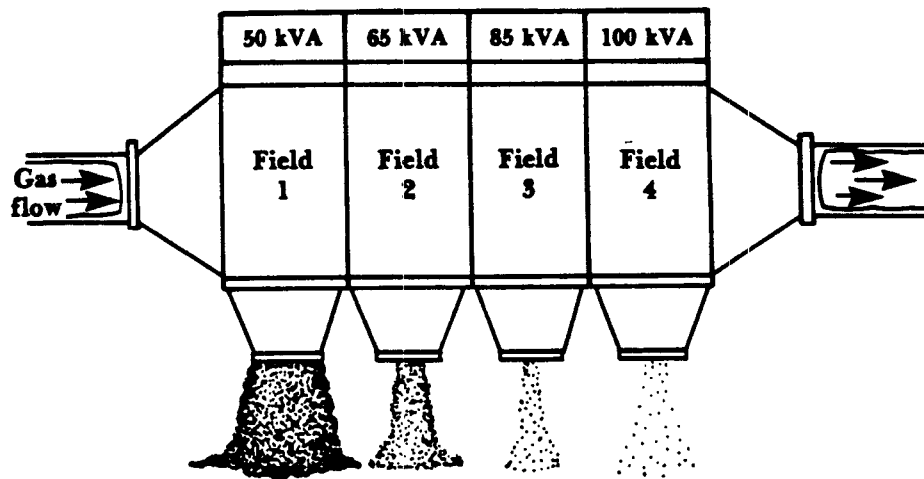


Figure 7-13. Stage or field sectionalization.

Parallel Sectionalization

Parallel sectionalization provides a means of coping with different power input needs due to uneven dust and gas distribution (Figure 7-14). Uneven gas distributions generally occur across the inlet face of the precipitator. Gains in collection efficiency from parallel sectionalization are likely to be small compared to field or stage sectionalization.

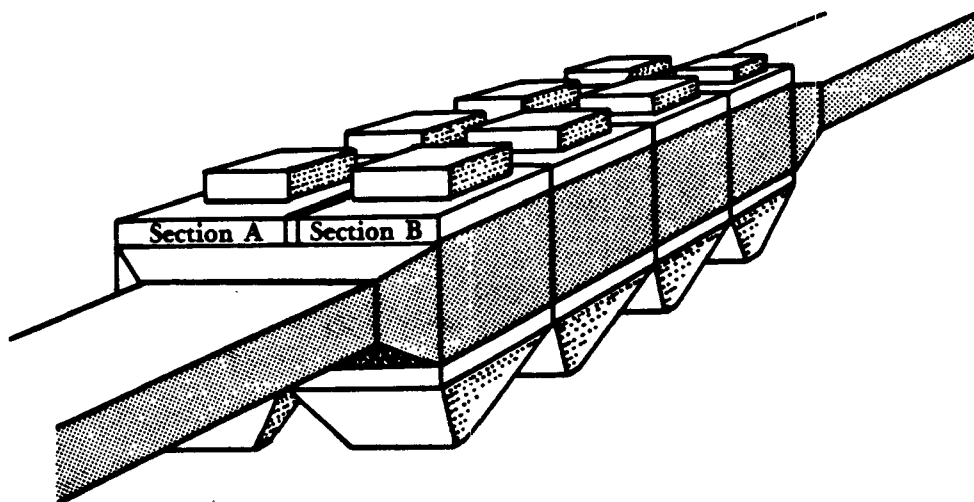


Figure 7-14. Parallel sectionalization.

Precipitator Equipment

Discharge Electrodes

The discharge electrodes (wires) in most U.S. precipitator designs are thin round wires varying from 0.05 to 0.15 inches (0.13 to 0.38 cm) in diameter. Most common designs use wires approximately 0.1 inch (0.25 cm) in diameter. The discharge electrodes consist of vertically hung wires supported at the top and held taut and plumb by a weight at the bottom. The wires are usually made from high carbon steel, but have also been constructed of stainless steel, copper, titanium alloy, and aluminum. The weights are made of cast iron and are generally 25 lbs (11.4 kg) or more.

Discharge wires are usually supported to help eliminate breakage due to mechanical fatigue. The wires move under the influence of aerodynamic and electrical forces and are subject to mechanical stress. The weights at the bottom of the wire are attached to guide frames to help maintain wire alignments. In addition, this will prevent the weights from falling into the hopper in the event that the wire breaks (Figure 7-15). The bottom and top of each wire is usually constructed with a shroud of steel tubing. The shroud helps minimize sparking and consequent metal erosion by sparks at these points on the wire.

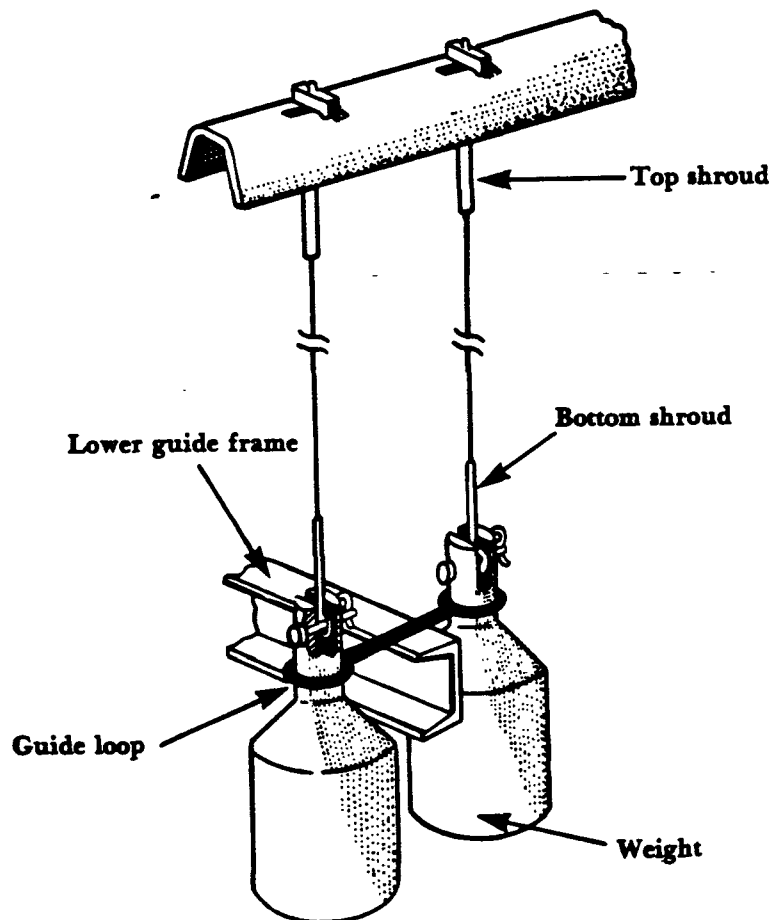


Figure 7-15. Guide frames and shrouds for discharge wires.

The size and shape of the electrodes are governed by the mechanical requirements of the system. Most U.S. designs have traditionally used thin, round wires for corona generation. Some designers have also used twisted wire, square wire, barbed wire or other configurations. Some of these are illustrated in Figure 7-16.

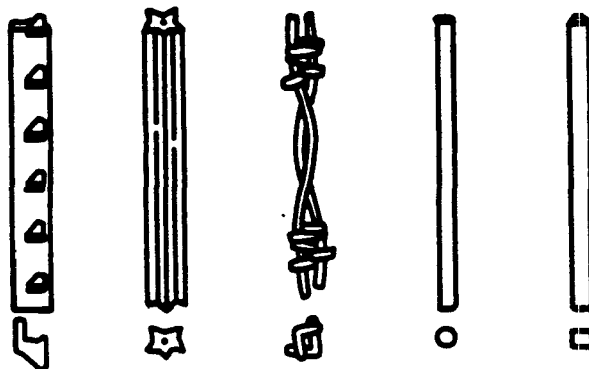


Figure 7-16. Typical discharge wire shapes.

European precipitator manufacturers favor the use of rigid support frames for discharge electrodes. The frames may consist of coiled spring wires, serrated strips, or needle points mounted on a supporting strip. An example is shown in Figure 7-17. The purpose of the rigid frame is to eliminate the possible swinging of the discharge wires. These designs have been used as successfully as the U.S. wire designs. One major disadvantage is the inability to remove a broken wire without removing the whole frame.

Collection Electrodes

Most precipitators use the plate collection electrodes because of the large gas volumes treated and high collection efficiencies needed. The plates are generally made of carbon steel, stainless steel, or some type of alloy, depending upon the gas stream conditions. The plates range from 0.02 to 0.08 inches (0.05-0.2 cm) in thickness. Plates are spaced from 4 inches (10 cm) to 12 inches (30 cm) apart. Normal spacing for high efficiency units is 8 to 9 inches (20-23 cm). Wider spaced ducts are preferred with large collection plates. Plates are usually between 20 and 50 ft (6 to 15 m) high, with higher efficiency precipitators having plates around 30 ft (9 m) high. Lower collection plate height reduces dust reentrainment since the particle has a shorter distance to fall to the hopper.

Collection plates consist of solid-sheet plates with structural stiffeners. In some designs the stiffeners have contours designed to improve gas flow and to lower turbulence in the collecting space near the plate surfaces (Figure 7-18). Baffles are commonly used to minimize particle reentrainment losses. The structural rigidity of the plates should be sufficient to maintain consistent electrode spacing. Distorted or misaligned electrodes contribute to reduced operating voltages and loss of collector efficiency.

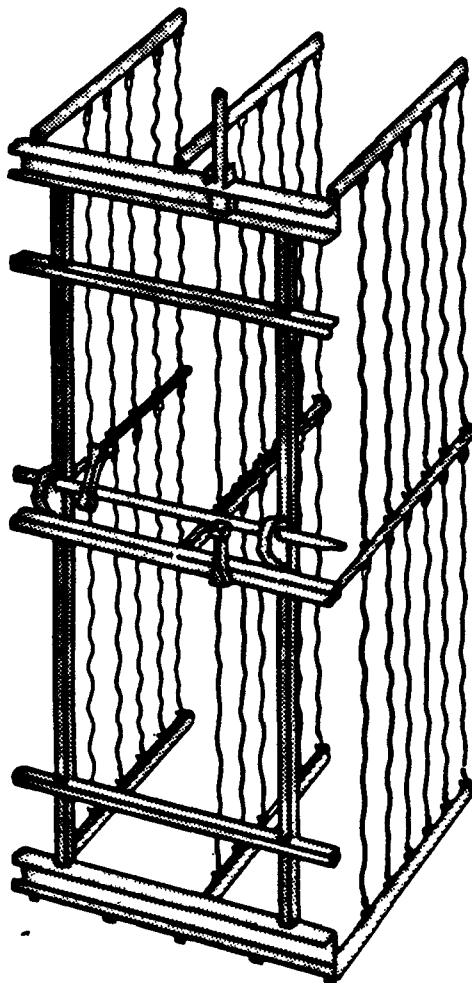


Figure 7-17. Rigid frame discharge electrode design.

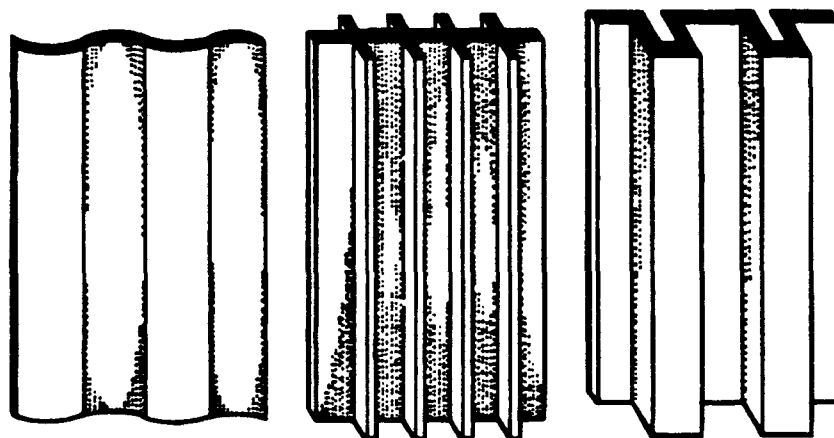


Figure 7-18. Typical collection plates.

Shell

The shell structure encloses the electrodes and supports the precipitator components in a rigid frame. This is done to maintain proper electrode alignment and configuration. Supporting structure and foundations for the entire precipitator and connecting flues must be properly designed. The support structure is especially critical for hot-side precipitators because of the large temperature expansions of precipitator components. Excessive temperature stresses can literally tear shell and hopper joints and welds apart.

Collecting plates and discharge electrodes are normally supported from the top so that the elements hang vertically under the force of gravity. This allows the elements to expand or contract with temperature changes without binding or distorting.

Shells, hoppers, and connecting flues should be covered with insulation to conserve heat, and to prevent corrosion due to condensation of moisture and acid on internal precipitator components. Insulation will also help minimize temperature differential stresses, especially on hot-side precipitators. Ash hoppers should be insulated and heated. Cold fly ash has a tendency to cake, making removal extremely difficult.

The precipitator design should also provide for easy access to strategic points of the collector. This permits the internal inspection of electrode alignment; facilitates maintenance; and allows for the cleaning of electrodes, hoppers, and connecting flues during outages.

Rappers

Removal of the accumulated dust deposit on collection and discharge electrodes is accomplished by rapping. Dust deposits are dislodged by mechanical impulses or vibrations imparted to the electrodes. A rapping system is designed so that rapping intensity and frequency can be adjusted for varying operational conditions. The system must also be capable of maintaining uniform rapping over long periods of time without attention.

Rapping of collection plates can be accomplished by a number of methods. One design uses mechanical rappers consisting of hammers mounted on a rotating shaft. As the shaft rotates, hammers drop by gravity and strike anvils attached to the collecting plates. The rappers can be mounted on the top of the collection plates or on the side as shown in Figure 7-19.

Rapping intensity is governed by the weight of the hammers and length of the hammer mounting arm. The frequency of rapping can be changed by changing the speed of the rotating shafts. Thus, rapping intensity and frequency adjustments can be made to deal with varying dust concentration to the precipitator.

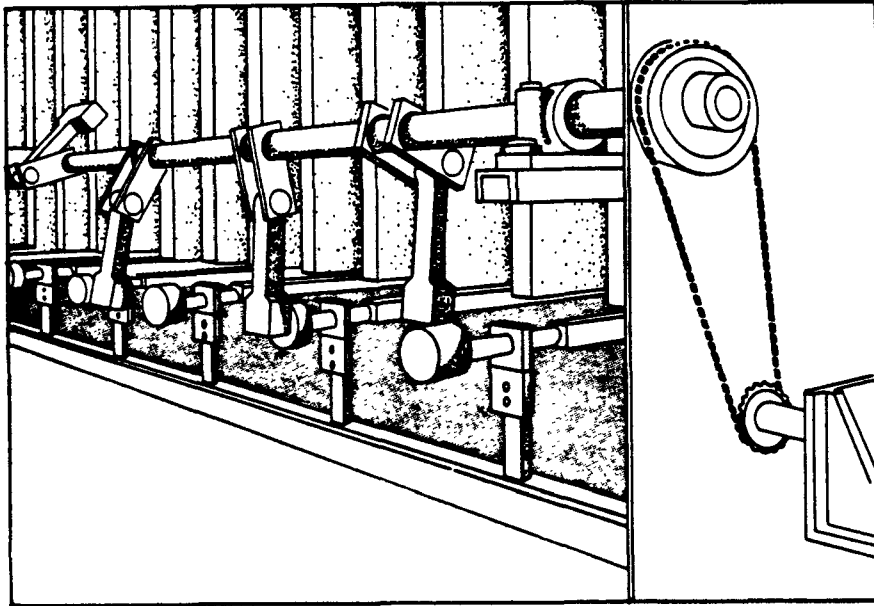


Figure 7-19. Typical hammer/anvil collection plate rapper.

Magnetic impulse rappers are frequently employed on many U.S. designs to remove accumulated dust layers from collection plates. A magnetic impulse rapper consists of a steel plunger that is raised by a current pulse in a coil. The raised plunger then drops back, due to gravity, striking a rod connected to a number of plates within the precipitator (Figure 7-20). Rapper frequency and intensity are easily regulated by an electrical control system. The frequency may be one rap every few minutes to one rap an hour with an intensity of 10-24 g's (Katz, 1979). Magnetic impulse rappers usually operate more frequently but with less intensity than the rotating hammer/anvil type rappers.

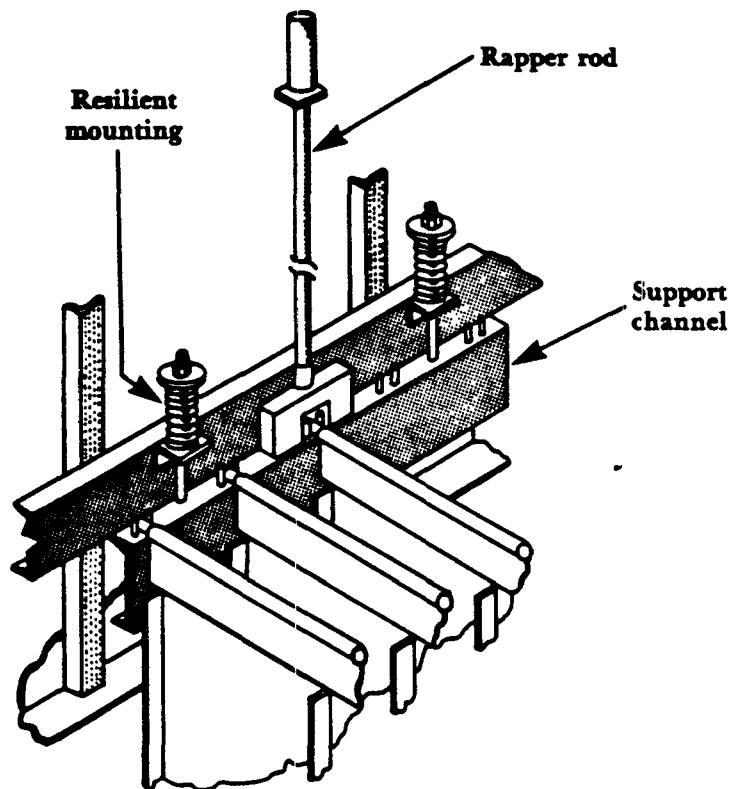


Figure 7-20. Typical impulse collection plate rappers.

The discharge or corona electrodes must also be rapped to prevent buildup of excessive dust deposits which interfere with corona generation. This is usually accomplished by the use of air or electric vibrators that gently vibrate the discharge wires. Vibrators are usually mounted externally on the roofs of the precipitators and are connected by rods to the high tension frames that support the corona electrodes (Figure 7-21). An insulator, located above the rod, electrically isolates the rapper while mechanically transmitting the rapping force.

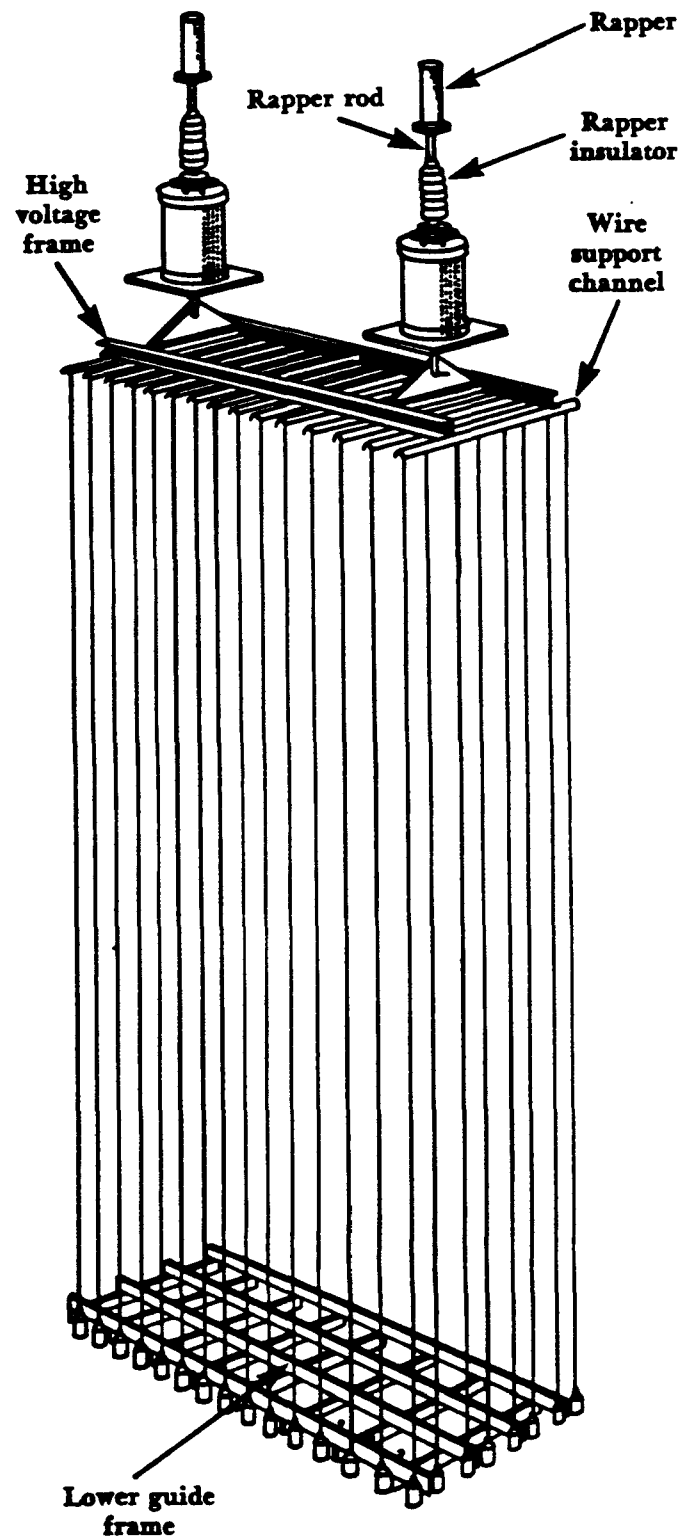


Figure 7-21. Typical vibrator rappers used for discharge electrodes.

High Voltage Equipment

Transformer-Rectifier Sets

The high voltage equipment is the heart of the electrostatic precipitator. The high voltage equipment controls the strength of the electric field generated between the discharge and collection electrodes. This is accomplished by using transformer-rectifier sets (T-R sets). The transformer-rectifier sets step up normal service voltages from 400-480 volts to approximately 50,000 volts and convert alternating to direct current. For fly ash applications, rectifier output ratings are typically 50 kilovolts and 500-2000 milliamperes DC rating.

Development of high voltage equipment to energize precipitators has been an evolutionary process. The earliest electrostatic precipitators were energized by mechanical rectifier sets but were consequently replaced by more efficient vacuum tube rectifiers. Modern precipitators use solid-state silicon type rectifiers and oil or askerel filled high voltage transformers (Figure 7-22). The T-R ratings usually range from 15-130 kVA, with more recent design between 60-95 kVA units. The T-R sets used in conjunction with spark rate, voltage, and current feedback signals automatically control electrical energization of the ESP.

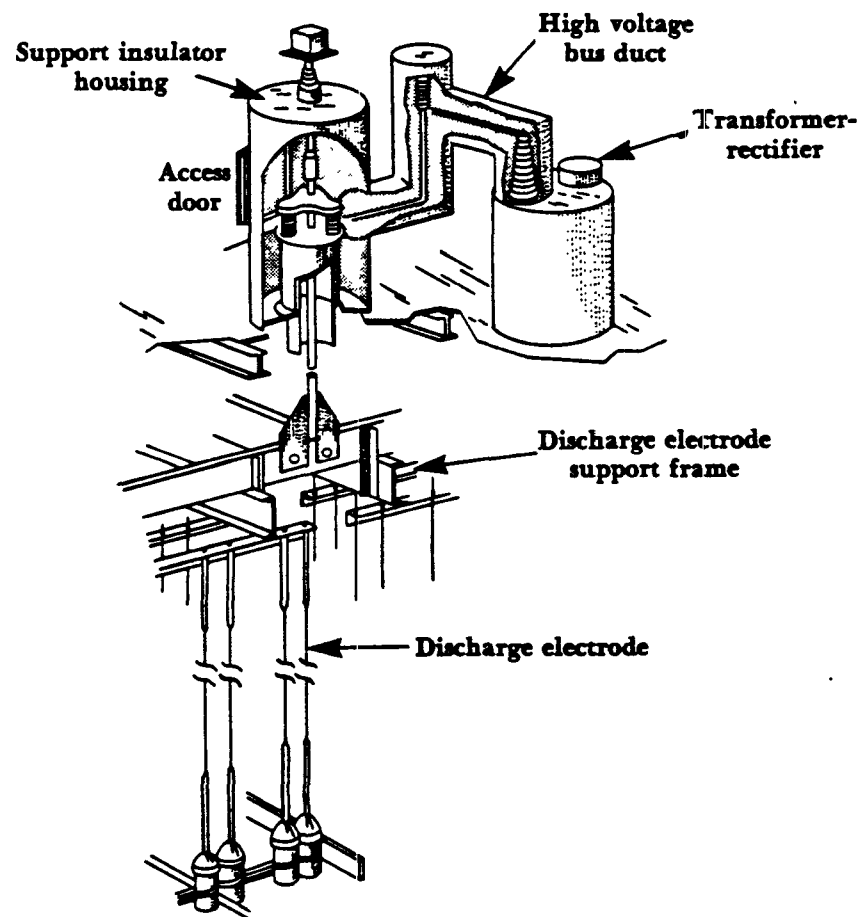


Figure 7-22. High voltage system.

Control Meters

Control meters are important parts of the control circuitry which monitors the variations in the electrical power output. Commonly used meters are voltage and current meters and sparkmeters. Primary voltage and current readings across the transformer reflect the precipitator power input. Spark meters measure the electrical breakdowns in the precipitator in sparks per minute. From the previous discussion, it is desirable to generate approximately 100 sparks per minute. These meters are generally located on the control panel of the precipitator.

Electrostatic Precipitator Applications

Electrostatic precipitators have been used for particulate emission reduction for many industrial applications. ESPs have been designed to collect particles in the submicron range with 99+ percent control efficiency. They are economical to operate since they have relatively low internal power requirements and low pressure drop losses across the collector. The ability of ESPs to handle large exhaust gas volumes at very high temperatures (175-700°C) make them very attractive for many industries. This is particularly desirable for both cement kiln emission reduction and control of emissions from basic oxygen furnaces in the steel industry where flue gas temperatures enter the precipitator at approximately 350°C. ESPs are commonly used for particulate emission reduction in the pulp and paper industry for black liquor operations, the steel industry for blast furnace and sintering operations, and for fly ash control from industrial and utility boilers.

Hot-Side Precipitators

Hot-side precipitators have been used in high temperature situations collecting cement kiln dust and utility boiler fly ash. The hot-side precipitator is located ahead of the air preheater in a boiler, as compared to the cold side precipitator which is located after the air preheater. The flue gas temperature for hot-side precipitators is in the range of 320-420°C. Popularity of hot-side precipitators has increased with the use of low sulfur coals that produce high resistivity fly ash that is difficult to collect in the precipitator. The use of hot-side precipitators also helps reduce corrosion and hopper plugging problems for easier emptying and dust disposal.

Hot-side precipitators have, however, some disadvantages. Since the temperature of the gas flow is higher, the volume of gas to be treated in the ESP is larger. Consequently the overall size of the precipitator will be larger. High gas temperature also has an effect on the corona, lowering the sparkover voltage and increasing the corona current. This could decrease the collection efficiency of the unit. Other major disadvantages include structural and mechanical problems that occur in the precipitator shell and support structure. Structural distortions stem mainly from differential thermal expansion between the shell and the support structure. This can be overcome with careful engineering and material design of precipitator components.

Review of ESP Design Plans

The first step in reviewing design plans for air pollution permits is to read the vendor literature and specifications of the precipitator design. The design specifications should include at least:

- exhaust gas flow rate and temperature,
- inlet dust concentration,
- specific collection area (SCA),
- gas velocity in the precipitator,
- distance between the plates
- aspect ratio,
- number and size of T-R sets,
- number of fields,
- design migration velocity,
- corona power/1000 m³/min,
- corona current/sq ft plate area,
- design collection efficiency, and
- outlet dust concentration.

The next review step is to determine if the design specifications are within the range that is typically used in practice by industry. The range of basic design parameters for fly ash precipitators are given in Table 7-2.

Table 7-2. Typical design parameter ranges for fly ash precipitators.

Parameter	Range (English units)	Range (metric units)
Distance between plates (duct width)	8-12 in. (8-9 in. optimum)	20-30 cm
Gas velocity in ESP	4-8 ft/sec (5-6 ft/sec optimum)	1.2-2.4 m/sec
SCA	200-800 ft ² /1000 cfm (300-400 ft ² /1000 cfm optimum)	11-45 m ² /1000 m ³ /hr (16.5-22.0 m ² /1000 m ³ /hr)
Aspect ratio (L/H)	1-1.5 (keep plate height less than 30 ft for high efficiency)	1.1-5 (keep plate height less than 9 m for high efficiency)
Design migration velocity	0.1-0.5 ft/sec	3.05-15.2 cm/sec
Number of fields	4-8	4-8
Corona power/1000 cfm	100-500 watts/1000 cfm	59-295 watts/1000 m ³ /hr
Corona current/ft ² plate area	10-80 microamp/ft ²	107-860 microamp/m ²
Plate area per electrical (T-R) set	5000-80,000 ft ² /T-R set (10,000-30,000 ft ² /T-R set optimum)	465-7,430 m ² /T-R set (930-2,790 m ² /T-R set optimum)

Source: White, 1977.

Finally, the outlet concentration from the ESP must meet the grain loading requirements of air pollution regulations. The design reviewer can determine if the calculated outlet values, using the Deutsch-Anderson equation, are within the regulation limits. In addition, requiring the source to perform a source test to verify the designed collection efficiency of the ESP would be extremely useful.

References

1. Deutsch, W. 1922. *Ann. Phys. (Leipzig)* 68:335.
2. Anderson, E., 1924. Report, Western Precipitator Co., Los Angeles, CA, 1919. *Trans, Amer. Inst. Chem. Eng.* 16:69.
3. White, H. J. 1963. *Industrial Electrostatic Precipitation*. Reading, Massachusetts: Addison-Wesley.
4. White, H. J. 1977. *Electrostatic Precipitation of Fly Ash*. APCA Reprint Series, J of Air Poll. Control Assoc.
5. Katz, J. 1979. *The Art of Electrostatic Precipitators*. Munhall, Pennsylvania: Precipitator Technology, Inc.
6. White, H. J. 1974. Resistivity Problems in Electrostatic Precipitation. *J of Air Poll. Control Assoc.* 24:315-338.
7. Schmidt, W. A. 1949. *Ind. and Eng. Chem.* 41:2428.
8. Rose, H. E. and Wood, A. J. 1956. *An Introduction to Electrostatic Precipitation in Theory and Practice*. London: Constable and Company LTD.
9. Bethea, R. M. 1978. *Air Pollution Control Technology—an Engineering Analysis Point of View*. New York: Van Nostrand Reinhold Company.
10. Theodore, L. and Buonicore, A. J. 1976. *Industrial Air Pollution Control Equipment for Particulates*. Cleveland: CRC Press.
11. Cheremisinoff, P. N. and Young, R. A., eds. 1977. *Air Pollution Control and Design Handbook Part 1*. New York: Marcel Dekker, Inc.
12. Hesketh, H. E. 1979. *Air Pollution Control*. Ann Arbor: Ann Arbor Science Publishers Inc.
13. Stern, A. C. ed. 1977. *Air Pollution Third Edition Volume IV Engineering Control of Air Pollution*. New York: Academic Press.
14. Cross, F. L. and Hesketh, H. E. eds. 1975. *Handbook for the Operation and Maintenance of Air Pollution Control Equipment*. Westport, Conn.: Technomic Publishing Co., Inc.
15. Environmental Protection Agency (EPA). 1979. *Particulate Control by Fabric Filtration on Coal-Fired Industrial Boilers*. EPA 625/2-79-021.
16. Environmental Protection Agency (EPA). 1976. *Capital and Operating Costs of Selected Air Pollution Control Systems*. EPA 450/3-76-014.
17. Sittig, M. 1977. *Particulates and Fine Dust Removal Processes and Equipment*. New Jersey: Noyes Data Corporation.
18. Environmental Protection Agency (EPA). 1973. *Air Pollution Engineering Manual*. 2nd ed. AP-40.

Chapter 8

Fabric Filtration

Filtration for Particle Collection

Fabric filtration is one of the most common techniques used to collect particulate matter. There are two basic types of filters: one is disposable; the other is not. Disposable filters are similar to those used in a home heating or air conditioning system. Disposable filters can be constructed as mats or as deep beds (12 inches or more). Mat filters are usually made using fiberglass bats with a thin metal plate on the outside of the filter used for structural reinforcement. Depth filters are generally constructed using fiberglass fibers, glass fiber paper or some other inert material such as fine grade steel to form a deep mesh. The filters are very efficient (99.97%) for the collection of $0.3\ \mu\text{m}$ and larger particles but must be replaced when they become loaded with particulate matter (when the pressure drop across the filter becomes excessive). Depth filters are widely useful for the collection of toxic dust materials.

Nondisposable fabric filters consist of some type of fabric material (nylon, wool, or others). This type is commonly used to clean dirty exhaust gas streams from industrial processes. The particles are retained on the fabric material, while the cleaned gas passes through the material.

The collected particles are then removed from the filter by a cleaning mechanism; by shaking or using blasts of air. The removed particles are stored in a collection hopper until they are disposed of or are reused in the process.

Collection Mechanisms

Particles are collected on a filter by a combination of the mechanisms described earlier in this manual. The most important here are impaction, direct interception and diffusion. In collection by *impaction*, the particles in the gas stream have too much inertia to follow the gas streamlines around the fiber and are impacted on the fiber surface (Figure 8-1).

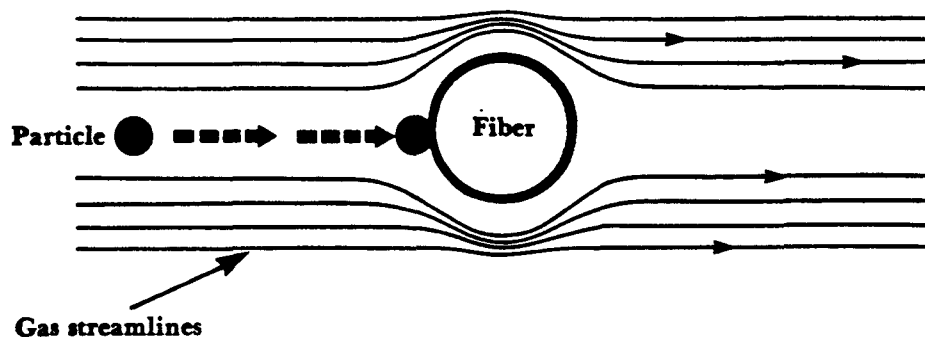


Figure 8-1. Impaction.

In the case of *direct interception* the particles have less inertia and barely follow the gas streamlines around the fiber. If the distance between the center of the particle and the outside of the fiber is less than the particle radius, the particle will graze or hit the fiber and be "intercepted" (Figure 8-2).

Impaction and direct interception mechanisms account for 99 percent collection of particles greater than $1\text{ }\mu\text{m}$ aerodynamic diameter in fabric filter systems.

The third collection mechanism is that of *diffusion*. In diffusion, small particles are affected by collisions on a molecular level. Particles less than $0.1\text{ }\mu\text{m}$ aerodynamic diameter have individual or random motion. The particles do not necessarily follow the gas streamlines, but move randomly throughout the fluid. This is known as *Brownian motion*. The particles may have a different velocity than the fluid and at some point could come in contact with the fiber and be collected (Figure 8-3).

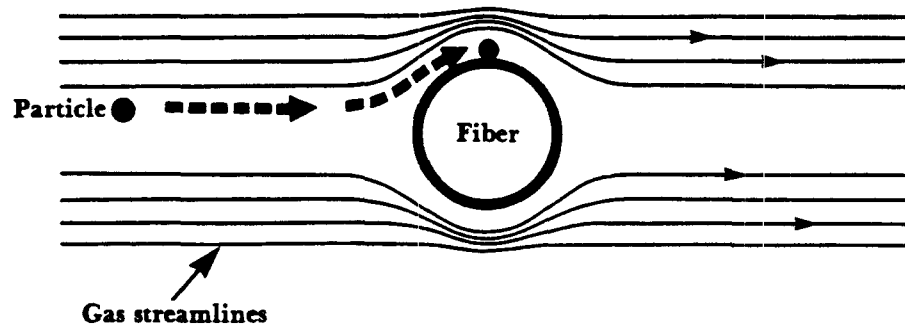


Figure 8-2. Direct interception.

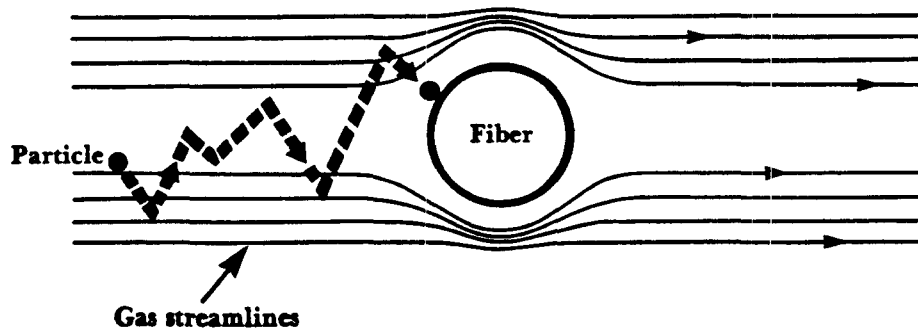


Figure 8-3. Diffusion.

Other collection mechanisms such as gravitational settling, agglomeration, and electrostatic attraction may contribute slightly to particle collection. Particles can agglomerate or grow in size and then be more easily collected by the fibers. Some particles have a small electrostatic charge and can be attracted to a material of opposite charge. Electrostatic charges could, on the other hand, have a bad affect if the charges of the particles and fiber are the same. Electrostatic charges can be particularly useful for the capture of particles in the submicron range. The use of a selected fiber material or a specially coated material may enhance particle capture (Frederick, 1974). Different materials will develop electrostatic charges of varying degree and sign. A series of these triboelectric effects or electrostatic charges for various fabric materials was developed by Frederick and is shown in Table 8-1.

Table 8-1. Triboelectric series for some production fabrics.

Positive	
+ 25	Wool felt
+ 20	
+ 15	Glass, filament, heat cleaned and silicone treated Glass, spun, heat cleaned and silicone treated Wool, woven felt, T-2
+ 10	Nylon 66, spun Nylon 66, spun, heat set Nylon 6, spun Cotton sateen
+ 5	Orlon 81, filament Orlon 42, needled fabrics Arnel, filament Dacron, filament Dacron, filament, silicone treated
0	Dacron, filament, M-31 Dacron, combination filament and spun Creslan, spun; Azoton, spun Verel, regular, spun; Orlon 81, spun (55200) Dynel, spun
- 5	Orlon 81, spun Orlon 42, spun Dacron, needled
- 10	Dacron, spun; Orlon 81, spun (79475) Dacron, spun and heat set Polypropylene 01, filament Orlon 39B, spun
- 15	Fibravyl, spun Darvan, needled Kodel
- 20	Polyethylene B, filament and spun
Negative	

Baghouses

General Description

Nondisposable fabric filter systems are developed for industrial application as baghouse systems. A baghouse consists of the following components:

- filter medium and support
- filter cleaning device
- collection hopper
- shell
- fan

The particle collection surface is composed of the filtering material and usually some type of support structure. Most U.S. baghouse designs employ long cylindrical tubes that contain felted fabric or woven cloth as the filtering medium. The cloth can be supported at the top and bottom of the bag by metal rings or by a cage that completely supports the entire bag (Figure 8-4). Some European baghouse designs employ an envelope filter arrangement as shown in Figure 8-5. In this case the baghouse consists of compartments that contain envelopes of fabric mounted on frames and attached to the walls of the collector (Figure 8-5).

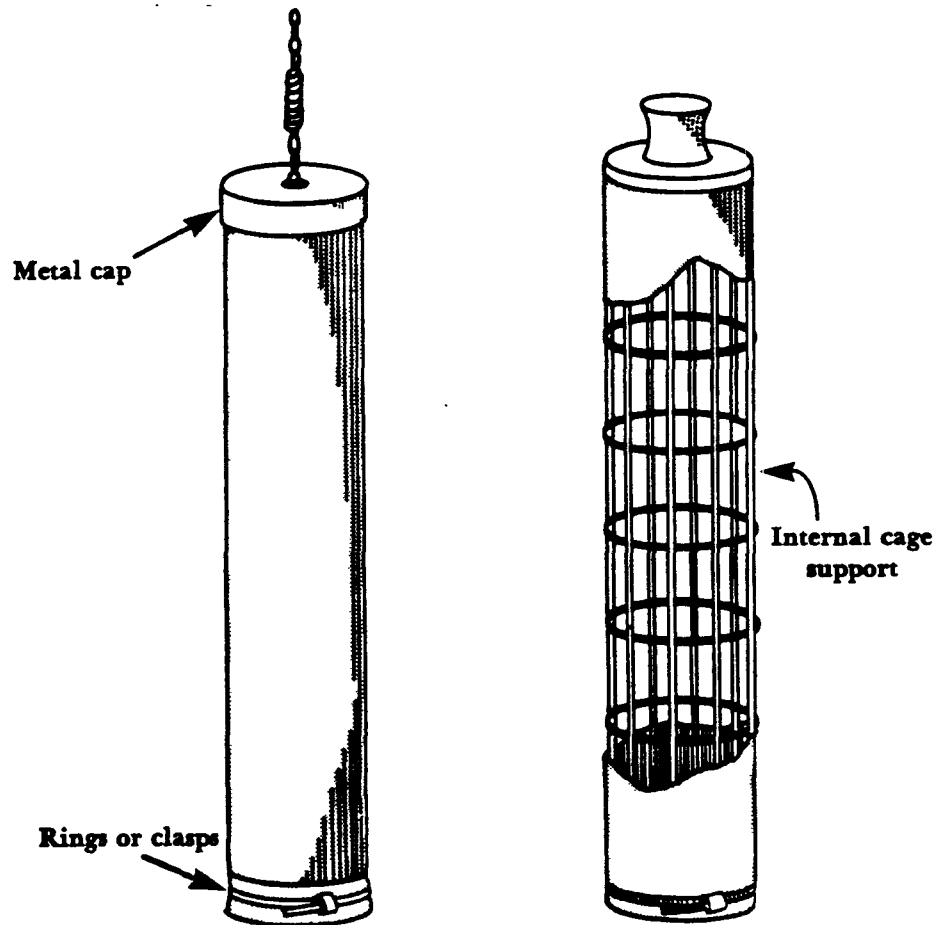


Figure 8-4. Bags and support.

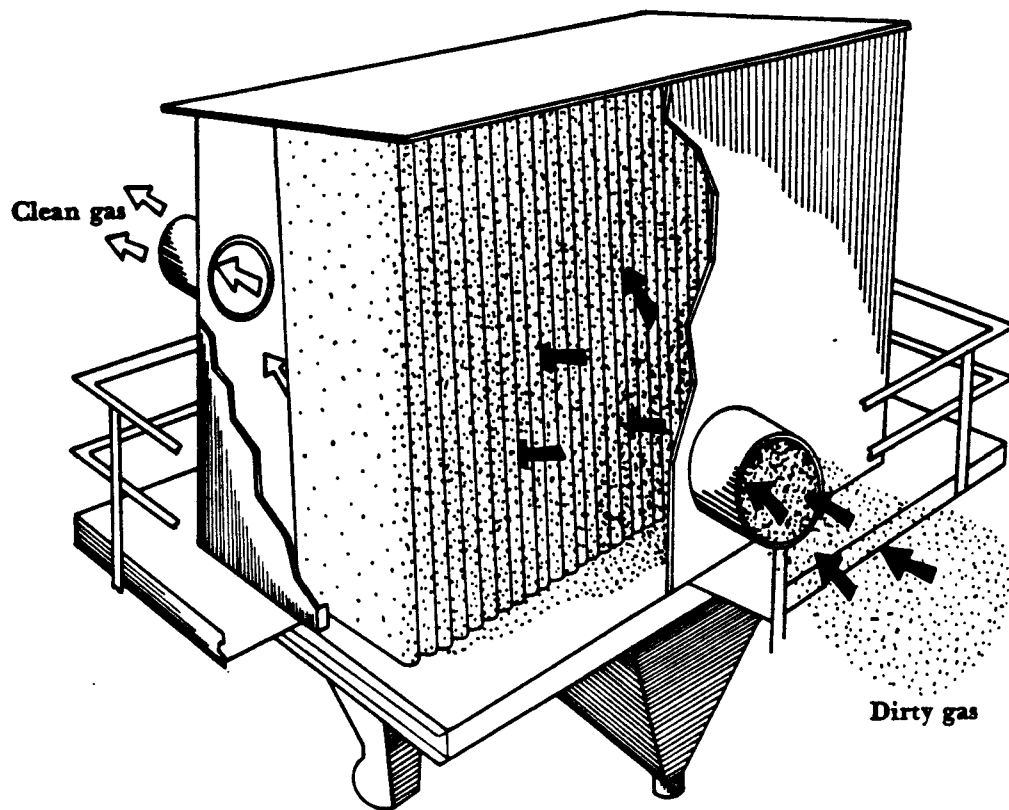


Figure 8-5. Envelope baghouse.

Baghouses are usually constructed using many cylindrical bags that hang vertically in the baghouse. The number of bags can vary from a few hundred to a thousand or more depending on the size of the baghouse. When dust layers have built up to a sufficient thickness, the bag is cleaned, causing the dust particles to fall into a collection hopper (Figure 8-6). Bag cleaning can be done by a number of methods. Particles are stored in the hopper and are usually removed by a pneumatic or screw conveyer. The baghouse is enclosed by sheet metal to contain the collected dust and to protect the bags from atmospheric environmental conditions.

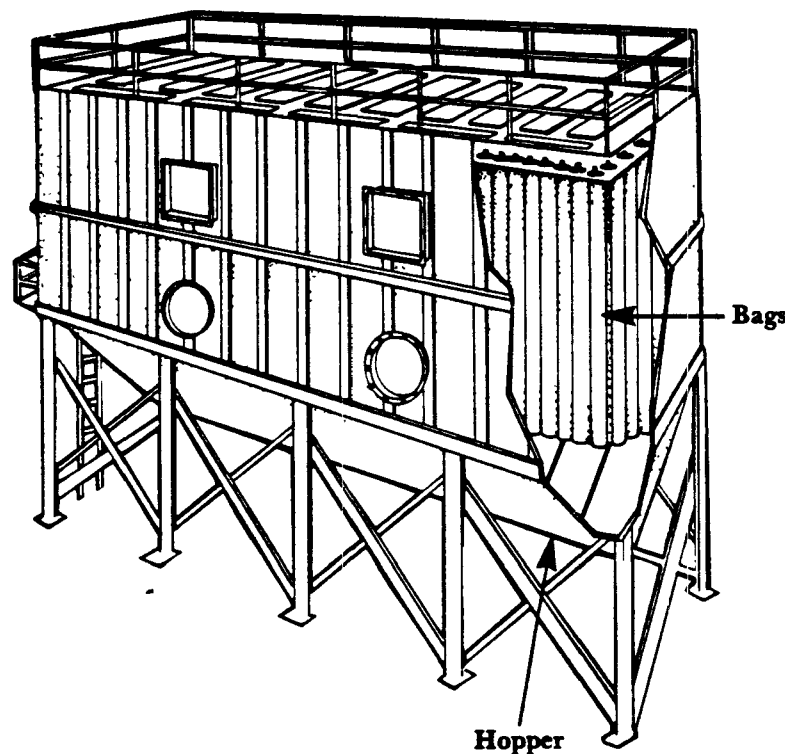
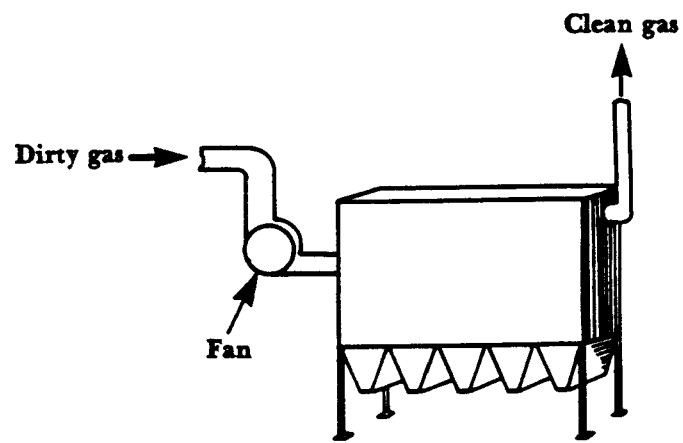
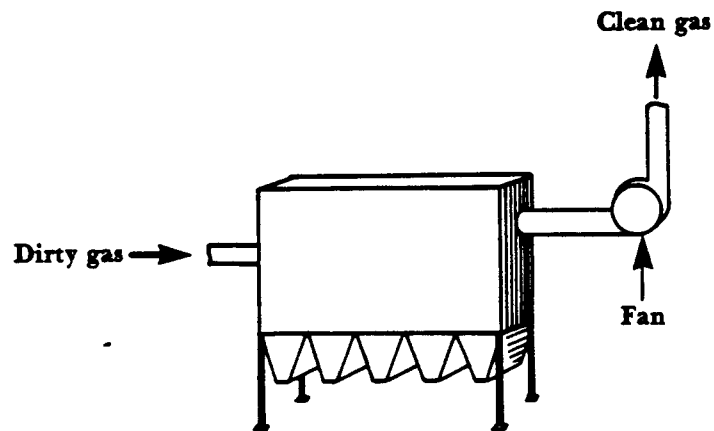


Figure 8-6. Bags and hopper.

Dirty gas is either pushed or pulled through the baghouse by a fan. When the dust laden gas is pushed through the baghouse, the collector is called a positive pressure baghouse. When the fan is on the downstream side of the baghouse, the dirty gas is pulled through the baghouse and the collector is called a negative pressure baghouse (Figure 8-7). The structure of the negative pressure baghouse must be reinforced because of the suction on the baghouse shell. Vendors can construct positive pressure baghouses with weaker support structure since the positive pressure will counterbalance the atmospheric pressure on the baghouse shell. Limitations, however, do exist since the fan is located on the dirty side of the system. Premature deterioration of fan blades and bearings can occur in this configuration.



Positive pressure baghouse



Negative pressure baghouse

Figure 8-7. Positive and negative pressure baghouses.

Filtration Designs

There are two filtration designs used in baghouses: *interior filtration* and *exterior filtration*. In baghouses using interior filtration, particles are collected on the inside of the bag. The dust laden gas enters either through the top or bottom of the collector and is directed inside the bag by diffuser vanes and a cell plate. The cell plate is a thin metal sheet surrounding the bag openings. The cell plate separates the clean gas section from the baghouse inlet. The particles are filtered by the bag and clean air exits through the outside of the bag (Figure 8-8).

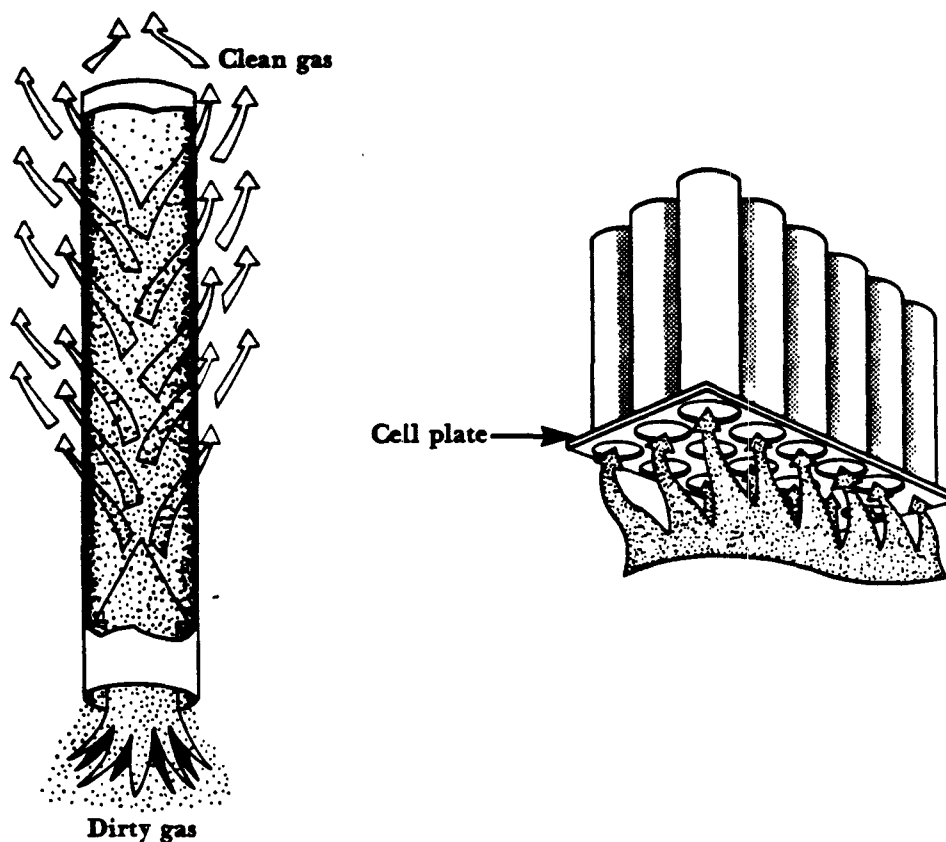


Figure 8-8. Interior filtration (particles collected on the inside of the bag).

In exterior filtration systems, dust is collected on the outside of the bags. The filtering process goes from the outside of the bag to the inside with clean gas exiting through the inside of the bag (Figure 8-9). Consequently, some type of bag support is necessary, such as an internal bag cage or rings sewn into the bag fabric.

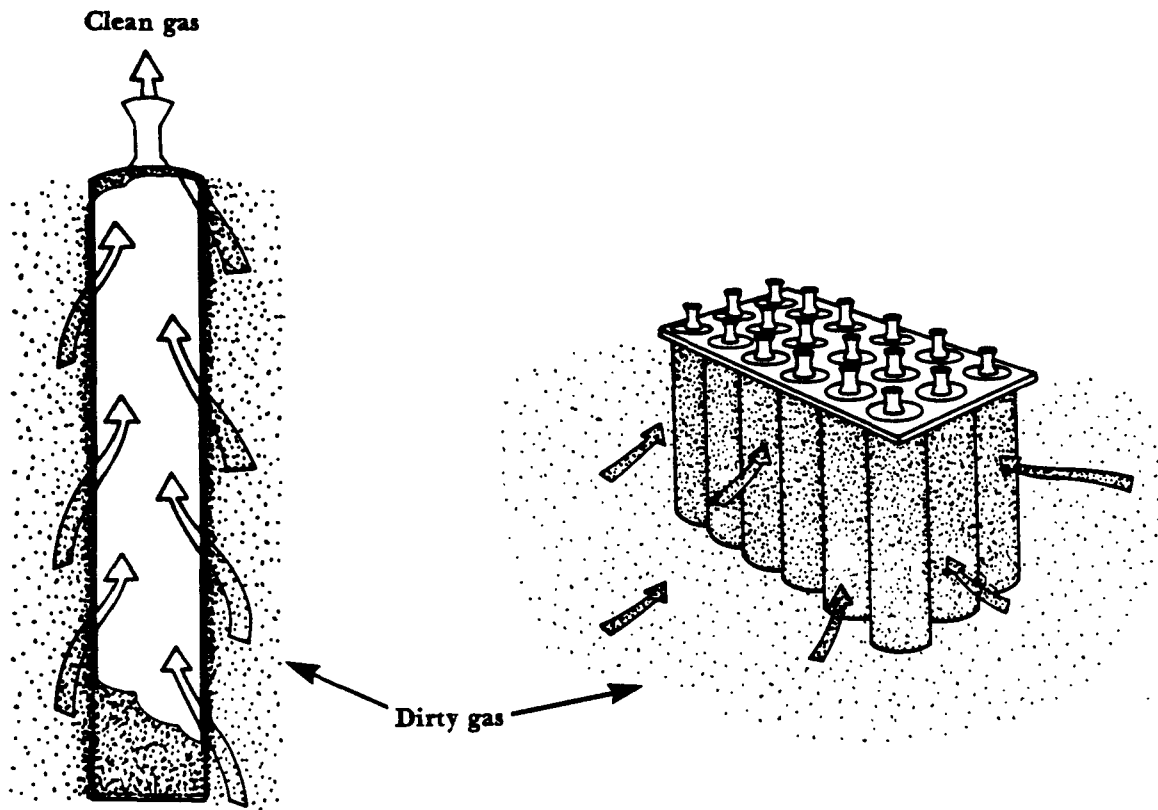


Figure 8-9. Exterior filtration (particles collected on the outside of the bag).

The dust-laden gas inlet position for both filtration systems often depends on the baghouse model and manufacturer. If the gas enters the top of the unit, a downwash of gas occurs which tends to clean the bags somewhat while the bags are filtering. This usually allows slightly higher gas volumes to be filtered through the baghouse before cleaning is required. If the gas enters the bottom of the unit, the inlet is positioned at the very top part of the dust hopper (Figure 8-10). Bottom or hopper inlets are easier to design and manufacture structurally than are the top inlets. However, when using hopper inlets, vendors must carefully design gas flows to avoid dust reentrainment from the hopper.

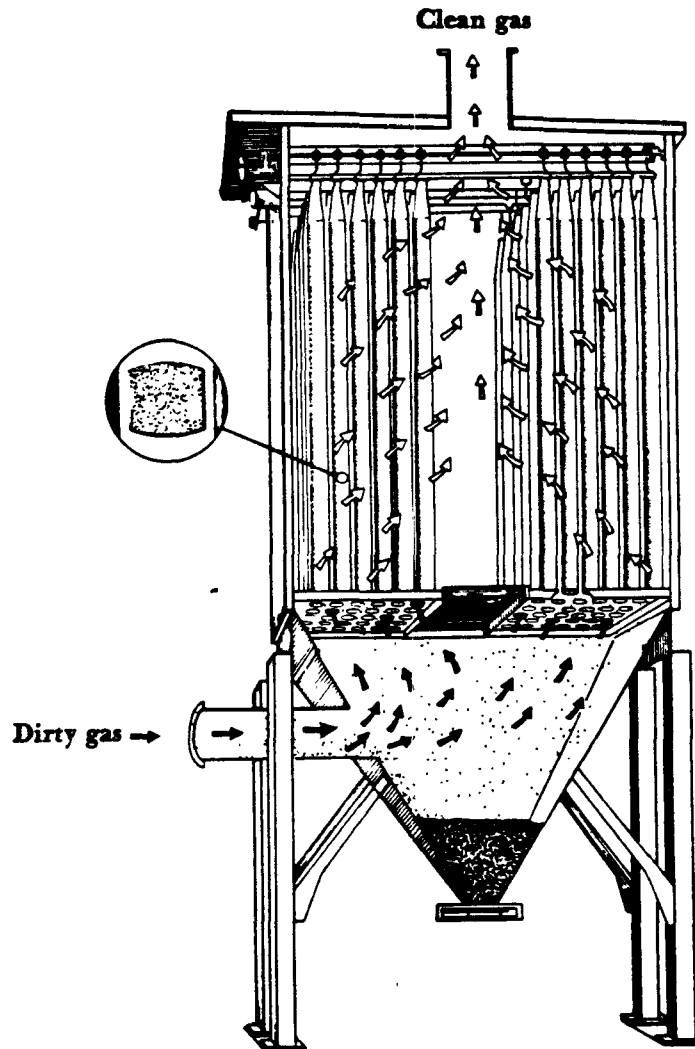


Figure 8-10. Dust inlet to the baghouse.

Bags

Tubular bags vary in both length and diameter depending on baghouse design and manufacturer. The length ranges from 10 to 40 feet and the diameter is usually between 6 and 18 inches. Bags are usually hung vertically in the baghouse and are attached at the top and bottom by some type of ring, cap, clamp or clasp (Figure 8-11).

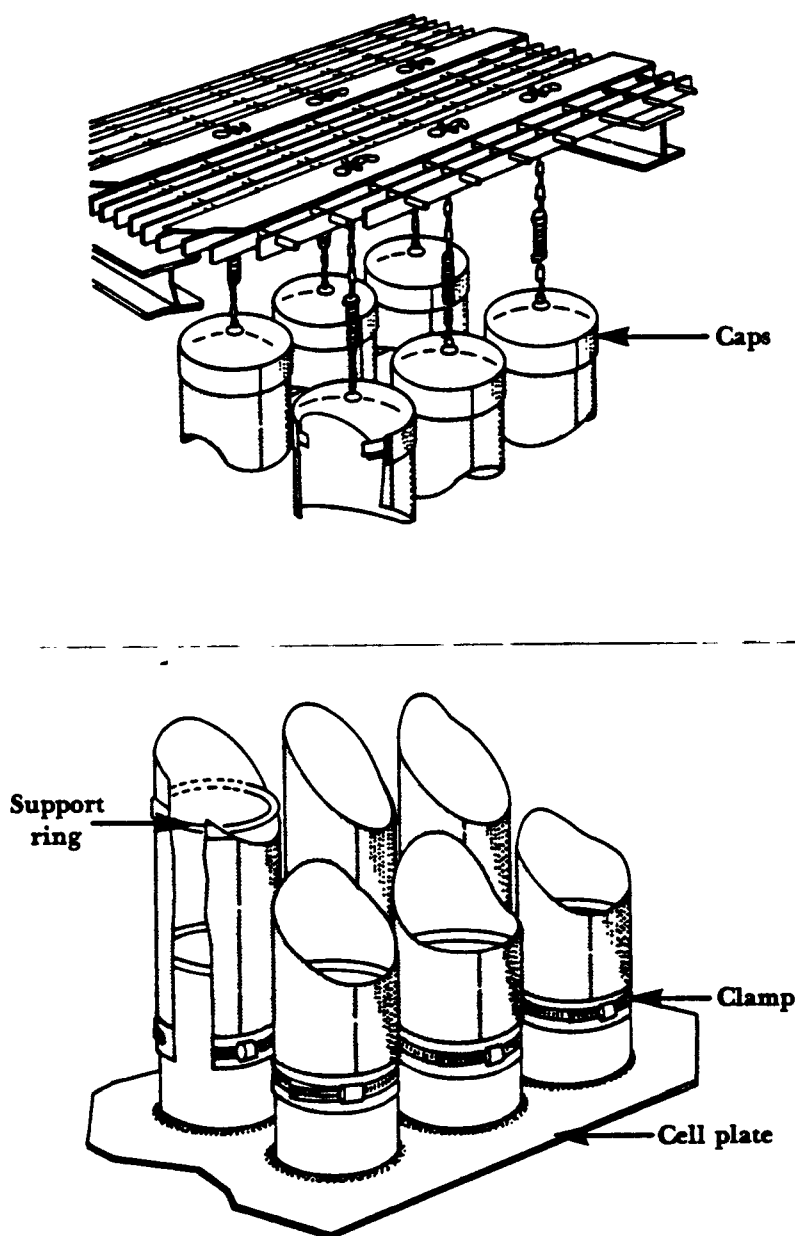


Figure 8-11. Bag attachment.

A cell plate (shown in Figure 8-11) is also used in some baghouse systems to secure bags in place. Exterior filtration baghouses usually have the bags supported by a cage and the bags are attached to the cage by a clasp.

Housing

Baghouses are constructed as single units or compartmental units. The single unit is generally used on small processes that are not in continuous operation such as grinding and paint spraying processes. Compartmental units consist of more than one baghouse compartment and are used in continuous operating processes with large exhaust volumes such as electric melt steel furnaces and industrial boilers. In both cases, the bags are housed in a shell made of a rigid metal material. Occasionally it is necessary to include insulation with the shell when treating high temperature flue gas. This is done to prevent moisture or acid mist from condensing in the unit, causing corrosion and rapid deterioration of the baghouse.

Hoppers

Hoppers are used to store the collected dust before it is disposed in a landfill or reused in the process. They are designed usually with a 60° slope to allow dust to flow freely from the top of the hopper to the bottom discharge opening. Some manufacturers add devices to the hopper to promote easy and quick discharge. These devices include strike plates, poke holes, vibrators, and rappers. Strike plates are simply pieces of flat steel which are bolted or welded to the center of the hopper wall. If dust becomes stuck in the hopper, rapping the strike plate several times with a mallet will free this material. Hopper designs also usually include access doors or ports. Access ports provide for easier cleaning, inspection and maintenance of the hopper (Figure 8-12).

Some type of discharge device is necessary for emptying the hopper. Discharge devices can be manual or automatic. The simplest manual discharge device is the *slide gate*, a plate held in place by a frame and sealed with gaskets. When the hopper needs to be emptied, the plate is removed and the material discharges. Other manual discharge devices include *hinged doors* or *drawers*. The collector must be shut down before opening any manual discharge device. Thus, manual discharge devices are used on baghouses that operate on a periodic basis.

Automatic continuous discharge devices are installed on baghouses that are used in continuous operation. Some devices include *trickle valves*, *rotary air lock valves*, *screw conveyors* or *pneumatic conveyers*. Trickle valves are shown in Figure 8-13. As dust collects in the hopper, the weight of the dust pushes down on the counterweight of the top flap and dust discharges downward (Figure 8-13). The top flap then closes, the bottom flap opens, and the material falls out. This type of valve is available in gravity-operated and motorized versions.

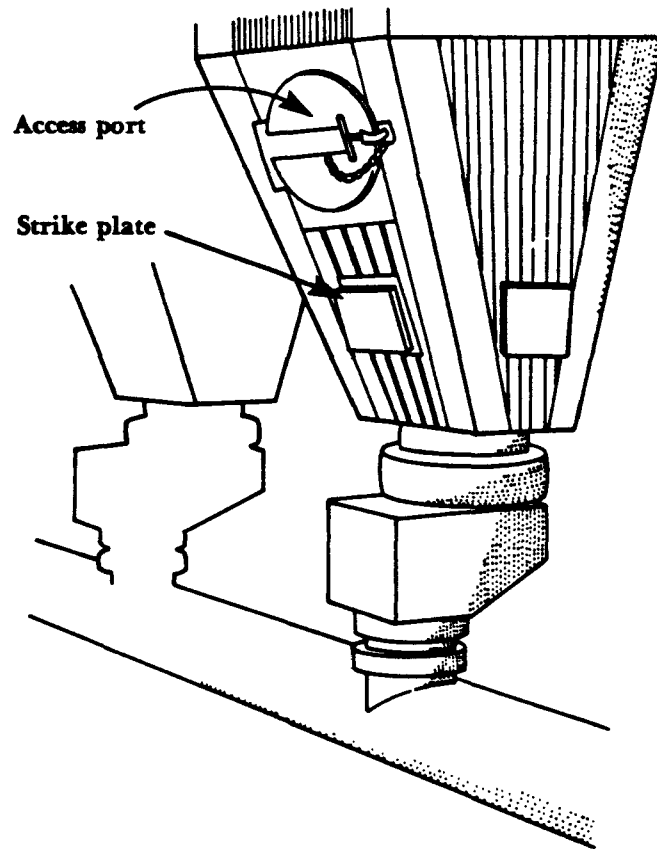


Figure 8-12. Hopper.

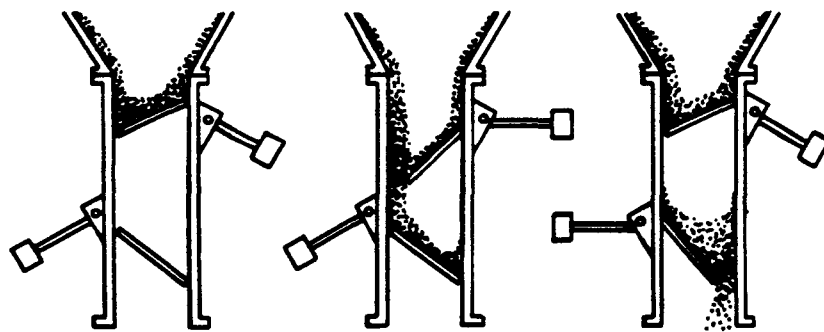


Figure 8-13. Trickle valve discharge device.

Rotary airlock valves are used on medium or large sized baghouses. The valve is designed with a paddle wheel which is shaft-mounted and driven by a motor (Figure 8-13). The rotary valve is similar to a revolving door: the paddles or blades form an airtight seal with the housing; the motor slowly moves the blades to allow the dust to discharge from the hopper.

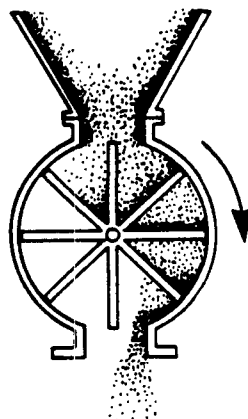


Figure 8-14. Rotary airlock discharge device.

Other automatic dust discharge devices include screw and pneumatic conveyers. Screw conveyers employ a revolving screw feeder located at the bottom of the hopper to remove the dust from the bin (Figure 8-15).

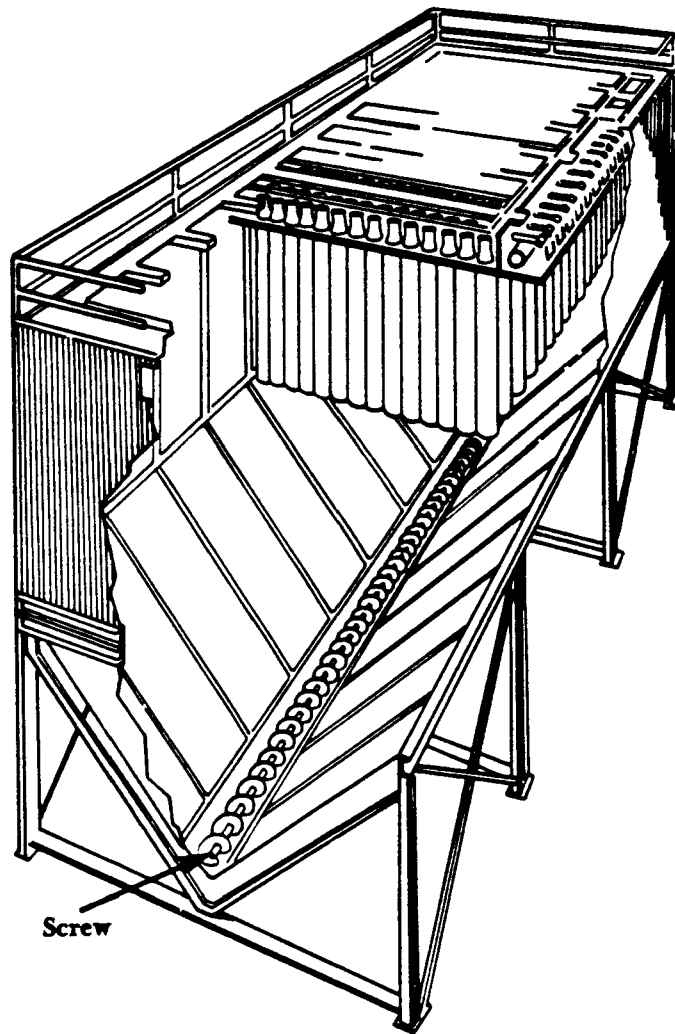


Figure 8-15. Screw conveyor.

Pneumatic conveyers use compressed air to blow (remove) dust from the hopper (Figure 8-16).

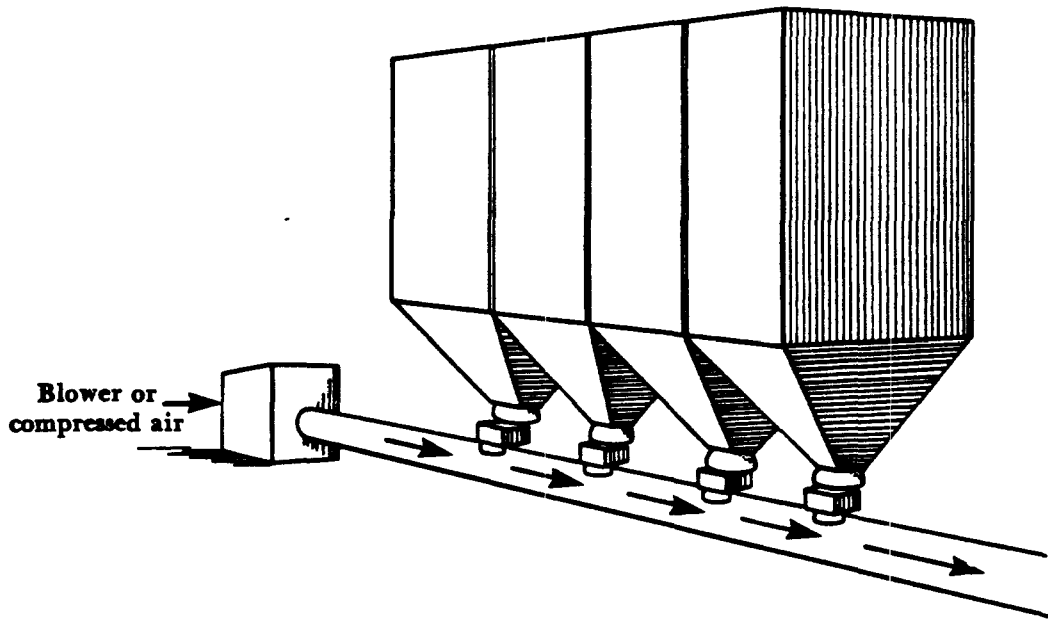


Figure 8-16. Pneumatic conveyor.

Fabric Filter Material

Construction Types

Woven and *felted* materials are used to make bag filters. Woven filters are made of yarn with a definite repeated pattern. Felted filters are composed of randomly-placed fibers compressed into a mat and attached to some loosely woven backing material. Woven filters are used with low energy cleaning methods such as shaking and reverse air. Felted fabrics are usually used with higher energy cleaning systems such as pulse jet cleaning.

Woven Filters

Woven filters have open spaces around the fibers. The type of weave used will depend on the design and the actual intended application of the woven filter. The simplest woven weave is the plain weave. The yarn is woven over and under to form a checkerboard pattern. This weave is not frequently used. Other weaves include the twill and sateen (satin). In the twill weave, yarn is woven over two and under one but in one direction only (Figure 8-17). This weave is tighter and more durable than the simple weave. Sateen weave goes one over and four under in both directions. Sateen weaves are very tight and allow the use of very fine yarns. Different weaving patterns increase or decrease the open spaces between the fibers.

This will affect both fabric strength and permeability. Fabric permeability affects the amount of air passing through the filter at a specified pressure drop. A tight weave, for instance, has low permeability and is better for the capture of small particles at the cost of increased pressure drop.

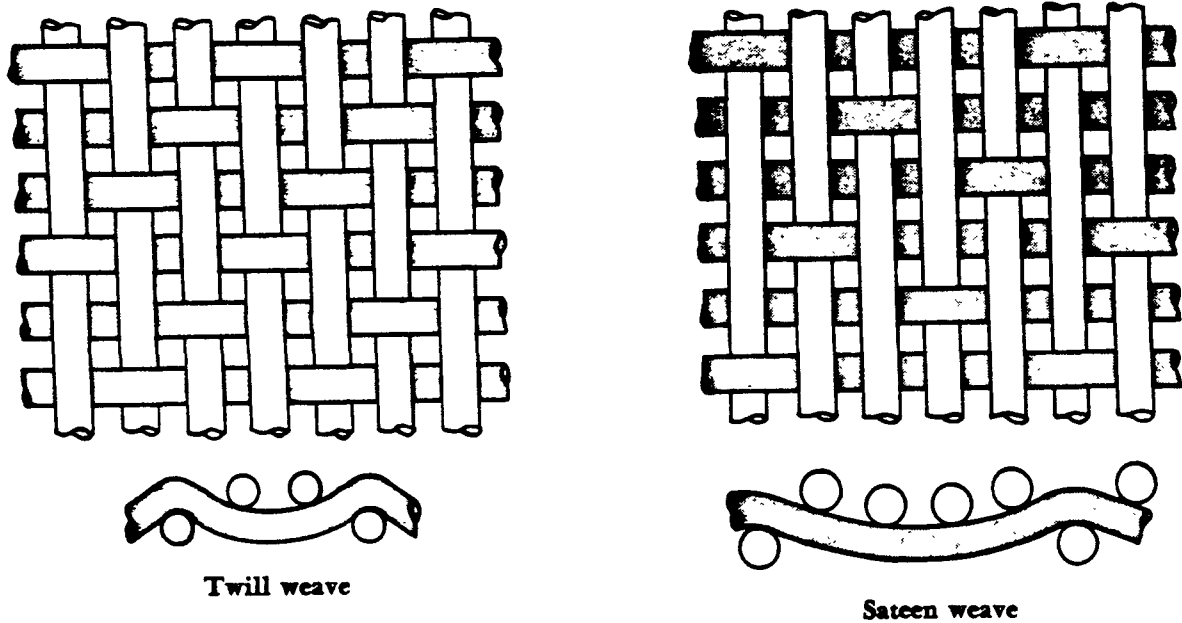


Figure 8-17. Woven fabric filter; twill weave and sateen weave.

The true filtering surface for the woven filter is not the bag itself, but the dust layer or *filter cake*. The bag simply provides the surface for capture of larger particles. Particles are collected by impaction or interception and the open areas in the weave are closed. This process is referred to as sieving (Figure 8-18). Some particles escape through the filter until the cake is formed. Once the cake builds up, effective filtering will occur until the bag becomes plugged and cleaning is required. At this point the pressure drop will be exceedingly high and filtering will no longer be cost effective. The effective filtering time will vary from a time of approximately 15-20 minutes to as long as a number of hours, depending on the concentration of particulate matter in the gas stream.

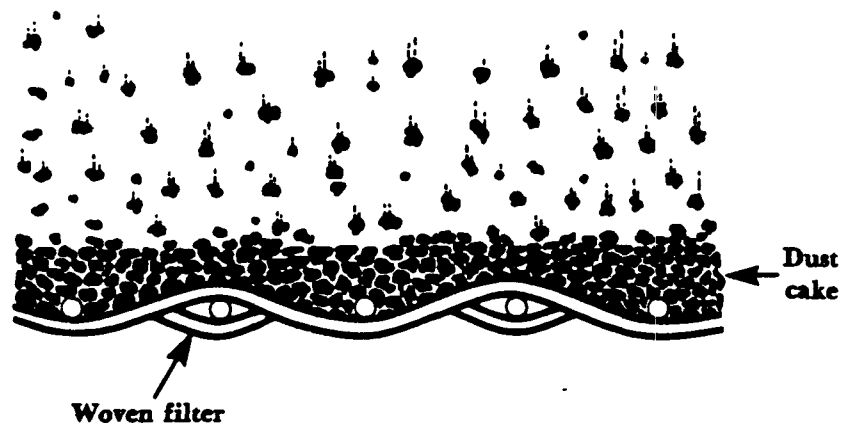


Figure 8-18. Sieving.

Felted Filters

Felted filters are made by needle punching fibers onto a woven backing called a scrim. The fibers are randomly placed as opposed to the definite repeated pattern of the woven filter. The felts are attached to the scrim by chemical, heat, resin and stitch-bonding methods.

To collect fine particles, the felted filters depend to a lesser degree on the initial dust deposits than do woven filters. The felted filters are generally 2 to 3 times thicker than woven filters. Each individual randomly oriented fiber acts as a target for particle capture by impaction and interception. Small particles can be collected on the outer surface of the filter (Figure 8-19).

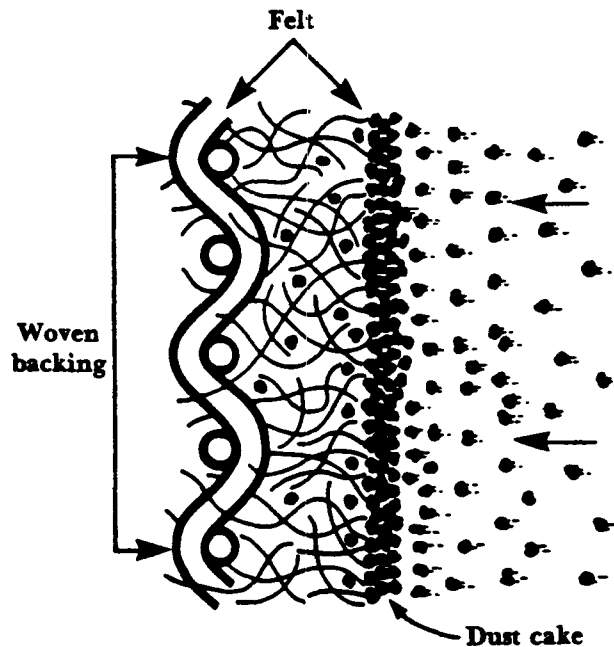


Figure 8-19. Felted fabric filter.

Felted filters are usually used in pulse jet baghouses. A pulse jet baghouse generally filters more air per cloth area (higher air-to-cloth ratio) than a shaker or reverse air unit. Felted bags should not be used in high humidity situations, especially if the particles are hygroscopic. Clogging and blinding could result in such situations.

Fibers

The fibers used for fabric filters vary depending on the industrial application to be controlled. Some filters are made from natural fibers such as cotton or wool. These fibers are relatively inexpensive but have temperature limitations ($< 100^{\circ}\text{C}$) and only average abrasion resistance. Synthetic fibers such as nylon, Orlon®, and polyester have slightly higher temperature limitations and chemical resistance. Synthetic fibers are more expensive than natural fibers. Nomex® is a registered trademark of fibers made by DuPont. DuPont makes the fibers, not filter fabrics or bags. Nomex® is widely used due to its relatively high temperature resistance and its resistance to abrasion. Other fibers such as Teflon® and Fiberglas® can be used in very high temperature situations (230 to 260°C). Both materials have good resistance to acid attack, but are generally more expensive than other fibers.

Table 8-2 lists a number of typical fibers used for fabric filters. The properties of the listed fibers include temperature limits, acid and alkali resistance, abrasion resistance, and relative bag costs.

Table 8-2. Typical fabrics used for bags.

Fabric	Maximum temperature (°C)		Acid resistance	Alkali resistance	Flex abrasion resistance	Relative cost
	Continuous	Surges				
Cotton	82	107	poor	very good	very good	2.0
Polypropylene	88	93	good to excellent	very good	excellent	1.5
Wool	93-102	121	very good	poor	fair to good	3.0
Nylon	93-107	121	poor to fair	good to excellent	excellent	2.5
Orlon®	116	127	good to excellent	fair to good	good	2.75
Acrylic	127	137	good	fair	good	3.0
Dacron®	135	163	good	good	very good	2.8
Nomex®	204	218	poor to good	good to excellent	excellent	8.0
Teflon®	204-232	260	excellent *except poor to fluorine	excellent *except poor to trifluoride, chlorine and molten alka- line metals	fair	25.0
Fiberglas®	260	288	fair to good	fair to good	fair	6.0

Sources: Bethea, 1978; EPA, 1979; Theodore and Buonicore, 1976.

Fabric Treatment

Fabrics are usually pretreated to improve their mechanical and dimensional stability. They can be treated with silicone to give them better cake release properties. Natural fabrics (wool and cotton) are usually preshrunk to eliminate bag shrinkage during operation. Both synthetic and natural fabrics usually undergo processes such as heat setting, flame retardation, and napping; these processes increase fabric life, improve dimensional stability and permeability, and ease of bag cleaning.

Bag Failure Mechanisms

There are three failure mechanisms that shorten the operating life of a bag. They are related to abrasion, thermal durability and chemical attack. The chief design variable is the upper temperature limit of the fabric. The process exhaust temperature will determine which fabric material should be used for dust collection. Exhaust gas cooling may be feasible, but one must be careful to keep the exhaust gas hot enough to prevent moisture or acid from condensing on the bags.

Another problem frequently encountered in baghouse operation is that of abrasion. Bag abrasion can result from bags rubbing against each other or from the type of bag cleaning employed in the baghouse. For instance, in a shaker baghouse, vigorous shaking may cause premature bag deterioration, particularly at the points where the bags are attached. In pulse jet units, the continual, slight motion of the bags against the supporting cages can also seriously affect bag life. As a result, a 25 percent per year bag replacement rate is usually encountered. This is the single biggest maintenance problem associated with baghouses.

Bag failure can also occur by chemical attack to the fabric. Changes in dust composition and exhaust gas temperatures from industrial processes can greatly affect the bag material. If the exhaust gas stream is lowered to its dew point or a new chemical species is created, the design of the baghouse (fabric choice) may be completely inadequate. Proper fabric selection and good process operating practices can help eliminate bag deterioration caused by chemical attack.

Gas Conditioning

Occasionally it is necessary to cool the process gas stream before the gas goes to the baghouse. Since there is an upper temperature limit on the fabrics used for bags, gas cooling is sometimes necessary to preserve bag life. This can be accomplished by a number of cooling methods.

Dilution of the exhaust gas stream by air is the easiest and cheapest method, especially at very high temperatures. However, air dilution requires the use of a larger baghouse to handle the increased volume of air. Other problems can arise due to the difficulty of controlling the intake of ambient moisture and other contaminants from the dilution air intake.

Radiation cooling can also be used to lower the process exhaust gas temperature. Radiation cooling involves the use of long uninsulated ducts that allow the gas stream to cool as heat radiates from the duct walls. Ducts can be designed in "U"

shapes to allow more duct surface area to be exposed for radiation cooling. Radiation cooling would not normally be very effective to cool gas temperatures below 300°C. This would require substantial surface area, lengthy duct runs, and increased fan horsepower. Precise temperature control is difficult to maintain and there is a possibility of the ducts becoming plugged due to particle sedimentation.

Evaporative cooling is also used to reduce exhaust gas stream temperature. Evaporative cooling is accomplished by injecting fine water droplets into the gas stream. The water droplets absorb heat from the gas stream as they evaporate. Spray nozzles are located in a quench chamber or somewhere in the duct preceding the baghouse. Evaporative cooling gives a great amount of controlled cooling at a relatively low installation cost. Temperature control can be flexible and accurate. However, this cooling method increases the exhaust volume to the baghouse. The biggest problem with evaporative cooling is keeping the gas temperature above the dewpoint of the gas (SO₂, NO₂, HCl, etc.). Otherwise, gases may condense on the bags causing rapid bag deterioration. In addition, all moisture injected into the gas must be evaporated to prevent corrosion of metal parts and blinding or plugging of caked dust on the bags.

Bag Cleaning

Cleaning Sequences

Three basic sequences are used for bag cleaning: *intermittent cleaning*, which is done on a demand basis; *periodic cleaning*, which is performed on a timed or scheduled basis; and *continuous filter cleaning*.

In intermittently cleaned baghouses, an entire compartment (or baghouse) is bypassed and the bags are cleaned either row by row or simultaneously. Intermittent baghouses are used for batch processes that can be shut down for bag cleaning.

Periodically cleaned baghouses consist of a number of compartments or sections. One compartment at a time is removed from service and cleaned on a regular rotation basis. The dirty gas stream is diverted from the compartment being cleaned to the other compartments in the baghouse, so it is not necessary to shut down the process.

Continuously cleaned baghouses, are fully automatic and can constantly remain on-line for filtering. The filtering process is momentarily interrupted by a blast of compressed air that cleans the bag, called pulse jet cleaning. In continuous cleaning, there is always a row of bags which are being cleaned somewhere in the baghouse. The advantage of continuous cleaning is that it is not necessary to take the baghouse out of service. Large continuous cleaning baghouses are built with compartments to help prevent total baghouse shutdown for bag maintenance and failures to the compressed air cleaning system or hopper conveyers. This allows the baghouse operator to take one compartment off-line to perform necessary maintenance.

Types of Bag Cleaning

A number of cleaning mechanisms are used to remove caked particles from bags. The three most common are *shaking*, *reverse air*, and *pulse jet*. Another mechanism called *blow ring* or *reverse jet* is normally not used in modern bag cleaning systems.

Shaking can be done manually, but is usually performed mechanically in industrial-scale baghouses. It is a low energy process that gently shakes the bags to remove deposited particles. The shaking motion and speed depends upon the vendors' design and the composition of dust deposited on the bag. The shaking motion can be either in a horizontal or vertical direction. The tops of the bags in shaker baghouses are sealed or closed and supported by some type of hook or clasp. Bags are open at the bottom and attached to a cell plate. The cell plate is shaken as a unit causing the bag to ripple, releasing the dust (Figure 8-20).

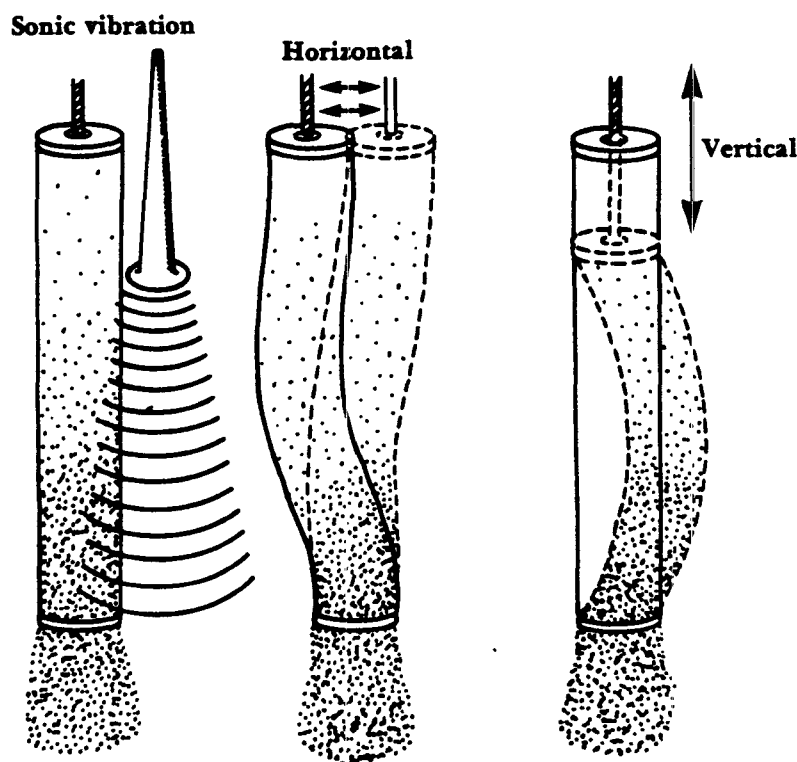


Figure 8-20. Shaking.

Shaking should not be used when collecting sticky dusts. The forces needed for removing sticky dust can cause the bag to be torn or ripped.

Bag wear on the whole is generally not a problem at the bottom of the bag which is attached to the cell plate; the greatest wear is at the top of the bag where the support loop attaches to the bag. Proper shaking frequency is therefore important to prevent premature bag failure.

In a few systems, shaking is accomplished by sonic vibration (Figure 8-20). A sound generator is used to produce a low frequency sound that causes the bags to vibrate. The noise level produced by the generator is barely discernable outside the baghouse. This type of cleaning, however, is not used on many newer baghouse systems.

Reverse air, the simplest cleaning mechanism, is accomplished by stopping the flow of dirty gas into the compartment and backwashing the compartment with a low pressure flow of air. Dust is removed by merely allowing the bags to collapse, thus causing the dust cake to break and fall into the hopper. The cleaning action is very gentle, allowing the use of less abrasion resistant fabrics such as Fiberglas® (Figure 8-21).

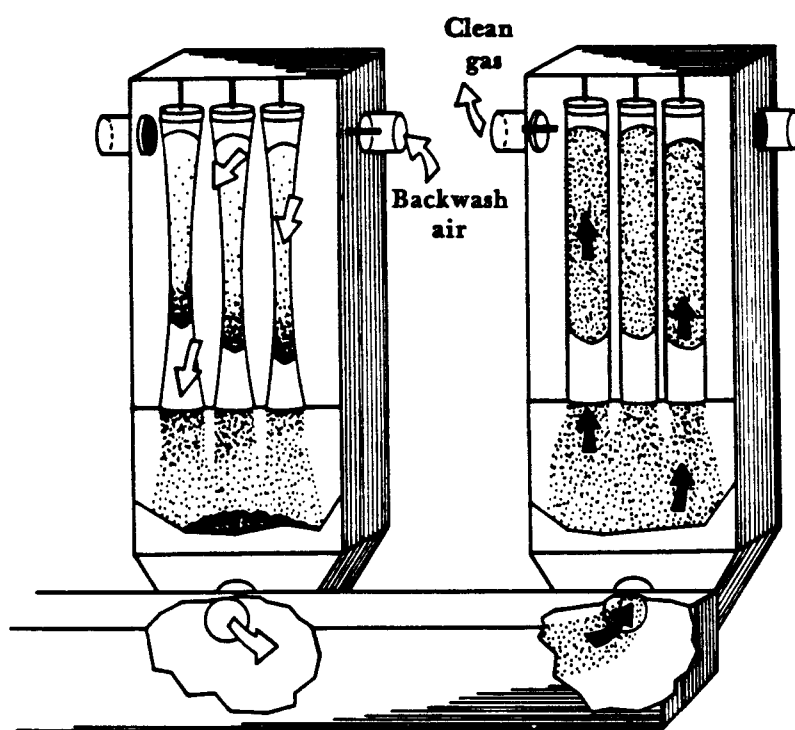


Figure 8-21. Reverse air cleaning.

Reverse air cleaning baghouses are usually compartmentalized to permit a section to be off-line for cleaning. Dust can be collected on either the inside or outside of the bag. If collected on the outside, some type of support is needed to prevent bag collapse during the filtering process. Bags can be supported by small steel rings sewn to the inside of the bag.

Reverse air cleaning baghouses generally have very low *air-to-cloth (A/C) ratios*. Air-to-cloth ratios describe how much dirty gas passes through a given surface area of filter in a given time. A high air-to-cloth ratio means a large volume of air passes through the fabric area. A low air-to-cloth ratio means a small volume of air passes through the fabric. The A/C ratios are usually expressed in units of $(\text{ft}^3/\text{min})/\text{ft}^2$ of cloth $[(\text{cm}^3/\text{sec})/\text{cm}^2 \text{ of cloth}]$. The A/C ratio can be used interchangeably with a term called *filtration velocity*. The units for filtration velocity are ft/min (cm/sec). When using the A/C ratios for comparison purposes one should use the units $(\text{ft}^3/\text{min})/\text{ft}^2$ or $(\text{cm}^3/\text{sec})/\text{cm}^2$. Likewise, when using filtration velocities one should use the units ft/min or cm/sec .

For reverse air baghouses, the filtering velocity (filtration velocity) range is usually between 1 and 3 ft/min (0.51 and 1.52 cm/sec). For shaker baghouses, the filtering velocity ranges between 2 and 6 ft/min (1.02 and 3.05 cm/sec). More cloth is generally needed for a given flow rate in a reverse air baghouse than in a shaker baghouse. Hence, reverse air baghouses tend to be larger in size.

Occasionally, baghouse cleaning is accomplished by two methods in combination. Many baghouses have been designed with both reverse air and gentle shaking to remove the dust cake from the bag.

The third bag cleaning mechanism most commonly used is the pulse jet or pressure jet cleaning. Baghouses using pulse jet cleaning make up approximately 40 to 50 percent of the new baghouse installations in the U.S. today. The pulse jet cleaning mechanism uses a high pressure jet of air to remove the dust from the bag. Bags in the baghouse compartment are supported internally by rings or cages. Bags are held firmly in place at the top by clasps and have an enclosed bottom. Dust-laden gas is filtered through the bag, depositing dust on the outside surface of the bag.

The dust cake is removed from the bag by a blast of compressed air injected into the top of the bag tube. The blast of high pressure air stops the normal flow of air through the filter. The air blast develops into a standing wave that causes the bag to expand as the bubble travels down the bag tube. As the bag flexes, the cake fractures and deposited particles are discharged from the bag (Figure 8-22). The air bubble travels down and back up the tube in approximately 0.5 seconds.

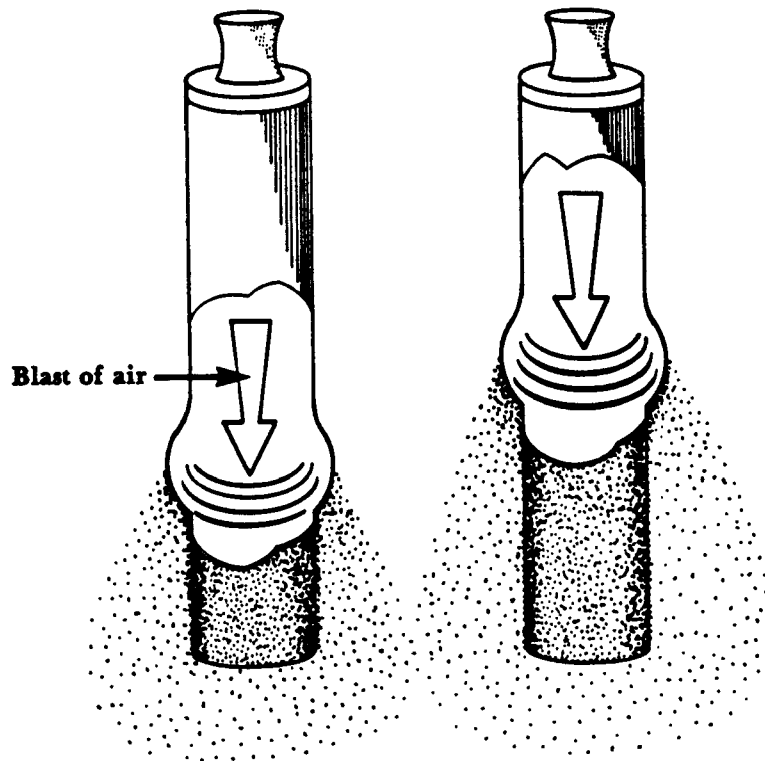


Figure 8-22. Pulse jet cleaning.

The blast of compressed air must be strong enough to travel the length of the bag and shatter or crack the dust cake. Pulse jet units use air supplies from a common header above each bag (Figure 8-23). In most baghouse designs, a venturi sealed at the top of each bag is used to create a large enough pulse to travel down and up the bag. This occurs in approximately 0.3 to 0.5 sec. The pressures involved are commonly between 60 and 100 psig (414 kPa and 689 kPa).

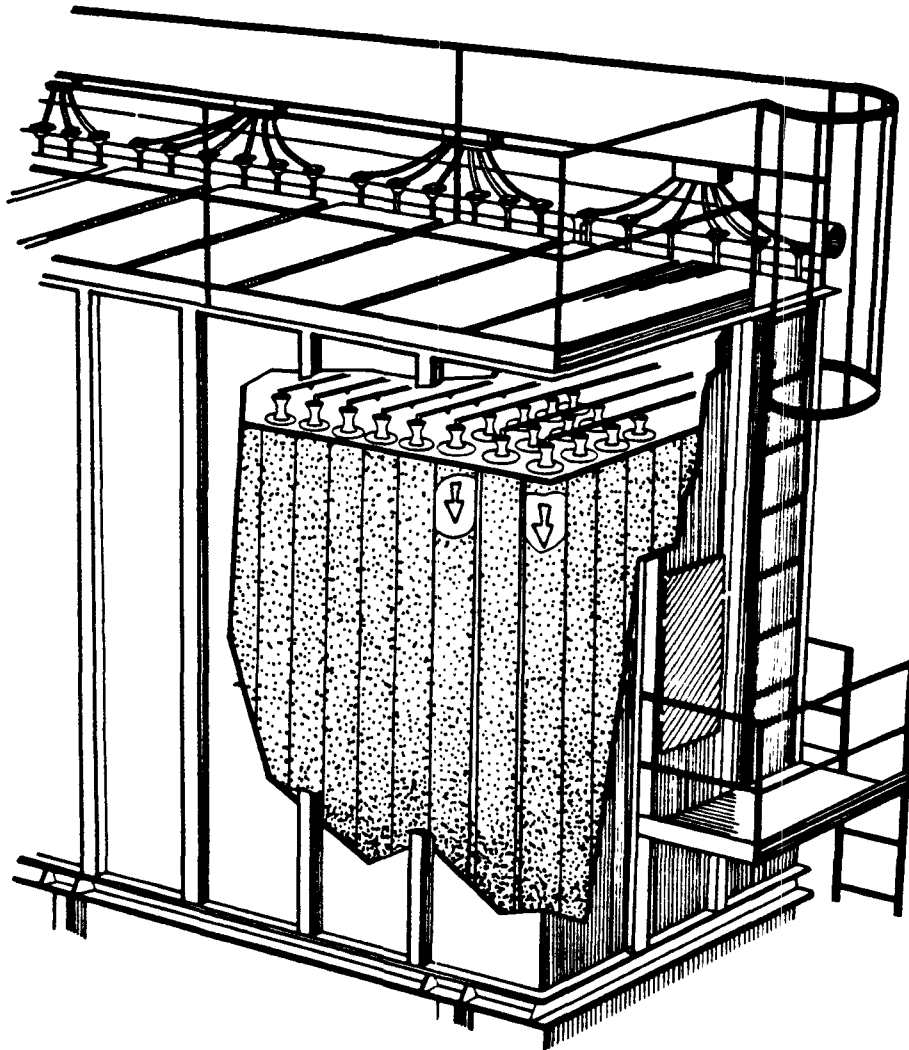


Figure 8-23. Pulse jet air supply.

Most pulse jet baghouses use bag tubes that are 4 to 6 in. (10.2 to 15.2 cm) in diameter. The length of the bag is usually around 10 to 12 ft (3.05 to 3.66 m), but can be as long as 25 ft (7.6 m). The shaker and reverse air baghouses use larger bags than the pulse jet units. The bags in these units are 6 to 18 in. (15.2 to 45.7 cm) in diameter and up to 40 ft (12.2 m) in length.

Pulse jet baghouses are designed with filtering velocities between 5 to 15 ft/min (2.5 to 7.5 cm/sec). Therefore, these units usually use felted fabrics as bag material. Felted material holds up very well under the high filtering rate and vigorous pulse jet cleaning. Pulse jet cleaning methods have the advantage of having no moving parts within the compartment. In addition, pulse jet units can clean bags on a continuous basis without isolating a compartment from service. The duration of the cleaning time is short (< 1.0 sec) when compared to the time length between cleaning intervals (approximately 20 minutes to several hours). The major disadvantage of high pressure cleaning methods is that the bags are subjected to more mechanical stress. Fabrics with higher dimensional stability and high tensile strength are required for these units.

Another bag cleaning mechanism is reverse jet cleaning using a blow ring. Some older baghouse designs employed this method, but it has lost popularity due to the great number of moving parts inside the baghouse. Blow ring cleaning involves reversing the air flow on each bag. This cleaning method does not depend on the collapse of each bag to crack the cake as in the reverse air baghouse. A traveling blow ring carriage moves up and down the bag compartment (Figure 8-24). Each ring has a number of slots where high velocity air jets penetrate the bag tube and dislodge the accumulated dust layer. The expense and complication of the blow ring mechanism (motors, drives, and switches for both ring and fan) limits the applicability of this equipment for air pollution control.

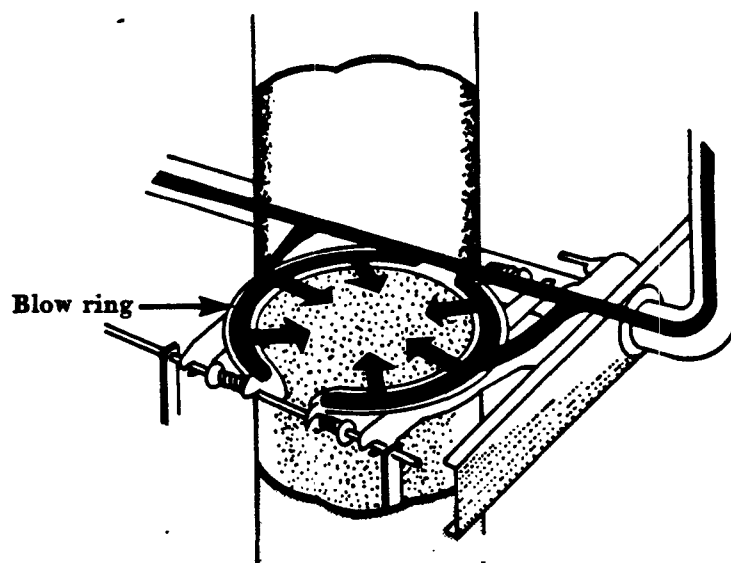
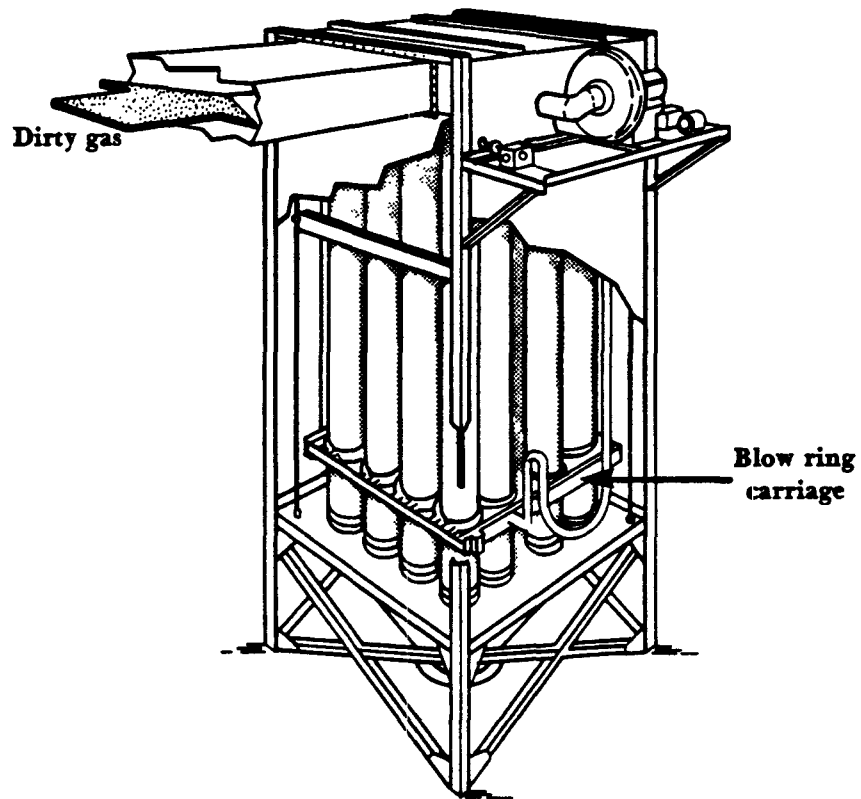


Figure 8-24. Reverse jet cleaning using blow rings.

Baghouse Design Variables

Baghouses are designed by considering a number of variables: *pressure drop*, *filter drag*, *air-to-cloth ratio*, *collection efficiency* and *gas conditioning*. Although not always possible or practical, it is a good idea to use a pilot scale baghouse during the initial stages of the baghouse design. However, previous vendor experience with the same or similar process to be controlled will generally be adequate for design purposes. Careful design will reduce the number of baghouse operating problems and possible air pollution violations.

Pressure Drop

Pressure drop, a very important baghouse design variable, describes the resistance to air flow across the baghouse. Pressure drop is usually expressed in mm of mercury or inches of water. It can be related to the size of the fan that would be necessary to either push or pull the exhaust gas through the baghouse. A baghouse with a high pressure drop would need a larger fan and more energy to move the exhaust gas through the baghouse.

Many different relationships have been used to estimate the pressure drop across a fabric filter. In a baghouse the total pressure drop is a function of the pressure drop across both the filter and the deposited dust cake. There are also some minor pressure losses due to friction occurring as the gas stream moves through the baghouse.

The simplest equation used to predict pressure drop across a *filter* is derived from Darcy's law governing the flow of fluids through porous materials and given as:

$$\text{(Eq. 8-1)} \quad \Delta p_f = k_1 v_f$$

Where: Δp_f = pressure drop across the clean fabric, in. H₂O (cm H₂O)
 k_1 = fabric resistance, in. H₂O/ft-min (cm H₂O/cm-sec)
 v_f = filtration velocity, ft/min (cm/sec)

The term k_1 is the fabric resistance and is a function of exhaust gas viscosity and filter characteristics such as thickness and porosity. Porosity describes the amount of void volume in the filter.

The pressure drop across the *deposited dust cake* can be estimated by using Equation 8-2 (Snyder and Pring, 1955). This formula is also derived from Darcy's law and the simplified form is given as:

$$\text{(Eq. 8-2)} \quad \Delta p_c = k_2 c_f v_f^2 t$$

Where: Δp_c = pressure drop across the cake, in. H₂O (cm H₂O)
 k_2 = resistance of the cake, in. H₂O/(lb/ft²•ft/min)
[cm H₂O/(g/cm²•cm/sec)]
 c_f = dust concentration loading, lb/ft³ (g/cm³)
 t = filtration time, min (sec)
 v_f = filtration velocity, ft/min (cm/sec)

The term k_2 is the dust-fabric filter resistance coefficient and is determined experimentally. The coefficient is dependent on gas viscosity, particle density and dust porosity. The dust porosity is the amount of void volume in the dust cake. The porosity is related to the permeability. Permeability is defined in ASTM standard D737-69 as the volume of air which can be passed through one square foot of filter medium with a pressure drop of no more than 0.5 inches of water.

The total pressure drop equals the pressure drop across the filter plus the pressure drop across the cake and is given as:

$$\begin{aligned} \text{(Eq. 8-3)} \quad \Delta p_T &= \Delta p_f + \Delta p_c \\ \Delta p_T &= k_1 v_f + k_2 c_i v_f^2 t \end{aligned}$$

Equation 8-3 should be used as only an estimate of pressure drop across shaker and reverse air cleaning baghouses. In the industrial filtration process, there are complicated particle-fabric interactions occurring just after the filtration cycle begins. In addition, the filter resistance factor k_1 can take on two values; one value for the clean filter and another after the filter has been cleaned. When the dust cake builds up to a significant thickness the pressure drop will become exceedingly high (> 12 in. H_2O or 30.5 cm H_2O). At this time the filter must be cleaned. Some dust will remain on the cloth even after cleaning; therefore, the filter resistance level will be higher than during original conditions.

Filter Drag

Filter drag is the filter resistance across the fabric-dust layer. It is a function of the quantity of dust accumulated on the filter and given as:

$$\text{(Eq. 8-4)} \quad S = \frac{\Delta p}{v_f}$$

Where: S = filter drag, in. H_2O /(ft/sec) [kPa/(cm/sec)]
 Δp = pressure drop across the filter and dust cake, in. H_2O (cm H_2O)
 v_f = filtration velocity, ft/sec (cm/sec)

It essentially gives the pressure drop occurring per unit velocity.

As previously mentioned, the true filtering surface is not the bag itself, but the dust layer. Dust bridges the pores or openings in the weave, increasing the drag rapidly. A filter performance curve of a single bag of a fabric is shown in Figure 8-25. The drag is plotted versus the dust mass deposited on the filter.

The point c , on the graph is the residual drag of the clean filter medium. The filter drag increases exponentially up to a constant rate of increase. This is the period of cake repair and initial cake buildup. Effective filtration takes place while the filter drag increases at a constant rate. When the total pressure drop reaches a value set by the system design, bag cleaning is initiated. At this point, the pressure drop decreases (almost vertically on the performance curve) to the initial point. Cake repair begins when the cleaning cycle stops and the cycle repeats.

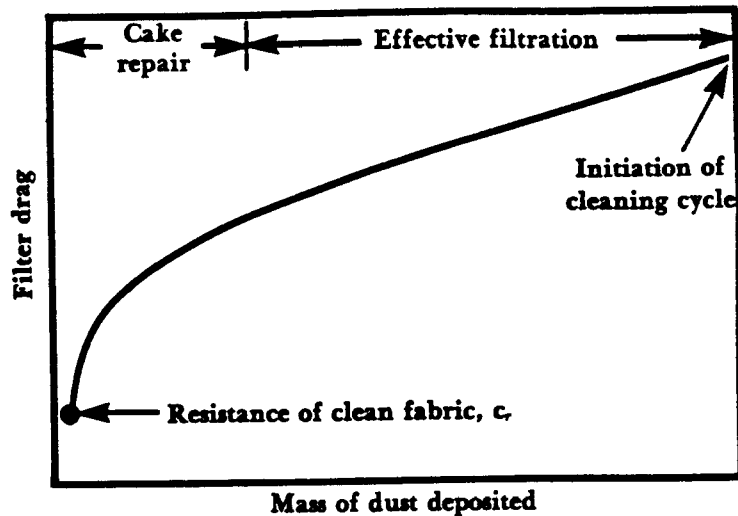


Figure 8-25. Performance curve for a single bag of a fabric filter.

In multicompartment baghouses where the various compartments are cleaned one at a time, the performance curve takes on a different shape. In this case the change in the curve is less pronounced than in Figure 8-25. The performance curve has a slight saw tooth shape for the net pressure drop across the entire baghouse (Figure 8-26). Each of the minima points on the curve represent the cleaning of an entire compartment. The average pressure drop would be represented by the dotted line. For optimum filtration rate and collection efficiency, the baghouse should be designed to operate at a pressure drop that approaches a constant value. This involves careful selection of fabrics and cleaning mechanisms for the baghouse. The weave, and any pretreatment of the fabric can affect the cake repair time. Poor cleaning will increase the filter drag; therefore, it is essential to thoroughly clean the bags to reduce the filter drag effect. If cake repair time can be minimized, the pressure drop will be lower. Consequently, the effective filtration rate will be longer for optimum filtering use.

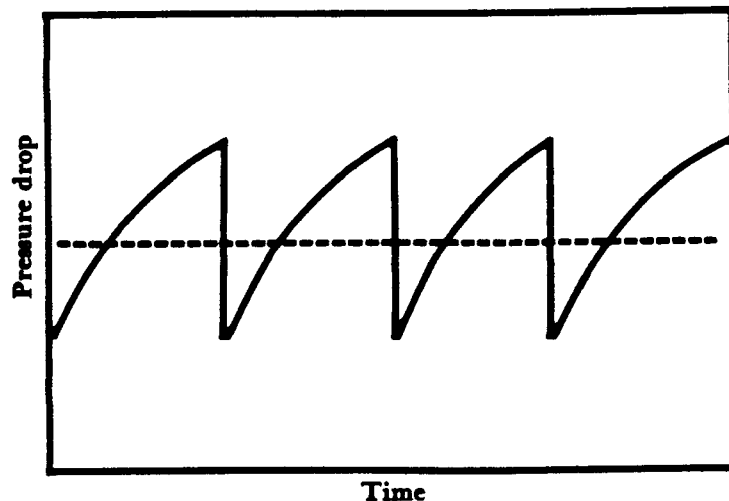


Figure 8-26. Overall pressure drop of a multicompartment baghouse.

Filtration Velocity: Air-to-Cloth Ratio

As previously mentioned, the terms filtration velocity and air-to-cloth ratio can be used interchangeably. The formula used to express filtration velocity is:

$$(Eq. 8-5) \quad v_f = \frac{Q}{A_c}$$

Where: v_f = filtration velocity, ft/min (cm/sec)
 Q = volumetric air flow rate, ft³/min (cm³/sec)
 A_c = area of cloth filter, ft² (cm²)

Air-to-cloth ratio is defined as the ratio of gas filtered in cubic feet per minute to the area of filtering media in square feet. Typical units used to express the A/C ratio are:

$$(ft^3/min)/ft^2 \text{ or } (cm^3/sec)/cm^2$$

These A/C ratio units essentially reduce to velocity units.

The A/C ratio (filtration velocity) varies for various baghouse designs. Shaker and reverse air baghouses generally have small A/C ratios. (Shaker units < 3:1 (cm³/sec)/cm² and reverse air units < 1.5:1 (cm³/sec)/cm²). On the other hand, pulse jet units usually operate at A/C ratios between 2.5 and 10:1 (cm³/sec)/cm². For a given flow rate, pulse jet units can be smaller in size (fewer bags) than the shaker and reverse air baghouse.

The A/C ratio (filtering velocity) is a very important factor used in the design and operation of a baghouse. Improper ratios can cause the baghouse to be in violation of air pollution regulations. Operating at an A/C ratio that is too high may lead to a number of problems. Very high ratios can cause compaction of dust on the bag resulting in excessive pressure drops. In addition, breakdown of the dust cake could also occur which in turn results in reduced collection efficiency. The major problem of a baghouse using a very low A/C ratio, is that the baghouse will be larger in size.

Collection Efficiency

Extremely small particles can be efficiently collected in a baghouse. Baghouse units designed with collection efficiencies of 99.99 percent are common. Exhaust air from baghouses can even be recirculated back into the plant for heating purposes, as long as the particles collected are not toxic.

Baghouses are not normally designed with the use of fractional efficiency curves as are some of the other particulate emission control devices. Vendors design and size the units strictly on experience. The baghouse units are designed to meet particulate emission outlet loading and opacity regulations. There is no one formula that can determine the collection efficiency of a specific baghouse. Some theoretical formulas for determining collection efficiency have been suggested, but these formulas contain numerous (3 to 4) experimentally determined coefficients in the equations. Therefore, these efficiency equations give at best only an estimate of baghouse performance.

Baghouse Design Review

The design of an industrial baghouse involves consideration of many factors including space restriction, cleaning method, fabric construction type, fiber, air-to-cloth ratio and many construction details such as inlet location, hopper design and dust discharge devices. Air pollution control agency personnel who review baghouse design plans should consider these factors during the review process.

A given process might often dictate one type of baghouse for particulate emission control. The manufacturer's previous experience with a particular industry is sometimes the key factor. For example, a pulse jet baghouse with its higher filter rates would take up less space and would be easier to maintain than a shaker or reverse air baghouse. But if the baghouse was to be used in a high temperature application (260°C), a reverse air cleaning baghouse with woven Fiberglas® bags might be chosen. This would prevent the need of exhaust gas cooling for the use of Nomex® felt bags (on the pulse jet unit) which are more expensive than Fiberglas® bags. All design factors must be weighed carefully in choosing the most appropriate baghouse design.

Review of Design Criteria

The principal design criterion is the gas flow rate to the baghouse, measured in cubic meters (cubic feet) per minute. The gas volume to be treated is set by the process exhaust, but the filtration velocity or air-to-cloth ratio is determined by the baghouse vendor's design. The air-to-cloth ratio depends on a number of variables. A thorough review of baghouse design plans should consider the following factors.

1. Type, shape, and density of dust; average and maximum concentrations; chemical properties such as abrasiveness, explosiveness, electrostatic charge and agglomerating tendencies.
2. Gas flow rate: average and maximum flow rate, temperature, moisture content, chemical properties such as dew point, corrosiveness and combustibility.
3. Fabric construction: woven or felt filters, filter thickness, fiber size, fiber density, filter treatments such as napping, resin and heat setting, and special coatings.
4. Fiber type: natural, synthetic, Nomex®, Teflon®, etc.
5. Cleaning methods: low energy which are shaker and reverse air cleaning; high energy which is pulse jet cleaning.
6. Cleaning time: ratio of filtering time to cleaning time is the measure of the percent of time the filters are performing; this should be at least 10:1 or greater.
7. Cleaning and filtering stress: amount of flexing and creasing to the fabric; reverse air is the gentlest, shaking and pulse jet have the most vigorous stress on the fabric.
8. Bag spacing: bags must be properly spaced to eliminate rubbing against each other; bags must be accessible for inspection and maintenance service.

9. Compartment design: allowance for proper cleaning of bags; design should include an extra compartment to allow for reserve capacity and off-line cleaning, and inspection and maintenance of broken bags.
10. Space and cost requirements: baghouses require a good deal of installation space; initial costs, and operating and maintenance costs can be high.
11. Emission requirements: efficiency in terms of opacity and grain-loading regulations.
12. Proper air-to-cloth ratio (A/C); reverse air lowest, shakers next, pulse jet baghouses allow the highest A/C ratio.

Simple Cloth Size Check

Baghouse sizing is done by the manufacturer. A simple check or estimate of the amount of baghouse cloth needed for a given process flow rate can be computed by using Equation 8-5.

$$v_f = \frac{Q}{A_c}$$

or

$$A_c = \frac{Q}{v_f}$$

For example, if the process gas exhaust rate is given as $4.72 \times 10^6 \text{ cm}^3/\text{sec}$ ($10,000 \text{ ft}^3/\text{min}$) and the filtration velocity is $4 \text{ cm}/\text{sec}$ (A/C is 4:1 ($\text{cm}^3/\text{sec})/(\text{cm}_2)$), the cloth area would be:

$$\begin{aligned} A_c &= \frac{4.72 \times 10^6 \text{ cm}^3/\text{sec}}{4 \text{ cm}/\text{sec}} \\ &= 1,179,875 \text{ cm}^2 \text{ (cloth required)} \\ &= 117.98 \text{ m}^2 \text{ (cloth required)} \end{aligned}$$

To determine the number of bags required in the baghouse, one would simply use the formula:

$$A_b = \pi d h$$

Where: A_b = area of bag, m (ft)
 d = bag diameter, m (ft)
 h = bag height, m (ft)

If the bag diameter is 0.203 m (8 in.) and bag height is 3.66 m (12 ft), the area of each bag is:

$$\begin{aligned} A_b &= 3.14 \times 0.203 \text{ m} \times 3.66 \text{ m} \\ &= 2.33 \text{ m}^2 \end{aligned}$$

The calculated number of bags in the baghouse is:

$$\begin{aligned}\text{Number of bags} &= \frac{117.98 \text{ m}^2}{2.33} \\ &= 51 \text{ bags}\end{aligned}$$

Typical Air-to-Cloth Ratios

During a permit review for baghouse installations the reviewer should check the A/C ratio. Typical A/C ratios for shakers, reverse air and pulse jet baghouses are listed in Table 8-3.

Table 8-3. Typical air-to-cloth ranges.

Baghouse cleaning method	Air-to-cloth range
Shaking	1-3 (cm ³ /sec)/cm ² 2-6 (ft ³ /min)/ft ²
Reverse air	0.5-1.5 (cm ³ /sec)/cm ² 1-3 (ft ³ /min)/ft ²
Pulse jet	2.5-7.5 (cm ³ /sec)/cm ² 5-15 (ft ³ /min)/ft ²

Note: Air-to-cloth ratios are occasionally given as 2.0:1 instead of 2.0 (cm³/sec)/cm²

Baghouses should be operated within a reasonable design A/C ratio range. For example, assume a permit was submitted indicating the use of a reverse air cleaning baghouse using woven Fiberglas® bags for reducing particulate emissions from a small foundry furnace. If the information supplied indicated that the baghouse would operate with an A/C ratio of 6 (cm³/sec)/cm² of fabric material, one should question this information. Reverse air units should be operated with a much lower A/C ratio. The fabric would probably not be able to withstand the stress from such high filtering rates and could cause premature bag deterioration. Too high an A/C ratio results in excessive pressure drops, reduced collection efficiency, blinding, and rapid wear. In this case a better design might include reducing the A/C ratio within the acceptable range, thus adding more bags. Another alternative would be to use a pulse jet baghouse with the original design A/C ratio of 6 (cm³/sec)/cm² and use felted bags made of Nomex® fibers. Either alternative would be more acceptable to the original permit submission.

Typical air-to-cloth ratios for baghouses used in industrial processes are listed in Tables 8-4 and 8-5. These values should be used as a rule of thumb or guide only. Actual design values may need to be reduced if the dust loading is high or the particle size is small. When compartmental baghouses are used, the design A/C ratio must be based upon having enough filter cloth available for filtering while one or two compartments are offstream for cleaning.

Table 8-4. Typical A/C ratios [(ft³/min)/ft²] for selected industries*.

Industry	Fabric filter air-to-cloth ratio		
	Reverse air	Pulse jet	Mechanical shaker
Basic oxygen furnaces	1.5-2.0	6-8	2.5-3.0
Brick manufacturing	1.5-2.0	9-10	2.5-3.2
Castable refractories	1.5-2.0	8-10	2.5-3.0
Clay refractories	1.5-2.0	8-10	2.5-3.2
Coal fired boilers	—	—	—
Conical incinerators	—	—	—
Cotton ginning	—	—	—
Detergent manufacturing	1.2-1.5	5-6	2.0-2.5
Electric arc furnaces	1.5-2.0	6-8	2.5-3.0
Feed mills	—	10-15	3.5-5.0
Ferroalloy plants	2.0	9	2.0
Glass manufacturing	1.5	—	—
Grey iron foundries	1.5-2.0	7-8	2.5-3.0
Iron and steel (sintering)	1.5-2.0	7-8	2.5-3.0
Kraft recovery furnaces	—	—	—
Lime kilns	1.5-2.0	8-9	2.5-3.0
Municipal incinerators	—	—	—
Petroleum catalytic cracking	—	—	—
Phosphate fertilizer	1.8-2.0	8-9	3.0-3.5
Phosphate rock crushing	—	5-10	3.0-3.5
Polyvinyl chloride production	—	7	—
Portland cement	1.2-1.5	7-10	2.0-3.0
Pulp and paper (fluidized bed reactor)	—	—	—
Secondary aluminum smelters	—	6-8	2.0
Secondary copper smelters	—	6-8	—
Sewage sludge incinerators	—	—	—
Surface coatings—spray booth	—	—	—

*High efficiency: a sufficiently low grain loading to expect a clear stack.

Source: EPA, 1976, EPA 450/3-76-014.

Table 8-5. Typical A/C ratios for fabric filters used for control of particulate emissions from industrial boilers.

Size of boiler (10 ³ lb steam per hour)	Temperature (°F)	Air-to-cloth ratio [(ft ³ /min)/ft ²]	Cleaning mechanism	Fabric material
260 (3 boilers)	400°	4.4:1	On- or off-line pulse or reverse air	Glass with 10% Teflon® coating (24 oz/yd ²)
170 (5 boilers)	500°	4.5:1	Reverse air with pulse-jet assist	Glass with 10% Teflon® coating
140 (2 boilers)	360°	2.0:1	Reverse air	No. 0004 fiberglass with silicone-graphite- Teflon® finish
250	338°	2.3:1	Shake and deflate	Woven fiberglass with silicone-graphite finish
200 (3 boilers)	300°	3.6:1	Shake and deflate	Woven fiberglass with silicone-graphite finish
400 (2 boilers)	Stoker, 285° to 300°; pul- verized coal, 350°	2.5:1	Reverse air	Glass with Teflon® finish
75	150°	2.8:1	Reverse air	Fiberglass with Teflon® coating
50	350°	3.0:1	On-line pulse	Glass with Teflon® finish
270 (2 boilers)	330°	3.7:1	On-line pulse	Teflon® felt (23 oz)
450 (4 boilers)	330°	3.7:1	On-line pulse	Teflon® felt (23 oz)
380	NA	2.0:1	Reverse air/vibrator assist	Glass with 10% Teflon® coating
645	NA	2.0:1	Reverse air/vibrator assist	Glass with 10% Teflon® coating
1,440 (3 boilers)	360°	3.4:1	Shake and deflate	Woven fiberglass with silicone-graphite finish

Source: EPA, 1979.

References

1. Bethea, R. M. 1978. *Air Pollution Control Technology: An Engineering Analysis Point of View*. New York: Van Nostrand Reinhold Company.
2. Theodore, L. and Buonicore, A. J. 1976. *Industrial Air Pollution Control Equipment for Particulates*. Cleveland: CRC Press.
3. Cheremisinoff, P. N. and Young, R. A., eds. 1977. *Air Pollution Control and Design Handbook, Part 1*. New York: Marcel Dekker, Inc.
4. Hesketh, H. E. 1979. *Air Pollution Control*. Ann Arbor: Ann Arbor Science Publishers Inc.
5. Stern, A. C. ed. 1977. *Air Pollution, 3rd ed. vol. IV. Engineering Control of Air Pollution*. New York: Academic Press.
6. Cross, F. L. and Hesketh, H. E. eds. 1975. *Handbook for the Operation and Maintenance of Air Pollution Control Equipment*. Westport, CN: Technomic Publishing Co., Inc.

7. Environmental Protection Agency (EPA). 1979. *Particulate Control by Fabric Filtration on Coal-Fired Industrial Boilers*. EPA 625/2-79-021.
8. Environmental Protection Agency (EPA). 1976. *Capital and Operating Costs of Selected Air Pollution Control Systems*. EPA 450/3-76-014.
9. Sittig, M. 1977. *Particulates and Fine Dust Removal Processes and Equipment*. New Jersey: Noyes Data Corporation.
10. Kraus, M. N. 1979. Baghouses: separating and collecting industrial dusts. *Chem. Eng.* 86:94-106.
11. Proceedings: Symposium on the use of fabric filters for the control of sub-micron particulates, April 8-10, 1974, Boston, MA. *J. Air Pol. Control Assoc.* 24:1139-1197, 1974.
12. Frederick, E. R. 1974. Some Effects of Electrostatic Charges in Fabric Filtration. *J. Air Pol. Control Assoc.* 24:1164-1168.
13. Environmental Protection Agency (EPA). 1973. *Air Pollution Engineering Manual*. 2nd ed. AP-40.
14. Proceedings: The User and Fabric Filtration Equipment III, October 1-3, 1978, Niagara Falls, NY. Air Pollution Control Association Specialty Conference.

Chapter 9

Wet Collectors

Wet collectors provide many options for the control of source emissions. These air pollution control devices can remove both particulate matter and gases from effluent gas streams. They can operate at low removal efficiencies or at high removal efficiencies. They also offer more versatility in design than other air pollution control devices. This versatility, however, does not come without problems. Higher efficiency requires higher operating costs; by-products are difficult to recover, and an air pollution problem can be transformed into a water pollution problem. In terms of cost, wet collectors are generally more expensive than simple settling chambers and cyclones but less expensive than high efficiency electrostatic precipitators and baghouses. They have often been specified as satisfying the requirements of Reasonably Available Control Technology (RACT) because of the number of design and cost options they can provide for existing stationary sources. This chapter will deal with the general characteristics of wet collectors, the design theories behind them, and their equipment descriptions.

General Characteristics—Particulate Matter Removal

As the name implies, wet collectors or wet scrubbers, are devices which use a liquid for removing particles or polluted gases from an exhaust gas stream. Water sprays can be injected into the gas stream; the gas can be forced to pass through sheets or films of liquid; or the gas can move through beds of plastic spheres covered with liquid. Each of these techniques can effectively remove particulate matter from process exhaust gases. They can also effectively remove gases such as HCl or SO₂, but removal conditions must be right. In many cases, the best conditions for removing particulate matter are the poorest for removing pollutant gases. In this chapter, emphasis will be placed on the design and application of wet scrubbers for the removal of particulate matter. Optimum operating conditions for particulate matter removal will be discussed. Effective techniques for removing gaseous components will be contrasted to particulate emission control methods. Gaseous emission control methods are discussed in greater detail in the manual for APTI Course 415—"Control of Gaseous Emissions".

Wet collectors exhibit some relative advantages compared to other particulate matter control equipment. These advantages follow:

Small space requirements: Systems can be designed for small locations, roof mounting, etc.

No secondary dust sources: Once the pollutant is collected, it cannot escape from hoppers or in transport. The collected slurries resulting from wet scrubbers can possibly be more easily handled than dry dust.

Collects gases and particulate matter: This can be an advantage for small industrial process industries unable to afford separate control systems; particularly useful for incineration processes.

Handles high temperature, high humidity gas streams: Temperature limits and condensation problems in baghouses and ESPs can be avoided since wet scrubbers cool incoming gases and wash away accumulated particulate matter.

Ability to humidify a gas stream: The scrubber can reduce the temperature and volume of an unsaturated gas stream at high temperature by the process of evaporation. Smaller ducting and fan sizes can then be used downstream of the collector.

Fire and explosion hazards are at a minimum: Fire and explosion hazards connected with various dry dusts can be eliminated by using water as the control medium.

Although wet collectors have many advantages, they may not be suitable for all applications. Some relative disadvantages follow:

Corrosion problems: Water and absorbed gaseous pollutants can form highly corrosive acid solutions; therefore, choosing proper construction materials for the control system is important.

Meteorological problems: Highly humidified exhaust gases can produce a wet, visible steam plume, especially during cold weather; fog and precipitation from the plume may cause local meteorological problems.

Pressure drop and power requirement: High collection efficiencies for particulate matter are attainable only at high pressure drops; the increased fan power required to move the exhaust gases through the scrubber may result in significant operating costs.

Water pollution: Adequate precautions must be taken before scrubber waste liquid is disposed; settling ponds and sludge clarifiers are often included in the design of wet collector systems to meet waste water regulations.

Difficulty of by-product recovery: Recovery of dust for re-use is difficult when wet collectors are used; costs associated with dewatering and drying of the scrubber sludge may make other control methods more practical.

A variety of wet collectors are commercially available. The evaluation and selection of a scrubber system is somewhat simplified by the observation that collection efficiency is a function of the amount of energy required to operate the scrubber (Lapple, 1955). This means simply, that independent of design, the more power put in the system the greater the collection efficiency. Therefore, for systems of nearly equivalent power inputs the collection efficiencies should be nearly equivalent. The selection or evaluation between two systems could then concentrate on ease of operation, potential maintenance problems, and comparative costs.

Theory of Operation

Wet collectors are designed to incorporate small dust particles into larger water droplets. Droplets ranging from 50 to 500 μm in diameter are produced and brought into contact with the particulate matter. These large droplets containing the captured particles are then collected by simple mechanisms such as gravity, impaction on baffles, or by cyclonic action. Many wet collectors can be represented as having two zones: a *contact zone* and a *separation zone* (Figure 9-1).

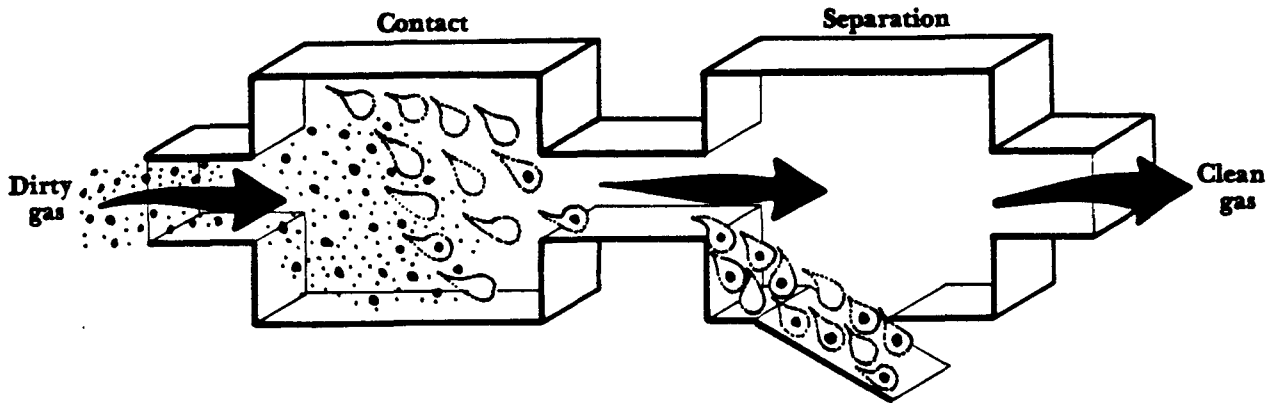
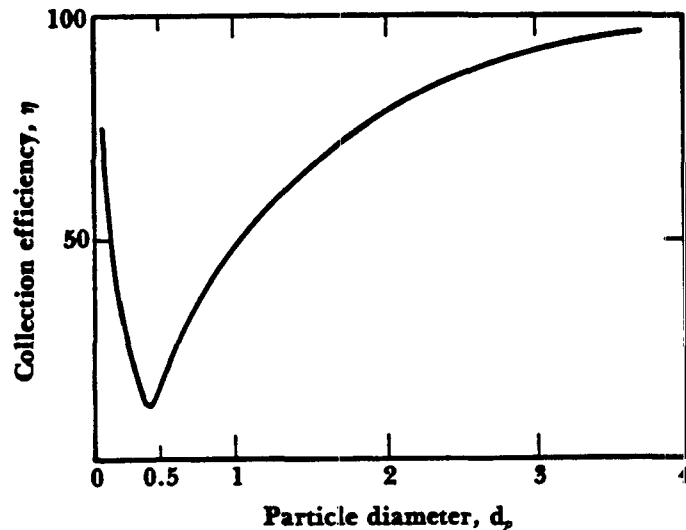


Figure 9-1. Zones of a wet scrubber.

Droplets can be produced by a spray nozzle, by the aspirating effect of the gas stream shearing a liquid film, or by the motion of a mechanically driven rotor. In the contact zone, the particulate matter approaches the water droplets. Contact is made by three primary mechanisms: *inertial impaction*, *direct interception*, and *diffusion* (see Chapter 1). Inertial impaction, the breaking through streamlines by particles, is the predominant collection mechanism for scrubbers having gas stream velocities greater than 1 ft/sec (0.3 m/sec) (Perry, 1973). At these and higher velocities, particles having diameters greater than 1.0 μm are collected by breaking through the streamlines encircling the water droplets.

Direct interception (the particle flows with the streamlines but "bumps" into the droplet because it gets too close) becomes important when the particle size (d_p) approaches that of the droplet (d_d) or when $d_p/d_d \rightarrow 1$. In scrubbers, droplet sizes are usually greater than 50 μm and dust particle sizes are usually 5 μm or less. Therefore, direct interception is a secondary effect compared to inertial impaction.

Diffusion effects become important for very small particle sizes (less than $0.5\ \mu\text{m}$). Here, the random motion of the small particles results in eventual contact with water droplets. The efficiency (η) of a scrubber can increase for smaller particle sizes because of the predominance of this effect (Figure 9-2).



Source: Calvert, 1977.

Figure 9-2. Collection efficiency for a mobile bed scrubber as a function of particle size.

Some scrubbing systems can increase collection efficiency through a combination of other effects. The condensation of steam on dust particles acting as nuclei, or the sweeping of particles into condensing water droplets provide mechanisms for particle collection. Charged droplet scrubbers impart an electrical charge to water droplets produced in the system. These are then collected much like in an electrostatic precipitator. These systems are effective in collecting particles in the range between 0.3 and $1\ \mu\text{m}$, the range where the impaction and diffusion mechanisms have the least effectiveness (Lear, 1975).

General Theories

A number of theories have been developed from basic particle movement principles to explain the action of wet scrubbing systems. Many of these start from firm scientific concepts, but give only qualitative results when predicting collection efficiencies or pressure drops. The interaction of particulate matter having a given particle size distribution with water droplets having another size distribution is not easy to express in quantitative terms. As a result of this complexity, experimentally determined parameters are usually needed in order to approach reality.

This section covers five topics:

- Collection Mechanisms
- The Johnstone Equation
- The Cut Power Method
- The Contact Power Theory
- Pilot Methods

An overview of a number of general methods that are used to evaluate wet collector systems will be presented. Each method described has limitations. One of the principal problems with most theoretical approaches is the lack of input data for the equations. Particle size information or specific equation parameters may not be available for a given process, particularly for a new process. For this reason, it is often necessary to obtain pilot plant information that can be scaled up to design the actual control system. Wet collector equipment manufacturers and various consultants also have developed methods and assembled data which can be used to design or evaluate these systems. However, much of this information is proprietary.

Collection Mechanisms

As stated earlier, wet collectors operate through three primary mechanisms: inertial impaction, direct interception, and diffusion. Each of these effects can be characterized by a mathematical expression called the *separation number*. The separation numbers are dimensionless groups of parameters—the higher the value of the separation number, the more effective the mechanism (Perry, 1973). From these basic expressions, theories have been derived to describe scrubber performance. Each of these mechanisms will be discussed in more detail here.

Inertial Impaction

Because of their mass, particles do not always follow the streamlines which diverge around an obstacle such as a droplet. An impacting particle is one which has broken through the streamlines and hits the droplet.

The separation number for impaction is obtained by balancing the force of the moving particle against the resistance of the gas stream to its motion. The separation number for impaction is known as the *impaction parameter*, ψ and is expressed by:

$$(Eq. 9-1) \quad \psi = \frac{C_f \rho_p d_p^2 v}{18 \mu d_o}$$

Where: C_f = Cunningham correction factor
 ρ_p = particle density (lb/ft³)
 d_p = particle diameter (ft)
 v = gas velocity (ft/sec)
 μ = gas viscosity (lb/ft•sec)
 d_o = droplet diameter (ft)

Note the similarity of this expression to the impaction parameter given for cyclones (Equation 6-7).

The impaction parameter can be used with a number of other concepts to develop a theoretical equation for the impaction collection efficiency, $\eta_{\text{Impaction}}$.

One of these concepts, *target efficiency*, is defined as the ratio of the actual number of particles hitting the droplet to the total number of particles which could hit it (Figure 9-3).

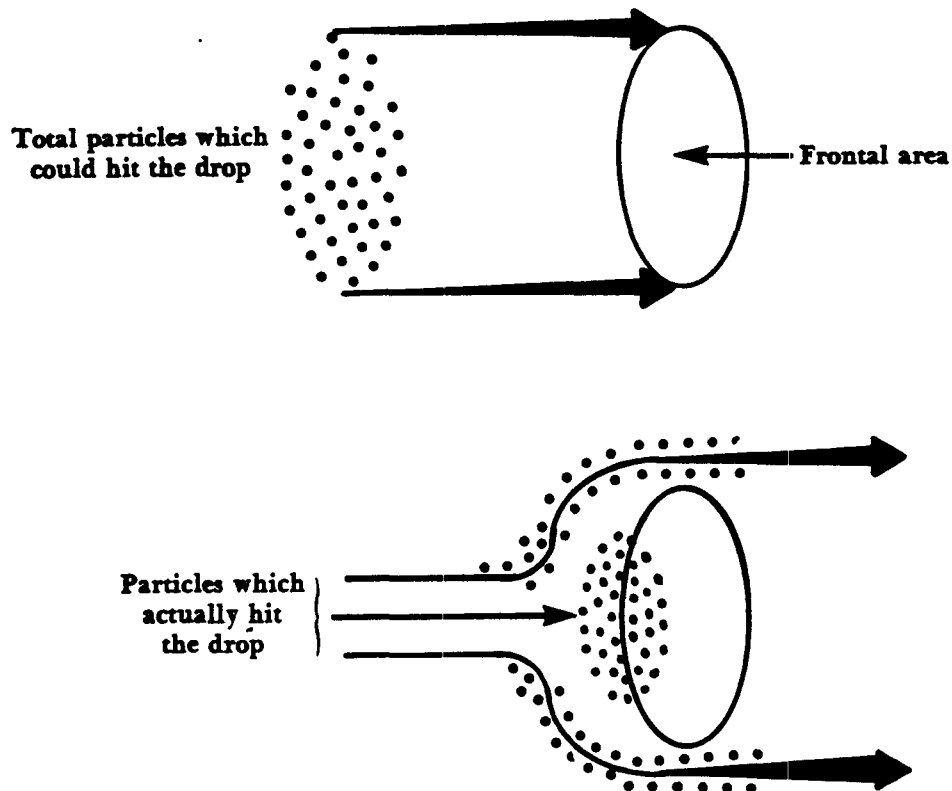


Figure 9-3. Inertial impaction collection efficiency: target efficiency.

Given a uniform distribution of particles, target efficiency can be thought of as a ratio of areas, i.e. the ratio of an area cleared of particles, to the frontal area of the drop (Figure 9-4).

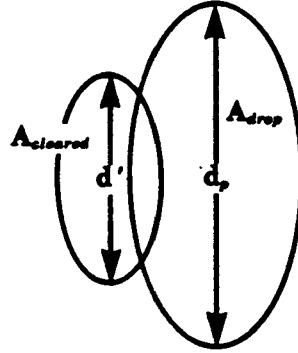


Figure 9-4. Target efficiency: the area ratios.

The target efficiency is thus the impaction collection efficiency, $\eta_{Impaction}$, and is expressed as:

$$(Eq. 9-2) \quad \eta_{Impaction} = \frac{A_{cleared}}{A_{drop}} = \frac{\pi \left(\frac{d'}{2} \right)^2}{\pi \left(\frac{d_p}{2} \right)^2} = \left(\frac{d'}{d_p} \right)^2$$

For large particles with high momentum, the area cleared (d') will be relatively large since the particles will be more likely to break the streamlines and be collected. Complete collection would correspond to $(d'/d_p)^2 = 1$. However, as d_p decreases, the particles tend to follow streamlines, so a point will be reached where $(d'/d_p) = 0$ and no particles are collected.

The path of a particle around a single droplet can be calculated by numerical techniques. Given parameters such as particle density, gas viscosity, and collector size, the conditions where the particle will be collected or follow the streamlines around the droplet can be predicted (Theodore, 1976). In other words, d' can be found numerically and a value for the single collector efficiency, $\eta_{Impaction}$, can be calculated.

Many other theoretical expressions for $\eta_{Impaction}$ do not rely on numerical methods. The impaction parameter, ψ , is common to many of them. In general, for a wet collector system having impaction as the predominant mechanism, the collection efficiency is expressed as a function of ψ , or:

$$(Eq. 9-3) \quad \eta_{Impaction} = f(\psi)$$

A number of these expressions are given for different flow regimes by Rimberg and Perry (1977). Another expression, developed by Johnstone, will be discussed later in this chapter.

Interception

The separation number characterizing inertial impaction (the impaction parameter) accounts for the effect that the mass of the particle has in penetrating streamlines. It does not account for the finite size of the particle as it nears the droplet.

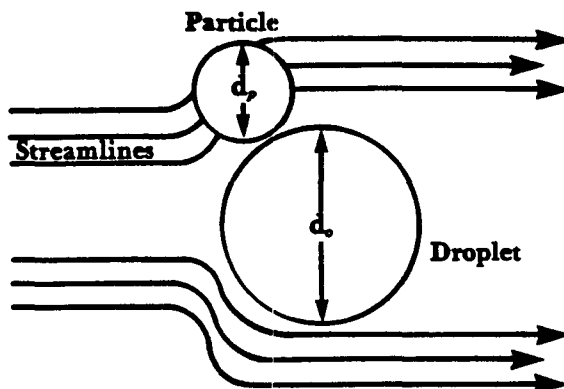


Figure 9-5. Collection by interception.

The center of the particle may follow streamlines around a droplet, but if the particle approaches the droplet by a distance less than $d_p/2$ (as measured from the particle's center), it will hit and be collected.

The separation number which characterizes this effect is the ratio of the particle diameter to the droplet diameter and expressed as:

(Eq. 9-4)
$$\frac{d_p}{d_o}$$

The collection efficiency associated with this effect is a function of d_p and d_o , or:

(Eq. 9-5)
$$\eta_{\text{Interception}} = f\left(\frac{d_p}{d_o}\right)$$

Again, a number of expressions have been developed for $\eta_{\text{Interception}}$ for different flow regimes and are reviewed by Rimberg (1977).

Diffusion

In the diffusion process, small particles (less than $0.5 \mu\text{m}$ diameter) are bombarded by gas molecules and are forced to move erratically in the gas stream. This irregular motion can cause them to move through streamlines and be collected by the larger water droplets.

The Brownian diffusion process leading to particle capture is most often described by a parameter called the Peclet number, Pe :

$$(Eq. 9-6) \quad Pe = \frac{3\pi\mu v d_p d_o}{C_f k_B T}$$

Where: μ = gas viscosity
 v = gas stream velocity
 d_p = particle diameter
 d_o = water droplet diameter
 k_B = Boltzmann's constant
 T = temperature of gas stream
 C_f = Cunningham correction factor

Expressions for collection efficiency by the diffusion process are generally in the form:

$$(Eq. 9-7) \quad \eta_{Diffusion} = f\left(\frac{1}{Pe}\right)$$

As the Peclet number decreases, collection efficiency by diffusion increases. In terms of Equation 9-6, as the temperature increases, Pe decreases. An increase in temperature means that gas molecules will move around faster than at lower temperatures. This will lead to increased bombardment of the small particles, increased random motion, and increased collection efficiency by this mechanism.

Combined Efficiency

When attempting to collect 100 particles using a collection mechanism having 80% efficiency, 80 particles would be collected and 20 would escape. If another mechanism with 60% efficiency was used to collect the remaining 20 particles, 8 would escape this time. Ninety two particles would therefore be collected, giving a total efficiency of $92/100 = 0.92$ or 92%. This can be expressed as:

$$\begin{aligned} \text{Collected particles} &= 100 - \{ [100 - 100(0.80)] - [100 - 100(0.80)](0.60) \} \\ &= 100 - \{ [100 - 100(0.80)](1 - 0.60) \} \\ &= 100 - \{ 100(1 - 0.8)(1 - 0.6) \} \\ &= 100 - 8 \\ &= 92 \end{aligned}$$

Generalizing in terms of the number of mechanisms which may be involved in wet collection devices, the combined efficiency can be expressed as:

$$(Eq. 9-8) \quad \eta_{Combined} = 1 - (1 - \eta_{Impaction})(1 - \eta_{Interception})(1 - \eta_{Diffusion}).$$

In terms of the separation numbers discussed earlier, the combined efficiency is then a function of many parameters.

$$(Eq. 9-9) \quad \eta_{Combined} = 1 - (1 - f(\psi))(1 - f\left(\frac{d_p}{d_o}\right))(1 - f\left(\frac{1}{Pe}\right))$$

Depending on flow conditions, (laminar, turbulent, etc.) other combinations of these parameters have been used to provide expressions for the efficiency of wet collectors. Actually, the number of variables are so great and the interaction between varying size distributions of both particulate matter and water droplets is so complex, that this type of theoretical approach is difficult to apply in practice.

This academic approach, although useful in understanding basic phenomena, is commonly sidestepped for more empirical approaches. Correction factors obtained from actual operating systems or pilot plant data are used to correct for complex interactions. A newer concept expressing efficiency in terms of power expended has led to several empirical techniques for evaluating scrubber performance. The subsequent sections of this chapter will describe some of these empirical methods.

The Johnstone Equation

Equations 9-8 and 9-9 represent the combined collection efficiency for a single droplet. The combined efficiency equation includes the efficiency for impaction, interception, and diffusion. A scrubber uses many droplets to collect particulate matter. This fact must be taken into consideration when developing a theory for scrubber collection efficiency. Each droplet will have a combined efficiency η_c , for collecting these particles.

In the first exposure to a drop:

Fraction of
particles captured
 η_c

Fraction of
particles escaped
 $1 - \eta_c$

Exposure two to another drop:

Fraction captured
 $\eta_c(1 - \eta_c)$

Fraction escaped
 $(1 - \eta_c) - \eta_c(1 - \eta_c)$
or $(1 - \eta_c)^2$

Exposure three to a third drop:

Fraction captured
 $\eta_c[1 - \eta_c - \eta_c(1 - \eta_c)]$

Fraction escaped
 $1 - \eta_c - \eta_c(1 - \eta_c) - \eta_c[1 - \eta_c - \eta_c(1 - \eta_c)]$
or $(1 - \eta_c)^3$

and so on.

If S_o is the total number of exposures, then generalizing, the *total fraction of particles which escape* can be written as:

$$(1 - \eta_c)^{S_o}$$

[NOTE: the exponential function e^{-x} can be expanded to $e^{-x} = 1 - x + \frac{x^2}{2!} - \frac{x^3}{3!} + \dots$. For small values of x , e^{-x} can be approximated as $e^{-x} \approx 1 - x$]

The overall collection efficiency η is then:

$$\begin{aligned}\eta &= 1 - (1 - \eta_c)^{S_o} \\ &= 1 - (e^{-\eta_c})^{S_o} \\ &= 1 - e^{-\eta_c S_o}\end{aligned}$$

(Eq. 9-10)

S_o depends on the type of scrubber and η_c is the collection efficiency for a single droplet. The terms in the exponent, $\eta_c S_o$, are a function of the many variables involved in the system. This exponent can be alternatively expressed as $f(\text{system})$, a function of the system. Therefore efficiency can be expressed as:

$$\eta = 1 - e^{-f(\text{system})}$$

(Eq. 9-11)

Semrau (1952), using chemical engineering terminology for absorption phenomena, expresses $f(\text{system})$ as N_r , the number of transfer units. This makes sense if we consider, for example, 100 particles moving through a gas stream. By impaction and other mechanisms, a number of the particles will be "transferred" to or collected by the first droplet they see. More will transfer to the second droplet, etc. The number of transfers therefore indicates the degree of collection, as expressed in Equation 9-11.

We will now look at a number of expressions for $f(\text{system})$ that have been used to calculate collection efficiencies.

Johnstone (1951) developed an expression for a venturi scrubber, considering only the predominant mechanism of inertial impaction.

The *Johnstone equation* is given as:

$$\eta = 1 - e^{-k \frac{Q_L}{Q_G} \sqrt{\psi}}$$

(Eq. 9-12)

Where: Q_L = liquid flow rate (gal/min)
 Q_G = gas flow rate (ft³/min)
 k = empirical constant

From Equation 9-1:

$$\psi = \frac{C_f Q_p v d_p^2}{18 d_o \mu}$$

Where: d_o = water droplet diameter (ft)
 C_f = Cunningham correction factor
 v = gas stream velocity (ft/sec)
 d_p = particle diameter (ft)
 μ = gas viscosity (lb/ft•sec)
 Q_p = particle density (lb/ft³)

Here k , an empirical constant, depends upon the geometry of the system and on the operating conditions. Typical values are 0.1 to 0.2 gal/acfm.

The droplet size, d_o , can be estimated by using the empirical relationship developed by Nukiyama and Tanasawa (1938), for gas atomized sprays.

The *Nukiyama Tanasawa equation* is:

$$(Eq. 9-13) \quad d_o = \frac{1920}{v_R} \left(\frac{\sigma_l}{\rho_l} \right)^{0.5} + 597 \left(\frac{\mu_l}{\sqrt{\sigma_l \rho_l}} \right)^{0.45} \left(1000 \frac{Q_L}{Q_G} \right)^{1.5}$$

Where: d_o = water droplet diameter (μm)
 v_R = relative velocity of gas to liquid (ft/sec)
 σ_l = liquid surface tension (dynes/cm)
 ρ_l = liquid density (g/cm^3)
 μ_l = liquid viscosity (lb/ft \cdot sec)
 Q_L = liquid flow rate (gal/min)
 Q_G = gas flow rate (ft 3 /min)

For air and water in a venturi scrubber, this expression reduces to:

$$(Eq. 9-14) \quad d_o = \frac{16400}{v_R} + 1.45 \left(\frac{Q_L}{Q_G} \right)^{1.5}$$

Where: v_R = relative velocity of gas to liquid at venturi throat (ft/sec)

It should be noted from the form of the impaction parameter ψ given in Equation 9-11, that η is dependent upon d_p , the particle size. The equation for the total efficiency of the scrubber η_{TOT} must be solved for each particle size range of the process. The sum of each η_i (for each d_p) multiplied times the distribution weight of the particle range will give the total efficiency of the scrubber denoted as η_{TOT} .

This discussion of the Johnstone equation is not intended to imply that the equation is the best predictive equation available for venturi scrubber performance. It is presented here because it demonstrates in a simple manner, the end result of a number of theoretical concepts associated with wet collector design. Other expressions, generally more complicated and also empirical in nature, have been developed (Calvert, 1972). The various theories, however, have never been adequately compared on a consistent basis.

The Cut Power Method

A generalized method of calculating the overall efficiency of a wet collector has been developed by Calvert (1972, 1974, 1977). This method assumes that the predominant collection mechanism is inertial impaction. It also requires a knowledge of the particle size distribution as does the Johnstone equation.

Several concepts previously discussed tie into the *cut power method*. The first concept considers the general form of overall efficiency equation such as that given in Equation 9-10. The second is cut size discussed in Chapter 6. Equation 9-11, gives overall efficiency expressed as:

$$\eta = 1 - e^{-f(\text{system})}$$

Where: $f(\text{system})$ = some function of the system variables

The cut power method uses the concept of *penetration*, where penetration is given as:

$$(Eq. 9-15) \quad Pt = 1 - \eta$$

Penetration is the fraction of particulate matter which gets through a collector, i.e. the opposite of the fraction collected.

In terms of penetration, then:

$$(Eq. 9-16) \quad \begin{aligned} Pt &= 1 - \eta \\ &= 1 - [1 - e^{-f(\text{system})}] \\ &= e^{-f(\text{system})} \end{aligned}$$

Calvert has chosen to define $f(\text{system})$ as an empirical function dependent upon the particle aerodynamic diameter d_p .

$$(Eq. 9-17) \quad f(\text{system}) = A_{cut} d_p^{B_{cut}}$$

Where: A_{cut} = parameter characterizing the particle size distribution
 B_{cut} = empirically determined constant dependent upon the type of scrubber

Combining Equations 9-16 and 9-17, penetration is:

$$(Eq. 9-18) \quad Pt = e^{-A_{cut} d_p^{B_{cut}}}$$

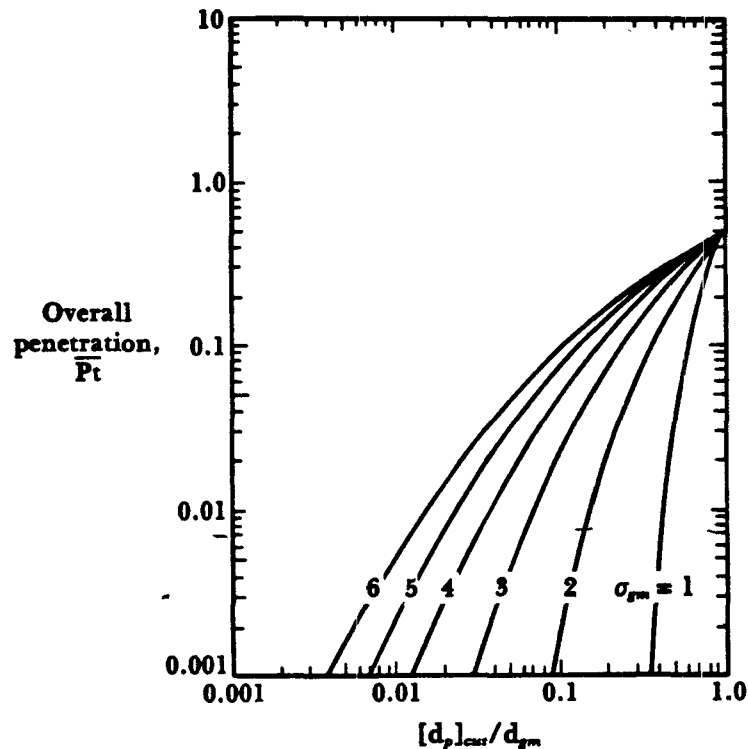
[NOTE: this function is given only for one particle size. Integrate this over a particle size distribution to obtain the *overall penetration*, \overline{Pt} for the wet collector.]

The cut diameter was discussed in Chapter 6. It is the diameter of the particles collected by the control system at 50% efficiency. Since wet collectors and other types of control equipment have limits to the size of particles they can collect, a knowledge of a required cut diameter is helpful in evaluating different scrubber systems.

Calvert has developed a method of determining the cut diameter that is required in order to achieve a given collection efficiency. By integrating Pt over a log normal distribution of particles and varying σ_{gm} (standard deviation of the distribution)

and d_{gm} (geometric mean particle diameter), \overline{Pt} can be obtained as a function of the required cut diameter $[d_p]_{cut}$, divided by the geometric mean particle diameter, d_{gm} (Figure 9-6).

[NOTE: A log normal distribution of particles can be statistically defined with only two terms, the geometric mean particle diameter, d_{gm} , and the geometric standard deviation, σ_{gm} , of the distribution. From stack test data or particle size information from a similar emission facility, the values of d_{gm} and σ_{gm} can be determined using the techniques discussed in Chapter 4 of this manual.]



Source: Calvert, 1977.

Figure 9-6. Penetration and the cut diameter.

Consider the following example: a particle size analysis indicated that $d_{gm} = 12 \mu m$ and $\sigma_{gm} = 3.0$. If a collection efficiency of 99% is required to meet emission standards what would the cut diameter of the scrubber have to be?

First:

$$\begin{aligned}\overline{Pt} &= 1 - \eta \\ &= 1 - 0.99 \\ &= 0.01\end{aligned}$$

From Figure 9-6, for $\overline{Pt} = 0.01$ and $\sigma_{gm} = 3.0$

$$\frac{[d_p]_{cut}}{d_{gm}} = 0.063$$

Since $d_{gm} = 12 \mu\text{m}$, then the scrubber must be able to collect particles of size $0.063 \times 12 = 0.76 \mu\text{m}$ with at least 50% efficiency to achieve an overall scrubber efficiency of 99%.

Figure 9-6 was developed using Equation 9-18, $P_t = e^{-A_{cut} P^{B_{cut}}}$, where $B = 2$. For plate towers, $B = 2$, but is only ≈ 2 for venturis under certain conditions. For centrifugal scrubbers $B \approx 0.7$ and therefore Figure 9-6 should not be used as is. Further limitations and models developed for specific devices using the cut power method are discussed by Calvert (1972). The application of these models to actual operating systems has been documented inadequately in the open literature.

The Contact Power Theory

Theoretical approaches based upon the dynamic interactions between particles and water droplets are limited in applicability since actual scrubber systems are very complex. For example, the Johnstone and cut power methods assume that the water droplets are uniformly distributed over the cross section of the scrubber. The actual turbulence and eddies existing in the contact zone are not accounted for, except by using empirically determined constants (Beg, 1976).

A more general theory which avoids the details of how particles and droplets hit each other, is the *contact power theory*. This theory is based upon a series of experimental observations made by Lapple (1955). The fundamental assumption of the theory is:

“When compared at the same power consumption, all scrubbers give substantially the same degree of collection of a given dispersed dust, regardless of the mechanism involved and regardless of whether the pressure drop is obtained by high gas flow rates or high water flow rates.” (Lapple, 1955)

In other words, collection efficiency is a function of how much power is used, and not upon details of design. This has a number of implications in the evaluation and selection of wet collectors. Once it is realized that a certain amount of power is needed for a required collection efficiency, the claims about specially located nozzles, baffles, etc. can be evaluated more objectively. The choice between two different scrubbers with the same power requirements may depend primarily on ease of maintenance.

Semrau (1959, 1963), developed the contact power theory from the work of Lapple and Kamack (1956). The theory as developed by Semrau, is empirical in approach and relates the *total pressure loss*, P_r , of the system to the collection efficiency.

The total pressure loss is expressed in terms of the power expended to inject the liquid into the scrubber plus the power needed to move the process gas through the system.

$$(Eq. 9-19) \quad \mathcal{P}_T = \mathcal{P}_G + \mathcal{P}_L \quad (\text{hp}/1000 \text{ acfm})$$

Where: \mathcal{P}_T = total contacting power (units of hp/1000 acfm)
 \mathcal{P}_G = power input from gas stream (hp/1000 acfm)
 \mathcal{P}_L = power input from liquid injection (hp/1000 acfm)

[NOTE: the total pressure loss, \mathcal{P}_T should not be confused with penetration, P_t defined in the previous section. Penetration is the symbol used by Calvert to express the fraction of particulate matter escaping from a collector.]

The power expended in moving the gas through the system, \mathcal{P}_G , is expressed in terms of the scrubber pressure drop:

$$(Eq. 9-20) \quad \mathcal{P}_G = 0.1575 \Delta p \quad (\text{hp}/1000 \text{ acfm})$$

Where: Δp = pressure drop (in. of H_2O)

The power expended in the liquid stream, \mathcal{P}_L , is expressed as:

$$(Eq. 9-21) \quad \mathcal{P}_L = 0.583 p_L \left(\frac{Q_L}{Q_G} \right) \quad (\text{hp}/1000 \text{ acfm})$$

Where: p_L = liquid inlet pressure (lb/in.²)
 Q_L = liquid feed rate (gal/min)
 Q_G = gas flow rate (ft³/min)

The constants given in the expressions for \mathcal{P}_G and \mathcal{P}_L incorporate conversion factors to put the terms on a consistent basis.

The total power can therefore be expressed as:

$$\mathcal{P}_T = \mathcal{P}_G + \mathcal{P}_L$$

$$(Eq. 9-22) \quad \mathcal{P}_T = 0.1575 \Delta p + 0.583 p_L \left(\frac{Q_L}{Q_G} \right)$$

The problem now is to correlate this with scrubber efficiency.

Equations 9-10 and 9-11 of this manual show that efficiency is an exponential function of the system variables for most types of collectors.

(Eq. 9-23)
$$\eta = 1 - e^{-f(s)}$$

Semrau defines:

(Eq. 9-24)
$$f(s) = N_t = \alpha \mathcal{P}_T^\beta$$

Where: N_t = number of transfer units
 α and β = empirical constants which are determined from experiment and are dependent upon the characteristics of the particulate matter

The efficiency then becomes:

(Eq. 9-25)
$$\eta = 1 - e^{-\alpha \mathcal{P}_T^\beta}$$

Table 9-1 gives values of α and β for different industries.

Table 9-1. Parameters α and β for the contact power theory.

Aerosol	Scrubber type	α	β
Raw gas (lime dust and soda fume)	Venturi and cyclonic spray	1.47	1.05
Prewashed gas (soda fume)	Venturi, pipeline, and cyclonic spray	0.915	1.05
Talc dust	Venturi	2.97	0.362
	Orifice and pipeline	2.70	0.362
Black liquor recovery furnace fume	Venturi and cyclonic spray	1.75	0.620
Cold scrubbing water humid gases			
Hot fume solution for scrubbing (humid gases)	Venturi, pipeline, and cyclonic spray	0.740	0.861
Hot black liquor for scrubbing (dry gases)	Venturi evaporator	0.522	0.861
Phosphoric acid mist	Venturi	1.33	0.647
Foundry cupola dust	Venturi	1.35	0.621
Open-hearth steel furnace fume	Venturi	1.26	0.569
Talc dust	Cyclone	1.16	0.655
Copper sulfate	Solivore (A) with mechanical spray generator	0.390	1.14
	(B) with hydraulic nozzles	0.562	1.06
Ferrosilicon furnace fume	Venturi and cyclonic spray	0.870	0.459
Odorous mist	Venturi	0.363	1.41

Source: Semrau, 1960.

The contact power theory cannot predict efficiency from a given particle size distribution as can the cut power and Johnstone theories. The contact power theory gives a relationship which is independent of the size of the scrubber. With this observation, a small pilot scrubber could first be used to determine the pressure drop needed for the required collection efficiency. The full-scale scrubber design could then be scaled up from the pilot information.

As an example, consider the following problem:

A wet scrubber is to be used to control particulate emissions from a foundry cupola. Stack test results reveal that the particulate emissions must be reduced by 85% to meet emission standards. If a 100 acfm pilot unit is operated with a water flow rate of 0.5 gal/min at a water pressure of 80 psi, what pressure drop (Δp) would be needed across a 10,000 acfm scrubber unit?

Solution:

From Table 9-1

$$\alpha = 1.35 \text{ and } \beta = 0.621$$

From Eq. 9-23

$$\eta = 1 - e^{-N_t}$$

$$N_t = \ln \frac{1}{1 - \eta} = \ln \frac{1}{1 - 0.85} = \ln 6.66 = 1.896$$

From Eq. 9-24

$$N_t = \alpha \mathcal{P}_T^\beta$$

$$1.896 = 1.35 \mathcal{P}_T^{0.621}$$

$$1.404 = \mathcal{P}_T^{0.621}$$

$$\mathcal{P}_T = 1.73 \text{ hp/1000 acfm}$$

From Eq. 9-22

$$\mathcal{P}_T = 0.1575 \Delta p + 0.583 p_L \left(\frac{Q_L}{Q_G} \right)$$

$$1.73 = 0.1575 \Delta p + 0.583(80) \left(\frac{0.5}{100} \right)$$

$$\Delta p = 9.5 \text{ in. H}_2\text{O}$$

The basic principle of the contact power theory can be applied in ways similar to Equation 9-25 developed by Semrau. For example, Kashdar (1979), in a regulatory analysis of wet scrubbing applied to coal-fired utility boilers, developed the correlation between outlet grain loading and power consumption shown in Figure 9-7.

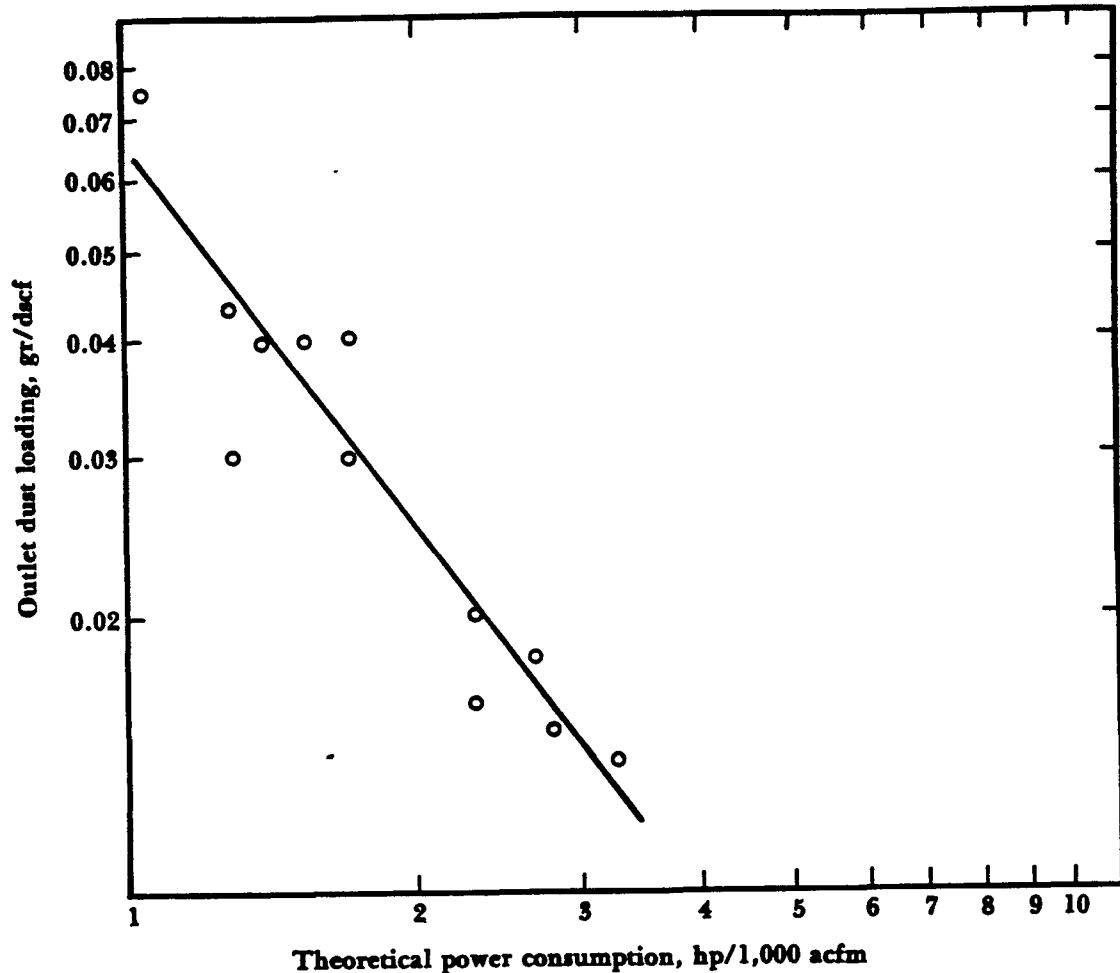


Figure 9-7. Correlation of scrubber outlet dust loading with theoretical power consumption.

Here the correlation is not made in terms of *transfer units* as in Equation 9-24, but directly with the particulate matter emission concentration. The good fit of the data to the format $y = 0.068 x^{-1.41}$ (where y = outlet grain loading (gr/dscf) and x = theoretical power consumption calculated using Equation 9-22) is encouraging support for the cut power theory.

Similarly, Calvert (1974, 1977) has used this approach to develop a relationship between the particle cut diameter and scrubber power. Using data from scrubber installations and relationships developed in the cut power approach, Calvert, in Figure 9-8, shows a similar improvement in performance (i.e. lower $[d_p]_{cut}$) with increased power consumption.

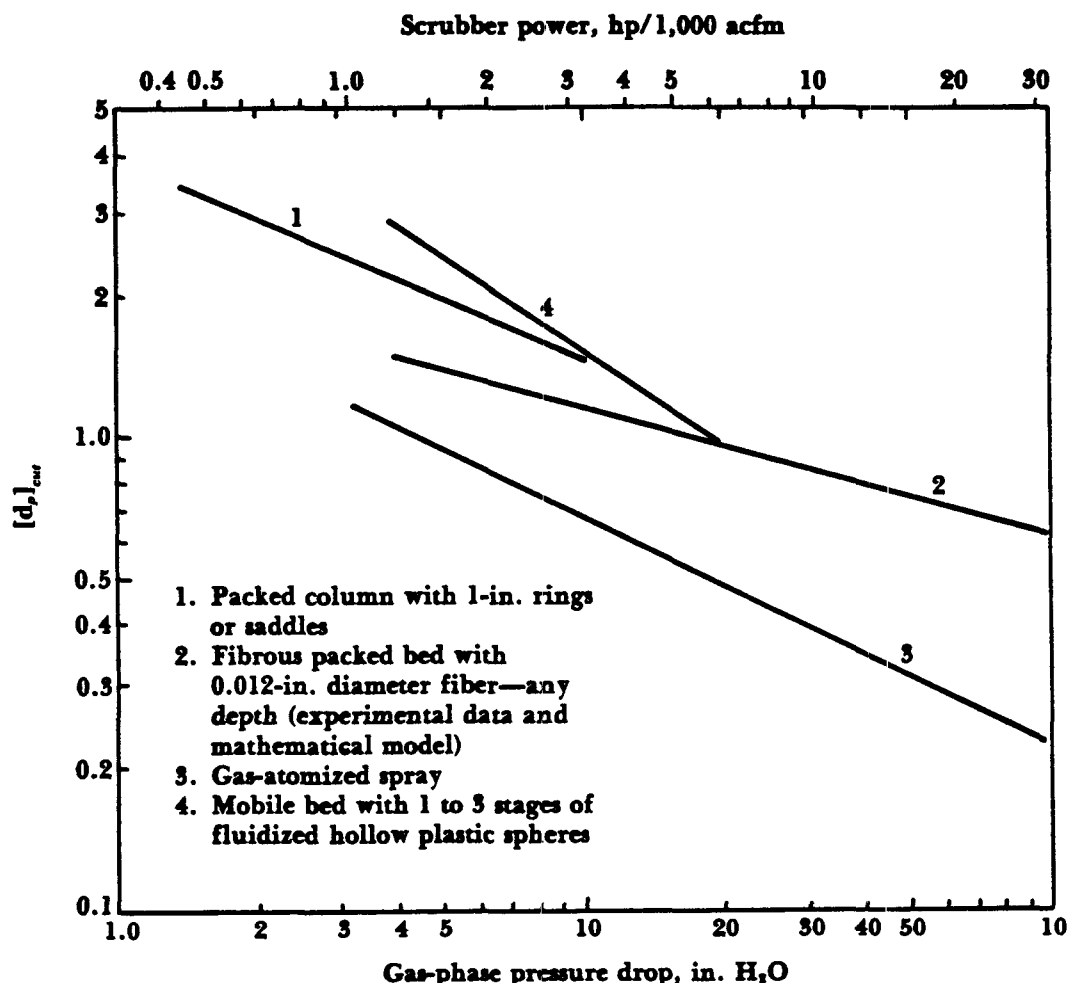


Figure 9-8. Cut diameter $[d_p]_{cut}$ as a function of gas pressure drop and power consumption.

The concept of the contact power theory does have limitations. It does not apply to a number of new wet collecting systems where a combination of collecting mechanisms are used, such as condensation scrubbers. Also, the theory applies best when the power is applied in one scrubbing area (McIlvane, 1977), such as in a venturi scrubber. Multiple staged devices and packed towers will have collection efficiencies varying from those of a venturi scrubber for a given power input.

Pilot Methods

The semi-empirical theories previously discussed are useful for scrubber design and evaluation exercises, since they can give qualitatively correct information. However, they have a number of practical limitations. It is not common practice to choose scrubber systems based only on this information. The uncertainties involved in particle size determinations and the questions associated with using empirically determined parameters restrict the use of theoretical methods. Basically, there are too many variables involved and it is too difficult to account for all of them in a simple theory. The time and expense needed to obtain good input data for these methods may be better spent in developing pilot plant information.

Scrubbers which work primarily through impaction mechanisms have certain performance characteristics (such as efficiency and pressure drop) which are independent of scale. This consequence of the contact power principle provides the basis for using pilot systems. By using a small scale scrubber (100 to 1000 cfm) on the exhaust gas stream, the effectiveness of the equipment for removing the actual particles in the gas can be experimentally determined.

Pilot systems ranging from 100 cfm units to 1/10 size full-scale plants have been developed in the past. McIlvane (1977) has compared the effectiveness of the various design methods. His work is summarized in Table 9-2.

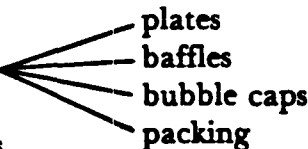
Table 9-2. Methods for predicting venturi scrubber pressure requirements.

Description		Expense (relative scale)	Time (months)
Most reliable	1710 size full-scale plants	100-1000	12-24
	2000 cfm pilot units	30	3-6
	100 cfm pilot units	5	2-3
	Empirical curves based on similar processes	0.2	0.2
	Impactor in situ particle sizing	2	1
Least reliable			

The design of a wet collector system for a particulate emission problem requires more than the application of a few design equations. The experience of scrubber manufacturers with specific industry installations coupled with the use of pilot units provides more reliable ways to determine the size of a system for a wide range of operating conditions. In many cases, theoretical models can complement such studies and provide qualitative data for wet collector evaluations.

Wet Collector Systems

Although many unique wet collector systems are available, commercially designed wet collectors use only a few basic components. Some of these components are:

- spray nozzles
 - venturi constrictions
 - impingement surfaces
 - cyclonic openings
 - spray inducing orifices
 - mechanically driven rotors
- 

The many possible combinations of these basic pieces of hardware has led to the development of numerous types of wet collectors. This is an advantage for the process engineer, who can specify a system in terms of size, cost, and collection efficiency. However, the profusion of devices can also be a disadvantage, especially when confronted with advertisements for such equipment. In this competitive market, the various claims and counterclaims can be confusing. This part of Chapter 9 will describe several commercially-marketed scrubbers; with emphasis on collection principles.

Although wet collection systems may vary greatly in complexity, most of them follow a general rule; collection efficiency increases with increased power input. Power is defined as energy applied per unit time. Energy from the gas stream, energy from the liquid stream, or energy from a mechanically driven rotor is used to bring gas stream particles into contact with the scrubbing liquor. The total energy applied per unit time is the *contacting power*. Scrubbers can be categorized in terms of how this power is applied in the system (Semrau, 1977). The categories used are given in Table 9-3.

Table 9-3. Categories of wet collectors and energy input.

Wet collector type	Scrubbers using energy from:
Gas phase contacting scrubbers	the gas stream
Liquid phase contacting scrubbers	the liquid stream
Liquid phase/gas phase contacting scrubbers	the gas and liquid streams
Mechanically aided scrubbers	a mechanically driven rotor

Scrubbers can also be classed by gas phase pressure drop: *low energy* scrubbers having a pressure drop of less than 5 in. (12.7 cm) of water; *medium energy* scrubbers, 5 to 15 in. (12.7 to 38.1 cm) of water; and *high energy* scrubbers having a pressure drop greater than 15 in. (38.1 cm) of water.

Gas Phase Contacting Scrubbers

Scrubbers using the process gas stream to provide the energy for particle-liquid contact are known as *gas phase contacting scrubbers*. By moving the gas across or through a liquid surface, the liquid is sheared to form small droplets. Particulate matter in the gas stream impacts on the larger droplets, which in turn are collected by cyclonic action or other means. A number of methods are used to develop this

shearing action in a scrubber. The gas can be forced through cascades of liquid falling over flat plates. Holes can be punched in the plates and the gas can aspirate the water flowing over the plate, or the gas can be forced through constricted passages wetted with liquid such as in orifice and venturi scrubbers. We will discuss three collectors which work primarily by this action: *plate scrubbers*, *orifice scrubbers*, and *venturi scrubbers*.

Plate Scrubbers

Plate scrubbers provide a simple means of interacting particulate matter with a liquid. A simple *sieve plate scrubber* is shown in Figure 9-9.

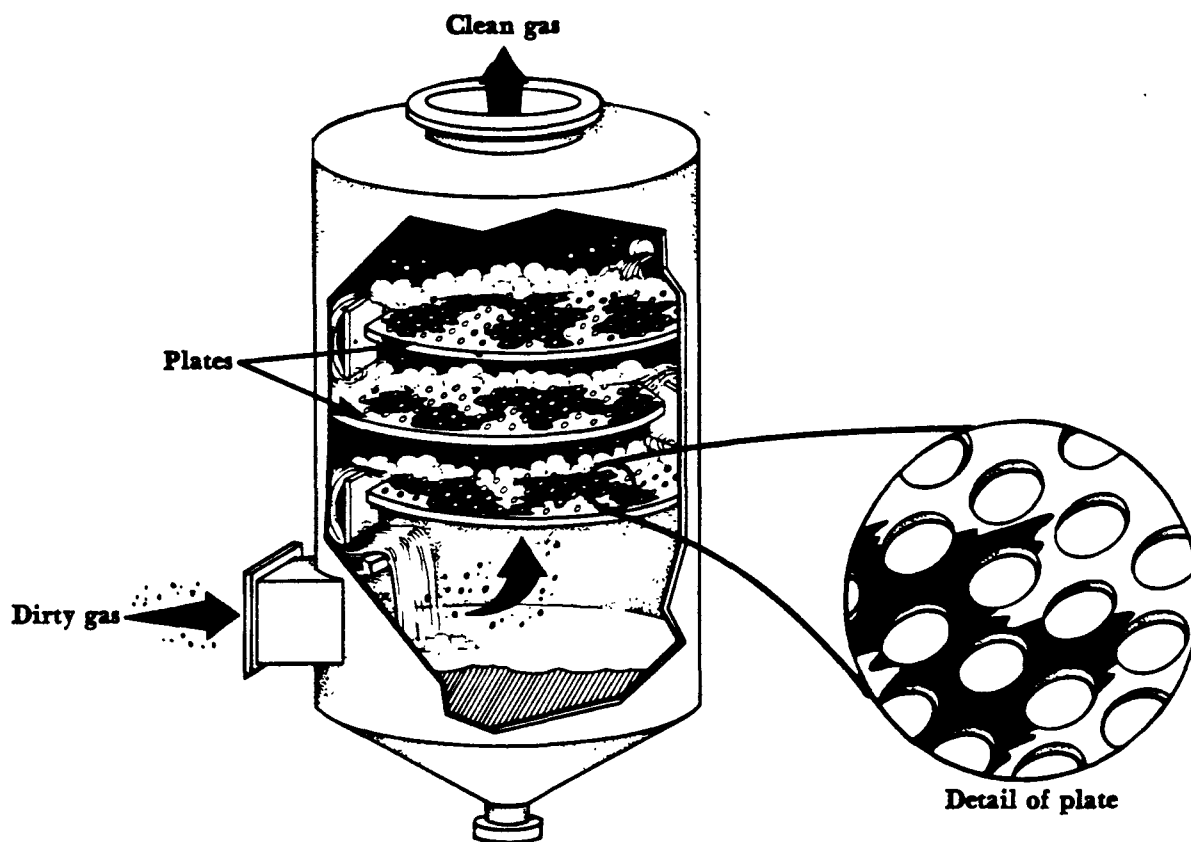


Figure 9-9. Sieve plate scrubber.

Water cascades down over the plates in the countercurrent system shown. The process exhaust gas moves up through the scrubbing chamber and atomizes the liquid at the edges of the holes. The plates (or trays) can contain from 600 to 3000 holes per square foot of surface. A sieve plate scrubber has two or three plates, adjusted so that the holes are not aligned between plates.

Particles are collected as the gas atomizes the liquid flowing over the holes in the plates. The droplets serve as impaction targets for the particulate matter. Liquid cascades from one tray to the other. In countercurrent flow, the cleanest liquid will

contact the cleanest gas at the top plate. In contrast to gas absorption systems where many plates may be used, systems designed for the collection of particles use only two or three plates in the scrubbing column. For particles, collection efficiency does not significantly increase by increasing the number of plates.

Collection efficiency can be improved by decreasing the hole size and increasing the number of holes per plate. More droplets of smaller size will be produced. Impaction targets placed above each hole of the plate can also improve efficiency. These targets can be of several types. In an *impingement plate scrubber* such as that shown in Figure 9-10, stationary impingement baffles force the gas to change direction.

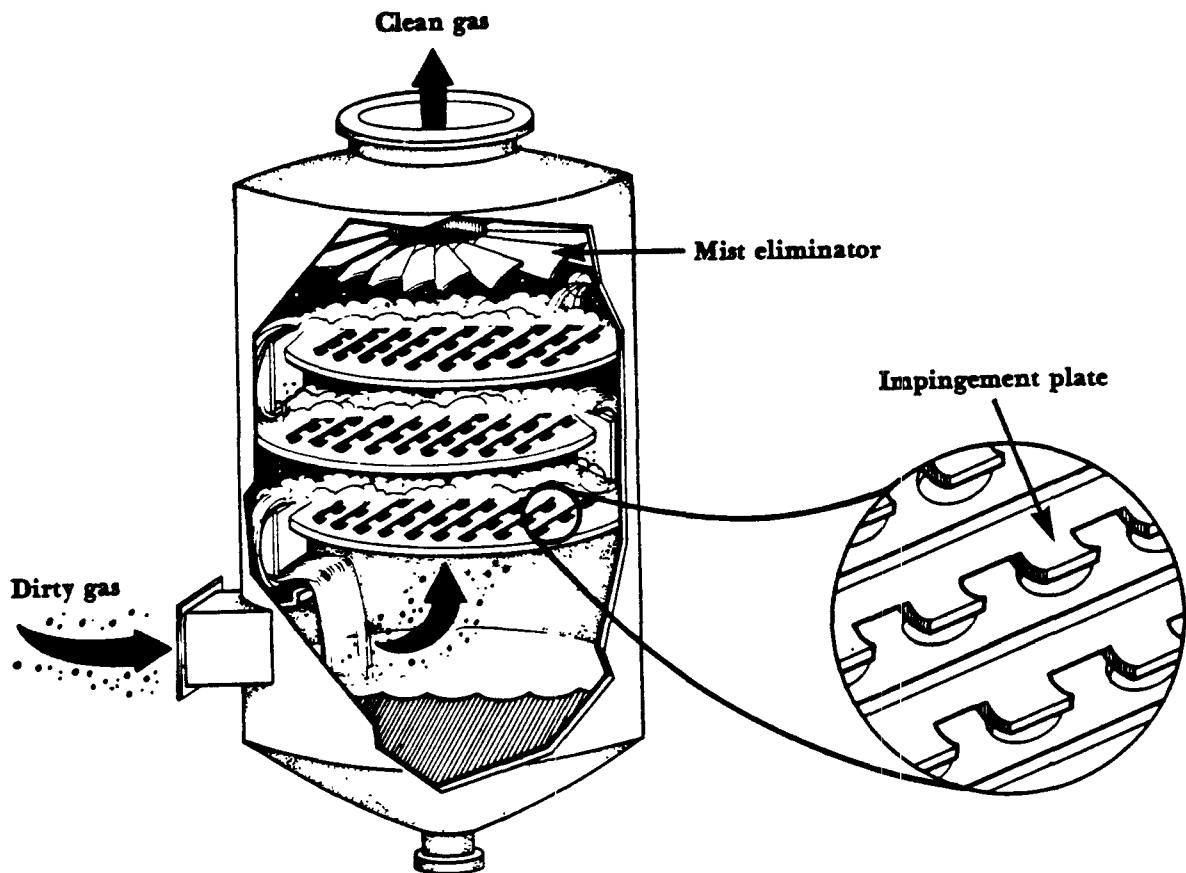


Figure 9-10. Impingement plate scrubber.

Particles and water droplets are forced against the small impingement plates (or baffle plates) with the consequent entrapment of particles in the liquid. Gas velocities range from 12 to 20 ft/sec (170 to 610 cm/sec) through the holes which may be from 1/8 (0.32 cm) to 1/4 inches (0.64 cm) in diameter. The change in flow direction of the gas, 90 degrees from the plate, also aids in liquid atomization and creates a turbulent froth on the plate surface. This provides an additional contact zone to collect the particulate matter (Figure 9-11).

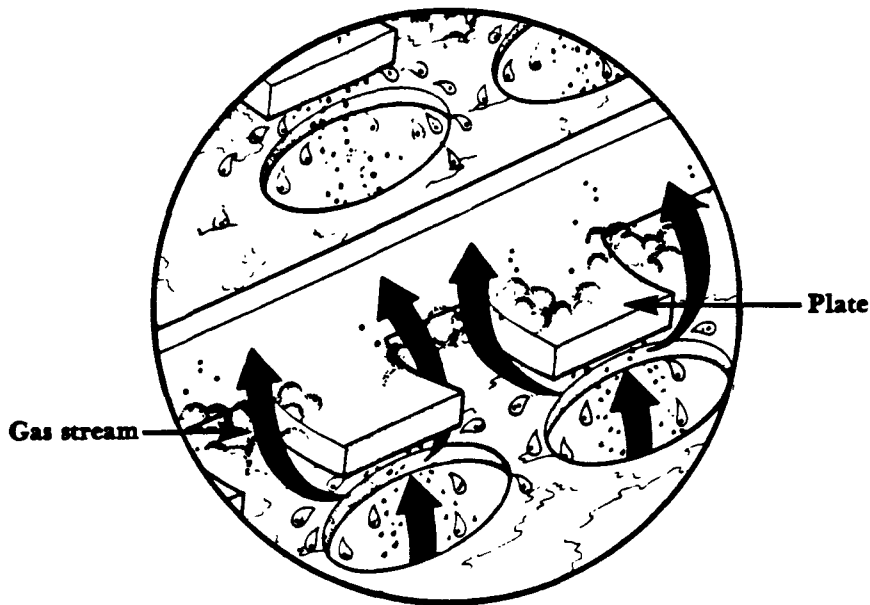


Figure 9-11. Detail of an impingement plate.

A problem that can occur with plate scrubbers is the weeping effect resulting from low gas velocities. If exhaust gas flow rates into the scrubber are variable and become too low, liquid can weep (drip) through the holes of the plate. Insufficient gas flow rates reduce the impingement velocities, the amount of frothing, and consequently, the collection efficiency. For cases of variable flow, *bubble cap* or *valve-type* impingement surfaces can be used. Figure 9-12 shows the detail of caps used in a bubble cap plate scrubber.

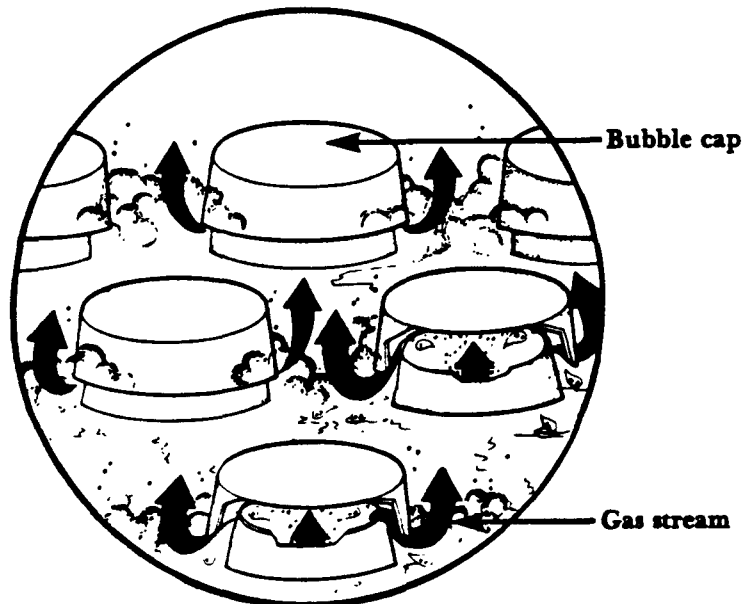


Figure 9-12. Detail of bubble caps.

In a number of systems the caps rise above the plate support. The height that the caps rise depends upon the gas stream velocity. Caps of different weights in alternate rows provide the required flexibility in the system.

The atomization and frothing of liquid in plate scrubbers results from energy supplied by the gas stream. Water sprays are sometimes added to wash over the bottom of the plates and humidify incoming hot, dry gas. In these cases, the liquid spray can also assist in the particle-droplet contacting process and will add to the system power requirements.

Plate scrubbers are medium energy devices and have moderate collection efficiencies. Problems arise if they are improperly applied to processes where heavy particle loading, sticky particles, or scaling plug the small holes in the plates. They have been applied to processes where it is desired to both collect particulate matter and absorb gaseous pollutants.

A summary of operating characteristics is given for the general class of plate scrubbers in Table 9-4.

Table 9-4. Operating characteristics of plate scrubbers.

Pressure drop (Δp)	Liquid to gas ratio (L/G)	Liquid inlet pressure (p_L)	Cut diameter ($[d_p]_{cut}$)	Applications
1-8 in. of water per tray	2-8 gpm/ 1000 acfm	< 5 psig	> 2.0 μm	Coal driers Copper roasting Industrial boilers Chemical process industries Petroleum refineries Incineration processes

Note: gpm = gallon per minute
acfm = actual cubic feet per minute
psig = pounds per inch squared gage pressure

Orifice Scrubbers

Orifice scrubbers have alternatively been called *self-induced spray scrubbers*, *impingement and entrainment scrubbers*, *submerged orifice* or *inertial orifice scrubbers*. Regardless of the term used, these scrubbers are designed so that the process gas stream breaks through a pool of liquid. The gas moves through restricted passages or orifices at velocities near 50 ft/sec (15.2 m/sec), to disperse and atomize the water and entrain droplets in the gas stream as shown in Figure 9-13.

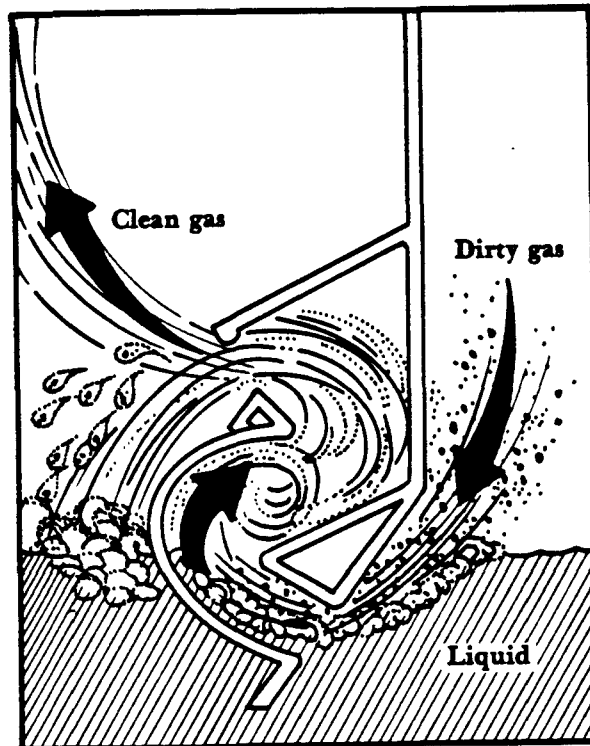


Figure 9-13. Detail of orifice action.

The larger particles in the incoming gas stream impinge upon the surface of the pool and are collected. Smaller particles impact upon the droplets produced by the high velocity gas skimming over the surface of the water. Baffles added in the scrubber serve as impingement surfaces for droplet collection. Since the high velocity gas enters into a large volume from the smaller orifice openings, the large droplets lose momentum and are collected by gravity (Figure 9-14).

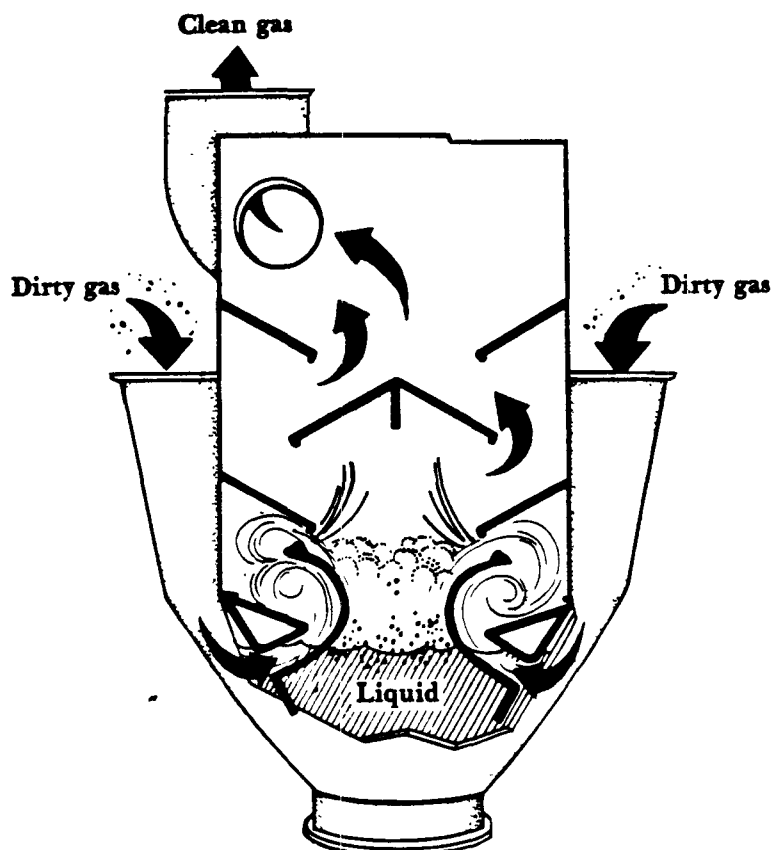


Figure 9-14. Swirl orifice scrubber.

Particulate matter is collected in the pool of scrubber liquid forming a sludge which must periodically be disposed of. Removal of the sludge can cause problems in the scrubber operation since the liquid level must be at a given height for optimum performance.

Orifice scrubbers are designed for specific gas stream velocities. A *turn-down* of the system, reducing the gas velocity, will result in less atomization and larger water droplets, with a consequent decrease in particle collection efficiency. The relatively large orifice openings can accommodate gas streams with high loadings of particulate matter. Plugging by sticky or stringy material is not as great a problem as with the sieve plate and impingement plate scrubbers. They are medium energy devices with moderate collection efficiencies. Operational characteristics for orifice scrubbers are given in Table 9-5.

Table 9-5. Operating characteristics of orifice scrubbers.

Pressure drop (Δp)	Liquid to gas ratio (L/G)	Liquid inlet pressure (p_L)	Cut diameter ($(d_p)_{cut}$)	Applications
2-10 in. of water	10-40 gpm/ 1000 acfm; $\frac{1}{2}$ -5 gpm/ 1000 acfm with recirculation	not applicable	0.8-1 μm	Mining operations Rock products industries Foundries Pulp and paper industries Chemical process industries

Venturi Scrubbers

Venturi scrubbers can give the highest collection efficiencies of any wet scrubbing system. High pressure drops are needed to achieve high efficiencies, but the versatility of venturi systems have made them attractive for many applications. One of the simplest of the venturi designs is shown in Figure 9-15.

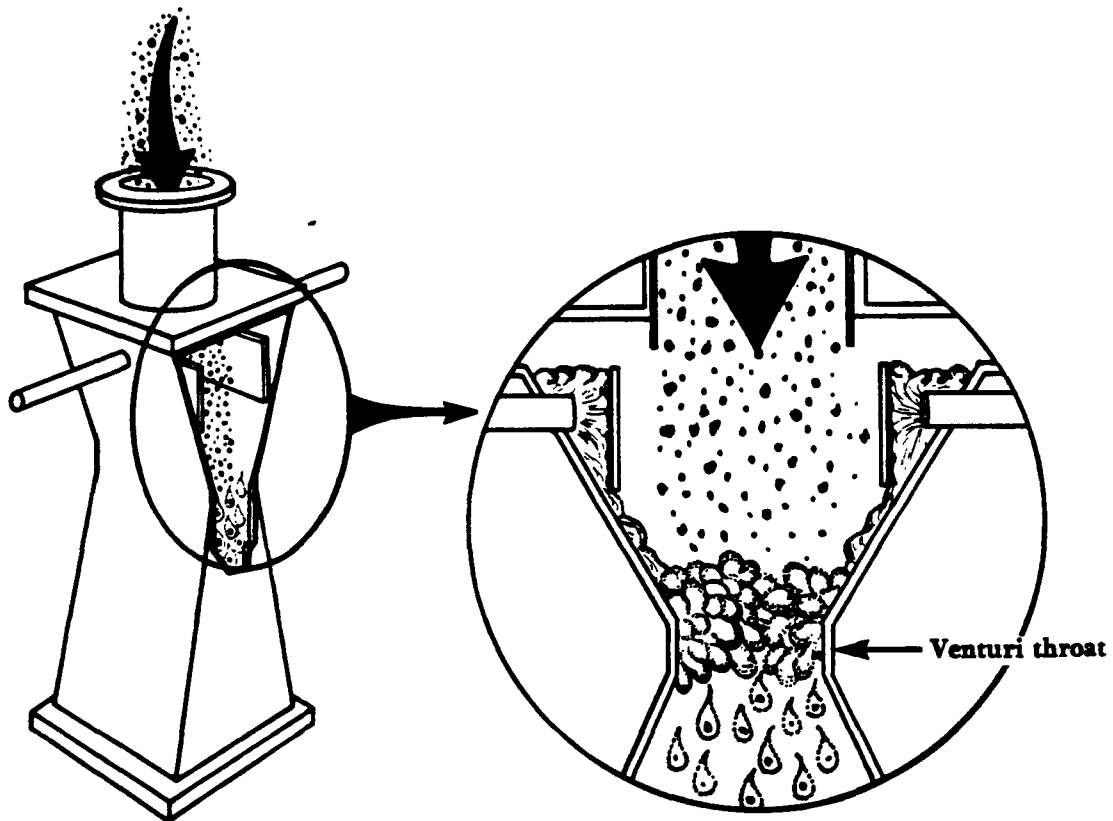


Figure 9-15. Typical venturi scrubber.

The venturi is designed to fan gas in and out of a constriction. Since the volumetric flow rate of the gas (Q) must be the same throughout the system, the velocity of the gas must increase at the throat of the venturi. That is, if

$$Q_{\text{entrance}} = Q_{\text{throat}}$$

$$v_{\text{entrance}} A_{\text{entrance}} = v_{\text{throat}} A_{\text{throat}}$$

Where: A = area
 v = velocity

the velocity at the throat must increase in order to make up for the decrease in area in the throat. Velocities at such a constriction can range from 200 to 800 ft/sec (61 to 244 m/sec). Now, if water is introduced into the throat, the gas forced to move at high velocity will shear the water into droplets. Particles in the gas stream then impact onto the droplets produced. Moving a large volume of gas through a small constriction gives a high velocity flow, but also a large pressure drop across the system. Collection efficiency for small particles increases with increased velocities (and corresponding increased pressure drops) since the water is sheared into more and smaller droplets than at lower velocities. The large number of small droplets combined with the turbulence in the throat section provides numerous impaction targets for particle collection.

Water injection rate can govern the production of water droplets. Depending upon design details, an increase in the liquid-to-gas ratio, (increase in liquid injection) can also improve collection efficiencies. There are, however, limits to the liquid injection rate, since once enough liquid is present, further amounts of liquid do not correspondingly increase efficiency.

The venturi design is merely a system for using the gas stream energy to atomize liquid, thus the contact power comes primarily from the process gas flow. The water droplets incorporating particulate matter must be subsequently collected for the system to be complete. The large bottom inlet cyclonic separators discussed in Chapter 6 are often used for this purpose (Figure 6-2). Mist eliminator pads are also used for this purpose. The droplets ranging from 50 to 500 μm in diameter are easily collected by these systems or by combinations of cyclonic separators and mist eliminators.

Many different venturi systems are commercially available. The primary distinctions between them are in method of water injection and in throat design. Figure 9-16 shows a venturi with water swirling down from the top to wet the walls before atomization at the throat.

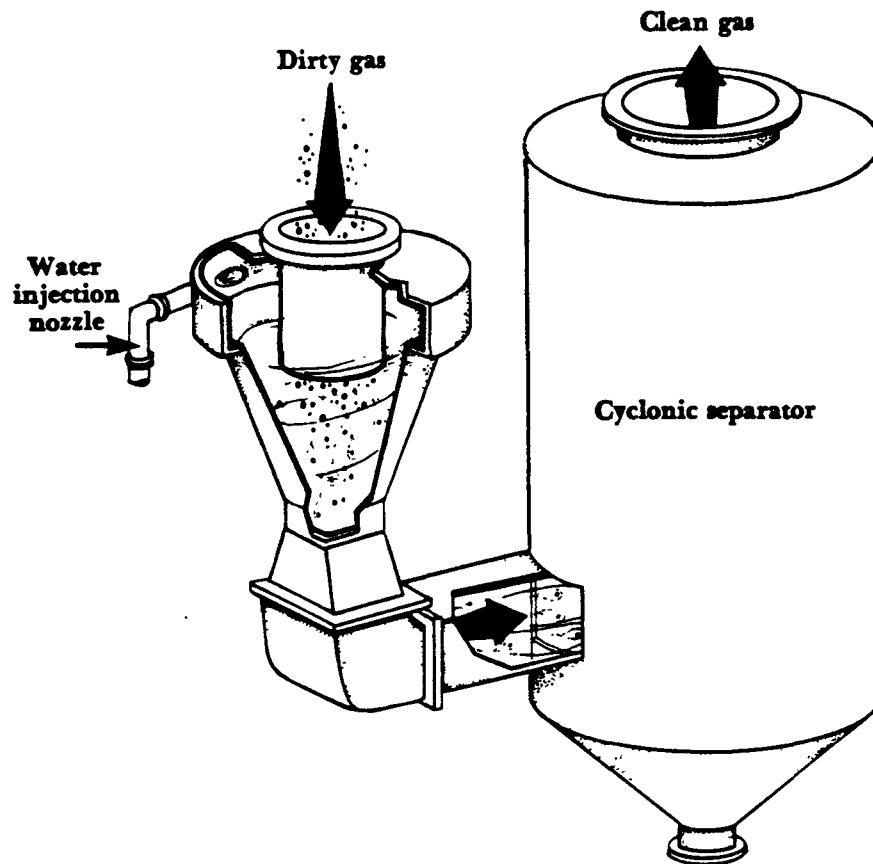


Figure 9-16. Swirl venturi scrubber.

Venturis with wetted walls such as those shown in Figures 9-15 and 9-16 have an advantage in preventing a buildup of wet particulate matter at the wet-dry transition which could occur in a scrubber such as that shown in Figure 9-17.

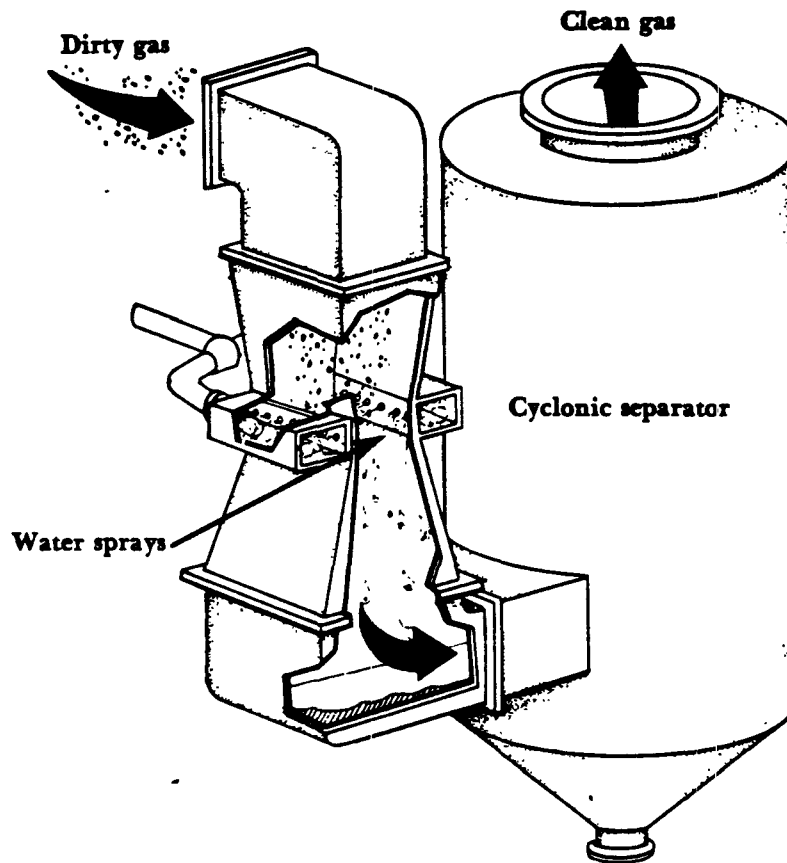


Figure 9-17. Spray venturi scrubber.

The spray venturi scrubber (Figure 9-17) injects the water through nozzles at the throat. Here, atomization can occur both by energy supplied by the gas stream and by energy supplied from the liquid stream. In these applications, however, low pressure sprays on the order of 5 to 15 psi (34.5 to 103 kPa) are normally used. The greatest energy contribution for droplet formation therefore comes from the gas stream. Spray injection can distribute liquid more uniformly over the throat area for venturis with large throat areas.

A problem that can occur with venturi scrubbers is maintaining a given pressure drop (and correspondingly, collection efficiency) under varying volumetric process flow rates. A number of methods have been designed to vary the venturi throat area under these conditions. Two of these designs are shown in Figure 9-18 and Figure 9-19.

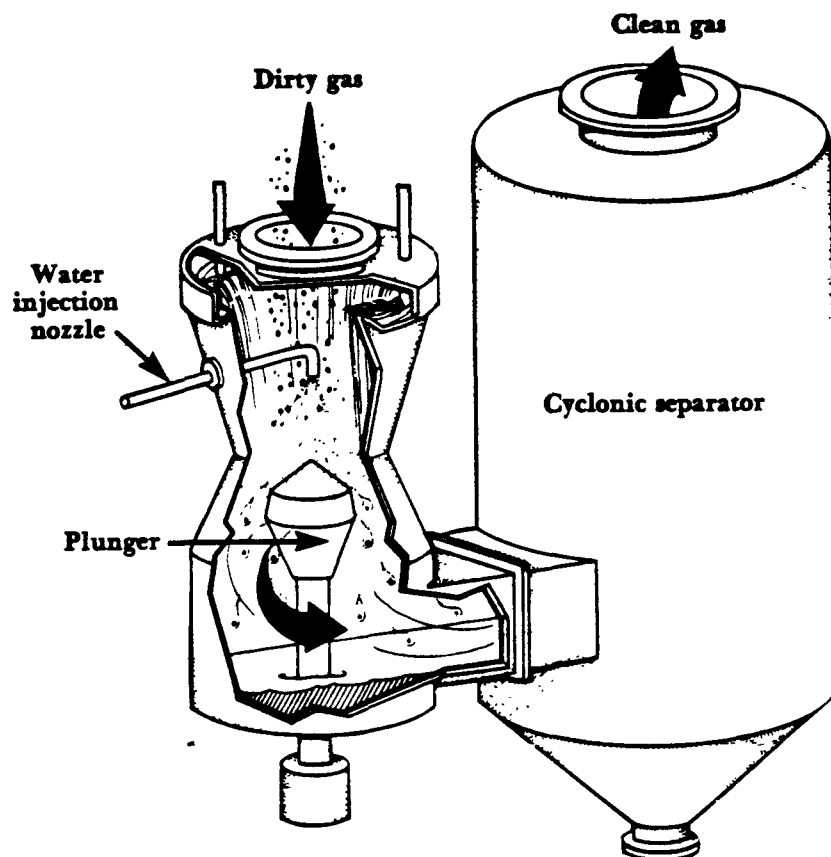


Figure 9-18. Variable throat venturi scrubber.

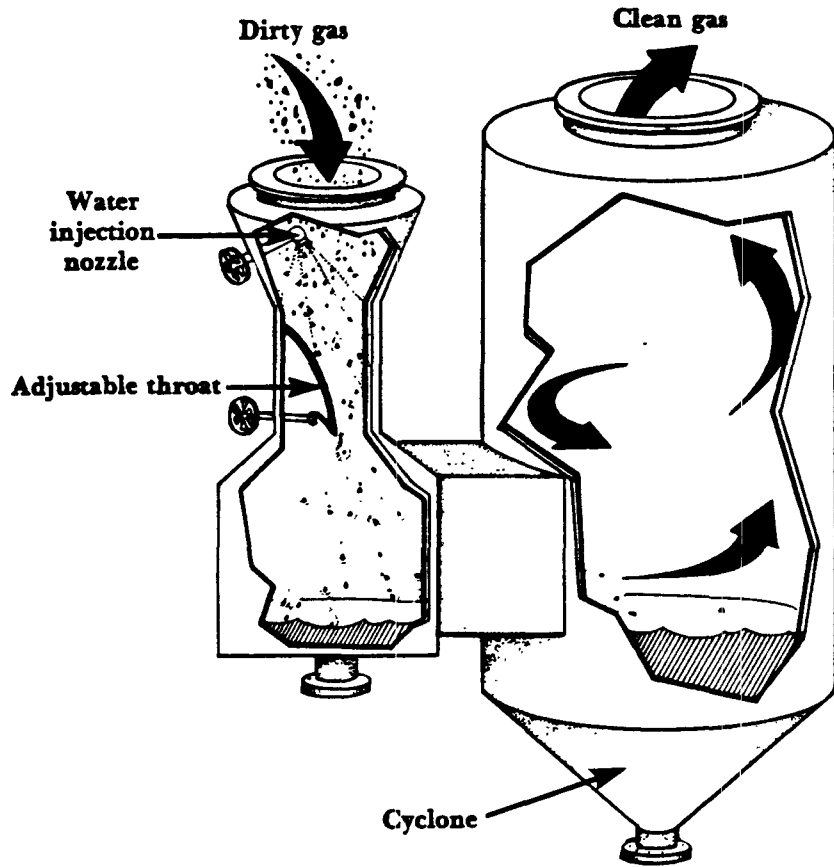


Figure 9-19. Variable throat venturi scrubber.

In the scrubber shown in Figure 9-18 the throat area is varied by moving a plunger up or down in the throat. Gas flows through the annular space to atomize water sprayed over the plunger or swirled in from the top. The purpose of the water spray is to continually wash collected matter from the top of the plunger cone and to provide water for atomization. Figure 9-19 illustrates the use of a movable plate to adjust the throat area with respect to process conditions. A water wash spray is also employed here for much the same purpose as in Figure 9-18.

A modification of the basic venturi design can be seen in the venturi-rod scrubber. By merely placing a number of pipes parallel to each other, a series of longitudinal venturi openings can be created as shown in Figure 9-20.

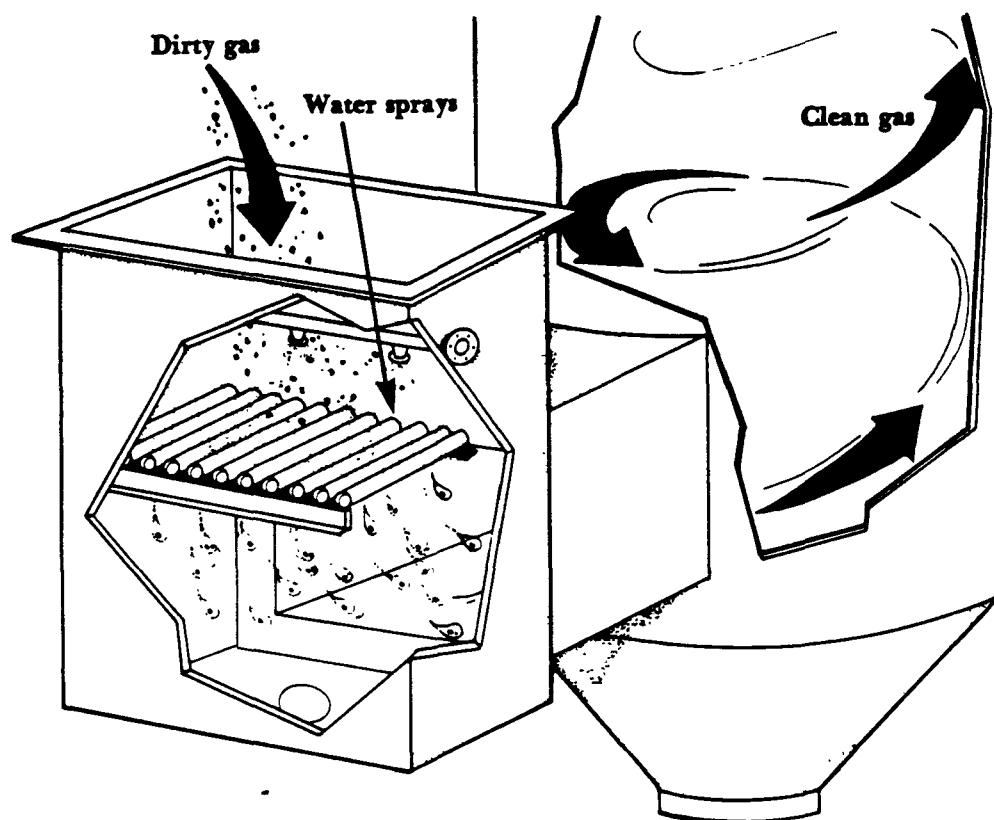


Figure 9-20. Venturi-rod scrubber.

Water sprays serve to prevent clogging the openings from solids build-up. The principle atomization of the liquid occurs at the rods, where the high velocity gas moving through spacings creates the small droplets necessary for fine particle collection.

Although venturi scrubbers have been used primarily for the collection of particulate matter, they have also been used to absorb gases. Lower gas rates and higher liquid-to-gas ratios are necessary for efficient absorption. The advantage of the venturi design for such an application is its relative freedom from scaling and plugging from accumulated solids. The contact time between gas and liquid is, however, relatively shorter than in other type absorption systems and high removal efficiencies for gases are more difficult to achieve. The basic design of the venturi can lead to high abrasion and, consequently, high maintenance. The high gas velocities can impel particles into the surfaces of the system and rapidly erode them. For this reason, silicon carbide brick has been used to line the throat section. The elbow at the bottom of the scrubber leading into the cyclonic separator can be

flooded. Particles and droplets impact into the pool of liquid, reducing abrasion of the scrubber itself. In designs using spray nozzles for liquid injection, recirculated water can cause the nozzles to plug. Automatic or manual reamers are used to correct this problem.

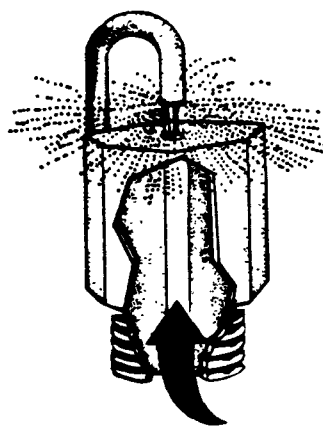
The operating characteristics of venturi scrubbers vary greatly, depending upon the application and specific design. An excellent and more detailed review of venturi scrubber systems is given in Cheremisinoff, 1977. A range of values for various performance parameters is given in Table 9-6.

Table 9-6. Operating characteristics of venturi scrubbers.

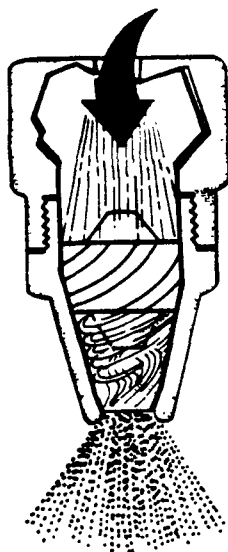
Pressure drop (Δp)	Liquid to gas ratio (L/G)	Liquid inlet pressure (p_L)	Cut diameter ($[d_p]_{cut}$)	Applications
5-100 in. water (20-60 common)	3-20 gpm/ 1000 acfm (7-8 common)	< 1-15 psig	0.2 μm (dependent upon Δp)	Pulp and paper industry Acid plants Mining industries Dryers Nonferrous metals industry Iron and steel industry Utility and industrial boilers Incinerators Chemical industry

Liquid Phase Contacting Scrubbers

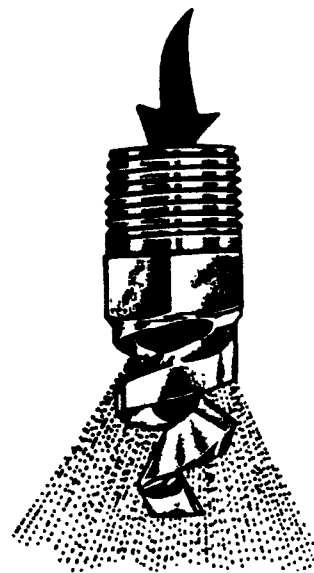
The previous section dealt with scrubbers which primarily used the process gas stream to atomize liquid into collection droplets. Energy can also be applied to a scrubbing system by injecting liquid at high pressure through specially designed nozzles. Nozzles produce droplets which fan out into a scrubber chamber to impact with particulate matter contained in a polluted gas stream. Three types of nozzles are shown in Figure 9-21 a-c; an *impingement spray nozzle*, a *solid cone spray nozzle*, and a *helical cone spray nozzle*.



a. Impingement spray nozzle



b. Solid cone spray nozzle



c. Helical cone spray nozzle

Figure 9-21. Types of spray nozzles.

In the impingement nozzle (Figure 9-21a), high pressure liquid strikes a plate or pin to give a spray of uniformly sized droplets. The solid cone nozzle (Figure 9-21b) directs the liquid through a central jet which strikes fluid rotating in from the side. The two streams interact to break the liquid up into a droplet spray. The helically shaped solid cone nozzle (Figure 9-21c) can provide a wide spray at high pressure with fewer plugging problems.

Two scrubber designs which most clearly characterize the liquid phase contacting class of wet collectors, are the *spray towers* and *ejector venturis*. Other scrubber designs use preformed sprays from nozzles to clean plates, packing surfaces, or orifices as were shown in the case of gas phase contacting venturis.

Spray Towers

Spray towers are alternatively called gravity spray towers, spray scrubbers, or spray chambers. The basic design is simple. Liquid is sprayed into a cylindrical or rectangular chamber using one nozzle or a series of nozzles as shown in Figure 9-22.

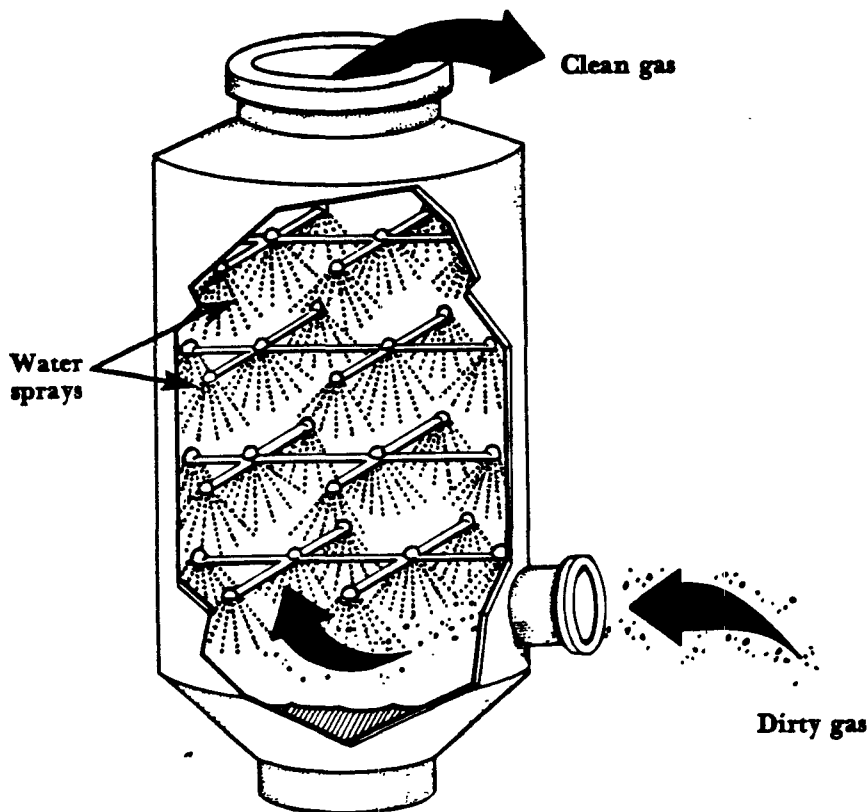


Figure 9-22. Simple spray chamber.

The gas flow is generally countercurrent to the liquid direction, moving up past the downward spraying droplets. The open space of the scrubbing chamber allows for few plugging or scaling problems. If the scrubber water is recirculated, however, the small nozzle openings can become plugged or severely eroded by suspended particulate matter in the recirculating liquid. Spray scrubbers are more successfully applied to systems using relatively clean water.

Spray towers are low energy devices. Contacting power is much lower than in venturi scrubbers and the gas pressure drop across such systems are generally less than 1 in. (2.5 cm) of water. The collection efficiency for small particles is correspondingly lower than more energy intensive devices. They are adequate for the collection of coarse particles larger than 10-25 μm , although with increased liquid inlet nozzle pressures, a cut diameter of 2.0 μm can be achieved. Higher liquid pressures at the nozzle imply the formation of smaller droplets. The highest collection efficiencies are achieved when small droplets are produced and the difference

between the velocity of the droplet and the velocity of the upward moving particles is high. Small droplets, however, have small terminal settling velocities, so there is an optimum range of droplet sizes for scrubbers which work by this mechanism. Stairmand (1956) found this range of droplet sizes to be between 500 and 1000 μm for gravity spray chambers. The injection of water at very high pressures, 300 to 450 psi (2070 to 3100 kPa), creates a fog of very fine droplets. Higher particle collection efficiencies can be achieved in such cases since collection mechanisms other than inertial impaction occur (Bethea, 1978).

Exhaust gases entering a spray chamber, expand into the large volume and cool down from both expansion and the water sprays. Large volumetric flows of hot gases can be conditioned in this way before being exhausted or undergoing further treatment in smaller systems. Gas velocities are generally low, on the order of 2 to 5 ft/sec (0.61 to 1.5 m/sec). Higher velocities will cause the smaller droplets to be swept up and entrained in the exhaust gas stream. In such cases, water droplet entrainment separators (mist eliminators) are needed to collect the escaping droplets. Chevron baffle or fiber type eliminators such as those shown in Figure 9-23 are often used.

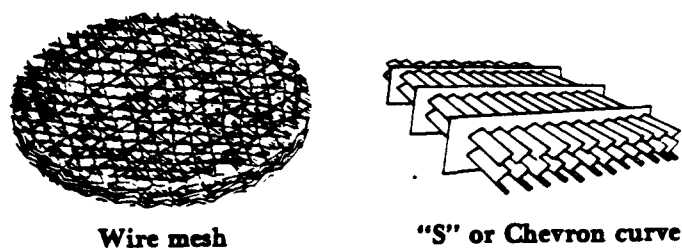


Figure 9-23. Mist eliminators.

These are placed at the top of the scrubber, before the gas exhausts into further parts of the duct system.

Spray towers find wide application as inexpensive control devices for large particles. They often serve to condition the gas, reduce its volume, and cool and humidify it before it is treated in a more efficient device. General characteristics of spray towers are given in Table 9-7.

Table 9-7. Operating characteristics of spray towers.

Pressure drop (Δp)	Liquid to gas ratio (L/G)	Liquid inlet pressure (p_L)	Cut diameter ($(d_p)_{cut}$)	Applications
$\frac{1}{2}$ -3 in. of water	0.5-20 gpm/1000 acfm (5 normal; > 10 when using high pressure sprays)	10-400 psig	2-8 μm	Mining industry Chemical process industry Boilers and incinerators Iron and steel industries

Ejector Venturi Scrubbers

The ejector venturi scrubber uses a preformed spray as does the simple spray tower. The difference is that only a single nozzle is used. This nozzle operates at higher pressures and higher liquid injection rates than those in most spray chambers. For example, liquid-to-gas ratios in such systems are on the order of 100 gpm/1000 acfm [(379 L/min)/(28 m³/min)] at liquid nozzle pressures near 100 psig (690 kPa). Figure 9-24 shows the ejector venturi design.

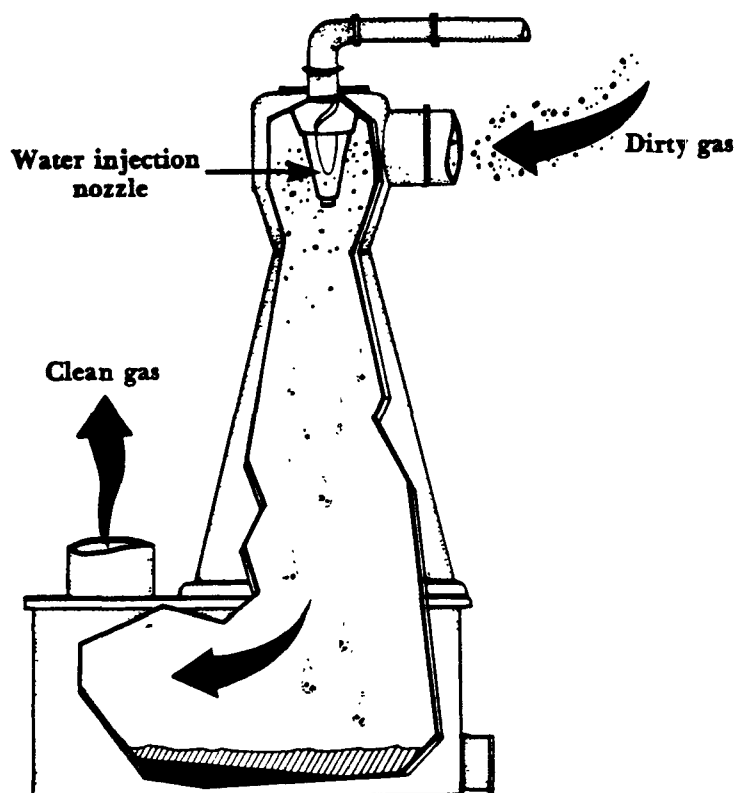


Figure 9-24. Ejector venturi scrubber.

The ejector venturi is unique among available scrubbing systems since it can move the process gas without the aid of a blower or fan. The liquid spray coming from the nozzle creates a partial vacuum in the side duct of the scrubber. This has the same effect as the water aspirator used in high school chemistry labs to pull a small vacuum for filtering precipitated materials (this is all due to the Bernoulli effect). This partial vacuum can be used to move the process gas through the control device as well as the process system. In the case of explosive or extremely corrosive atmospheres, the elimination of a fan in the system can avoid many potential problems.

The energy for the formation of scrubbing droplets comes from the injected liquid. Particulate collection occurs primarily by impaction as the process gas enters into the spray area from the side. The gas motion is initially in a crossflow

direction with respect to the liquid, but then becomes cocurrent as it moves down the venturi tube. The turbulence which occurs in the throat area of the venturi also aids in the collection of the particulate matter. Since the flow is cocurrent once the gas is in the system, the gas will remain in contact with the liquid longer than in some other systems. This longer time improves absorption efficiency for pollutant gases soluble in the scrubbing liquor.

Very high liquid injection rates are used to provide the gas-moving capability and higher efficiencies. As with other types of venturis, a means of separating entrained liquid from the gas stream must be applied. Ejector systems commonly use a liquid sump, directing the gas flow at a right angle, to continuing duct work. Mist eliminators are commonly used to remove remaining small droplets.

Ejector venturis have an advantage in being able to handle small, large, and variable gas volumetric flows. In fact, 10 cfm units have been made using this principle. Other design ranges are given in Table 9-8.

Table 9-8. Operating characteristics of ejector venturis.

Pressure drop (Δp)	Liquid to gas ratio (L/G)	Liquid inlet pressure (p_L)	Cut diameter ($(d_p)_{cut}$)	Applications
$\frac{1}{2}$ -5 in. of water	50-100 gpm/ 1000 acfm	15-120 psig	1 μm	Pulp and paper industry Chemical process industries

Liquid Phase/Gas Phase Contacting Scrubbers

A number of wet collector designs utilize energy from both the gas stream and liquid stream to collect particulate matter. A few of these have already been discussed in the section on venturi scrubbers. Many of these combination devices are currently available commercially. A seemingly unending number of scrubber designs have been developed by changing system geometry, incorporating vanes, nozzles, and baffles. This section will describe several systems which incorporate features of both liquid phase and gas phase contacting wet collectors.

Cyclonic Spray Scrubbers

Scrubbers which remove particulate matter from a gas stream by the mechanism of inertial impaction show improved collection efficiency when the relative velocity between the particles and the water droplets increases. This is evident from the Johnstone equation (Equation 9-12), one of the simplest expressions characterizing this collection mechanism. The faster a particle moves toward a droplet, the greater its momentum. If the particle has high momentum, following the streamlines around the droplet will be difficult. Hence, it will break through the streamlines and impact upon the droplet. The question here is, what does this have to do with cyclonic spray scrubbers? In a simple gravity spray tower, the relative velocity between the particles carried at the velocity of the gas stream and the droplets is low; on the order of 2-5 ft/sec (0.6 to 1.5 m/sec). However, by intro-

ducing the gas tangentially into a scrubber, a cyclonic motion can be given to the gas (see Chapter 6). The resultant increased relative particle/droplet velocities, v_R , can lead to improved collection efficiency.

Gas phase contacting power was previously discussed in terms of the gas acting to shear liquid into dispersed droplets in a venturi or orifice scrubber. In the case of a cyclonic scrubber, energy is utilized to develop the cyclonic action which leads to greater particle velocities. The pressure drops and energy requirements associated with the gas flow are the same as the dry cyclone collectors discussed in Chapter 6. By adding spray nozzles, a contribution is made from the energy of the liquid stream to the collector. The total energy required to run the system is higher, but the efficiency for particle collection is correspondingly improved.

Many combination devices use cyclonic action and liquid sprays. Modifying an existing dry cyclone by adding spray nozzles at the top, as in Figure 9-25, promotes significant improvements in efficiency.

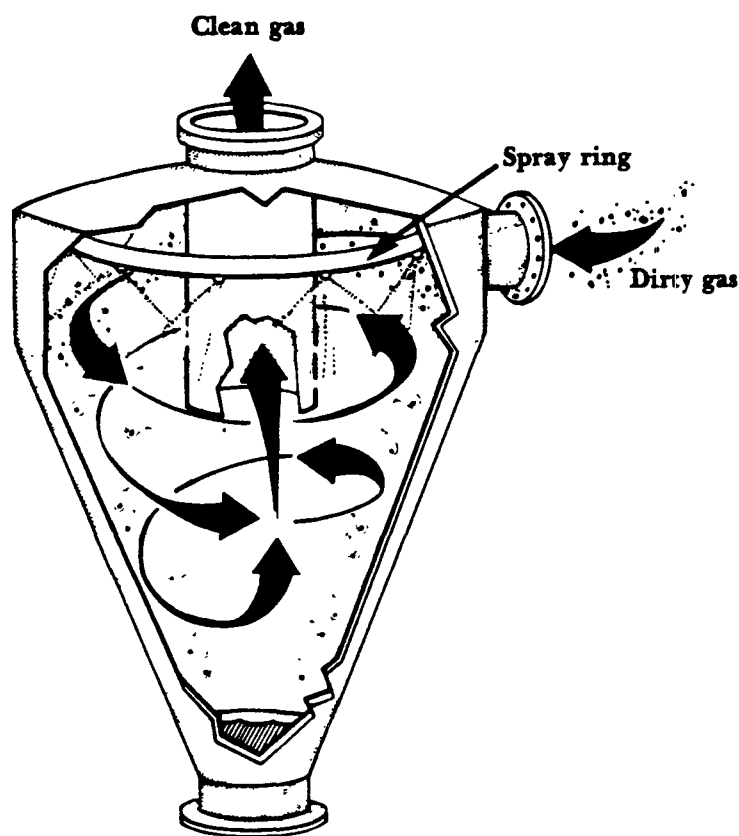


Figure 9-25. Irrigated cyclone scrubber.

The liquid droplets serve as impaction targets and sweep up the smaller particles. The larger droplets containing the particles are more easily collected in the cyclone and the additional feature of the sprays wetting the walls of the system reduces

particle reentrainment. Reentrainment is a significant problem in dry cyclones and the use of spray rings or other spray nozzle configurations to wet the walls is an effective way of minimizing this problem.

A variation of the simple spray chamber directs the gas flow tangentially into the chamber to induce cyclonic flow, thus improving efficiency. Figure 9-26 shows such a system with spray nozzles mounted on a central post, directed toward the walls of the chamber.

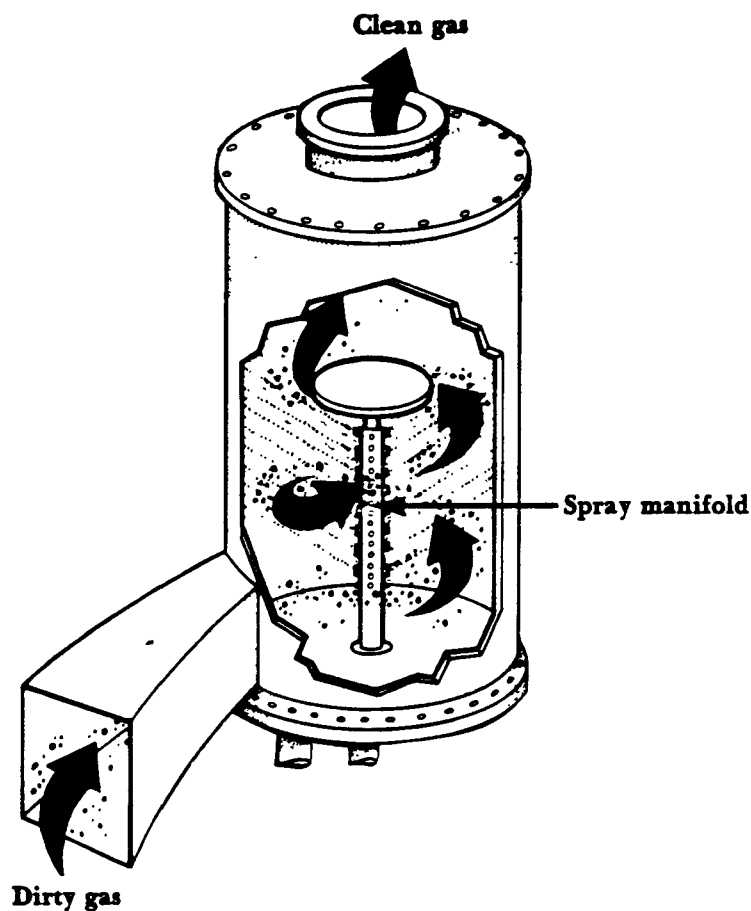


Figure 9-26. Cyclonic spray scrubber.

Other systems are designed with spray nozzles on the outside of the chamber. This configuration allows for easier maintenance and nozzle replacement. Systems have also been designed with directional vanes placed inside the chamber (Figure 9-27).

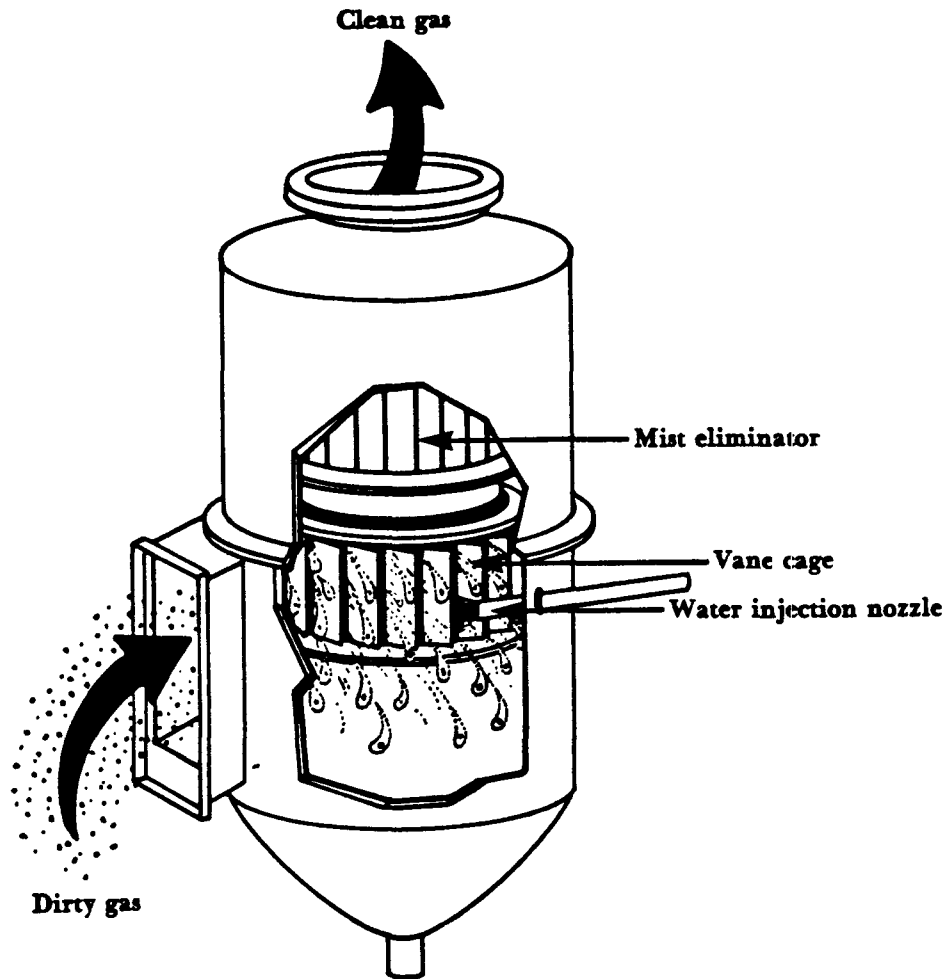


Figure 9-27. Centrifugal scrubber.

These vanes can be used to accentuate the cyclonic motion and force the collecting droplets to the walls for separation from the gas stream. A summary of operational characteristics for the general class of cyclonic scrubbers is given in Table 9-9.

Table 9-9. Operating characteristics of cyclonic scrubbers.

Pressure drop (Δp)	Liquid to gas ratio (L/G)	Liquid inlet pressure (p_L)	Cut diameter ($[d_p]_{cut}$)	Applications
1.5-10 in. of water	2-10 gpm/1000 acfm	40-400 psig	2-3 μm	Mining operations Drying operations Food process Foundries Fertilizer industry Asphalt production Cupolas

Moving Bed Scrubbers

Moving bed scrubbers utilize gas stream energy in a unique way to provide impaction surfaces for particle collection. Figure 9-28 shows the basic components of the moving bed or mobile bed scrubber.

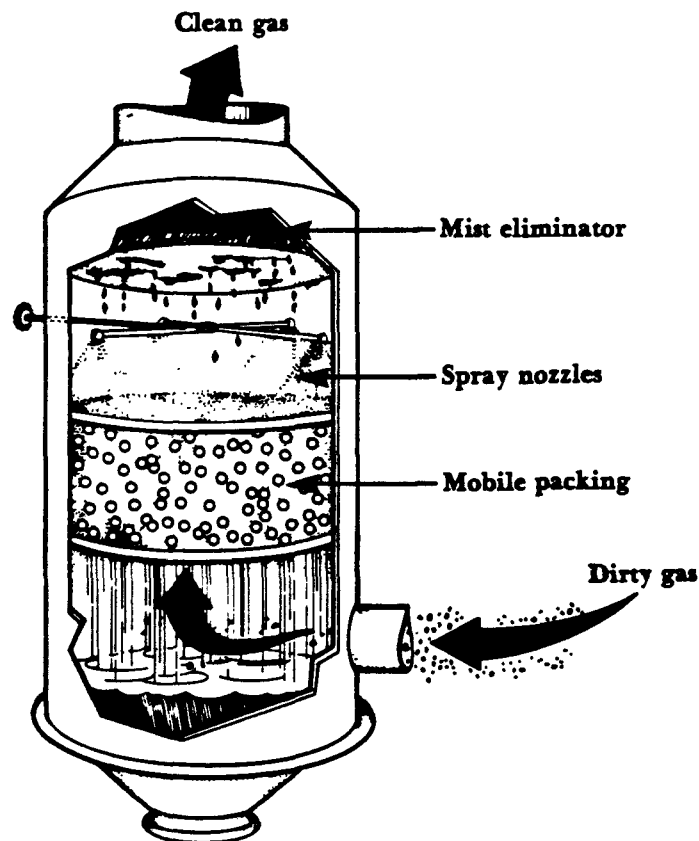


Figure 9-28. Moving bed scrubber.

In one type of mobile bed scrubber, the *fluidized bed scrubber*, process gas is injected at the bottom, keeping a bed of plastic spheres in constant motion. The spheres, resembling ping pong balls, bounce between two perforated plates or screens. Water is sprayed from nozzles over these moving spheres. Particles in the gas stream impact upon the spheres, the liquid which runs over the spheres, and the droplets directed down from the spray nozzles. The gas will also atomize liquid circulating within the moving bed to create a turbulent zone for particle collection. The continual movement of the bed combined with the washing effect of the water sprays, prevents plugging by collected particulate matter.

Energy is supplied by the gas stream to support the packing material and generate the turbulent froth layer. Energy is also supplied by the liquid stream to produce droplets in the water spray.

A similar device is commercially marketed which uses glass marbles in the packing bed (*flooded bed scrubber*). Liquid is sprayed cocurrently into the bed from the bottom. Fluidization is not as pronounced in this case, but the marbles still jiggle by action of the gas stream.

These systems can also be used for gas absorption and in this sense have been termed *turbulent contact absorbers*. They have found application in removing both particulate matter and SO_2 from coal-fired steam generator exhausts. General characteristics of the moving bed scrubber are given in Table 9-10.

Table 9-10. Operating characteristics of moving bed scrubbers.

Pressure drop (Δp)	Liquid to gas ratio (L/G)	Liquid inlet pressure (p_L)	Cut diameter ($(d_p)_{cut}$)	Applications
3-5 in. of water per stage	3-5 gpm/1000 acfm	—	2-3 μm	Mining operations Pulp mills Utility boilers Food industry

Baffle Spray Scrubbers

Baffles are commonly used in entrainment separators to remove droplets from the outlet gas stream. Single baffles are placed in a chamber to redirect the gas flow, or they can be arranged together in Chevron or parallel patterns as in mist eliminators (shown in Figure 9-23). Water is sprayed on the plates to remove accumulated particulate matter and to aid in collecting particles. A simple baffle scrubber system is shown in Figure 9-29.

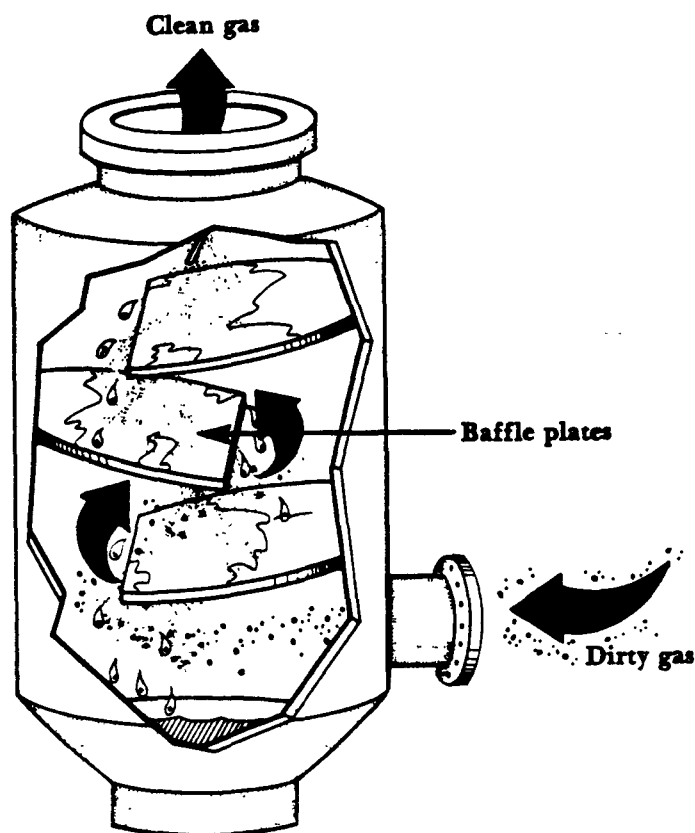


Figure 9-29. Baffle spray scrubber.

Liquid cascading over baffles can be atomized by the gas stream under appropriate conditions (Figure 9-29). Depending upon the scrubber design, liquid and gas streams will contribute to the collection of particulate matter by varying degrees. Pressure drops are normally low for these simple systems as are collection efficiencies for small particles (Table 9-11).

Table 9-11. Operating characteristics of baffle spray scrubbers.

Pressure drop (Δp)	Liquid to gas ratio (L/G)	Liquid inlet pressure (p_L)	Cut diameter ($[d_p]_{cut}$)	Applications
1-3 in. of water	1 gpm/ 1000 acfm	< 15 psig	$\approx 10 \mu m$	Mining Incineration Chemical process industry

Combination Devices

As mentioned previously, new wet collectors can be devised by modifying scrubber geometry or adding hardware. The incorporation of a number of scrubbing principles often improves the collection efficiency for small particles. The addition of baffles, cyclonic motion, or spray nozzles generally raises the energy requirements of the system. The improved efficiency would of course be consistent then with the contact power principle. Two of these combination designs are shown in Figures 9-30 and 31. As an exercise, the reader can evaluate the mechanisms used for particle collection in each scrubber.

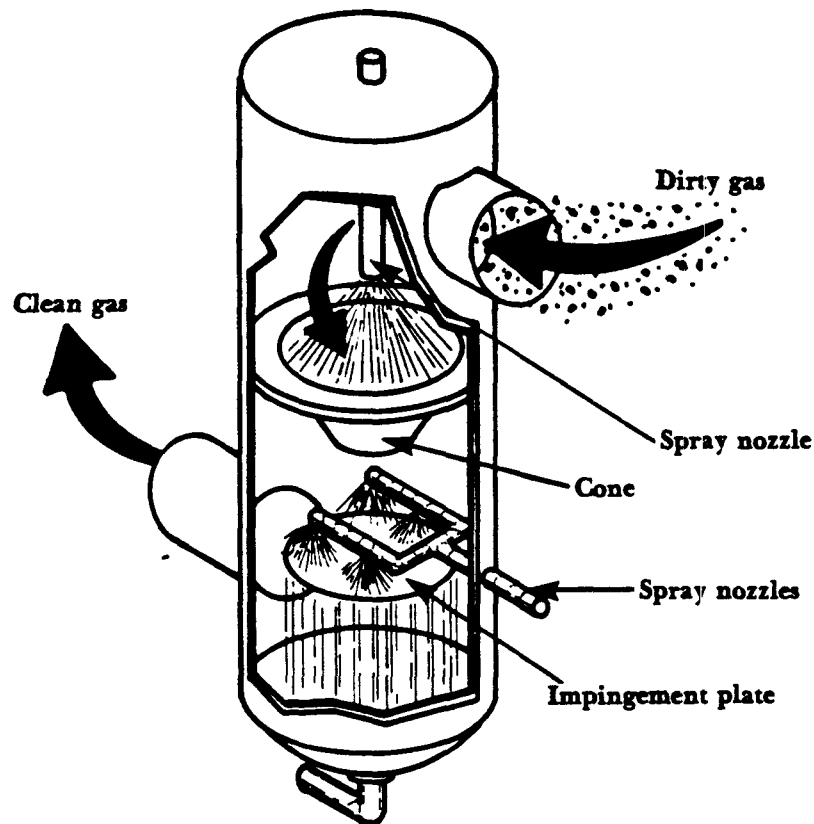


Figure 9-30. Combination device A.

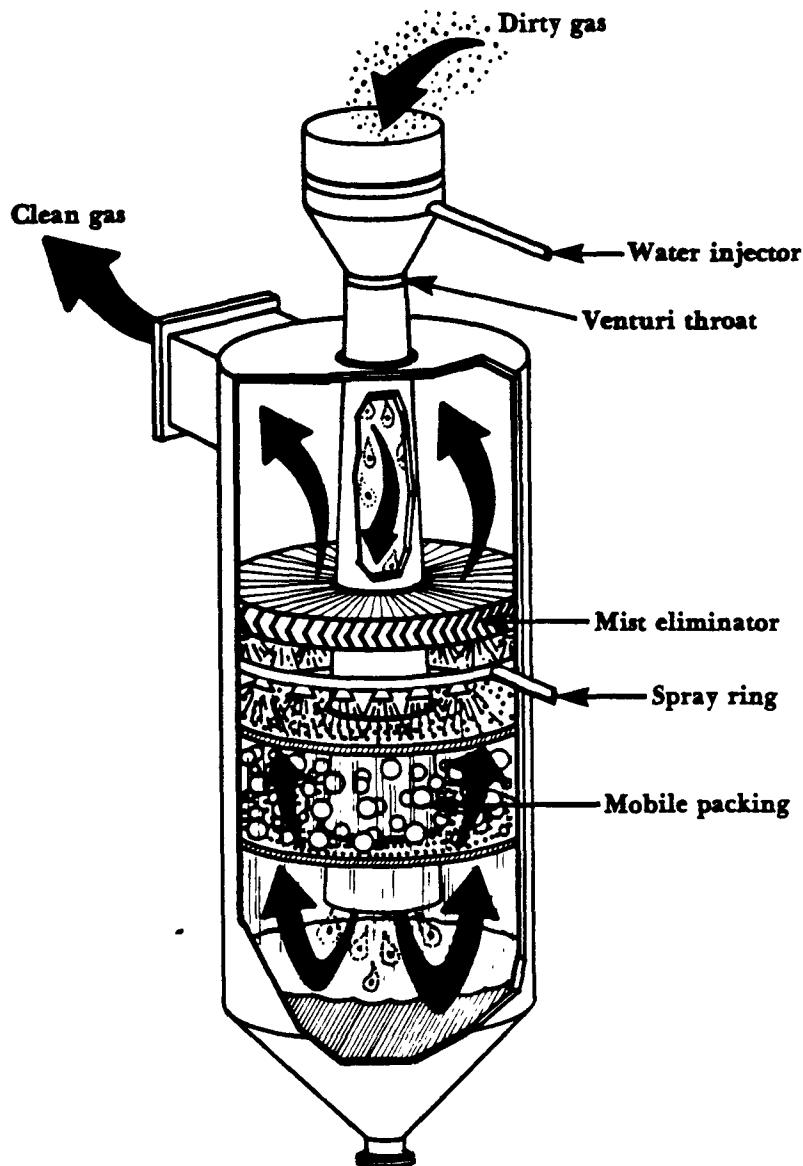


Figure 9-31. Combination device B.

Mechanically Aided Scrubbers

Energy can be supplied externally to a scrubber system by using a motor. A motor serves to drive a rotor or paddles to generate water droplets for particle impaction. Systems designed in this manner have an advantage of requiring less space than other scrubbers, but the overall power requirements tend to be higher than other scrubbers of equivalent efficiency. This point might appear to contradict the contact power principle, but it must be realized that significant power losses occur in driving the rotor and is not expended to provide for particle-liquid contact.

Mechanically aided scrubbers have higher maintenance costs than other wet collector systems. The moving parts can be particularly susceptible to corrosion and fouling. Caking or sticky materials should be collected by simpler devices. Mechanical scrubbers are not normally used for absorbing gaseous pollutants since residence times are short.

Fewer different mechanically aided scrubber systems are available than liquid and gas phase contacting collectors. Two basic designs will be discussed here; the *centrifugal fan scrubbers* and *mechanically induced spray scrubbers*.

Centrifugal Fan Scrubbers

A centrifugal fan scrubber can serve both as an air mover and a collection device. Figure 9-32 shows such a system, where water is sprayed onto the fan blades concurrently with the moving gas.

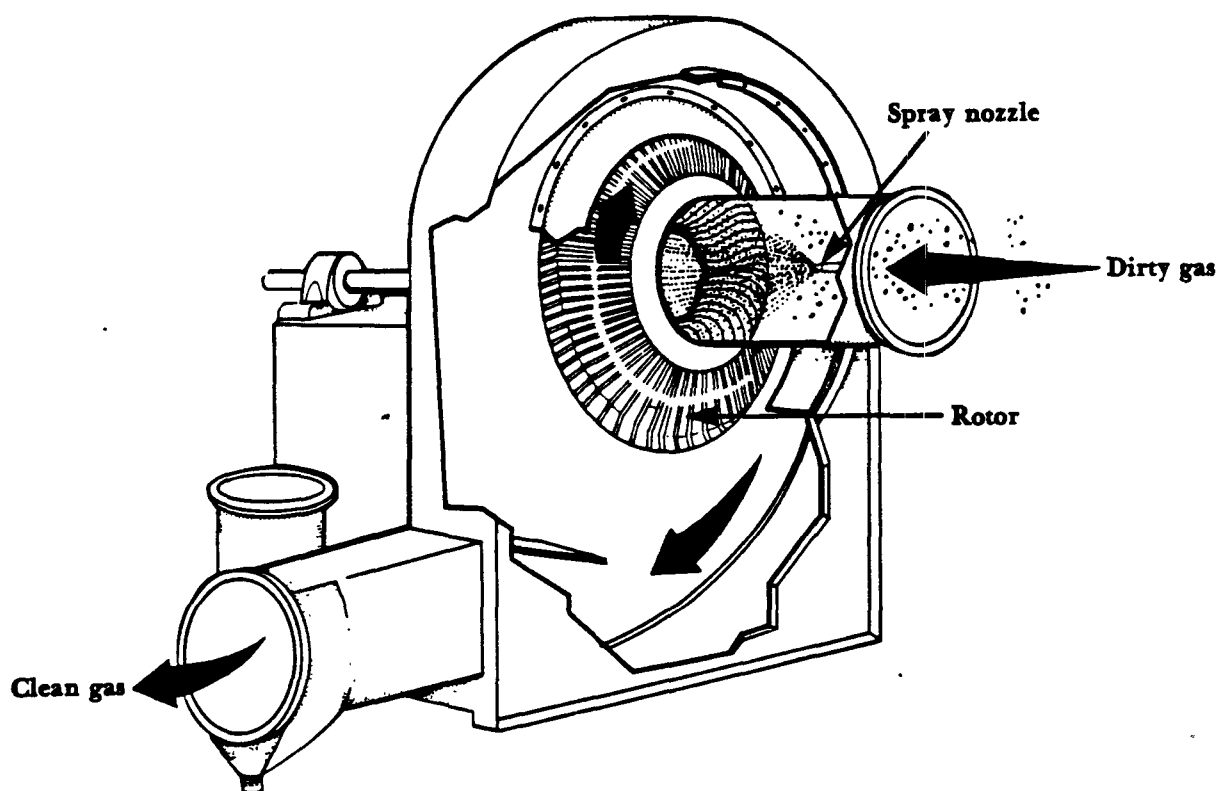


Figure 9-32. Centrifugal fan scrubber.

Droplets from the spray nozzle will initially collect some particulate matter. These will atomize when impacting the blades to create smaller droplets for additional particle collection. The particles will also impact on the blades and be collected. Liquid film on the blades, in conjunction with the centrifugal effects of the

rotating blades, will force both particulate matter and liquid together off the blade ends. The particles and liquid fly off the blades with great acceleration, and are subsequently collected.

Centrifugal fan collectors are the most compact of the wet scrubbers since the fan and collector comprise a combined unit. No internal pressure loss occurs across the scrubber, but a power loss equivalent to a pressure drop of 4 to 6 in. (10.2 to 15.2 cm) of water occurs due to a lower blower efficiency.

Mechanically Induced Spray Scrubbers

A whirling rotor submerged in a pool of liquid produces a fine droplet spray. By moving the process gas through the spray, particles can subsequently be collected. Figure 9-33 shows a vertical spray rotor which operates by this method.

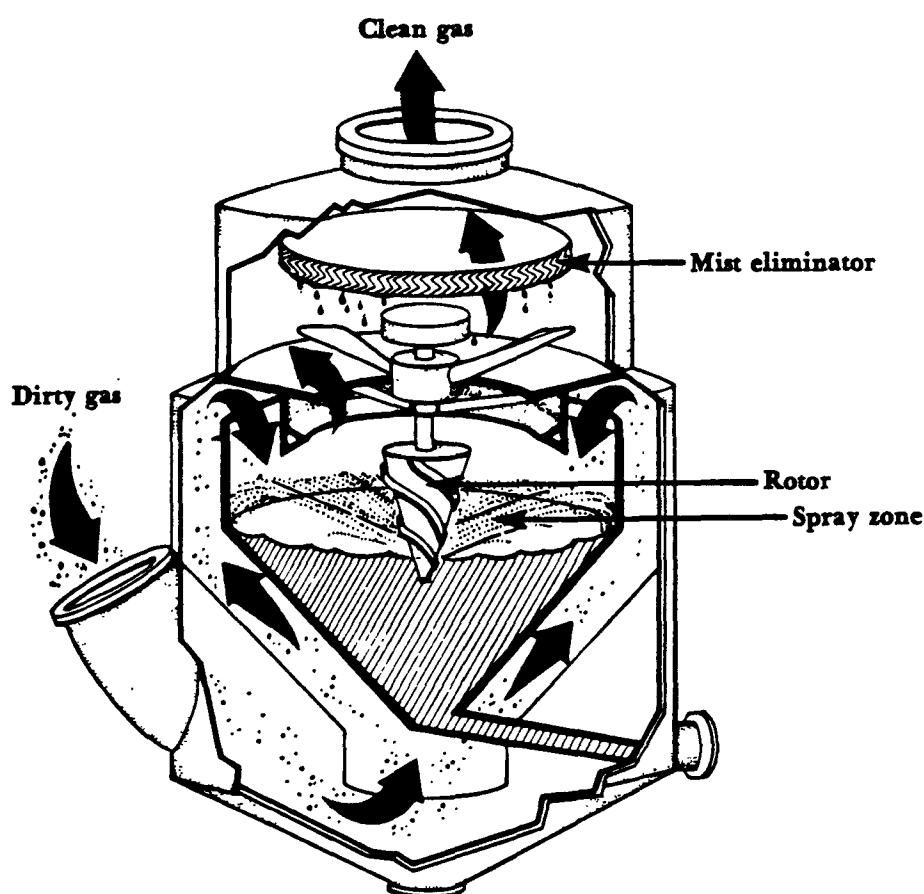


Figure 9-33. Vertical spray rotor scrubber.

The high radial droplet velocity provides good collection efficiencies for submicron sized particles.

Another system, the *disintegrator scrubber*, is used to treat blast furnace gas. Water injected into a rotating apparatus is atomized into small droplets. This scrubber operates well only at low grain loadings, has high operating costs, and requires frequent maintenance. Further performance characteristics for mechanically aided scrubbers are given in Table 9-12.

Table 9-12. Operating characteristics of mechanically aided scrubbers.

Pressure drop (Δp)	Liquid to gas ratio (L/G)	Liquid inlet pressure (p_L)	Cut diameter ($(d_p)_{cut}$)	Applications
4-6 in. of water (nominal)	0.5-1.5 gpm/1000 acfm (centrifugal) 4-5 (spray rotor)	20-60 psig (centrifugal)	$< 1 \mu m$	Mining operations Food product industries Chemical industry Foundries and steel mills

Miscellaneous Devices

Many other systems also use a liquid to aid in the collection of particulate matter. *Wet film scrubbers*, for example, are commonly used to remove gaseous substances from exhaust streams, but under proper conditions, have been successfully used to control particulate emissions. The introduction of new collection mechanisms such as electrostatic charging or condensation has improved collection efficiencies for a number of newer devices. As previously discussed, many collection mechanisms are involved in some of the simplest appearing scrubbers. The generation of a fog or foam, or the electrostatic charging of collecting droplets require extra increments of energy. The efficiency relationships however, differ from those given by the simple contact power theory discussed in this chapter. This section will first discuss the use of wet film scrubbers for particle control and will then briefly discuss some of the new types of wet collection equipment.

Wet Film Scrubbers

A film of liquid will form by spraying or cascading water over packing material. Packing materials are made of plastic or ceramic in many shapes. Figure 9-34 shows a number of forms commonly used. These convoluted forms of packing material are designed so that a large wetted surface area is provided without greatly impeding either the flow of gas or liquid.

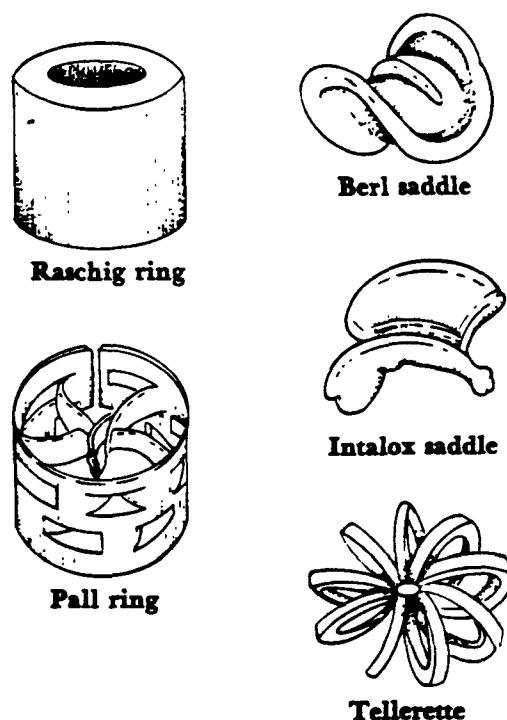


Figure 9-34. Common packing materials.

Packing materials are literally packed in a column or in sectional compartments. Liquid is sprayed on the material and allowed to flow through the system. Process exhaust gas is introduced into this system and the particles in the gas stream move through the packing or are collected. Figure 9-35 shows a packed tower with countercurrent flow (gas and liquid moving in opposite directions). Figure 9-36 shows a packed tower with cocurrent flow (gas and liquid moving in the same direction). Cocurrent flow, provides better particle collection than countercurrent flow since higher gas velocities can be used. With higher velocities, smaller particles can be collected than in similar countercurrent scrubbers.

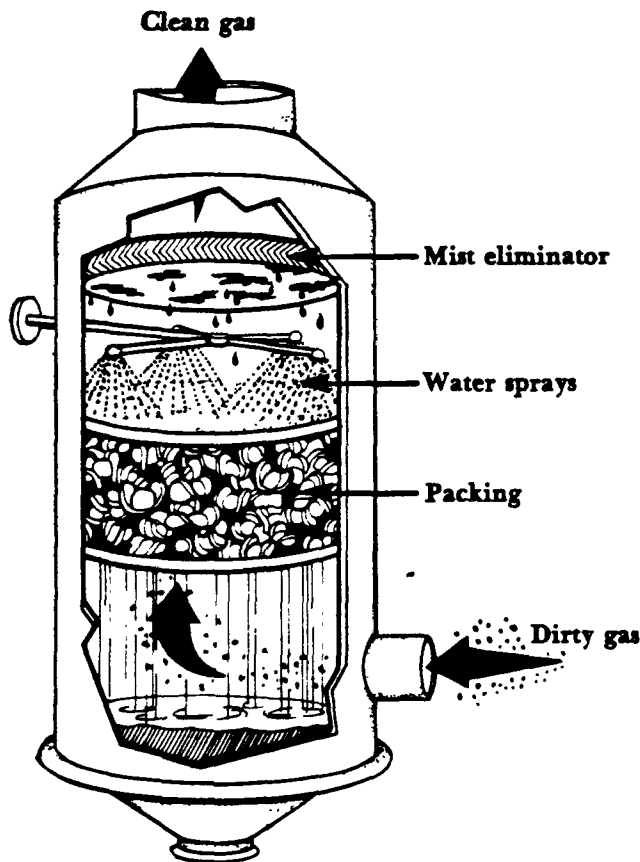


Figure 9-35. Countercurrent packed tower.

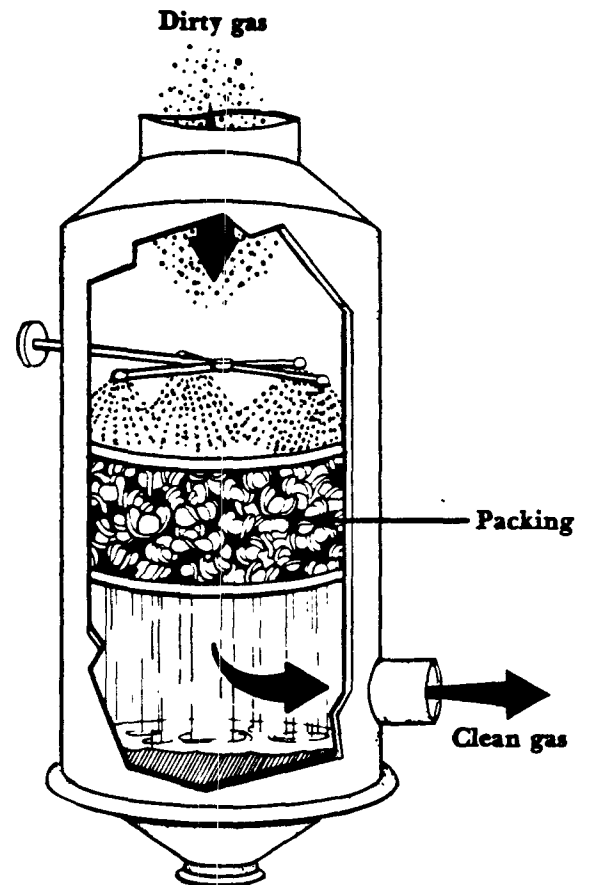


Figure 9-36. Cocurrent packed tower.

The particles impinge upon the liquid film covering the packing and are drained off with the liquid as it flows through the system. Many changes of direction occur as the gas winds through the openings of the packing materials. Larger particles unable to follow the streamlines associated with this flow will consequently hit the packing and be collected.

The packed column or tower can have several problems when not operated under proper conditions. Heavy loadings of particulate matter can plug beds of packing material. Deep beds will provide high pressure drops and higher efficiencies, but can be more susceptible to plugging. However, gas channeling is more likely to occur in thin beds. The gas flows through the path of least resistance and may channel through a certain section of the bed if the bed is not thick enough. In the countercurrent design, if the liquid rates are too high or the gas rates too low, the tower will flood and begin to fill with liquid.

An alternative means of using packing material for particle collection is in a crossflow design such as that shown in Figure 9-37. The water sprays can be positioned in front of the packing, above the packing, or behind the packing. This configuration has an advantage since particulate matter accumulated on the face of the packing can be washed off by water sprays.

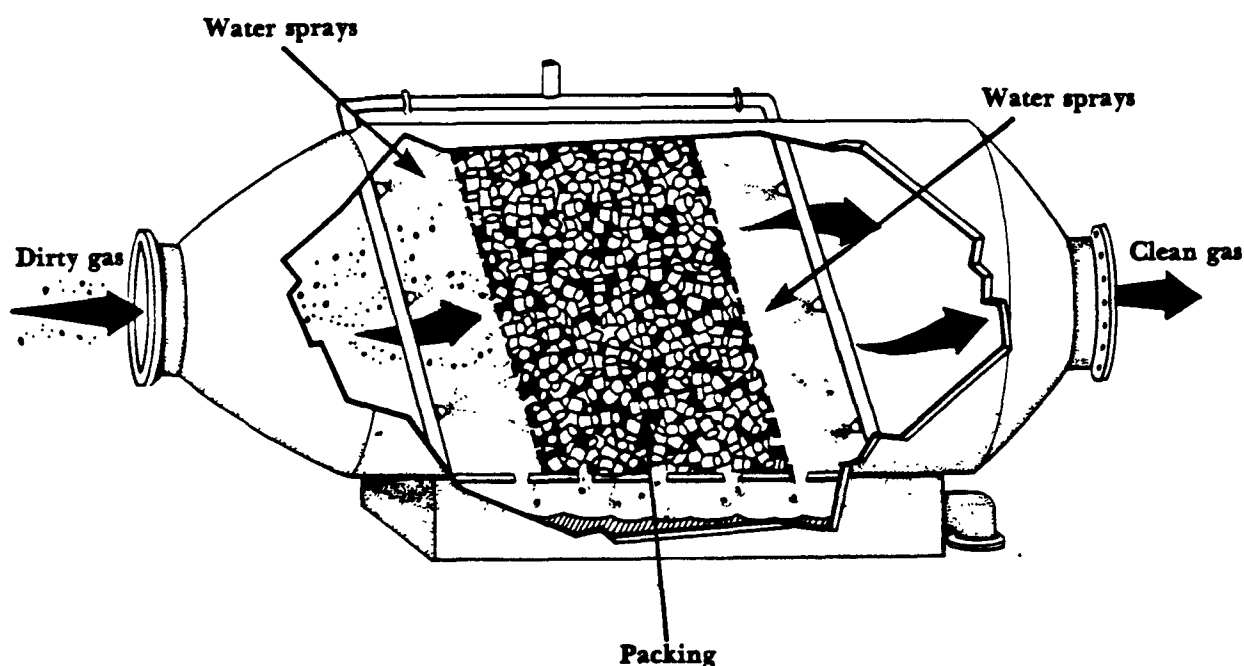


Figure 9-37. Crossflow scrubber.

Another type of arrangement, the *fiber bed scrubber*, uses fibrous material such as fiberglass or plastic in beds with water sprays that wash away collected material (Figure 9-38).

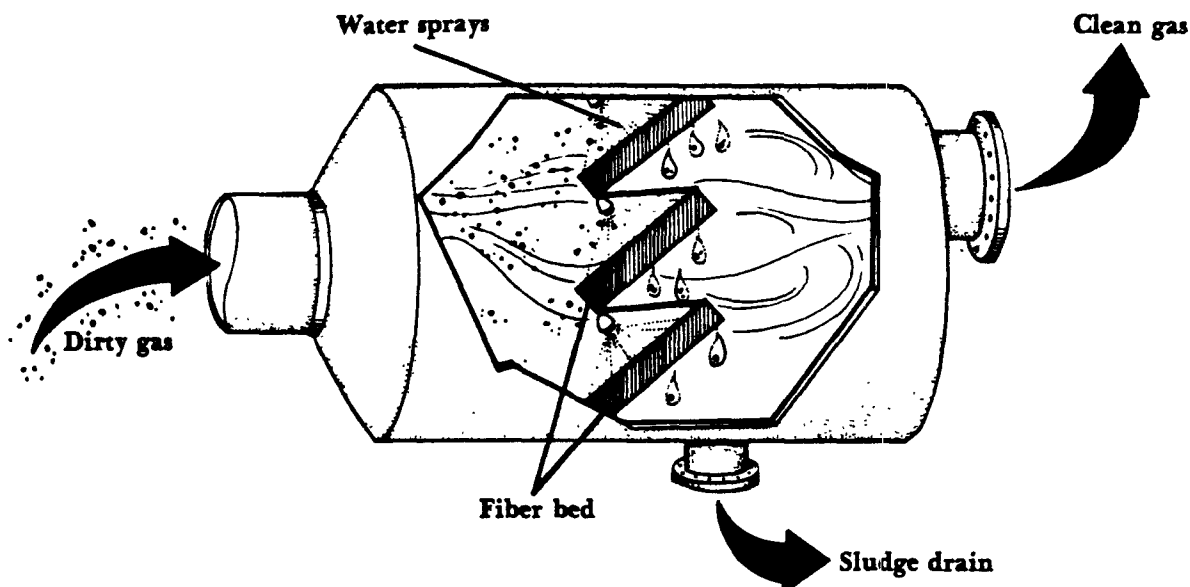


Figure 9-38. Fiber bed scrubber.

Some operational characteristics of the general class of wet film scrubbers are given in Table 9-13.

Table 9-13. Operating characteristics of wet film scrubbers.

Pressure drop (Δp)	Liquid to gas ratio (L/G)	Liquid inlet pressure (p_L)	Cut diameter ($[d_p]_{cut}$)	Applications
1.5-10 in. of water (depending on packing depth)	1-15 gpm/1000 acfm (depending upon countercurrent, cocurrent or crossflow operation)	5-15 psig	$> 1.5 \mu m$ (depending upon size of packing)	Mainly used for liquid aerosol or gaseous pollutant removal Metal operations Acid plants Chemical process industries

New Methods

Mechanisms other than impingement or diffusion can be used for the wet collection of particulate matter. Electrostatic effects, for example, are used to aid in droplet collection. By charging droplets in a special nozzle or by charging particles in a high voltage ionization section, a *charged droplet scrubber* can be produced.

Condensation effects can be used to grow droplets about *particle nuclei*. By reducing the temperature of a hot, saturated gas stream, the condensation effect is used to improve the collection of small particles.

Wet collectors have also been designed which utilize a foam consisting of numerous bubbles. Long lasting bubbles in the foam can increase the likelihood of capturing small particles by diffusional processes.

Selecting a Scrubber

The large number of commercially available wet collector systems has often led to confusion in selecting one for a given application. Vendors do, however, supply extensive information and performance data on their own systems. Evaluations of scrubber designs should be made carefully. Literature on possible systems should be obtained from as many vendors as possible with a list of previous users. These customers should then be contacted for information on actual performance characteristics. Process industry trade associations should also be contacted to identify successful systems applied to processes similar to the one needing control.

References

- American Petroleum Institute. 1974. *Manual on Disposal of Refinery Wastes—Volume on Atmospheric Emissions*. API Publication 931, Chapter 13—Filters and Wet Collectors for the Removal of Particulate Matter.
- Beg, S. A. and Taheri, M. 1977. Test of Mathematical Modeling for the Design of High Energy Scrubbers. *J. Atmos. Environ.* 11:911-915.
- Bethea, R. M. 1978. *Air Pollution Control Technology—An Engineering Analysis Point of View*. New York: Van Nostrand Reinhold Co., pp. 253-328.
- Brady, J. D. and Legatski, L. K. 1977. Venturi Scrubbers, *Air Pollution Control and Design Handbook*, eds. P. N. Cheremisinoff and R. A. Young, pp. 729-745. New York: Marcel Dekker, Inc.
- Busch, J. S., MacMath, W. E. and Lin, M. S. 1973. Part 1—The Basic Scrubber. *Pollut. Eng.* Jan. 1973: 28-32.
- Calvert, S., Lundgren, D. and Mehta, D. S. 1972. Venturi Scrubber Performance. *J. Air Poll. Control Assoc.* 22:529-532.
- Calvert, S. 1974. Engineering Design of Fine Particle Scrubbers. *J. Air Poll. Control Assoc.* 24:929-934.
- Calvert, S. 1977. Scrubbing. In *Air Pollution* Vol. IV, ed. A. C. Stern. New York: Academic Press, pp. 257-291.
- Calvert, S. 1977. How to Choose a Particulate Scrubber. *Chem. Eng.* Aug. 1977: 54-68.
- Calvert, S. 1977. Get Better Performance from Particulate Scrubbers. *Chem. Eng.* Oct. 1977: 133-140.
- Cheremisinoff, P. N. and Young, R. A. 1974. Wet Scrubbers—A Special Report. *Pollut. Eng.* May 1974: 33-43.
- Cheremisinoff, P. N. and Young, R. A. 1976. Control of Fine Particulate Air Pollutants: Equipment Update Report. *Pollut. Eng.* Aug. 1976: 22-29.

- Cheremisinoff, P. N. and Young, R. A. 1977. *Air Pollution Control and Design Handbook*. New York: Marcel Dekker, Inc.
- Crews, B. D. 1978. The Selection of Wet Scrubbing Equipment. In *Proceedings of the International Clean Air Conference*, ed. E. T. White, pp. 277-291. Ann Arbor: Ann Arbor Science.
- Dickie, L. 1967. All About Wet Collectors—Part I. *Air Eng.* Jan. 1967: 14-19.
- Dickie, L. 1967. All About Wet Collectors—Part II. *Air Eng.* Feb. 1967: 24-27.
- Environmental Protection Agency (EPA). 1969. *Control Techniques for Particulate Air Pollutants*. AP-51, pp. 50-81.
- Environmental Protection Agency (EPA). 1972. *Wet Scrubber System Study*. EPA-R2-72-118a.
- Environmental Protection Agency (EPA). 1979. *Design Guidelines for an Optimum Scrubber System*. EPA-600/7-79-018.
- Environmental Protection Agency (EPA). 1978. *Particle Collection by a Venturi Scrubber Downstream from an Electrostatic Precipitator*. EPA-600/7-78-193.
- Environmental Protection Agency (EPA). 1978. *SR-52 Programmable Calculator Programs for Venturi Scrubbers and Electrostatic Precipitators*. EPA-600/7-78-026.
- Gardenier, H. E. 1974. Submicron Particulate Scrubbing with a Two Phase Jet Scrubber. *J. Air Poll. Control Assoc.* 24:954-957.
- Gilbert, N. 1961. *Removal of Particulate Matter from Gaseous Wastes-Wet Collectors*. American Petroleum Institute.
- Gilbert, W. 1977. Troubleshooting Wet Scrubbers. *Chem. Eng.* Oct. 1977: 140-144.
- Gleason, T. G. 1977. Halt Corrosion in Particulate Scrubbers. *Chem. Eng.* Oct. 1977: 145-148.
- Hesketh, H. 1974. The Particle Collection Efficiency Related to Pressure Drop, Scrubbant and Particle Properties, and Contact Mechanism. *J. Air Poll. Control Assoc.* 24:939-942.
- Hesketh, H. E. 1979. *Air Pollution Control*. Ann Arbor: Ann Arbor Science, pp. 217-261.
- Imperato, N. F. 1968. Gas Scrubbers. *Chem. Eng.* Oct. 1968: 152-155.
- Johnstone, H. F., and Roberts, M. H. 1949. Deposition of Aerosol Particles from Moving Gas Streams. *Ind. and Eng. Chem.* 41:2417-2423.
- Johnstone, H. F., Field, R. B., and Tassler, M. C. 1954. Gas Absorption and Aerosol Collection in a Venturi Atomizer. *Ind. and Eng. Chem.* 46:1601-1607.
- Klugman, W. and Sheppard, S. V. 1977. The Ionizing Wet Scrubber. *Air Pollution Control and Design Handbook*, eds. P. N. Cheremisinoff and R. A. Young, pp. 799-811. New York: Marcel Dekker, Inc.

- Krockta, H. and Lucas, R. L. 1972. Information Required for the Selection and Performance Evaluation of Wet Scrubbers. *J. Air Poll. Control Assoc.* 22:459-462.
- Lapple, C. E. and Kamack, H. J. 1955. Performance of Wet Dust Scrubbers. *Chem. Eng. Prog.* 51:110-121.
- Lear, C. W., Krieve, W. F. and Cohen, E. 1975. Charged Droplet Scrubbing for Fine Particle Control. *J. Air Poll. Control Assoc.* 25:184-189.
- Licht, W. 1980. *Air Pollution Control Engineering—Basic Calculations for Particulate Collection*. New York: Marcel Dekker, Inc. pp. 333-370.
- MacDonald, J. W. 1977. Packed Wet Scrubbers. In *Air Pollution Control and Design Handbook*, ed. P. N. Cheremisinoff and R. A. Young, pp. 699-720. New York: Marcel Dekker, Inc.
- Marchello, J. M. 1976. *Control of Air Pollution Sources*. New York: Marcel Dekker, Inc., pp. 187-207.
- McCarthy, J. E. 1980. Scrubber Types and Selection Criteria. *Chem. Eng. Prog.* May 1980: 58-62.
- McIlvaine, R. W. 1977. When to Pilot and When to Use Theoretical Predictions of Required Venturi Pressure Drop. Air Poll. Control Assoc. Meeting Paper, Toronto: 77-17.1.
- Nukiyama, S. and Tanasawa, Y. 1983. An Experiment on Atomization of Liquid by Means of Air Stream (in Japanese) *Trans. Soc. Mech. Eng. Japan*: 4, 86.
- Onnen, J. H. 1972. Wet Scrubbers Tackle Pollution. *Environ. Sci. Technol.* 6:994-998.
- Ostojc, N., Yankura, E. S. and Buonicore, J. A. 1977. Energy Savings with the Centripetal Vortex Scrubber. *Air Poll. Control Assoc. Annual Meeting Paper* 77-17-8. Toronto.
- Perry, J. H. and Chilton, C. H. (eds). 1973. *Chemical Engineers Handbook* 5th ed. New York, McGraw-Hill Book Co., pp. 20-94 to 20-104.
- Rimberg, D. and Peng, Y. M. 1977. Aerosol Collection by Falling Droplets. *Air Pollution Control and Design Handbook*, eds. P. N. Cheremisinoff and R. A. Young, pp. 747-777. New York: Marcel Dekker, Inc.
- Rimberg, D. B. 1979. Tips and Techniques on Air Pollution Control Equipment O & M. *Pollut. Eng.* March 1979: 32-35.
- Semrau, K. T. 1960. Correlation of Dust Scrubber Efficiency. *J. Air Poll. Control Assoc.* 10:200-207.
- Semrau, K. T. 1963. Dust Scrubber Design—A Critique on the State of the Art. *J. Air Poll. Control Assoc.* 13:587-593.

- Semrau, K. T. 1977. Practical Process Design of Particulate Scrubbers. *Chem. Eng.* Sept. 1972: 87-91.
- Sparks, L. E., McCain, J. D. and Smith, W. B. 1974. Performance of a Steam Ejector Scrubber. *J. Air Poll. Control Assoc.* 24:958-960.
- Stairmand, C. J. 1956. The Design and Performance of Modern Gas-cleaning Equipment. *J. Inst. Fuel.* 29:58-81.
- Strauss, W. 1975. *Industrial Gas Cleaning*. Oxford: Pergamon Press, pp. 367-408.
- Theodore, L. and Buonicore, A. J. 1976. *Industrial Air Pollution Control Equipment for Particulates*. Cleveland: CRC Press, pp. 191-250.

Appendix A

Common SI Units

Quantity (1)	Some common units	Symbol	Equivalent	Symbol
length	kilometer	km		
	meter	m		
	centimeter	cm		
	millimeter	mm		
	micrometer	μm		
area	square kilometer	km^2	hectare (2)	ha
	square hectometer	hm^2		
	square meter	m^2		
	square centimeter	cm^2		
	square millimeter	mm^2		
volume	cubic meter	m^3	liter (3)	L
	cubic decimeter	dm^3		
	cubic centimeter	cm^3	milliliter (3)	mL
speed or velocity	meter per second (12)	m/s		
	kilometer per hour (4)	km/h		
acceleration	meter per second squared	m/s^2		
rotational frequency	revolution per second	r/s		
	revolution per minute (4)	r/min		
mass (5)	megagram	Mg	metric ton	t
	kilogram	kg		
	gram	g		
	milligram	mg		
density	kilogram per cubic meter	kg/m^3	gram per liter	g/L
force	kilonewton	kN	kilogram meter per second squared	$\text{kg}\cdot\text{m/s}^2$
	newton	N		
movement of force (6)	newton meter	$\text{N}\cdot\text{m}$		
pressure (or vacuum)	kilopascal	kPa	Newton per meter squared	N/m^2
	pascal	Pa		
stress	megapascal	MPa		
viscosity (dynamic)	millipascal second (7)	$\text{mPa}\cdot\text{s}$		
	pascal second	$\text{Pa}\cdot\text{s}$		
viscosity (kinematic)	square millimeter per second (8)	mm^2/s		
energy, work, or quantity of heat	joule (9)	J	Newton meter	$\text{N}\cdot\text{m}$
	kilowatt hour (10)	$\text{kW}\cdot\text{h}$	kilowatthour	kWh
power, or heat flow rate	kilowatt	kW		
	watt	W		
temperature, or tem- perature interval	kelvin	K		
	degree Celsius (11)	$^{\circ}\text{C}$		

NOTES

(1) Any measurable property (such as length, area, temperature) is called a *quantity*. Listed in same sequence as ISO 1000 and ISO 31, except plane angle.

(2) For land or water area only.

(3) To be used only for fluids (both gases and liquids), and for dry ingredients in recipes, or for volumetric capacities. Do not use any prefix with liter except *milli*.

(4) The symbols for minute, hour, and day are min, h, and d, respectively.

(5) Commonly called *weight*.

(6) Torque or bending movement.

(7) $1 \text{ mPa}\cdot\text{s} = 1 \text{ cP}$ (centipoise, which is obsolete).

(8) $1 \text{ mm}^2/\text{s} = 1 \text{ cSt}$ (centistokes, which is obsolete).

(9) The unit-multiples kilojoule (kJ) and megajoule (MJ) are also commonly used.

(10) To be abandoned eventually. $1 \text{ kW}\cdot\text{h} = 3.6 \text{ MJ}$.

(11) The degree mark $^{\circ}$ is always used in $^{\circ}\text{C}$ to avoid confusion with coulomb (C), but never with K for kelvin.

(12) Second is denoted by s in SI units.

Source: The American National Metric Council, 1978.

Appendix B

Conversion Factors

Length

$$1 \text{ inch} = 2.54 \text{ cm}$$

$$1 \text{ m} = 3.048 \text{ ft}$$

$$1 \text{ ft} = 0.305 \text{ m}$$

Mass

$$1 \text{ lb} = 453.6 \text{ g}$$

$$1 \text{ lb} = 7000 \text{ grains}$$

$$1 \text{ kg} = 2.2 \text{ lb}$$

Pressure

$$\begin{aligned} 1 \text{ atm} &= 101,325 \text{ Pa} \\ &= 760 \text{ mm Hg (0°C)} \\ &= 14.7 \text{ psia} \end{aligned}$$

Force

$$1 \text{ N} = 1 \text{ kg} \cdot \text{m/s}^2$$

$$1 \text{ N} = 0.225 \text{ lb}_f$$

Energy

$$1 \text{ cal} = 4.184 \text{ J}$$

$$1 \text{ J} = 9.48 \times 10^{-4} \text{ Btu}$$

$$1 \text{ Btu} = 252.2 \text{ cal}$$

Kinematic viscosity

$$1 \text{ m}^2/\text{s} = 10^4 \text{ stokes}$$

$$1 \text{ m}^2/\text{s} = 3.875 \times 10^4 \text{ ft}^2/\text{hr}$$

Power

$$1 \text{ W} = 1 \text{ J/s}$$

$$1 \text{ W} = 3.414 \text{ Btu/hr}$$

$$1 \text{ W} = 1.341 \times 10^{-3} \text{ hp}$$

$$1 \text{ hp} = 33,479 \text{ Btu/hr}$$

Area

$$1 \text{ m}^2 = 10.764 \text{ ft}^2$$

$$1 \text{ cm}^2 = 0.155 \text{ in}^2$$

$$1 \text{ m}^2 = 1.196 \text{ yd}^2$$

Volume

$$1 \text{ m}^3 = 35.31 \text{ ft}^3$$

$$1 \text{ cm}^3 = 0.061 \text{ in}^3$$

$$1 \text{ m}^3 = 264 \text{ gal (US)}$$

$$1 \text{ ft}^3 = 28.317 \text{ L}$$

$$1 \text{ m}^3 = 10^3 \text{ L}$$

$$1 \text{ barrel (oil)} = 42 \text{ gal}$$

$$1 \text{ ft}^3 = 7.48 \text{ gal}$$

Density

$$1 \text{ kg/m}^3 = 0.0624 \text{ lb/ft}^3$$

Dynamic viscosity

$$1 \text{ Pa} \cdot \text{s} = 1 \text{ N} \cdot \text{m/s} = 1000 \text{ centipoise}$$

$$1 \text{ cp} = 0.000672 \text{ lb/ft} \cdot \text{sec}$$

Volume flow

$$1 \text{ m}^3/\text{s} = 35.3 \text{ ft}^3/\text{sec}$$

$$1 \text{ m}^3/\text{min} = 35.3 \text{ ft}^3/\text{min}$$

$$1 \text{ scfm} = 1.7 \text{ m}^3/\text{h}$$

$$1 \text{ gpm} = 0.227 \text{ m}^3/\text{h}$$

Velocity

$$1 \text{ m/s} = 3.28 \text{ ft/sec}$$

$$1 \text{ m/s} = 196.85 \text{ ft/min}$$

$$1 \text{ mi/hr} = 0.447 \text{ m/s}$$

Geometry

$$\text{area of circle} = \pi r^2$$

$$\text{circumference of circle} = 2 \pi r$$

$$\text{surface area of sphere} = 4 \pi r^2$$

$$\text{volume of sphere} = 4/3 \pi r^3$$

$$\text{area of cylinder} = 2 \pi r h$$

Appendix C

Constants and Useful Information

Gas constants

$$\begin{aligned}
 R &= 0.0821 \text{ atm liter/g mol} \cdot \text{K} \\
 &= 83.14 \times 10^6 \text{ g} \cdot \text{cm}^3/\text{s}^2 \cdot \text{g mol} \cdot \text{K} \\
 &= 8.314 \text{ N} \cdot \text{m/g mol} \cdot \text{K} \\
 &= 0.7302 \text{ atm} \cdot \text{ft}^3/\text{lb mol} \cdot ^\circ\text{R} \\
 &= 1.987 \text{ g} \cdot \text{cal/g mol} \cdot \text{K} \text{ or Btu/lb mol} \cdot ^\circ\text{R}
 \end{aligned}$$

Acceleration of gravity

$$g = 32.17 \text{ ft/sec}^2 = 980.7 \text{ cm/s}^2 = 9.8 \text{ m/s}^2$$

Newton's conversion constant

$$g_c = 32.17 (\text{lb}_{\text{mass}})(\text{ft})/(\text{lb}_{\text{force}})(\text{sec}^2)$$

1 lb mol = 359 ft³ of ideal gas at STP (32°F and 14.7 psia)

1 g mol = 22.4 L of ideal gas at STP (0°C and 760 mm Hg)

C_p for water $\approx 1 \text{ Btu/lb} \cdot ^\circ\text{R} \approx 1 \text{ cal/g } ^\circ\text{C}$ (at 20°C and 1 atm)

C_p for air $\approx 0.26 \text{ Btu/lb} \cdot ^\circ\text{R} \approx 0.26 \text{ cal/g } ^\circ\text{C}$

viscosity of water, $\mu = 1 \text{ cp} = 0.01 \text{ g/cm} \cdot \text{s}$ (at 20°C and 1 atm)

viscosity of air, $\mu_a = 4.1 \times 10^{-7} \text{ lb} \cdot \text{sec/ft}^2 = 2 \times 10^{-5} \text{ N} \cdot \text{s/m}^2$ (at 20°C and 1 atm)

density of air = $1.29 \text{ kg/m}^3 = 7.49 \times 10^{-2} \text{ lb/ft}^3$ (at 20°C and 1 atm)

density of water = $1 \text{ g/cm}^3 = 62.4 \text{ lb/ft}^3$ (at 4°C and 1 atm)

1 cubic foot of air weighs 34.11 g

conversion from ppm to g/m³ at STP (273.15 K and 1 atm)

$$\frac{\text{g}}{\text{dscm}} = \frac{\text{ppm} \times \text{MW} \left(\frac{\text{g}}{\text{g mol}} \right)}{22.414 \frac{\text{liters}}{\text{g mol}} \times 10^{-3} \frac{\text{m}^3}{10^3 \text{ L}} \left(\frac{293.15 \text{ K}}{273.15 \text{ K}} \right)} \times \frac{1}{1 \times 10^6 \text{ ppm}}$$

Appendix D

Capital and Operating Cost Estimations

This appendix contains generalized cost data for air pollution control systems described throughout this manual. These data should be used only as an estimate to determine systems costs. In some cases the cost of the control device may represent only a very small portion (< 20 percent) of the total installed cost; in other cases it may represent the total cost. Variations in the total cost can be attributed to a number of variable factors such as cost of auxiliary equipment, new or retrofitted installation, local labor costs, engineering overhead, location and accessibility of plant site, and type of installation (factory or field assembled).

This cost estimation data, included in this appendix, first appeared in an EPA publication (EPA, 1976) and then in a series of articles published in the Journal of the Air Pollution Control Association (JAPCA, 1978). The reader should refer to these publications for additional information concerning this subject. These estimations represent equipment costs based on a reference date of December 1977 and are estimated to be accurate to within ± 20 percent on a component basis, except where noted (JAPCA, 1978).

Electrostatic Precipitators

The cost of a basic electrostatic precipitator is a function of the collection area which is specified by the desired collection efficiency. Dust resistivity varies with the temperature and moisture content of the exhaust gas stream. For proper operation, the gas may therefore require some type of conditioning prior to entering the ESP. High moisture contents combined with low operating temperatures will necessitate insulating the ESP to prevent corrosion of precipitator components. Figure D-1 gives cost data for dry precipitators utilizing mechanical or vibrator rappers. This figure has curves for both insulated and uninsulated precipitators.

The collection plate area can be estimated using the Deutsch-Anderson equation:

(Eq. 7-3)
$$\eta = 1 - e^{(-wA/Q)}$$

The equation can be rearranged to give the plate area:

$$A = -Q \ln(1 - \eta) / w$$

Where:

- η = collection efficiency
- w = migration velocity, ft/sec (m/sec)
- A = plate area, ft² (m²)
- Q = exhaust gas flow rate, ft³/sec (m³/sec)

Example:

For dust generated by a coal fired industrial boiler the migration velocity of a dust particle is approximately 0.25 ft/sec. If a 99.5 percent collection efficiency is required with a flow rate of 50,000 cfm into the precipitator, the net plate area is calculated as follows:

$$A = (-50,000 \text{ cfm}) \ln(1 - 0.995) / (0.25 \text{ ft/sec})(60 \text{ sec/min}) \\ = 17,661 \text{ ft}^2$$

The price of an uninsulated precipitator (Figure D-1) would be approximately \$138,500.00. For an insulated precipitator the price would be approximately \$212,000.00

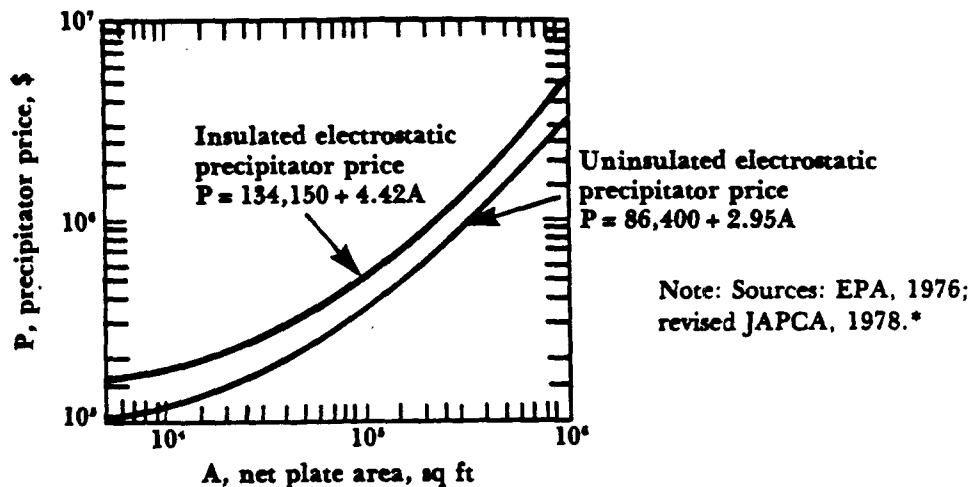


Figure D-1. Dry type electrostatic precipitator purchase prices versus plate area.
Data valid for December 1977.

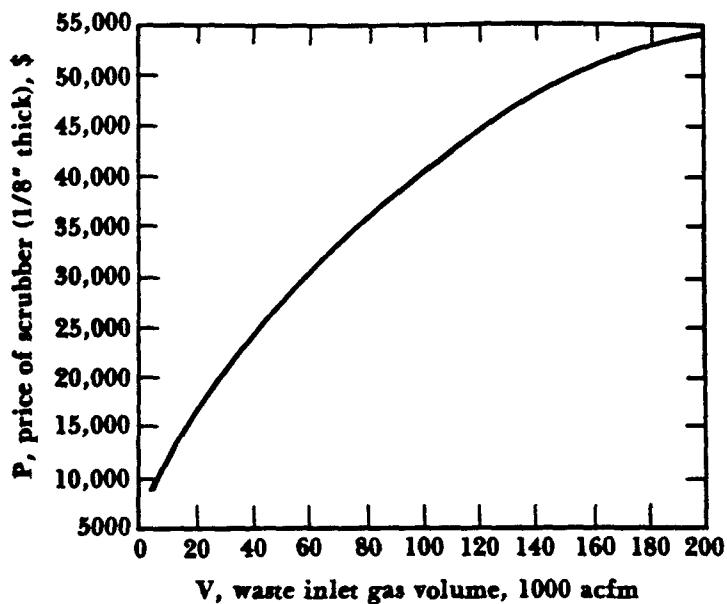
Venturi Scrubbers

The cost of a venturi scrubber and separator (mist eliminator) depends upon the volumetric flow rate, operating pressure and materials of construction. The size of the scrubber, separator, and elbows are determined from the actual inlet gas flow rate (acfm) and priced accordingly for a scrubber with a plate thickness of 1/8 in. Additional cost factors are provided for pricing scrubbers with different metal thicknesses, stainless steel construction, rubber and Fiberglas liners, and manual and automatic variable throats (Figure D-2). Prices for venturi scrubbers are contained in Figure D-2 through D-6. To estimate the scrubber costs using these curves, use the following steps:

- "A. Determine the gas volume entering the venturi section and read the price for 1/8 in. thick carbon steel scrubber from Figure D-2. For example, at 100,000 acfm the price is approximately \$39,000.

*All figures in Appendix D (Figures D-1 through D-18) are from EPA, 1976; revised JAPCA, 1978.

- B. Determine the pressure drop across the scrubber required to obtain the desired efficiency and find the required metal thickness for the design inlet volume from Figure D-3. For 100,000 acfm and 30 in. the required metal thickness is $\frac{1}{4}$ in. plate (always round up to the next standard plate thickness).
- C. From Figure D-4, find the price adjustment factor for the design inlet volume and the material thickness found in Step B. For 100,000 acfm and $\frac{1}{4}$ in. plate, the factor is approximately 1.6. Thus, the carbon steel scrubber price is now $\$39,000 \times 1.6 = \$62,400$.
- D. If stainless steel construction, rubber or fiberglass lining, or variable venturi section is to be included, refer to Figure D-2 and adjust price accordingly. For 304 stainless steel construction, the adjusted price would be $\$62,400 \times 2.3 = \$143,520$. If rubber linings are required, refer to Figure D-5 to determine total square footage.
- E. If an internal gas cooler is to be used, determine the number of trays that can be fitted into the separator (from separator height, Figure D-5), and determine the diameter of each tray (from separator diameter, Figure D-5). Read price for one tray from Figure 6. For 100,000 acfm the separator diameter is approximately 13.5 ft. Thus the price for one tray is about \$14,800." (JAPCA, 1978)



Note:

1. Prices are for 1/8" carbon steel scrubbers.
2. Includes: venturi, elbow, separator, pumps and controls, flange-to-flange.
3. Do not use price equation for above 200,000 acfm.

Scrubber price

$$P = 7117 + 408V - .85V^2$$

Price adjustments

Item

- A. Other metal thickness
- B. 316 stainless steel
- C. 304 stainless steel
- D. 3/16" rubber liner
- E. Manual variable venturi
- F. Automatic variable venturi
- G. Fiberglass lined

Factor

See Figure D-4

x 3.20

x 2.3

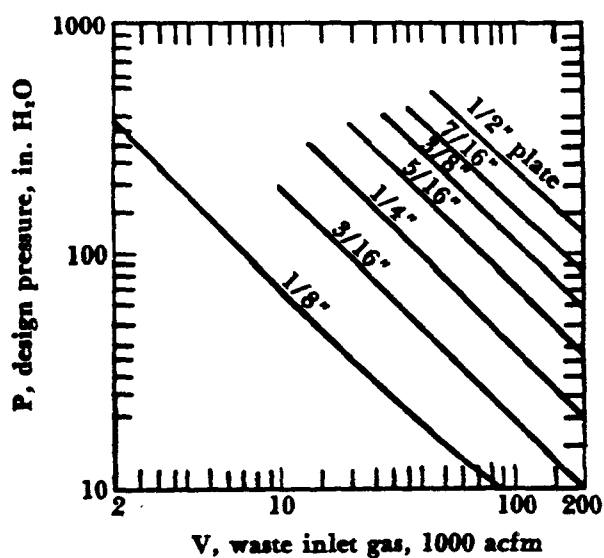
\$4.69/ft²

\$3450

\$6350

Add 15% of price
for 1/8" carbon
steel scrubber
to total price

Figure D-2. 1/8" thick carbon steel fabricated scrubber price versus volume.
Data valid for December 1977.



Note: 1. Safety factor = 2

2. No corrosion/erosion allowance

Figure D-3. Metal thickness required versus volume and design pressure.

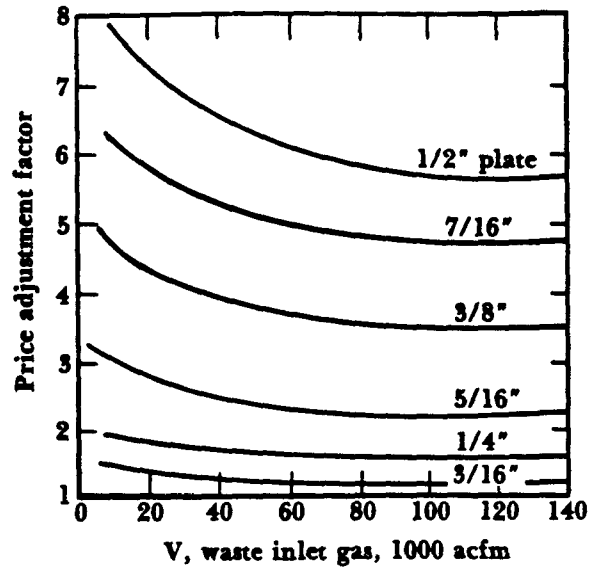
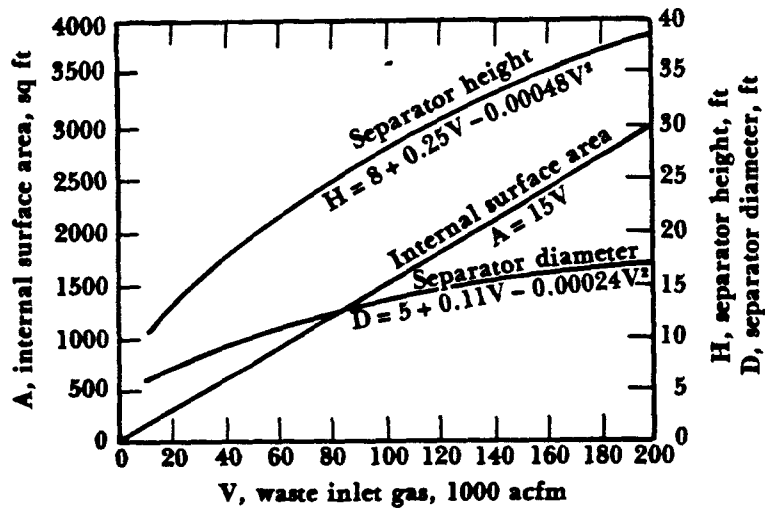


Figure D-4. Price adjustment factors versus plate thickness and volume.
Data valid for December 1977.



Scrubber internal surface area

Part	Fraction
Venturi	0.12
Elbow	0.10
Separator	0.78
	<hr/> 1.00

Figure D-5. Scrubber internal surface area and separator diameter and height versus waste inlet gas volume.

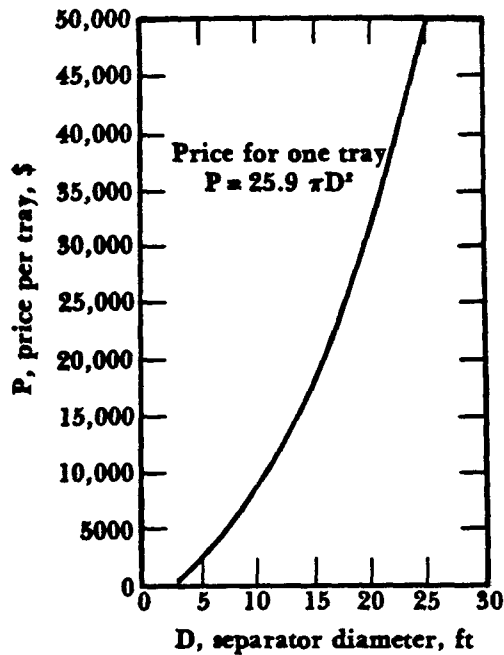


Figure D-6. Internal gas cooler bubble tray cost versus separator diameter.
Data valid for December 1977.

Fabric Filters

The cost data for fabric filters is based on the *net cloth area*. The net cloth area is the total filter area available for on-stream filtration. This would not include the isolated compartment being cleaned in the case of an intermittently cleaned baghouse. For intermittently cleaned baghouses requiring an off-line compartment, the total cloth area must be calculated as the *gross cloth area*. The gross cloth area is the net cloth area of the baghouse plus the cloth area for an extra compartment. The gross cloth area can be calculated for various values of net cloth area from Table D-1.

Table D-1. Approximate guide to estimate gross cloth area.

Net cloth area (ft ²)	Gross cloth area (ft ²)
1-4000	Multiply by 2
4401-12000	1.5
12001-24000	1.25
24001-36000	1.17
36001-48000	1.125
48001-60000	1.11
60001-72000	1.10
72001-84000	1.09
84001-96000	1.08
96001-108000	1.07
108001-132000	1.06
132001-180000	1.05
180001 on up	1.04

The cost for various type baghouses—shaker, reverse air, or pulse jet units—are listed in Figures D-7 through D-11. These figures include curves of additional prices for stainless steel construction, insulation, suction baghouses, and standard or custom designed units. Suction baghouses are negative pressure systems with the fan located on the clean side of the baghouse. Standard baghouses are predesigned and built as modules which can be operated singly or combined to form units for larger capacity. Custom baghouses are designed for a specific application, are erected in the field, and are used most often for large capacity applications. The cost of the baghouse units in Figures D-7 through D-11 are for the baghouse only (bags are not included). The costs for bags using various fabrics can be calculated from Table D-2.

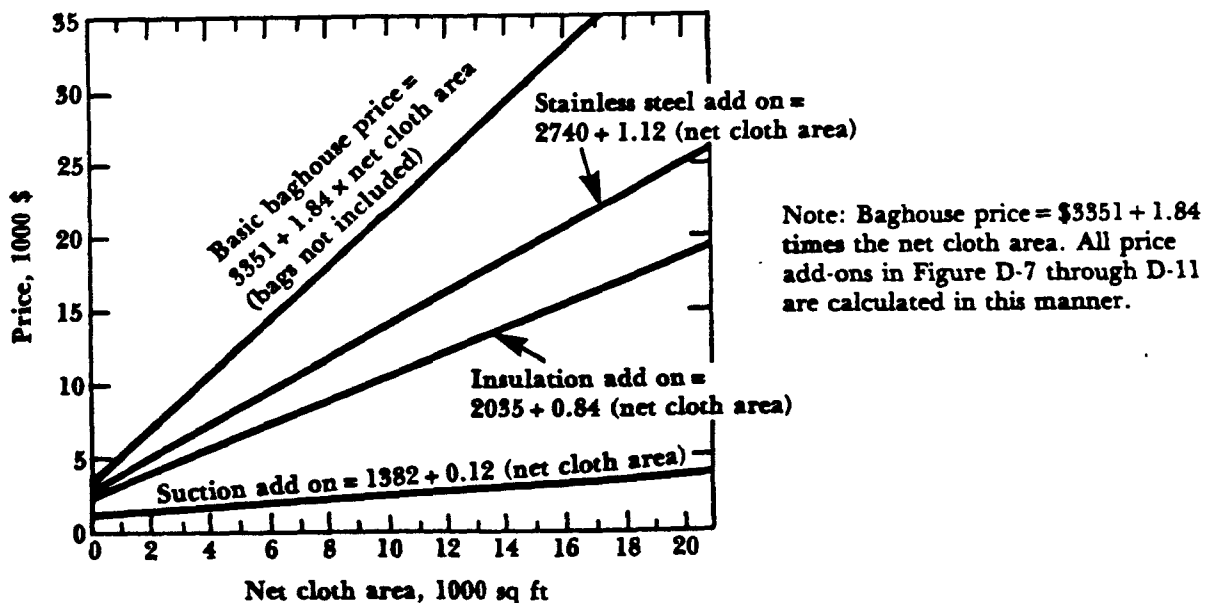


Figure D-7. Intermittent, pressure, mechanical shaker baghouse prices versus net cloth area. Data valid for December 1977.

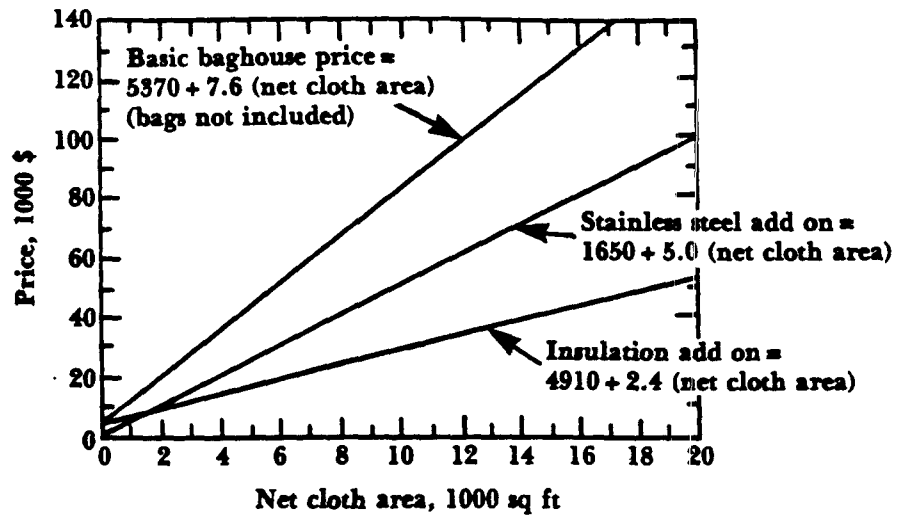


Figure D-8. Continuous, suction or pressure, pulse jet baghouse prices versus net cloth area.
Data valid for December 1977.

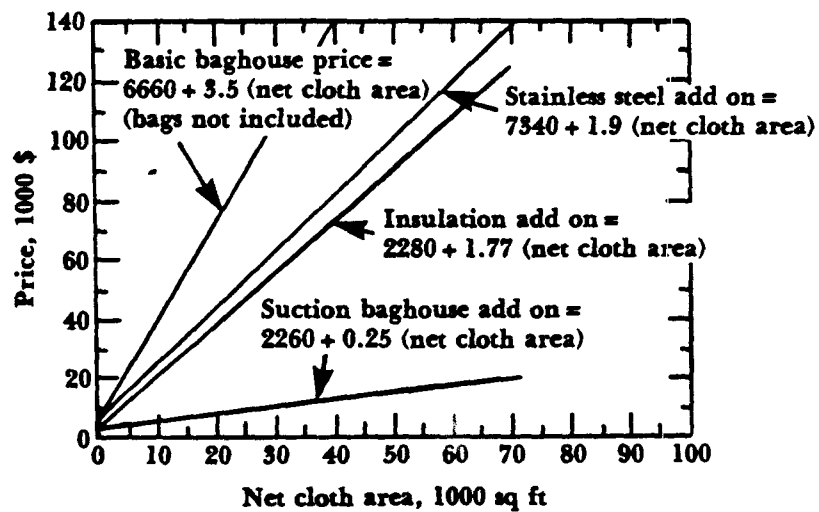


Figure D-9. Continuous, pressure, mechanical shaker baghouse prices versus net cloth area.
Data valid for December 1977.

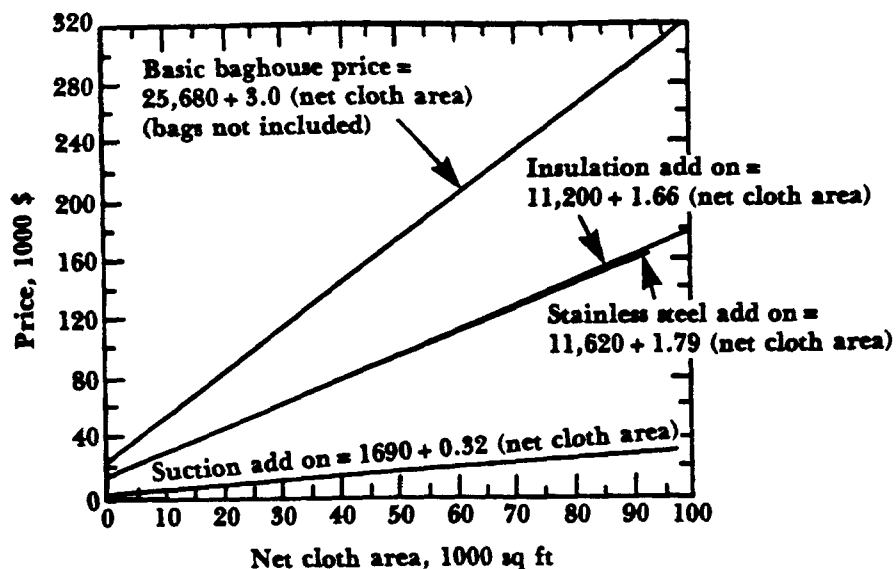


Figure D-10. Continuous, pressure, reverse air baghouse prices versus net cloth area.
 Data valid for December 1977.

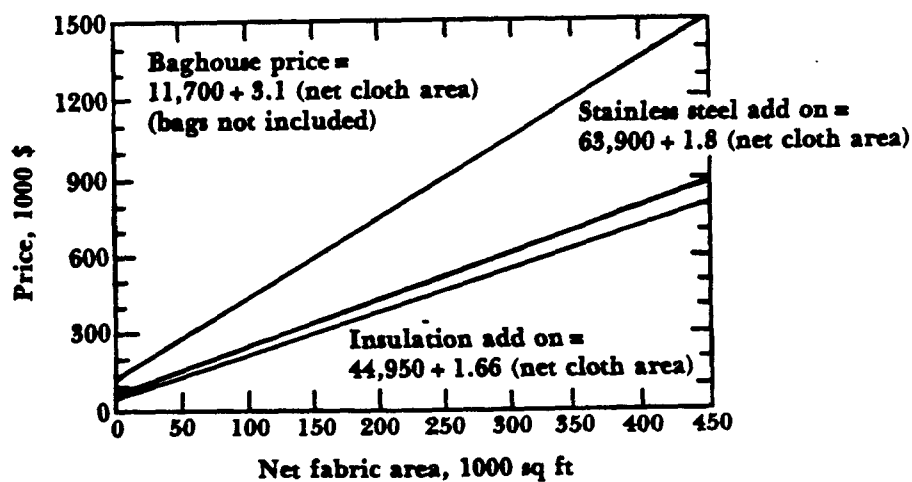


Figure D-11. Custom pressure or suction baghouse prices versus net cloth area.
 Data valid for December 1977.

Table D-2. Bag prices (\$/ft²). Data valid for December 1977.

Class	Type	Dacron	Orlon	Nylon	Nomex	Glass	Polypropylene	Cotton
Standard	Mechanical shaker, < 20,000 ft ²	0.36	0.62	0.73	1.14	0.47	0.62	0.43
	Mechanical shaker, > 20,000 ft ²	0.31	0.57	0.67	1.04	0.42	0.52	0.38
	Pulse jet*	0.57	0.93		1.30		0.67	
	Reverse air	0.31	0.57	0.67	1.04	0.42	0.52	0.38
	Mechanical shaker	0.21	0.31	0.42	0.62	0.26	0.31	0.38
Custom	Reverse air	0.21	0.31	0.42	0.62	0.26	0.31	0.38

*For heavy felt, multiply price by 1.5.

Sources: EPA, 1976; revised JAPCA, 1978.

Example:

A baghouse is used to clean the exhaust from an industrial boiler with a flow rate of 50,000 cfm. The baghouse is a reverse air unit, suction type, using glass bags and an air-to-cloth ratio of 1.5. The baghouse should include an extra compartment for off-line cleaning.

$$\begin{aligned}\text{Net cloth area} &= \frac{50,000}{1.5} \\ &= 33,333 \text{ ft}^2\end{aligned}$$

From Table D-1:

$$\begin{aligned}\text{Gross cloth area} &= 33,333 \times 1.125 \\ &= 37,500 \text{ ft}^2\end{aligned}$$

The price of the unit is:

Baghouse	\$138,180	(Figure D-10)
Suction	13,690	(Figure D-10)
Insulation	73,470	(Figure D-10)
Bags	15,750	(Table D-2)
Total	241,090	

Cyclones

Cyclones are used to remove larger sized particulate matter from gas exhaust streams (usually > 20 μm diameter particles). They are not as efficient as scrubbers, electrostatic precipitators, or baghouses and consequently are cheaper to install. The size of a cyclone is usually based on an inlet velocity of approximately 3600 ft/min, and therefore the cost of the cyclone is based on the inlet area size. The inlet area size (ft²) can be determined from an exhaust gas capacity for various pressure drops by using Figure D-12. An inlet area can also be estimated from a critical particle size, $[d_p]_{crit}$, (particle size collected with 100 percent efficiency), by using Figure D-13. Figure D-14 gives cyclone prices for carbon steel construction

and Figure D-15 gives prices for stainless steel construction. Support, hopper, and scroll outlet price additions can be determined from Figures D-16, D-17 and D-18 respectively.

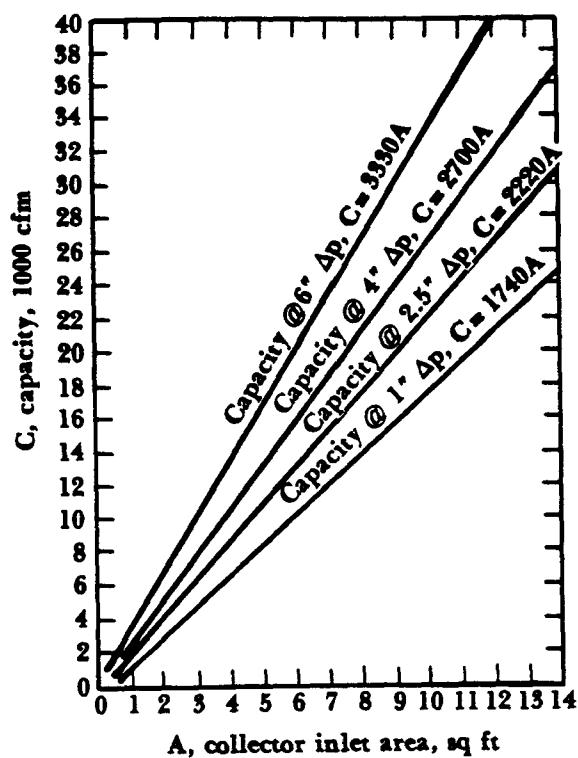


Figure D-12. Capacity estimates for cyclones.

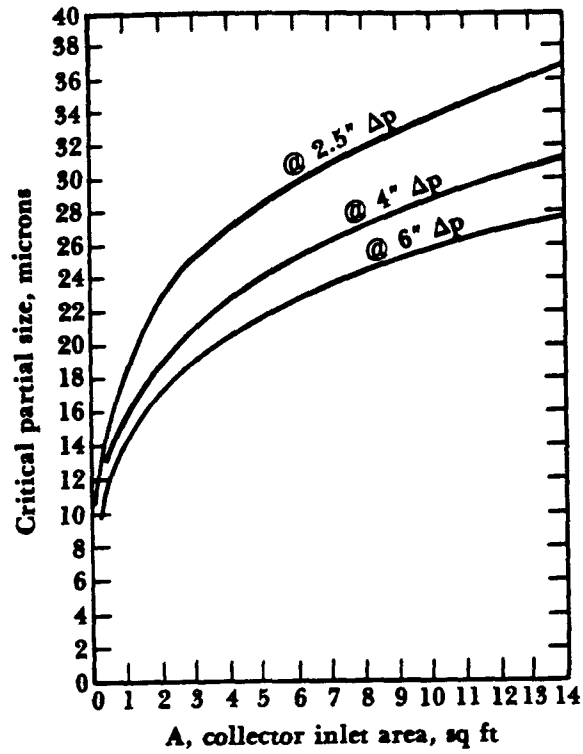


Figure D-13. Critical partical size estimates for cyclones.

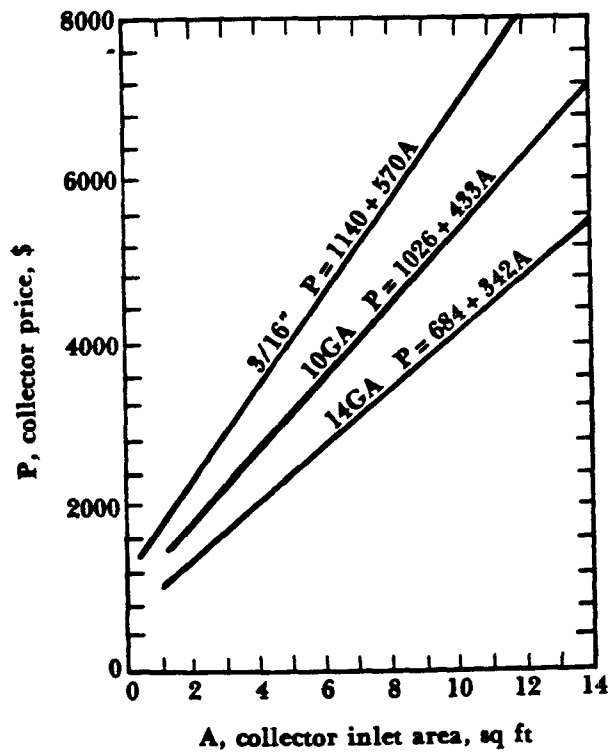


Figure D-14. Cyclone prices for carbon steel construction versus inlet area.
Data valid for December 1977.

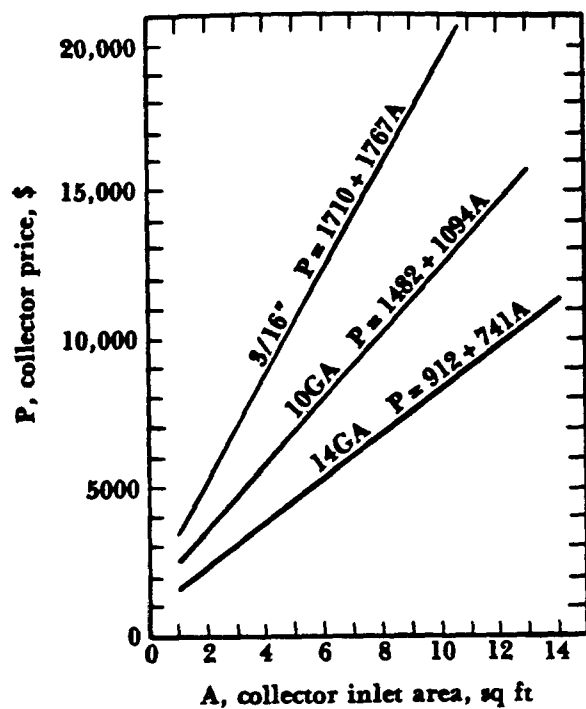


Figure D-15. Cyclone prices for stainless steel construction versus inlet area.
Data valid for December 1977.

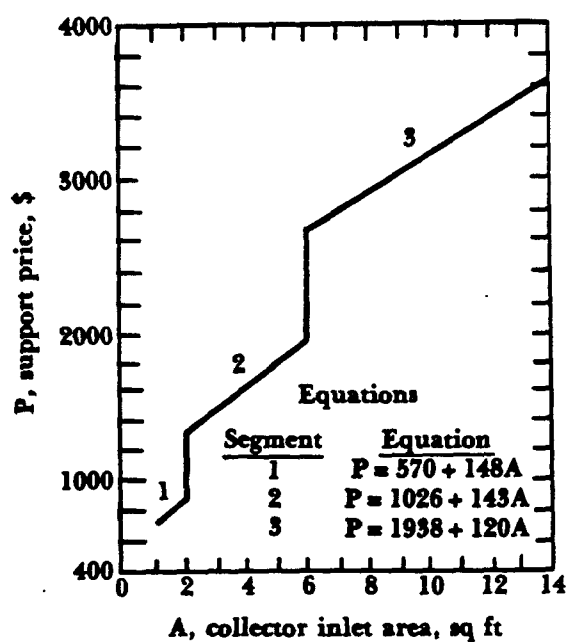


Figure D-16. Cyclone support prices versus collector inlet area.
Data valid for December 1977.

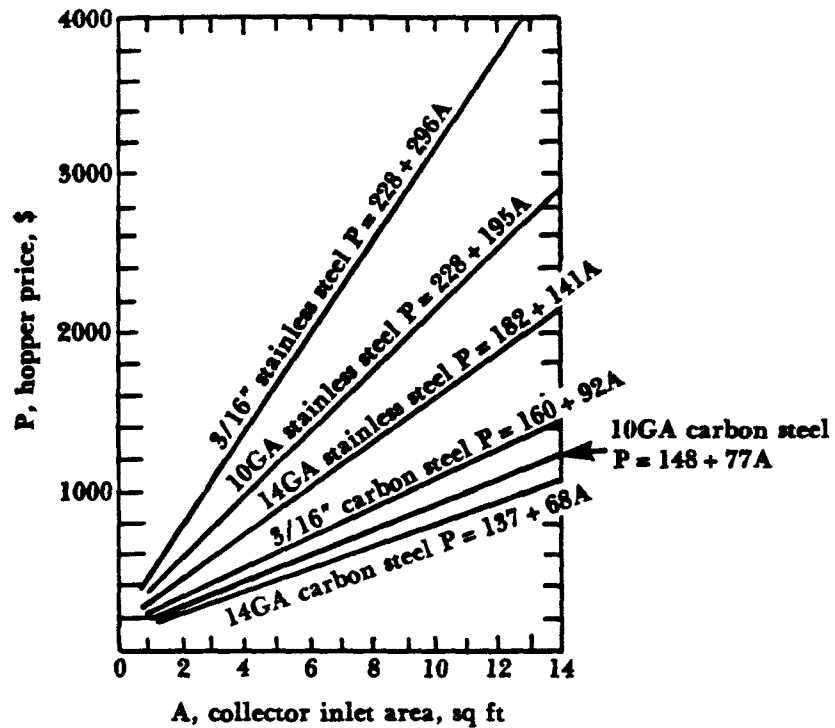


Figure D-17. Cyclone dust hopper prices for carbon and stainless steel construction versus collector inlet area. Data valid for December 1977.

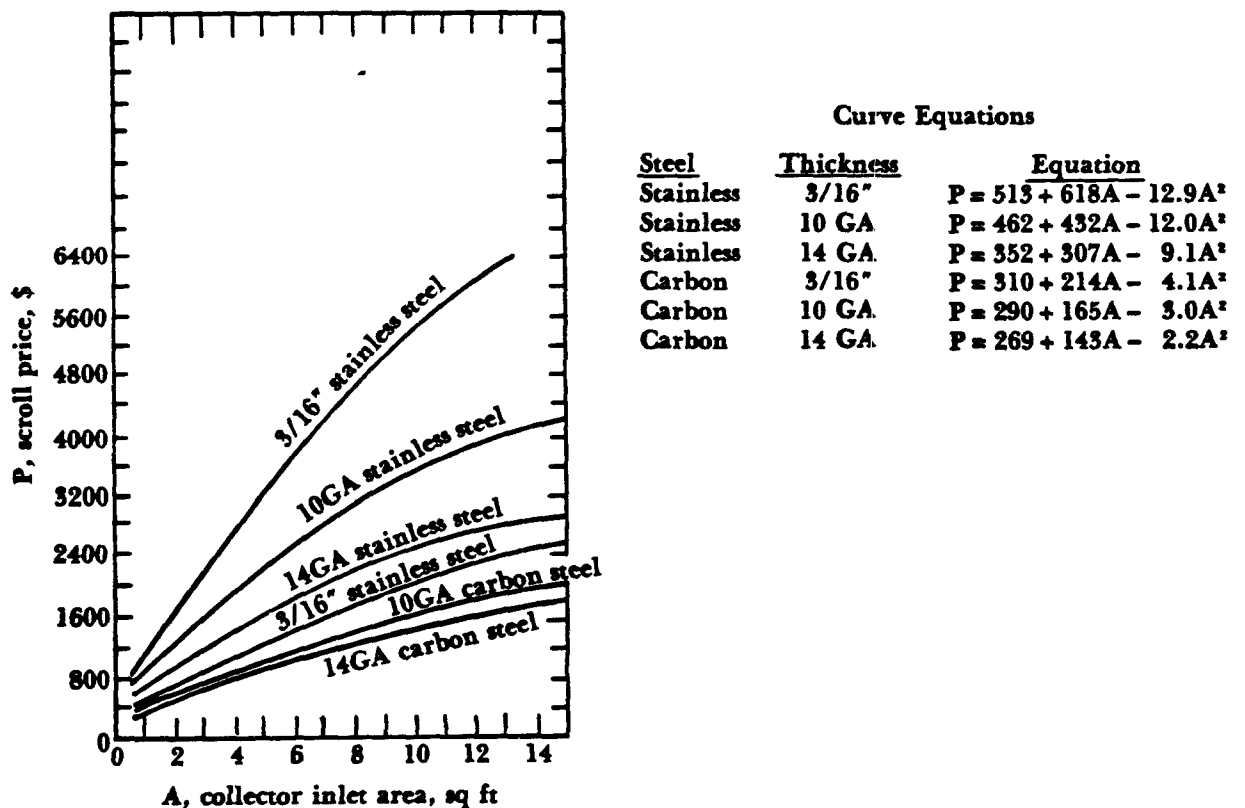


Figure D-18. Cyclone scroll outlet prices for carbon and stainless steel construction versus collector inlet area. Data valid for December 1977.

Example:

A cyclone is used to clean the exhaust from an industrial process with a flow rate of 25,000 cfm. The cyclone should be constructed of 3/16 in. carbon steel and the price should include a hopper, support, and a scroll outlet. The pressure drop across the cyclone is 4 in. H₂O.

From Figure D-12: Inlet area = 9.5 ft²

The price of the cyclone:

Cyclone	\$ 6,600	(Figure D-14)
Support	3,100	(Figure D-16)
Hopper	1,050	(Figure D-17)
Scroll outlet	<u>2,000</u>	(Figure D-18)
Total	\$12,750	

The figures in Appendix D must only be used as an estimate for determining the cost of a control device. As previously mentioned, these costs are based on 1977 dollars and do not include ancilliary equipment (hoods, fans, ducting, stacks), engineering overhead, labor erection cost and others. The reader should consult vendors of air pollution control equipment when an actual price quote is needed. A listing of air pollution control equipment vendors can be obtained by consulting the following sources:

Journal of the Air Pollution Control Association. March 1981. 31:205-326.

Pollution Equipment News. November 1980. 13: No. 6.

Pollution Engineering. December 1980.

Appendix E

Characteristics of Air Pollution Control Equipment

Name of device		Description	$[d_p]_{\text{minimum}}$ (μm)	Water pressure (psig)	Liquid to gas ratio Q_L/Q_G (gpm/cfm)	Pressure drop (inches of H_2O)	Application	Limitations
General	Specific type							
Scrubbers	Plate	Plates with openings and impingement targets	> 2.0	< 5	2-8	1-8	Simultaneous gas absorption and particle removal	Corrosion, erosion problems
	Orifice	Gas skims through and over liquid	0.8-1	—	0.5-5 (with recirculation)	2-10	Ability to cool and clean high-temperature, moisture-laden gases	Added cost of wastewater treatment and reclamation
	Venturi	Constricted section increasing velocity	0.2	1-15	3-20	5-100	Corrosive gases and mists can be recovered and neutralized	Lower efficiency on submicron particles
	Spray	Water sprays for droplet formation	2-8	10-400	0.5-20	0.5-5	Reduced dust explosion risk	Contamination of effluent stream by liquid entrainment
	Ejector	Water activated pump producing spray	> 1	15-120	50-100	0.5-5	Efficiency can be varied	Freezing problems in cold weather
	Cyclonic spray	Use of cyclonic motion and water for collection	2-5	40-400	2-10	1.5-10	Gas and particulate emission removal	Reduction in buoyancy and plume rise
	Moving bed	Moving spheres for impingement	2-5	—	3-5	3-5		Water vapor contributes to visible plume under some atmospheric conditions
	Baffle spray	Baffles for targets plus use of sprays	10	< 15	1	1-3		
	Mechanical	Mechanically driven rotors to develop droplets	< 1	20-60	0.5-1.5	4-6		
	Packed towers	Column packed with inert material	> 1.5	5-15	1-15	1.5-10		

Source: Adapted from Bethua, 1978.

Name of device		Description	Optimum size particles (µm)	Temperature limitations (°F)	Utility requirements (HP, water, kW, Btu)	Pressure drop (inches of H ₂ O)	Efficiency (% by weight)	Application	Limitations
General	Specific type								
Industrial filters	Cloth bag	Bags made of synthetic or natural fiber fabrics	> 0.3	0-180-550	—	> 4	> 99	Dry collection possible Collection of small particles possible High efficiencies possible (> 99%)	Sensitivity to filtering velocity High-temperature gases must be cooled to 550°F Affected by relative humidity (condensation) Susceptibility of fabric to chemical attack
	Cloth envelope	Envelopes made of natural or synthetic fibers; fabrics over screen cages	> 0.3	0-180-550	—	> 4	> 99		
Electrostatic precipitators (high voltage)	Single stage (plate)	Ionizing (—) wires between parallel collecting (+) plates	> 0.3	0-850	0.2-0.6 kW/1000 cfm	< 1	> 99	99% efficiency obtainable Very small particles can be collected Particles may be collected wet or dry Pressure drop and power requirement are small compared to other high-efficiency collectors Maintenance is nominal unless corrosive or adhesive materials are handled Few moving parts	Relatively high initial cost Precipitators are sensitive to variable dust loadings or flow rates Resistivity causes some materials to be economically uncollectable Precautions are required to safeguard personnel from high voltage Collection efficiencies can deteriorate gradually and imperceptibly
	Single stage (pipe)	Ionizing (—) wires inside concentric collecting (+) pipes	> 0.3	0-1200	0.2-0.6 kW/1000 cfm	< 1	> 99		
Dry inertial collectors	Settling chamber	Straight chamber expansion	> 50	0-700	—	< 0.1	< 50	Low pressure loss, simplicity of design and maintenance	Much space required Low collection efficiency Much head room required
	Baffle chamber	Straight chamber expansion (with baffles)	> 30	0-700	—	< 0.5	< 50		
	Cyclone	Chamber with spiral flow	> 10	0-700	—	< 2.0	< 80	Dry continuous disposal of collected dusts Low to moderate pressure loss	Sensitive to variable dust loadings and flow rates High efficiency for only small diameter cyclones
	Multiple cyclone	Small cyclones in parallel	> 5	0-700	—	4.6	< 90	Higher collection efficiency than single cyclones	Tendency to clog

Appendix F

Industry Pollutant Sources and Typical Control Devices

Industry	Source	Control system	Capture device	Typical gas flow design rate	Typical gas temperature
Brick manufacturing	1. Tunnel kiln 2. Crusher, mill 3. Dryer 4. Periodic kiln	1. Scrubber, baghouse precipitator 2. Baghouse, scrubber 3. Same as 1 4. Same as 1	1. Direct tap 2. Canopy hood 3. Same as 1 4. Same as 1	1. Combustion air fan capacity 2. 250 fpm hood face 3. Same as 1 4. Same as 1	1. 200-600°F 2. 70°F mill 3. 250°F 4. Same as 1
Casable refractories	1. Electric arc 2. Crusher, mill 3. Dryer 4. Mold and shakeout	1. Baghouse, scrubber 2. Same as 1 3. Same as 1 4. Same as 1	1. Direct tap 2. Canopy hood 3. Direct tap 4. Canopy hood	1. Infiltrated air 2. 250 fpm hood face 3. Fan capacity 4. Same as 2	1. 3000-4000°F 2. 70°F 3. 300°F 4. 150°F
Clay refractories	1. Shuttle kiln 2. Calciner 3. Dryer 4. Crusher, mill	1. Baghouse, precipitator, scrubber 2. Same as 1 3. Same as 1 4. Baghouse, precipitator	1. Direct tap 2. Same as 1 3. Same as 1 4. Canopy hood	1. Fan capacity 2. Same as 1 3. Same as 1 4. 250 fpm hood face	1. 150-800°F kiln 2. Same as 1 3. 250°F 4. 70°F
Coal-fired boilers	1. Steam generator	1. Precipitator, scrubber, baghouse	1. Direct tap	1. Induced draft fan capacity	1. 300°F
Conical incinerators	1. Incinerator	1. Scrubber	1. Direct tap	1. Combustion air rate	1. 400-700°F
Cotton ginning	1. Incinerator	1. Scrubber	1. Direct tap	1. Combustion air rate	1. 500-700°F
Detergent manufacturing	1. Spray dryer	1. Scrubber, baghouse	1. Direct tap	1. Fan capacity	1. 180-250°F
Feed mills	1. Storage bins 2. Mills/grinders 3. Flash dryer 4. Conveyors	1. Baghouse, scrubber 2. Same as 1 3. Same as 1 4. Same as 1	1. Direct tap 2. Canopy hood 3. Direct tap 4. Canopy hood	1. 250 fpm canopy hood face velocity 2. Same as 1 3. Air heater flow rate (dryer) 4. Same as 1	1. 70°F 2. 70°F 3. 170-250°F 4. 70°F
Ferroalloy plants a. HC Fe Mn b. 50% Fe Si c. HC Fe Cr	1. Submerged arc furnace (open) 2. Submerged arc furnace (closed) 3. Tap fume	1. Scrubber, baghouse, precipitator 2. Scrubber 3. Scrubber or baghouse	1. Full or canopy hood 2. Direct tap 3. Canopy	1. 2500-5500 acfm/MW with scrubber 2. a. 220 b. 180 acfm/MW c. 190 3. 200 fpm/ft ²	1. 400-500°F open arc 2. 1000-1200°F closed arc 3. 150°F hood
Glass manufacturing	1. Regenerative tank furnace 2. Weight hoppers and mixers	1. Baghouse, scrubber precipitator 2. Same as 1	1. Direct tap 2. Canopy	1. Fan capacity 2. 200 fpm/ft ²	1. 600-850°F furnace 2. 100°F mixers
Grey iron foundries	1. Cupola 2. Electric arc furnace 3. Core oven 4. Shakeout	1. Afterburner-baghouse for closed cap; afterburner-precipitator for closed cap; scrubber precipitator 2. Baghouse, scrubber precipitator 3. Afterburner 4. Baghouse	1. Direct tap 2. Direct tap, full/side draft hood 3. Direct tap 4. Full/side draft hood	1. Tuyere air + infiltrated door air + afterburner second air 2. 2000 fpm/ft ² hood 3. Fan capacity 4. 200-500 cfm/ft ² hood	1. 1200-2200°F 2. ~2500°F direct tap ~400°F hood 3. 150°F 4. ~150°F

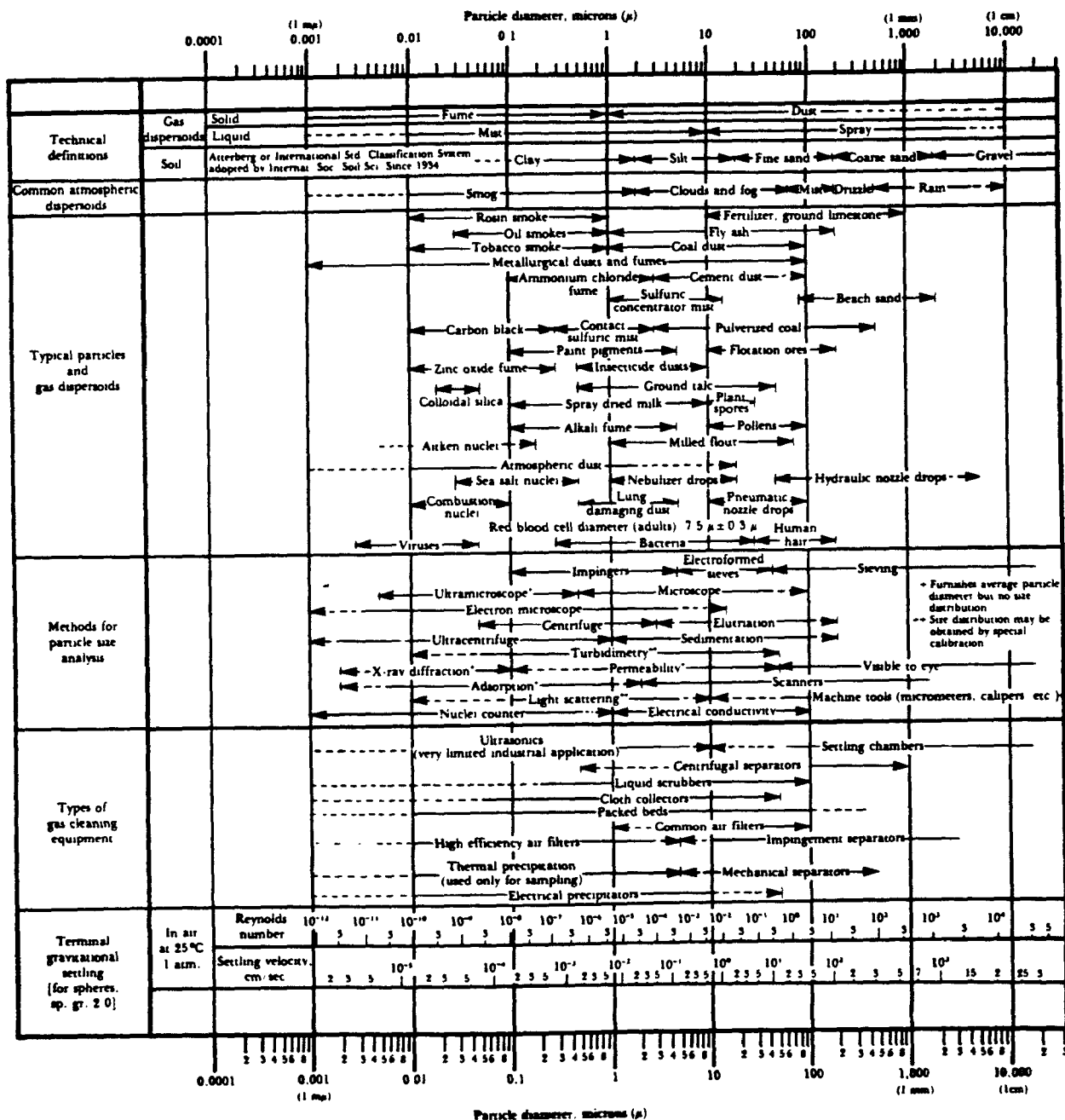
Industry	Source	Control system	Capture device	Typical gas flow design rate	Typical gas temperature
Iron and steel (sintering)	1. Sinter machine a. Sinter bed b. Ignition fce. c. Wind boxes	1. Precipitator, baghouse, scrubber	1. Down draft hood	1. Based on bed size	1. 150-400°F sinter machine
	2. a. Sinter crusher b. Conveyors c. Feeders	2. Baghouse, scrubber	2. Canopy hood	2. 250 fpm hood face	2. 70°F conveyors
Kraft recovery furnaces	1. Recovery furnace and direct contact evaporator	1. Precipitator, scrubber	1. Direct tap	1. Primary and secondary air supply capacity	1. 350°F
Lime kilns	1. Vertical kilns	1. Baghouse, scrubber, precipitator	1. Direct tap	1. Combustion air rate	1. 200-1200°F
	2. Rotary sludge kiln	2. Scrubber, precipitator	2. Direct tap	2. Combustion air rate	2. 200-1200°F
Municipal incinerator	1. Incinerator	1. Scrubber, precipitator, baghouse, afterburner	1. Direct tap	1. Combustion air far applicable	1. 500-700°F capacity where
Petroleum catalytic cracking	1. Catalyst regenerator	1. Precipitator, (boiler)-precipitator, scrubber	1. Direct tap a. High pressure b. Low pressure	1. Regeneration air rate + boiler combustion air	1. 1100°F regenerator, 500°F from boiler
Phosphate rock crushing	1. Crusher and screens	1. Baghouse, scrubber, precipitator	1. Canopy hood	1. 350 cfm/ft belt width at speeds ~200 fpm 500 cfm/ft belt width at speeds ~200 fpm	1. 70°F hoods
	2. Conveyor	2. Same as 1	2. Same as 1	2. 100 cfm/ft of casing cross-section (elevator) 50 cfm/ft of screen area	2. Same as 1
	3. Elevators	3. Same as 1	3. Same as 1	3. Combustion air rate	3. Same as 1
	4. Fluidized bed calciner	4. Same as 1	4. Same as 1	4. Blower rate	4. 600-1500°F calciner
Polyvinyl chloride production	1. Process equipment vents	1. Adsorbers, afterburners, precipitators	1. Direct tap	1. Process gas stream rate	1. -15 to 130°F
Pulp and paper	1. Fluidized bed reactor	1. Scrubber	1. Direct tap	1. Combustion air rate	1. 600-1500°F
Secondary aluminum	1. Reveratory furnace	1. Scrubber (low energy) + baghouse precipitator	1. Canopy hood (hearth), direct tap	1. Max. plume vol. + 20% (hearth)	1. 1600°F fluxing, 600°F holding hearth
	2. Electric induction furnace	2. Same as 1	2. Same as 1	2. Infiltrated air	2. Based on type capture
	3. Crucible furnace	3. Same as 1	3. Same as 1	3. Same as 2	3. Same as 2
	4. Chlorinating station	4. Same as 1	4. Same as 1	4. Same as 2	4. Same as 2
	5. Dross processing	5. Same as 1	5. Same as 1	5. Same as 2	5. Same as 2
	6. Sweating furnace	6. Same as 1	6. Same as 1	6. Same as 2	6. Same as 2
Secondary copper smelters	1. Reveratory furnace	1. Baghouse, scrubber precipitator	1. Direct tap, canopy hood, full hood	1. 200 fpm/ft ² canopy hood	1. 2500°F direct tap
	2. Crucible furnace	2. Same as 1	2. Same as 1	2. Max. plume vol. + 20%	2. Based on type capture
	3. Cupola and blast furnaces	3. Same as 1	3. Same as 1	3. 1800 fpm infiltrated air (full hood)	3. Same as 2
	4. Converters	4. Same as 1	4. Same as 1	4. Based on type capture	4. Same as 2
	5. Electric induction furnace	5. Same as 1	5. Same as 1	5. Same as 4	5. Same as 2

Industry	Source	Control system	Capture device	Typical gas flow design rate	Typical gas temperature
Sewage sludge incinerators	1. Multiple hearth incinerator 2. Fluidized bed incinerator	1. Scrubber 2. Same as 1	1. Direct tap 2. Same as 1	1. Combustion air blower capacity 2. Same as 1	1. 600 to 1500°F 2. Same as 1
Surface coatings— spray booths	1. Spray booth	1. Adsorber	1. Canopy hood	1. 150 fpm/ft ² hood, 100 fpm booth face velocity	1. 70°F
Portland cement	1. Rotary kiln a. Wet 2. Crushers and conveyors 3. Dryers	1. Precipitators, baghouses 2. Baghouses 3. Precipitators, baghouses	1. Direct tap 2. Canopy hoods 3. Direct tap	1. Combustion air rate where applicable 2. 250 fpm hood face 3. Same as 1	1. 150-850°F kilns 2. 70°F crushers and conveyors 3. 200°F dryers
Basic oxygen	1. Basic oxygen furnace	1. Precipitator, scrubber, baghouse	1. Full-canopy hood	1. Function of lance rate and hood design—up to 1,000,000 acfm	1. 3500-4000°F
Electric arc furnaces	2. Charging hood	2. Same as 1	2. Canopy hood	2. 3000 fpm hood face	2. 150-400°F
	1. Arc furnace	1. Baghouse, scrubber, precipitator	1. Direct tap, full/side draft hood	1. Function of lance rate and hood design—up to 200,000 acfm	1. 3500°F (direct tap)
	2. Charging and tapping	2. Same as 1	2. Canopy hood	2. 250 fpm hood face	2. 150°F (canopy)
Phosphate fertilizer	1. Digester vent air 2. Filters 3. Sumps	1. Scrubber, baghouse 2. Same as 1 3. Same as 1	1. Hood 2. Same as 1 3. Same as 1	1. Process stream rate 2. Same as 1 3. Same as 1	1. 150°F 2. Same as 1 3. Same as 1

Source: EPA, 1976.

Appendix G

Characteristics of Particles



Source: Stanford Research Institute Journal, 1961.

Appendix References

- The American National Metric Council. 1978. *Metric Editorial Guide*. 3rd ed.
- Environmental Protection Agency (EPA). 1976. *Capital and Operating Costs of Selected Air Pollution Control Systems*. EPA 450/3-76-014. PB 258, 484.
- Neveril, R. B., Price, J. U. and Engdahl, K. L. 1978. Capital and Operating Costs of Selected Air Pollution Control Systems—I. *J. Air Poll. Control Assoc.* 28:829-836.
- Neveril, R. B., Price, J. U. and Engdahl, K. L. 1978. Capital and Operating Costs of Selected Air Pollution Control Systems—I. *J. Air Poll. Control Assoc.* 28:963-968.
- Bethea, R. M. 1978. *Air Pollution Control Technology—an Engineering Analysis Point of View*. New York: Van Nostrand Reinhold Company.
- Vandegrift, A. E., Shannon, L. J., Gorman, P. G., Lawless, E. W., Sallee, E. E. and Reichel, M. 1971. *Particulate Pollutant Systems Study I, Mass Emissions*. Report PB 203, 128. Midwest Research Institute. Kansas City, MO.
- Stanford Research Institute Journal*. 1961. Menlo Park, CA: SRI International.

TECHNICAL REPORT DATA <i>(Please read instructions on the reverse before completing)</i>		
1. REPORT NO. EPA 450/2-80-066	2.	3. RECIPIENT'S ACCESSION NO.
4. TITLE AND SUBTITLE APTI Course 413 Control of Particulate Emissions Student Manual	5. REPORT DATE October 1981	6. PERFORMING ORGANIZATION CODE
	8. PERFORMING ORGANIZATION REPORT NO.	
7. AUTHOR(S) David S. Beachler, James A. Jahnke	10. PROGRAM ELEMENT NO. B18A2C	11. CONTRACT/GRANT NO. 68-02-2374
9. PERFORMING ORGANIZATION NAME AND ADDRESS Northrop Services Inc. P.O. Box 12313 Research Triangle Park, NC 27709	13. TYPE OF REPORT AND PERIOD COVERED Student Manual	
	14. SPONSORING AGENCY CODE	
12. SPONSORING AGENCY NAME AND ADDRESS U.S. Environmental Protection Agency Manpower and Technical Information Branch Research Triangle Park, NC 27711		
15. SUPPLEMENTARY NOTES EPA Project Officer for this Student Manual is R. E. Townsend, EPA-ERC, MD-20, Research Triangle Park, NC 27711		
16. ABSTRACT The Student Manual is to be used in conducting APTI Course 413 "Control of Particulate Emissions". This manual supplements the course lecture material, presenting detailed discussions on particulate emission control equipment. The major topics include: Basic Gas Properties, Particle Dynamics, Particle Sizing, Settling Chambers, Cyclones, Electrostatic Precipitators, Fabric Filters, and Wet Collectors. This manual will assist the reader in evaluating plans for particulate emission control systems and in conducting plan reviews. This guide is intended for use in conjunction with the Instructor's Guide (EPA 450/2-80-068) and the Student Workbook (EPA 450/2-80-067) for APTI Course 413.		
17. KEY WORDS AND DOCUMENT ANALYSIS		
a. DESCRIPTORS	b. IDENTIFIERS/OPEN ENDED TERMS	c. COSATI Field/Group
Air Pollution Control Particulate Emission Control Training Manual	Student Manual	13B 5I 68A
18. DISTRIBUTION STATEMENT Unlimited Available from National Technical Information Service, 5285 Port Royal Rd., Springfield, VA 22161	19. SECURITY CLASS (This Report) Unclassified	21. NO. OF PAGES 264
	20. SECURITY CLASS (This page) Unclassified	22. PRICE

U.S. Environmental Protection Agency
Region 5, Library (5PL-16)
230 S. Dearborn Street, Room 1670
Chicago, IL 60604